THE INFLUENCES OF GEOGRAPHIC FACTORS ON THE COMPLEMENTARY NATURE OF WIND POWER AND INSOLATION

By

WEIPING LI

Bachelor of Science in Economic Geography and Urban and Regional Planning
Nanjing University
Nanjing, China
1989

Master of Science in Computer Science
Oklahoma State University
Stillwater, Oklahoma
2000

Submitted to the Faculty of the
Graduate College of the
Oklahoma State University
in partial fulfillment of
the requirements for
the Degree of
DOCTOR OF PHILOSOPHY
December, 2012

THE INFLUENCES OF GEOGRAPHIC FACTORS ON THE COMPLEMENTARY NATURE OF WIND POWER AND INSOLATION

Dissertation Approved:

Dr. Steve Stadler

Dissertation Adviser

Dr. Jonathan Comer

Dr. G. Allen Finchum

Dr. R. Ramakumar

ACKNOWLEDGEMENTS

I owe sincere and earnest thankfulness to my advisor, Dr. Steve Stadler, who provided me with the opportunity to work for OWPI first and initiated my interests in the area of renewable energy study, which has fascinated me greatly ever since. Dr. Stadler has helped me through the whole study, and helped me to overcome many hurdles during the study. He taught me how to 'think aloud' and keep a positive attitude in both study and life. I thank him for his constructive guidance, support, patience, and motivation throughout my study. Without his constant push and encouragement, this work would not have been completed.

I would express special thanks to Dr. Ramakumar who has co-advised and oriented this research. His expertise in renewable energy field, in computational methods and even in writing was invaluable in helping me to achieve the project goals. His inputs to this study, including helping me to design the topic, develop the quantification approach, and clarify many concepts and issues I met during the study, are irreplaceable and highly appreciated. I learned a lot from Dr. Ramakumar.

My deep gratitude also goes to the members of my doctoral committee, Dr. Comer and Dr. Finchum for their committed service, support, and suggestions that helped to conduct and improve this work. The convenient access to the GWR software provided by Dr. Comer was extremely helpful to this study, his assistance in my grasp of the methodology of GWR, and his rigorous attitude and meticulous review of the writing was priceless and indispensable. The technical support from Dr. Finchum, especially the exceptional permission of my dominant usage of some computers was also helpful.

I wish to convey my sincere gratitude and appreciation to Michael Larson and Bruce Battles for their help in searching for a person to help edit my writing and introduced Helen Agnew to me; Helen helped me to edit the dissertation draft in a rush period. I also got assistance from Bruce in providing a computer for me to conduct my data-intensive computation. To all of them, words are not enough to say thanks.

I am deeply indebted to my parents, and my brothers who gave me constant support on each of my step. Without their love, understanding, and sacrifices, I would not be able to keep on my pursuits.

This work was partially supported by the Department of Commerce of Oklahoma and the U.S. Department of Energy. Their financial support is gratefully acknowledged.

Name: WEIPING LI

Date of Degree: DECEMBER, 2012

Title of Study: THE INFLUENCES OF GEOGRAPHIC FACTORS ON THE COMPLEMENTARY NATURE OF WIND POWER AND INSOLATION

Major Field: Geography

Abstract: The major objective of this study is to investigate the spatial variation of the complementary nature of wind power and solar radiation (***CWS***), and how geographic factors impact this nature. Quantification approaches, spatial analysis, especially local geographically weighted regression (GWR) methodology are employed to conduct this study. Local geographic factors from micro to mesoscale are associated with the ***CWS***. Their relationships are further examined through statistics, principal components analysis, and GWR modeling. Oklahoma with typical terrain variations and high-resolution Mesonet data is used as an exemplary case for this study. Because of time limitation, this study is basically preliminary. The variation of the complementary nature in a wider spatial and temporal scale, and many theoretical and practical issues related with this topic are not explored by this study.

Through applying quantification approach and local spatial analysis methods on the exemplary case of Oklahoma, this study found that there exist complementarity of wind power and solar radiation (***CWS***) in different levels during different temporal span at different places. In Oklahoma, the average annual level of ***CWS*** can range from 0.28 to 0.62 where 1 means the highest. Geographic factors like moisture, landscape focusing on slope/forest coverage, landscape focusing on curvature, landscape focusing on barren and residential land percentage, and landscape focusing on aspect/relative elevation are found significantly related with ***CWS***. In global model, except that the dimension of landscape focusing on barren and residential land percentage is found negatively impacting the ***CWS,*** all other three dimensions are positively affecting the ***CWS***. However, in local GWR model, the sign of their relations with the ***CWS*** vary with space, and may hold opposite signs in different regions. Through local GWR modeling, it is also found that only the influences of the moisture dimension on the ***CWS*** indicate significant spatial variation. By examining the statistics of local GWR models and corresponding global models, it is found local models did not outperform global models in most cases. Therefore there is probably a global model to estimate the level of ***CWS*** based on local or regional geographic factors.

TABLE OF CONTENTS

Chapter Page

Chapter Page

LIST OF TABLES

Table Page

LIST OF FIGURES

Figure Page

Figure Page

ACRONYMS

AIC	Akaike Information Criterion
CINDX	Long-term Annual Cloud Index
CIWS	Complementarity Index between Wind Power and Solar Radiation
CWS	Complementarity between wind power and solar radiation
DEM	Digital Elevation Model
DPG	Distributed Power Generation Systems
INSOLATION	Incident Solar Radiation
GIS	Geographic Information Systems
GWR	Geographically Weighted Regression
OLS	Ordinary Least Squares Regression
PC	Principal Component
PCA	Principal Components Analysis
MAUP	Modifiable Area Unit Problem
MESONET	Oklahoma Mesoscale Network

CHAPTER I

INTRODUCTION

1.1 Overview

In recent years, environmental degradation and energy depletion have become prominent concerns in relation to human overconsumption of nonrenewable fossil fuels (Energy Information Administration, 2010). Fossil fuels, including coal, oil, and natural gas, have been the major resources energizing human industrialized civilization in the past several decades. However, fossil fuel combustion produces many greenhouse gases and other pollutants impacting the environment. Moreover, it is projected that by the middle of this century, the provision of fossil fuels as primary energy sources will not keep up with accelerating demand (Lincoln, 2005). The current soaring market prices of gas and oil are a reflection of this concern. Societies are facing an urgent need to explore alternative energy sources.

Renewable energy is an ideal alternative energy source for human sustainable development because it is clean and inexhaustible. According to the US Department of Energy (2010), renewable energy is "energy derived from resources that are regenerative or for all practical purposes cannot be depleted". Renewable energy includes solar energy, wind power, hydropower, tidal and wave power, geothermal energy, and biofuels. Fundamentally, with the exception of geothermal, most energy sources on the earth, including both the renewable and the non-renewable resources, are directly or indirectly derived from solar energy. However, renewable energy can be renewed in short-term cycles, such as diurnal, seasonal, annual time scales, while

non-renewable resources usually take much longer geological cycles to regenerate (Ramakumar, 2001). Renewable energy resources could better meet human needs for energy because of its regenerability and endurance compared with non-renewable energy resources. In addition, the cleanness of renewable energy has also been proven. Through long term human experience, the existence and usage of renewable energy resources has not brought destructive impacts to human societies in the past.

Renewable energy resources can be an important way forward for the next generation of energy solutions for several reasons. First, compared with non-renewable energy, renewable energy resources are inexhaustible and free of human concern of fossil energy depletion, and therefore most ideal for human sustainability. Second, all renewable energy resources, except bio-fuel, have low-carbon footprint or zero-emission which is a favorable feature to help reverse the current tendency of increasing carbon dioxide concentration in the atmosphere. Third, renewable energy distribution is widespread, and easily accessible, which makes it especially feasible for the design of future decentralized energy generation systems. Fourth, renewable resources are site-specific, that is, different places have different types and amounts of renewable resources, just as energy demands, production processes, and consumption patterns vary from place to place. Although local demand and renewable resources do not necessarily coincide with each other, they provide the possibility to match them. With improvement of the design of modularized power systems in the future, this feature might become especially beneficial for comprehensive deployment of various renewable energy resources locally. Lastly, renewable energy resources are free to obtain, even though it is not free to convert them to a usable form of energy such as electricity (Ramakumar, 2001).

Among various types of renewable resources, wind and solar energy (insolation) are unique and especially worthy of further investigation. They are the most abundant and ubiquitous sources of energy (Sawin, 2004). It has been estimated that energy delivered from the sun to earth's surface is about 5500 times the current world energy consumption (Meyer, 2008). The global wind power

potential is assessed to be at least five times current global power demand (Archer and Jacobson, 2005). Moreover, compared with other renewable energy types, both wind and solar power indicate some special advantages. Unlike biomass fuels, wind and solar energy are completely emission-free and have little or no competition with human food needs for existing arable and grazable land. Unlike hydropower, wind and solar energy are less limited by geographic location and more accessible globally. Unlike geothermal power, deployment of wind and solar energy consumes no water. These special characteristics of wind and solar resources make both of them logical choices for sustainable development.

There is another salient feature observed between wind and solar resources that could greatly increase their credentials for human pursuit of sustainability, that is, the complementary nature between the wind and solar energy. It has long been noticed that there is usually more sunlight during calm, cloud-free daylight hours, and more windy weather during cloudy periods of times (Ramakumar, 2001). This is usually referred to as the complementary nature of wind and solar energy in diurnal cycle. In many places in the US and many other parts of the world, wind speeds are lower in the summer, when the sun shines brightest and longest; and the wind can be stronger in the winter, when less sunlight is available (Ramakumar, 2001). This is referred to as the complementary nature of wind and solar energy in annual cycle.

The complementary nature of wind and solar energy may especially make wind-plus-solar resources - an integrated deployment of both resources - a better renewable energy combination for future energy solutions, by combining their advantages and lessening the impacts of their shortcomings. It has been recognized by power engineers that the deployment of wind and solar resources faces some bottlenecks from their natural drawbacks. Both wind and solar flows are volatile in nature, intermittent in time, non-transportable, and non-storable in their original forms. These characteristics make them qualitatively different from conventional fossil fuels, which are available to use whenever the appropriate combination of supply source and conversion device are available. Energy converted

directly from the sunlight or wind inherently fluctuates. Manipulation of either resource to satisfy end user demand faces a greater difficulty than using fossil fuels. To some extent, this implies that power generation from wind or solar resources is not as dependable or as competitive as using conventional fossil energy. However, the complementarity observed between wind and solar power may help to somewhat lift this constraint. Studies have found that the complementary nature of wind and solar energy can make the combined usage of the two to be a better load match (meeting the total momentary power demand) than using either resource exclusively (Ai et al., 2003; Reichling and Kulacki, 2008). Further exploration of the complementary nature of the two, including a meaningful assessment of their complementarities in various locations, is therefore essential for helping better deployment of the two resources and for a better understanding of the relations between the two energy forms.

1.2 Research Problem

Although the complementary nature of wind and solar energy, abbreviated as ***CWS*** in this dissertation study, has been revealed by a few studies in the past (see chapter 2), existing work is limited in scope. There are many questions still unanswered, such as: how to define the complementary nature of wind and solar radiation? What method can be used to quantify the complementary nature between the two energy forms? And, does this nature vary from place to place, since wind and solar energy are site-specific? More specifically, are there significant differences in the complementarity at different places? That is, is there notable spatial heterogeneity of the complementarity? If spatial heterogeneity exists, how do geographic factors affect this nature? Are there significant correlations between geographic factors and the complementary nature of wind power and solar energy? What are those geographical factors? How is the complementary nature shaped by various spatial factors and spatial processes? In addition, what kind of locations might be expected to have higher level of ***CWS***? Is there any way to estimate and predict the complementarity level for different places? Finally, does the feature vary during different periods of time? And, if so, how? None of these issues have been

studied, even though the ***CWS*** has been asserted by meteorologists, engineers, researchers, and lay observers. Future effective deployment of hybrid systems using both wind and solar resources will depend on more detailed and accurate knowledge of this complementary nature. This study makes a preliminary attempt to answer these questions.

Chapter Two of this dissertation reviews previous studies related to ***CWS*** and the general concepts and methodologies regarding complementarity as used in other fields. Chapter Three outlines the definitions and research problems, some key concepts regarding ***CWS***, the objectives of this study, and the methodology used. Chapter Four introduces an approach to quantify the complementarity of wind and solar radiation. This methodology is applied to the case of Oklahoma to obtain the quantified index of complementarity of wind and solar energy for all of Oklahoma. Chapter Five discusses the spatial variation revealed through quantified ***CWS*** by examining the example of Oklahoma. Major geographic factors, including location, local topographic factors and climatological factors have been examined and linked to the spatial variations of ***CWS***. Impacting factors were compressed through correlation analysis and principal components analysis. Chapter Six uses geographic weighted regression (GWR) to model and investigate the potential relationships of various geographic factors and the quantified ***CWS*** values for Oklahoma. Analysis of modeling results, discussions of modeling results and some suggestions about the approach of local model are presented in Chapter Six. In the last chapter, conclusions, tentative explanations about mechanisms behind the nature of ***CWS***, some potential applications of results from this study, and future work to be done regarding this topic are discussed.

1.3 Significance

In the context of rising energy concerns and environmental awareness, there are increasing demands toward developing renewable energy resources such as wind and solar energy. A better understanding of the characteristics of wind and solar resources and their complementarity will help to develop economically and technically viable wind-solar hybrid power systems and assist the development of

optimized multi-sourced distributive renewable energy systems in the future. Studies of the influences of geographic factors on the complementary nature of wind and solar resources provide a basis to investigate and predict geographic and temporal variations of the ***CWS***. In the future, the gradual transition of the world economy to a carbon-independent growth will not only involve deployment of hybrid renewable energy systems by taking advantage of their complementary nature, but also include development of distributive power generation systems using the complementary nature of these abundantly available renewable energy resources. The increased knowledge of various renewable energy resources and their relationships, including the complementary nature of wind and solar energy investigated in this study, will benefit this effort.

1.3.1 Optimized Design of Hybrid Systems Using both Wind and Solar Resources

A hybrid system that combines both wind and photovoltaic (PV) technologies is considered to be one of the renewable energy systems with the best prospects. Wind and PV hybrid systems may provide better performance potential in case of converse availability of solar and wind power. An optimally configured wind/PV system might be designed for producing electricity on a 24/7 basis to meet end users' demands based on three things: the complementary tendency and characteristics discovered between wind and solar power potential at a location, assumptions of market cost of both wind and solar energy, and knowledge of the local power demand (Sahin, 2000).

Although at the current time capital cost of energy favors wind plants, electric load matching usually favors a hybrid wind/solar plant (Reichling and Kulacki, 2008). Since wind and solar energy technologies continue to advance, and because solar power generation is getting cheaper, adding solar thermal electrical generating capacity to a wind farm will provide better cost-benefit tradeoffs than expanding current wind farm capacity (Reichling and Kulacki, 2008). Therefore, a detailed knowledge of the complementary nature of wind and solar energy for individual sites helps to develop optimal configuration of hybrid systems using both resources at a specific site.

In addition, in consideration of the design of hybrid systems using wind and solar resources, energy storage systems such as batteries, hydropower dams, or other peak adjustment measures are usually needed to counter the intermittency and fluctuation of the energy outputs from wind and solar resources. If the complementarity level between wind and solar energy is known, it is possible to estimate how much backup energy storage and reconversion may be needed to provide on-demand supply of power. A quantitative assessment of the complementary feature of wind and solar energy therefore not only helps to determine the amount of wind and PV ratings needed, but also helps to decide the storage capacity or backup systems needed.

Hybrid systems based on the complementary nature of wind and solar energy are especially applicable to remote and underdeveloped areas without any grid connections but with abundant sunshine and wind power (Gül, 2004). It is estimated there are about two billion people living in about two million villages without access to power grid around the world (Ramakumar, 2001). For these households in remote areas, to build new grid connections is expensive. Besides, many of those remote areas are in vulnerable ecosystems. Installing hybrid system using wind/PV will increase their access to electricity and improve their lives in an economical and environmentally friendly way.

For areas with grid-connected, the use of hybrid renewable resources, especially wind and solar energy, will decrease the dependence on fossil fuels and lower the carbon footprint. The deployment of hybrid systems for grid-support, uninterruptible power supplies and peak-shaving applications in grid-connected urban areas can be both economically and environmentally beneficial.

In the long term, deployment of hybrid systems with solar and wind inputs, plus some other renewable resources, will help to stabilize the carbon-concentration in the atmosphere and slow the rate of use of fossil fuels, forming a new sustainable electrification strategy for the entire planet. Findings from this study regarding the complementarities between wind and solar energy at a specific location hopefully will also help to develop the temporal profile of wind and solar power in places

where specific geographic variables and conditions are known. Optimum design configuration of hybrid systems using wind/PV will be based on the local temporal profiles of wind and solar potential so that they can best meet the local demand in the most economical and technologically viable way (Ai et al., 2003; Zhou et al., 2010). It is expected that the end-use energy demand can be better met by the combined use of the two energy sources by exploiting their complementary nature rather than using only either one, even though backup systems will still be needed with the combined systems (Ai et al., 2003). How well the combined system can improve the provision of energy partially depends on the complementarity between the two energy resources. Therefore, a detailed exploration of the complementarity between the two, such as its spatial and temporal variations and the factors and processes behind the variations, is useful.

1.3.2 In-depth Understanding of Relations between Wind and Solar Energy

Solar energy is the fundamental source of most energy types on earth, and it is also the original source of wind power. How solar energy is redistributed into different energy types through the work of moving air and static earth landforms is a significant topic. Since wind and solar radiation are both impacted by local and global natural processes, the study of the complementary nature of wind and solar energy from a spatial perspective improves knowledge of wind and solar energy and their relations in a bigger picture. It may also deepen the understandings about spatial factors and dynamic spatial processes that have helped to shape the two energy forms and their special relations. In the future, models built to connect various factors and processes for dynamically estimating wind and solar distributions at a specific site and time within a large spatial context might be possible.

Fundamentally, wind is caused by the sun heating the atmosphere non-uniformly over different locations leading to air flows from higher pressure to lower pressure. It transports excess heat from one place to another (NEED, 2011). Larger pressure gradients of the air lead to stronger winds. On the other hand, ground surfaces of the earth having static features and varied levels of friction slow down winds at varied rates. Farther above the earth's surface, where the amount of friction lessens,

the wind is usually stronger. Therefore, wind as an air flow is strengthened by larger gradients of air pressure and weakened by friction from the earth's surface.

Wind power is the conversion of kinetic energy of air flow into forms useful for humans, usually electricity, by turning wind turbines (IEC, 2007). Since the amount of power contained in wind is a cubic function of wind speed, even small differences in wind speed can result in large differences in wind power (IEC, 2007).

Regarding solar energy, the total incident solar radiation on a unit of the earth's surface is called the "insolation", or incident solar radiation. It is comprised of two parts: direct beam radiation and diffuse radiation from the sun (SRML, 2007). The direct beam irradiance is solar radiation coming from the direction of the sun. The diffuse radiation refers to atmospherically scattered radiation reaching the earth's surface (SRML, 2007). The sun's rays are attenuated as they pass though the atmosphere. Therefore, insolation is dramatically affected by the angle at which the sun strikes a surface. The average insolation over a location determines its climate zone, daily and seasonal temperature changes. On the other hand, daily and seasonal climate conditions affect the insolation through the extent of cloud cover, humidity level, and atmospheric contents as well. In addition, insolation may also be influenced by factors such as latitude, topography, orientation, and shading conditions of the site (Dogniaux, 1994). In general, the total amount of insolation at a site, both direct and diffuse types, is affected by climate, location, and terrain factors.

In summary, at a specific site, during a unit of time, the amount of wind power and solar radiation received is a function of many parameters: the relative movement of the earth and the sun, which can be represented by time and location; the atmosphere and its movement; and local topographic and climatic factors. When sunlight passes through the atmosphere onto the earth's surface, part of it is absorbed by the atmosphere and converted to wind power, while the other part reaches the earth's surface and becomes the measured insolation. Possibly, inverse work done by same set of geographic

and climatic factors toward wind and solar radiation at a place creates the complementarity between wind and solar energy. Exploring the level of complementarity between wind and solar energy along with those affecting geographic factors may help to reveal the inverse functions of various spatial factors and processes behind various wind and solar energy scenarios over space and time dimensions. It is expected that, in the future, models integrating space, time and detailed spatial features to predict the potentials of solar and wind energy in a more dynamic and real time manner could be created.

1.3.3 Transition to Carbon-neutral Growth through Distributed Generation of Alternatives

The history of human civilization is also a history of human beings growing proficient in deploying varied energy sources and energy technologies based on varying human demand in time. In the era of pre-industry, fire was called the first Promethean energy technology, fueled by wood or biomass (Cleveland, 2007). Entering the era of industrialization, Promethean II was the heat engine powered first by wood and coal, and then by oil and natural gas (Cleveland, 2007). Heat engines achieved a greater conversion of energy from heat into mechanical work, by supplying more surplus energy compared to animate energy converters, which brought changes to all aspects of the human sphere (Cleveland, 2007). Entering the modern era of post-industrialization and information technology, new energy technologies with foci on renewable resources and distributed power generation technologies are arising urged by human desires for a more sustainable path of development (see Figure 1.1).

1.3.3.1 Unsustainable Carbon-economy

Carbon-based energy has been a major energy source behind human survival since the beginning of human civilization. This is because carbon is the basic element for photosynthesis and the raw material of which human beings are made of (Rockwell, 1998). Carbon-based fuels, also referred to as fossil fuels, have been used to heat and light homes and workplaces since fire was invented (Rockwell, 1998). It is the carbon fuels that made the Industrial Revolution possible, and it is because of the ever increasing use of carbon fuels that the world has changed profoundly. Today, nearly

everything pertaining to human consumption, from transportation and electricity to foodstuff, from fertilizer to pesticide, is entirely carbon dependent (Rockwell, 1998). Carbon-based fuels can be considered as the growth engine of the world economy.

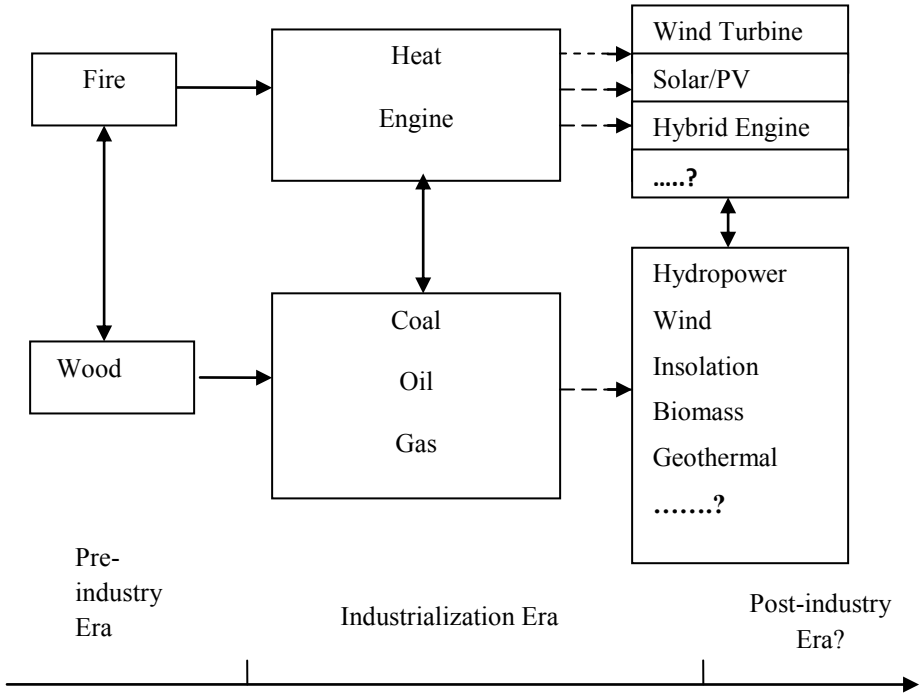

Figure 1.1 History of Energy Transition
(Based on Cleveland, 2007)

The carbon engine can work in two ways. It has been realized that over-exploitation of stored carbon energy has incurred an enormous negative impact on human sustainability. Human societies today have to face two pressing concerns deriving from the carbon dependent economy: the environmental degradation because of global warming and pollution (See Figure 1.2), and the nearing of fossil energy exhaustion. According to the Intergovernmental Panel on Climate Change (2007), if human beings follow the current path of carbon fuel dependency, the average temperature of the earth will be expected to increase 2^0C to 5^0C in the next 100 years. The most direct result of this climate change will be the alteration of the timing and distribution of precipitation and therefore a severe disturbance to current ecosystems of which human lives and economic activities rely on very much (Rockwell,

1998). Sea levels might also rise to inundate islands and several of the most populated metropolitan coastal areas so that the world map may become different (Rockwell, 1998). Another environmental impact of human overuse of stored carbon energy is severe pollution. Toxic smog generated from fossil fuel combustion may occur and spread; acid rains and sand storms are occurring more frequently than in the past; human health problems, such as lung disease, are reported in higher rates than ever before in the most affected areas (Rockwell, 1998). In addition, human's concentrated use of nonrenewable fossil fuels has evoked the specter of the fossil energy exhaustion. If human beings continue the current rate of consumption, the energy supply system to meet the needs of the world economy over the next 25 years may fail (IEA, 2012). According to BP Review (2011), in 2011 known natural gas reserves are sufficient for production for about 63 years at current rate; the known oil reserves can meet demand for 40 years at current rate; coal as the most abundant fossil fuel with known reserves estimated to meet demand for 155 years at current production rates. Unfortunately, human consumption of carbon fuels is not at a fixed rate but accelerating as developing countries aspire for a higher level of economic security and the developed countries expect to maintain their leading level of prosperity.

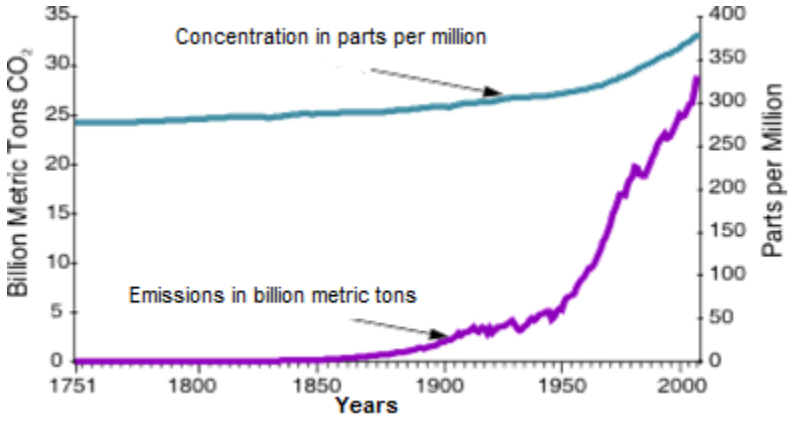

Figure 1.2 Carbon Dioxide Emissions and Carbon Dioxide Concentrations during 1751-2004 (Original Source: Oak Ridge National Laboratory, Carbon Dioxide Information Analysis Center) (EIA, 2010)

The current trends in fossil energy consumption are neither secure nor sustainable. A study by Aitken,

Billman and Bull (2004) found that, if assuming a modest one percent growth of world energy demand, to stabilize the atmospheric concentration of carbon dioxide within the safe range of 550-750 ppm, the world would have to adopt a zero-emission energy source for total primary energy at a pace roughly equal to 10 percent by 2010, 20 percent by 2020, and 50 percent by 2050. Therefore, human societies are facing a pressing demand to start the transition toward a carbon independent growth path, involving new energy sources and technologies.

Wind and solar energy, as the most clean, abundant, accessible, and affordable renewable energy resources, can play important roles in the transition to a carbon-neutral path. It is estimated that in the US, the developable wind resources in the top 12 states with high wind energy potential (this excludes offshore wind energy) can have a total output equivalent to over twice of the total electricity generation of the US in 2004 (OWPI, 2007); the total electricity demand (418GW in 2002) could be satisfied by covering a land surface of 180 square km with photovoltaic. This size represents 0.35 percent of the total land area and roughly corresponds to the surface covered by roads in the country (Sims, 2004). For the past decade, wind and solar power have been the fastest growing energy resources for world electricity generation. According to IEA (2012), the world wind capacity had an average annual growth of 25 percent from 2007-2011, and solar PV had average annual growth of over 50 percent.

1.3.3.2 Distributed Power Generation and Distributive Energy Resources

According to Wang and Nehrir (2005), in recent years in the U.S., with the power deregulation and utility restructuring, plus the shortage of transmission line capacities and increasing environmental concerns, more emphasis has been put on the use of distributed power generation (referred to as DPG). DPG is also called on-site generation or dispersed generation. It contains scattered power generation from many small energy sources and usually near the end use of electricity. DPG systems could either be connected to grid or stand-alone. DPG systems might be integrated in current power systems for grid reinforcement. They would be helpful in “reducing power losses and on-peak

operating costs, improving voltage profiles and load factors, deferring or eliminating the need for system upgrades, and improving system integrity, reliability and efficiency" (Wang and Nehrir, 2005, p.2068). The sizes of DPG systems are usually relatively small and in modules.

Most traditional power generation consist of large centralized facilities, using fossil fuels (coal, oil or natural gas), and nuclear or hydropower plants, which is good based on economies of scale, but usually transmit electricity over long distances, which may affect the environment. With the advancement in technology, combustion turbines, combined cycle turbine, and other co-generation units using diesel or natural gas have become first-generation distributive power systems. Now with perpetuated concerns on environment and eco-systems, distributed power generation using more distributive and renewable energy resources is gaining favor. New DPG systems have expanded to include low-head hydro, photovoltaic, solar thermal storage units, wind, fuel cell, ocean thermal gradient, tidal power, geothermal, trash burning and biomass. There is a great potential that in the near future, the multi-sourced and multi-layered DPG systems depending less on fossil fuels but more on distributive renewable resources will become more economically and technologically feasible for new electric generation strategy.

1.3.3.3 Wind and Solar Energy as Ideal Distributed Power Generation Resources

Wind and solar radiation, because of their widely distributed nature, are especially suitable for DPG systems. No place on the earth's surface exists without exposure to wind flow and solar radiation, no matter how varied their strengths are from place to place and time to time. No other renewable energy resources are so widely accessible as wind and insolation. The complementarity between wind and insolation may even make them better choices for DPG because better power management and reliability can be achieved with this nature (Wang and Nehrir, 2005). It is believed that the better the complementarities between the two at a location, the more effective coordination, reliability, and efficiency in an integrated system which uses both resources can be expected (Macken, Bollen, and Belmans, 2004). In some cases, the features of geographically unbalanced distribution and temporal

intermittency of wind and solar radiation could be beneficial features for geographically distributed DPG systems, considering the spatial and temporal complementarities of these resources (McPherson et al., 2007). In the future, distributive energy generation infrastructure using plural-sources of alternative energies, both the coordinating feature of wind and solar energy in time and in space could be useful, helping to provide power close to end users with a varied load demand in time and space also. In the long run, hybrid or multi-layer renewable energy systems using multiple renewable resources including wind and solar power may become a major component in the sustainable electrification strategy (Ramakumar, 2001). To design DPG systems meeting specific regions' needs which mainly depend on various local renewable energy resources such as wind and solar power, the assessment of the ***CWS*** level, plus an end-use energy demand analysis for each location will help to better estimate the gap between the total of local end-use demand and the total of local wind and solar supply over time (Felder, 2004).

It is hoped that this dissertation would help to improve knowledge about the spatial variability of both wind and solar power and the spatial features of their complementary relations. In addition, results from this study might also be helpful in understanding the influences of geographic factors on the complementary nature. With some modification to models generated in this study, it might even be possible to estimate the complementarity level of wind and solar energy for places without detailed wind and solar data, but with available geographic information.

CHAPTER II

LITERATURE REVIEW

The complementary nature between wind and solar radiation (***CWS***) has been informally observed at different places for a long time. However, there have been very few studies directly targeting the complementary nature of wind and solar energy. One of the earliest explorations on this topic was done by Takle and Shaw (1979). Their article called the "complimentary nature of wind and solar energy at a continental mid-latitude station" examined the combined renewable energy resources of solar and wind year-round in one Iowa location (Takle and Shaw, 1979). Some more recent studies, motivated by the prospect of deploying hybrid renewable energy systems using both wind and solar resources, also investigated the complementarity between wind and solar sources. At the same time, many studies have indirectly revealed the existence of the nature of complementarity. However, how to measure the level of ***CWS*** at a specific site, how to assess the spatial and temporal variations of ***CWS***, and how to explain the influences of geographic factors on the spatial variations of the ***CWS*** have been little studied and are the focus of the present study.

In this chapter, past studies related with the ***CWS*** are reviewed. A summary of literatures related with studies of the complementary features in other disciplines is also included considering that complementarity is a general but complicated phenomenon in many fields, and the concepts and methodologies from other fields might be used for this study. Studies attempting to explain the

influences of geographic factors on either wind or solar resources are also examined in this chapter. Since spatial analysis methodology is used to explore the relationship of the ***CWS*** and geographic factors in this study, a review of applicable quantitative geographic methods is also presented.

2.1 Some Direct Studies on the Complementary Nature of Wind and Solar Energy

There are three studies directly targeting on the complementary nature of wind and solar energy introduced in this part. One studied the ***CWS*** in a located in Iowa, one is based on data obtained in a Japanese site, and another one explored the complementary nature in a Saudi Arabian station.

2.1.1 Complementary Nature of Wind and Solar Energy at Stations of Iowa

In 1977, Tackle and Shaw studied the complementarity between wind and solar energy based on observed wind data during July 1 of 1959 to June 30 of 1970 for the site of Des Moines and the solar radiation data for Ames, Iowa. They first created the annual cycle solar radiation curve based on averaged daily solar radiation data (Figure 2.1.). To define a smoothly varying curve of solar energy in annual cycle, a sinusoidal function for calculating estimated daily average solar radiation using a Fourier transform was generated. The formula is as:

$$Es(d) = 3.9278 - 0.8578\sin(2\pi t/365) + 1.9956\cos(2\pi t/365) + 0.2034\sin(4\pi t/365) + 0.1474\cos(4\pi t/365) \quad \text{(Takle and Shaw, 1979; } \textit{Equ}\text{. 2.1)}$$

where Es(d) is the estimated solar radiation in units of KWH/M^2 for day number d of the year, and t = d - Mar 1 (Takle and Shaw, 1979). Figure 2.1 shows the actual data and smoothed trend of data generated using the raw data of the Ames station, which was used to represent the solar radiation at station of Des Moines.

For wind energy, they extrapolated the 10m hourly wind speed data to 32m and then calculated the hourly wind power. The 24 hour daily total potential wind power density was a sum of hourly wind power. One analytical expression similar to that for solar energy was also generated. It is:

$$Ew(d) = 5.9736 + 2.7960\sin(2\pi t/365) + 0.1720\cos(2\pi t/365) + 0.1052\sin(4\pi t/365) + 1.2332\cos(4\pi t/365)$$ (Takle and Shaw, 1979; *Equ*. 2.2)

where d is day of the year, t = d-Mar 1 and Ew (d) is the estimated daily wind power density in KWH/M^2 (Takle and Shaw, 1979). The actual and smoothed wind curve created based on actual data for Des Moines station is shown in Figure 2.2.

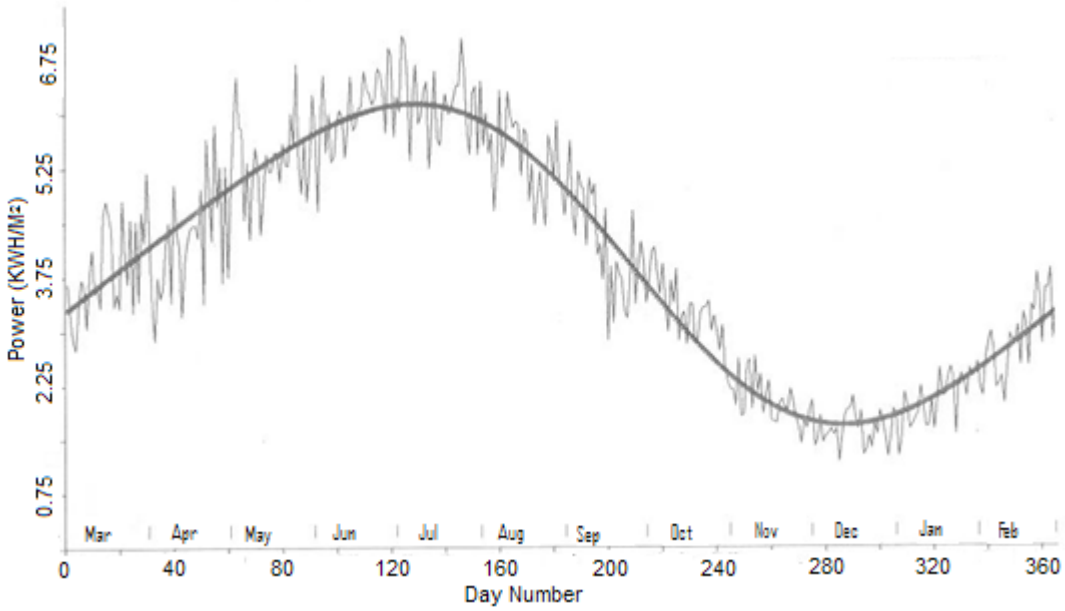

Figure 2.1 Annual Cycle of Solar Energy at Ames over the Period of 7/1/1959-6/30/1970 (Source: Takle and Shaw, 1979; axis relabeled to improve clarity)

Figure 2.3 shows the combined solar-wind energy graph for the annual cycle of the Des Moines station based on the two analytical expressions derived.

To further analyze the complementary nature between wind and solar energy, the authors examined the day-by-day relationships of the two energy forms in annual, summer, and winter periods. They compared the actual solar and wind potential with the expected solar and wind energy calculated from the derived analytical expression by decomposing the actual amount into two parts:

$$S(d) = \hat{S}(d) + S'(d)$$ (Takle and Shaw, 1979; *Equ*. 2.3)

where S(d) is the actual daily total solar energy, $\hat{S}(d)$ is the estimated one calculated from *Equ. 2.1*, S'(d) is the amount the actual daily total deviated from $\hat{S}(d)$ (Takle and Shaw, 1979);

$$W(d) = \hat{W}(d) + W'(d)$$ (Takle and Shaw, 1979; *Equ*. 2.4)

where W(d) is the actual daily wind potential measured, $\hat{W}(d)$ is the estimated amount from *equ. 2.2*, and W'(d) is the amount the actual daily wind potential deviated from $\hat{W}(d)$ (Takle and Shaw, 1979).

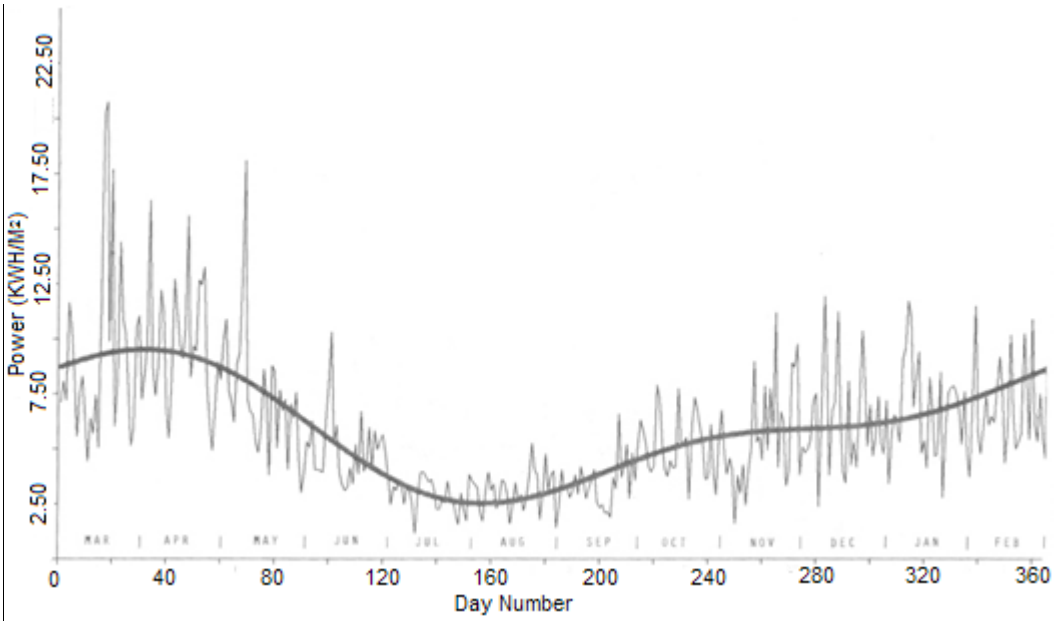

Figure 2.2 Annual Cycles of Daily Wind Energy Totals at Des Moines
(Source: Takle and Shaw, 1979; axis relabeled to improve clarity)

Complementarity was evaluated through the calculated product W'S' for each day. According to the authors (1979), the product was positive if wind and solar energy were both higher than the expected value of the day or both lower than expected values; if one was higher, the other was lower, the product was negative and compensation occurred. Table 2.1 shows their summarized results by month based on calculations for a total of 2922 days during the period of July 1 1959 to June 30 1970.

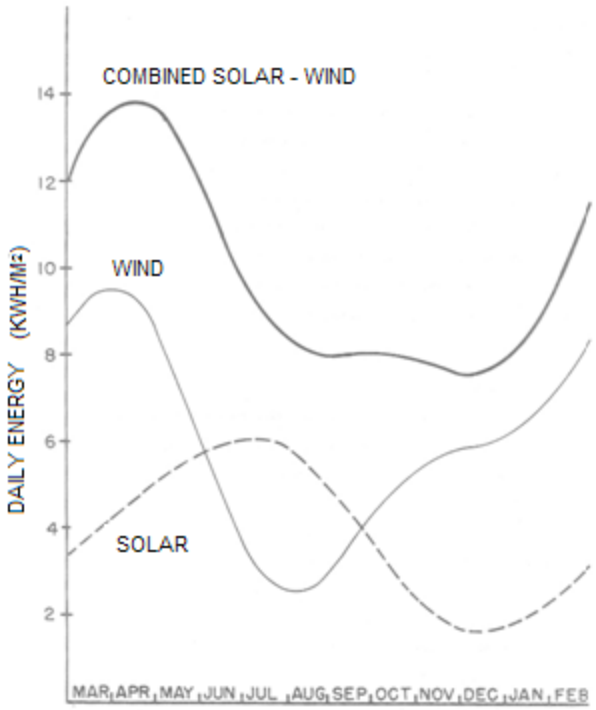

Figure 2.3 Expected Seasonal Cycle of Solar and Wind Energy and Combined Total
(Takle and Shaw, 1979; relabeled to improve clarity)

Month	*S'*>0, % Days	*W'*>0, Ave. *S'W'*	*S'*>0, % Days	*W'*<0 Ave. *S'W'*	*S'*<0, %Days	*W'*>0 Ave. *S'W'*	*S'*<0, %Days	*W'*<0 Ave. *S'W'*	All *S'W'* Ave. *S'W'*
Mar	18	8.70	43	-7.61	18	-19.24	21	8.76	-3.28
Apr	18	13.82	30	-10.74	19	-27.31	33	9.88	-2.68
May	21	10.98	34	-9.11	15	-14.59	30	8.49	-0.57
Jun	22	4.78	39	-3.98	18	-10.80	22	5.94	-1.02
Jul	25	2.23	37	-2.28	19	-4.25	20	3.36	-0.43
Aug	23	3.03	35	-2.00	20	-6.53	22	2.80	-0.71
Sep	20	2.72	37	-3.56	15	-5.84	28	3.67	-0.64
Oct	23	5.39	45	-3.65	13	-9.45	19	4.07	-0.92
Nov	18	4.85	35	-3.01	15	-5.75	32	3.58	+0.03
Dec	20	3.25	31	-2.54	22	-5.72	27	2.95	-0.64
Jan	17	4.12	37	-2.24	19	-6.87	28	4.12	-0.26
Feb	18	7.56	41	-5.13	15	-6.45	27	6.13	-0.01
Annual	20	5.74	37	-4.60	17	-10.19	26	5.46	-0.93

Table 2.1 Occurrences and Magnitudes of the Products S'W' of Solar and Wind
(Takle and Shaw, 1979)

According to the report and article published by Takle and Shaw (1979), there are several important findings in their study:

(1) There is an overall mild tendency of wind and solar energy to complement each other on an annual basis in the studied locations;

(2) During the months of June through February, wind and solar energy complement each other in a way that the higher one raises the lower one and makes it stable for the combined of the two resources. However, in March and April, solar energy typically reaches its minimum when wind energy is at its seasonal peak; in the summer months of July and August there is a tendency for both energy types to rise and fall in concert instead of being complementary;

(3) The observed diurnal variation of wind and solar suggests complementary behavior in daily cycle, though not highly significant, and weaker than as shown in annual cycle;

(4) The fluctuating range of wind power density is larger than the range for solar power density;

(5) Distributions of daily wind energy totals for all seasons are unimodal, but the distributions of daily solar energy is bimodal in winter seasons;

(6) Solar radiation data are weakly dependent on distance, but wind speed measurements are highly site-specific and vary markedly over short distance in space;

(7) Cloudy weather and low pressure systems are believed to be associated with each other and cause higher wind speeds than high pressure systems under clear or less cloudy weather;

(8) Statistical analysis shows the monthly average maximum temperature is positively correlated with monthly average wind speed;

(9) The authors believed, based on their experience, the predictability of daily amount of wind and solar energy from climatological data is highly tenuous.

The study conducted by Takle and Shaw (1979) over thirty years ago is quite enlightening to further exploration of the complementary nature of wind and solar energy. The statistical methods

they used combined with decomposing input data into annual, seasonal, weekly, bi-weekly, diurnal periods helped them to examine the compensation feature between two energy forms in a more detailed way. Their association of wind and solar resources with climatological factors like temperature, pressure, and cloudiness to explain the complementary behavior of the two resources is developmental. However, only one site in Iowa was investigated. As the authors realized, wind energy can be very site specific though solar radiation is less spatially sensitive and the complementarity of wind and solar might vary from place to place. In addition, in assessing the wind and solar resources, the analytical expressions generated by the authors are only applicable for their studied site, which limited the applicability of their findings. Besides, when the authors tried to explain the cause of the complementary nature, no other geographic factors except climatologic conditions were considered, even though they realized climatological variables only explain partial variations of both resources. With the help of the stronger computation capacity today, this dissertation study attempts to expand their effort to study ***CWS*** by trying a different approach, covering more sites and including more geographic factors.

2.1.2 Demonstrative Study of the Wind and Solar Hybrid Power System

In March of 1995, to explore the complementary relationship between wind and solar energy, researchers Kimura, Onai, and Ushiyama (1996) installed a small scale of wind and solar hybrid system in Ashikaga, Japan. They obtained actual power output data from both wind and solar energy systems at the same site. The nine-month data they acquired confirmed there is complementarity between wind and solar energy.

As shown in Figure 2.4, solar energy in summer season is greater while wind energy is greater in winter at the site (Kimura, Onai, and Ushiyama, 1996). Figure 2.5 and Figure 2.6, indicating the daily wind and solar output in May 22 of 1995 and December 30 of 1995 respectively, demonstrate the existence of complementarity between wind and solar energy in diurnal cycle.

This demonstration provided a simple but solid proof of the existence of complementarity of wind and solar energy at one site through the actual power output of an installed hybrid system. However, considering the factor of cost, studies like this might not be feasible at other sites. To better estimate and assess the complementarity of wind and solar energy for different locations requires other approaches such as using secondary data and modeling. This is one of the major goals of the present dissertation study - to explore an approach applicable to any site for estimating the ***CWS*** level.

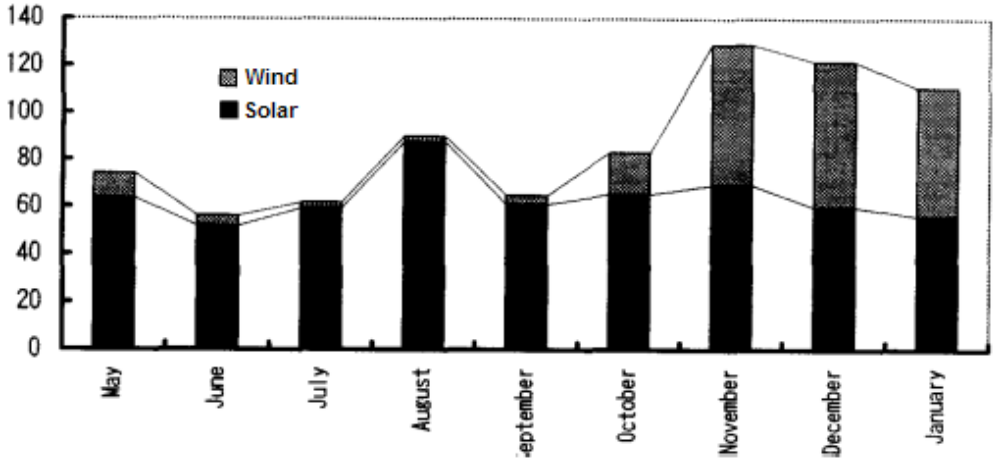

Figure 2.4 Cumulative Output of Hybrid WTG and PV Cell
(Kimura, Onai, and Ushiyama, 1996)

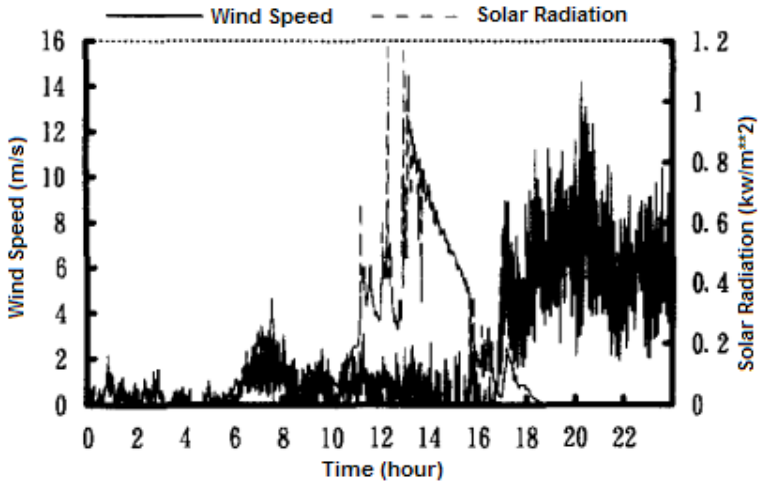

Figure 2.5 Wind Speed and Solar Radiation in May 22 of 1995
(Kimura, Onai, and Ushiyama, 1996)

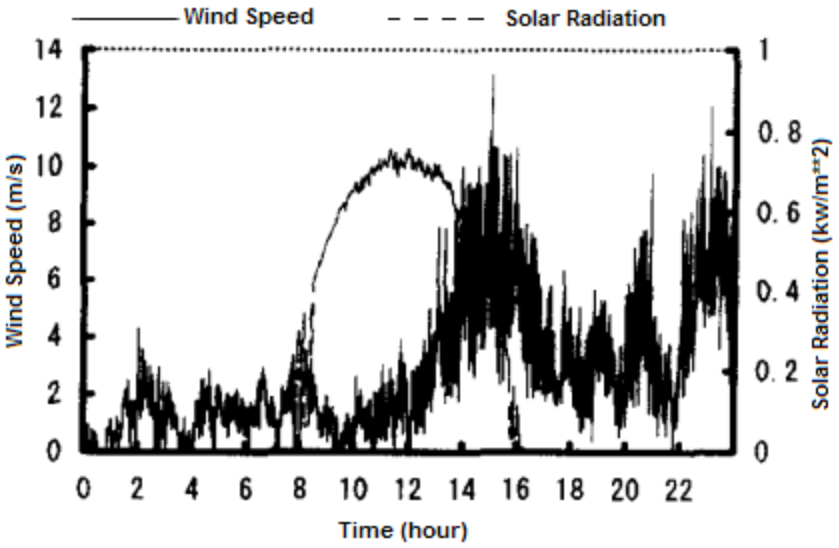

Figure 2.6 Wind Speed and Solar Radiation in December 30 of 1995
(Kimura, Onai, and Ushiyama, 1996)

2.1.3 Applicability of Wind-Solar Hybrid Power Systems in Northeastern Saudi Arabia

Sahin (2000) studied the complementary nature of wind and solar power and the economically optimal configuration of the hybrid systems using wind and solar at one site on the shoreline of the Arabian Gulf in northeastern Saudi Arabia. The site is located in a semi-desert area in Northeastern Arabian Peninsula, with low pressure, high temperature and frequent wind storms (Sahin, 2000). One-minute data were collected during the year of 1995 at a height of 2m for solar radiation and at 10m for wind speed data (Sahin, 2000).

The approach the author used to evaluate the complementary nature was to calculate the correlation $\boldsymbol{\rho_{s,w}}$ between the solar and wind power availability using the formula as following:

$$\rho_{s,w} = \mathrm{Cov}\,(W_s,\ W_w) \,/\, \tau_s\, \tau_w \qquad \textit{(Sahin, 2000; Equ. 2.5)}$$

Where *Ws* and *Ww* are solar and wind power density in watt/m^2. The covariance is:

$$\mathrm{Cov}\,(W_s\ ,\ W_w) = \left(\frac{1}{n}\right) \sum_i^n [\ (W_s\ )_i\ -\ \overline{W_s}\ ]\ [(W_w\ )_i\ -\ \overline{W_w}] \qquad \textit{(Sahin, 2000; Equ. 2.6)}$$

and the standard deviation is:

$$\tau_s = \{\left(\frac{1}{n}\right) \sum_{i=1}^{n}[\,(W_s)_i - \overline{W_s}]^2\}^{1/2} \text{ and } \tau_w = \{\left(\frac{1}{n}\right) \sum_{i=1}^{n}[(W_w)_i - \overline{W_w}]^2\}^{1/2}$$

(Sahin, 2000; *Equ. 2.7)*

The calculated correlation values ranged from -1 to +1 with -1 representing the highest complementarity and +1 indicating no complementarity between wind and solar potential.

The daily average solar and wind power density for the site is shown in Figure 2.7, in which the daily average solar power shows a great consistency while the wind potential is scattered in a larger range (Sahin, 2000). The monthly average of solar, wind, and total power potential obtained are displayed in Figure 2.8, indicating a clear complementary tendency of wind and solar energy at the site. The calculated correlation value between daily wind and solar power amount was -0.75.

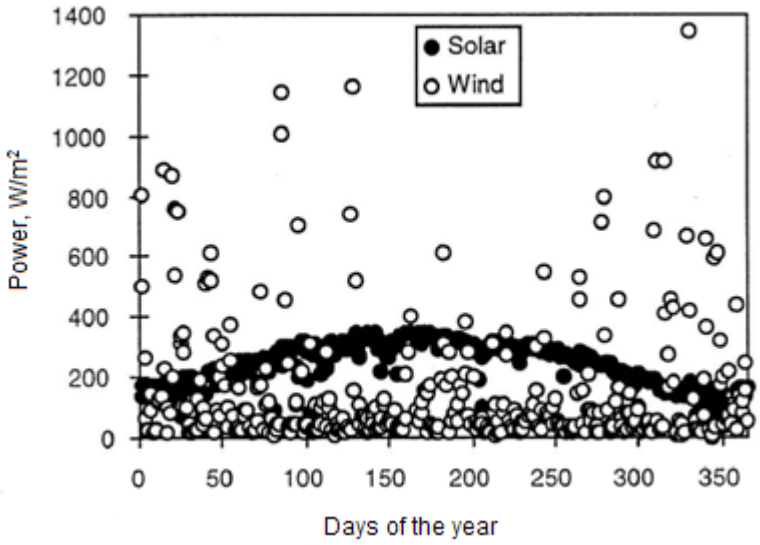

Figure 2.7 Daily Averages of Solar and Wind Power through the Year
(Sahin, 2000)

The study conducted by Sahin provided a statistical approach to assess the complementarity of wind and solar energy using Pearson's *r*, which is based on normal distributive assumptions of data. However, because of the prominent fluctuation characteristics of wind power, the

assumption of a normal distribution is tenuous. The present dissertation study attempts a different approach to quantify the complementarity unlimited by the normal assumption.

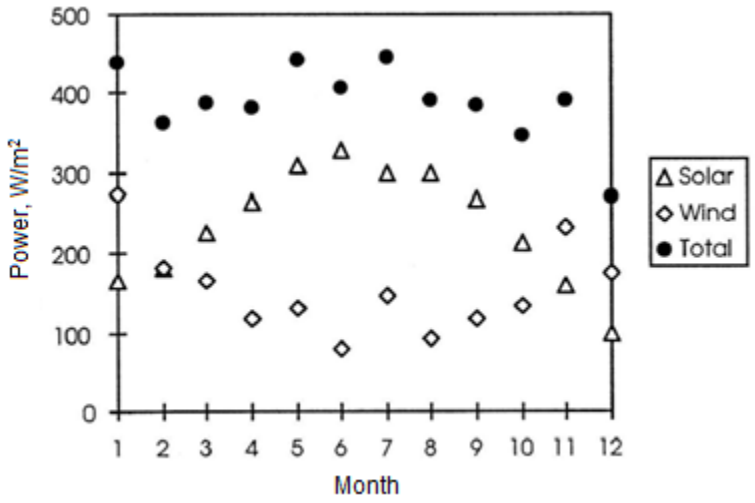

Figure 2.8 Monthly Averages of Solar and Wind Power through the Year (Sahin, 2000)

2.2 Studies Indirectly Revealing Existence of Complementarity of Wind and Solar Energy

Although in the past there has not been much research focused on studying the complementary nature between wind and solar energy, the complementary nature has been assumed in side discussions of many studies. In the work examined below, complementarities between wind and solar radiation are mostly indicated by empirical data on which the researchers based their studies, even though the complementary nature itself was not intended as their research subject. Locations in these studies ranged from Pennsylvania to Oklahoma City, to Inner Mongolia, to a small island near Hong Kong, which also suggests that the complementarity between wind and solar energy is a global phenomenon.

In a study regarding regional end-use energy strategy, Felder (2004) used the cases from Centre Country of Pennsylvania and further advanced an alternative strategy to match regional end-use energy demand with regional renewable energy resources. Her study found that over the annual cycle, a big portion of end-use energy demand can be satisfied through a combination of local

wind, solar, super-insulated housing, and hydropower. In the two case studies conducted in one county of Pennsylvania, she compared the total energy demand of end-users with total supplies of selected renewable energy resources in these two places. A gap between the demand and supply, either in surplus or shortage, is shown for both places (see Figures 2.9 and 2.10).

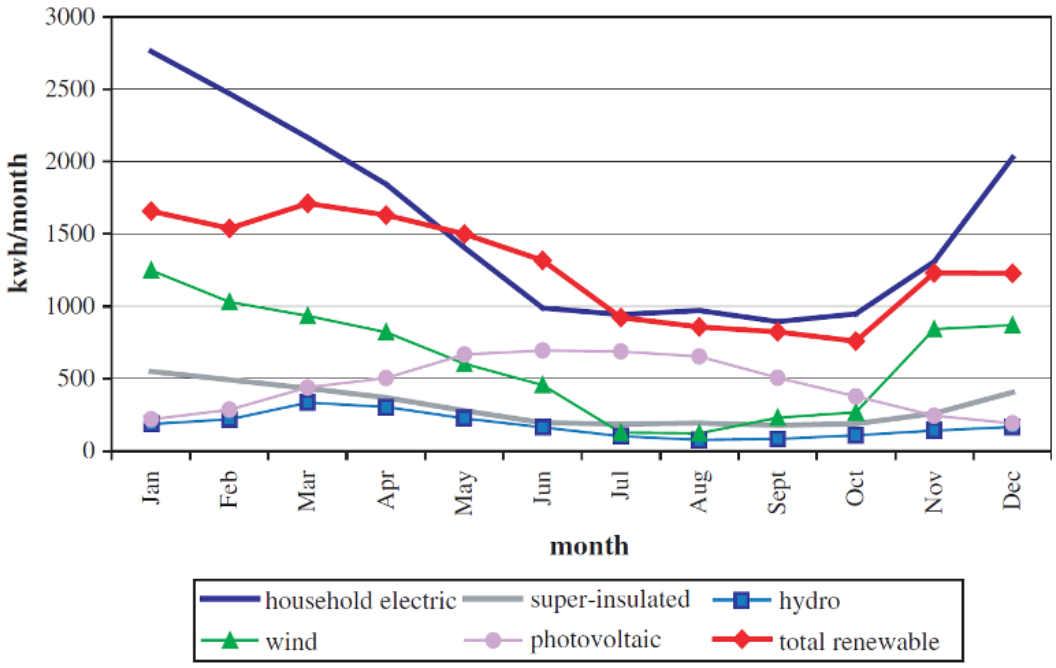

Figure 2.9 Average Monthly Household Electric Demand and Potential Renewable Resources at Laurel Run, PA (Felder, 2004)

Though Felder's study focused on relating the end use demand with local renewable energy supply, it provides a proof of the existence of complementarities between wind and solar power in the site she studied through both the basic data used and the graphs generated.

The schematic chart shown in Figure 2.11 extracted from an early study about wind resources in Oklahoma City (OSU Report, 1962) provided more proof of the assumed complementary nature of wind and solar energy. This theoretical chart is one of the earliest attempts found revealing the complementarities between the wind and solar energy within annual cycle.

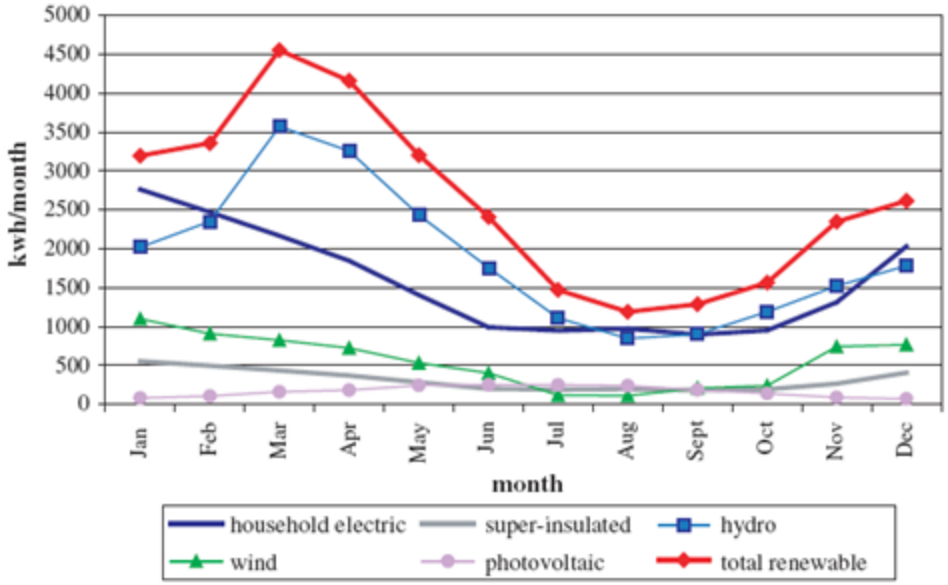

Figure 2.10 Average Monthly Household Electric Demand and Potential Renewable Resources at Elk Creek, PA (Felder, 2004)

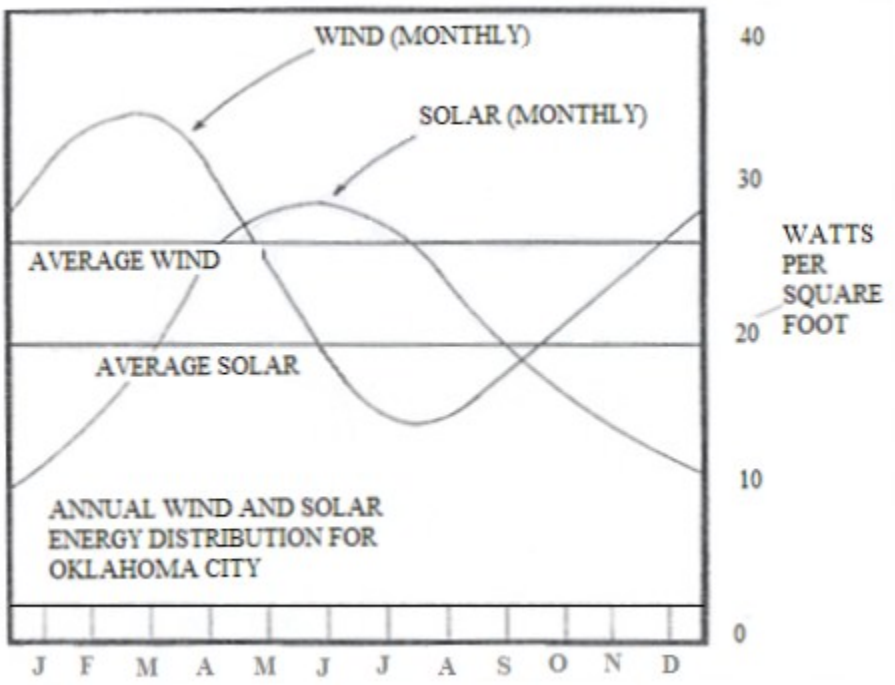

Figure 2.11 Annual Wind and Solar Energy Distribution for Oklahoma City (From Original: OSU Report, 1962)

In an investigation of sizing the wind/photovoltaic hybrids for households in Inner Mongolia, Barley, Lew, and Flowers (1997) compared two scenarios of balancing the unmet load and the cost of wind/photovoltaic hybrids systems in Inner Mogolia of China. They proved that "combinations of wind and PV are more cost-effective than using either one alone", and that from an economic view, "the relative amount of PV in the design shall increase as the acceptable unmet load decreases and as the average wind speed decreases" (Barley, Lew and Flowers, 1997). Figure 2.12 shows the seasonal profiles based on the resource assessment of wind and solar power and the load in the studied area with a wind system hub height of about 6 meters. It shows some seasonal complementarities between wind and solar power even though the estimated wind output is much lower than solar because of the generator system used.

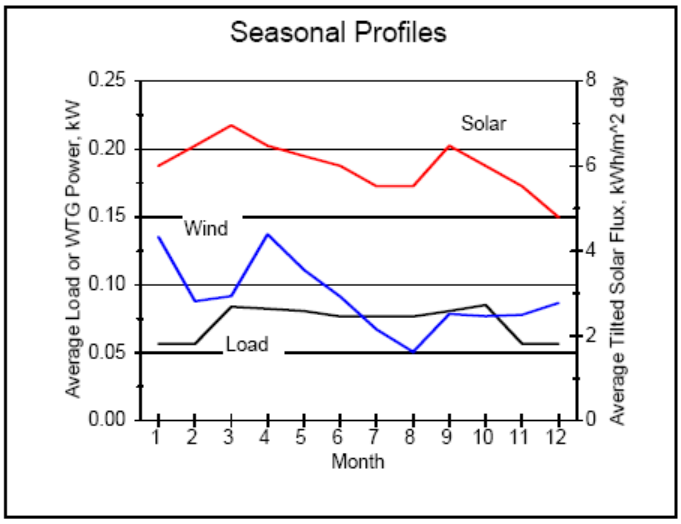

Figure 2.12 Seasonal Profiles of the Load, Wind Power and Solar Power in Jurh, Inner Mongolia (Barley, Lew and Flowers, 1997)

According to the authors, by taking advantage of the complementarities between wind and solar power, it is possible to trade between some solar photovoltaic power with cheaper wind power. They also suggest that more effectiveness can be achieved and cost could be saved for people in remote areas when proper hybrid systems were chosen to fit their seasonal profiles. Less excess energy will be produced if properly-sized hybrids systems are installed (Barley, Lew and

Flowers, 1997). Since the focus of their study was about sizing the hybrid system fitting local wind and solar profiles, the detailed features and causes of complementary nature and the geographic factors behind the complementarities were not studied further.

In a study called "computer-aided design of PV/wind hybrid system" by Ai et al. (2003), the researchers developed a set of match calculation programs for optimum sizing of PV/wind hybrid system. Using this program, the optimum configuration which can meet the energy demand with the minimum cost can be found. The authors applied the programs to Wagland Island, southeast of Hong Kong, where hourly measured meteorological data of wind and solar radiation and load data are available. In this study, the seasonal complementary tendency between wind and solar radiation are evident. Again, their study provided no further analysis of the complementary nature.

2.3 Geographic Factors Related with Wind and Solar Resources

The potentials of wind and solar resources are highly site specific and region based in addition to changing with time. Though there are few studies devoted to studying the relationship of complementarity and geographic factors, there have been many studies exploring the spatial characteristics behind the variation of wind or solar resources by linking them with various geographic factors. In this dissertation, geographic factors refer to all location related factors, such as longitude and latitude, elevation, geomorphology, climate, bio-system coverage, and human activities. Considering time is a special form of space and a result of the relative solar-earth movement, the association of various geographic factors with the temporal and spatial variation of the wind or solar resources and with their complementarity is defendable. In section 2.3, a review of a few past studies involving discussions of relations of geographic factors with either wind or solar resources is presented.

2.3.1 Wind and Geography

Wind is defined as the movement of air. It is a special climatologic phenomenon caused by the heat and pressure gradient of the atmosphere (NEED, 2011). As a result, heat and moisture are redistributed through the wind over the atmosphere and the earth surface. The rotation of earth itself and the friction from the earth's surface usually alter the strength and direction of the wind during its path. Therefore, both the absolute location of a place on the earth's surface, and the relative terrain forms of a location, contribute to determination of the average wind resources and wind resource class of a location. The National Renewable Energy Laboratory-NREL (OWPI, 2007) has classified the wind power potentials of different places into 7 different classes based on the average wind power density estimated (see Table 2.2).

Power Class	Wind Power	Wind Speed*
1	<200	<5.6
2	200-300	5.6-6.4
3	300-400	6.4-7.0
4	400-500	7.0-7.5
5	500-600	7.5-8.0
6	600-800	8.0-8.8
7	>800	>8.8

Table 2.2 Classes of Wind Resources (OWPI, 2007)
(*Equivalent wind speed at sea level for a Rayleigh Distribution)

Most places around the world have been assessed and classified of their potential wind resources and presented with wind resource maps ranging in local, regional, and global scales. During various assessments of wind potential, models were developed and geographic variables were the core factors considered, especially for studies requiring accurate assessment of local and micro-site wind resources.

In assessing wind power of Oklahoma, Oklahoma Wind Power Initiative project team (OWPI) tried two different approaches, WindMap and Neural Network model. In both models, geographic

factors such as vegetation roughness, elevation, terrain, and weather patterns were weighted to obtain estimations of wind resources at height of 10 meters and 50 meters respectively. In the WindMap model, a horizon resolution of 372 by 372 meter grid cell is used (OWPI, 2007). The ground measurement of wind speeds at Mesonet stations, distance from the chosen stations, elevation variation around stations, and surface roughness calculated from satellite-derived vegetation types were input into commercial WindMap software to extrapolate wind power density for large grid cells. The WindMap approach is based on a mass-conserving model for predicting and mapping the wind over an area (OWPI, 2007). In the neural model developed by OWPI, for each chosen Mesonet station, besides the calculated wind power density, geographic information such as elevation, terrain exposure, and roughness length were also obtained. The terrain exposure is referred to as "relative elevation", defined as the distance a point sits above or below the average elevation of a surrounding area (OWPI, 2007). The roughness length is defined as a height above ground below which friction from obstacles effectively stifles air currents and at which the neutral wind profile extrapolates to zero (OWPI, 2007). In the neural net model, 10-meter height wind power density values were empirically related to elevation, terrain exposures (north and south), and roughness-length averages (north and south) at sample Mesonet stations. The model created several possible nonlinear formulas based on historical data. Then each formula was applied to predict values of wind power density for control Mesonet stations. The formula with the least root-mean-square error was chosen as the formula applicable to the whole state of Oklahoma (OWPI, 2007).

In 2002, consultants from TrueWind Solution were assigned the task of developing a more accurate and reliable wind resource map for California. They used both the Mesoscale Atmospheric Simulation System and the simpler WindMap models (CECCR, 2002). According to their “California Energy Commission Consultant Report” (2002), the blocking and channeling effects of mountains, effects of tree heights and density, and impact of complex terrain to

atmospheric circulation, plus mountain impacts to vertical and horizontal wind profiles and nocturnal boundary layers in desert areas, are some geographic factors considered significant for California.

In a study titled "Geographic Information Systems in Support of Wind Energy Activities at NREL's WARM model" (Heimiller and Haymes, 2001), scientists from the National Renewable Energy Laboratory, developed the automated GIS Wind Resource Assessment Model (WRAM). It allowed consistent application of analytical techniques in a regional scale and detailed analysis of wind resources performed. It produced high-quality maps easily distributed to clients (Heimiller and Haymes, 2001). According to the scientists, wind resource potential is strongly influenced by "the exposure and the orientation of the terrain relative to the prevailing wind direction" (Heimiller and Haymes, 2001). The topography may boost or reduce the wind resource (Heimiller and Haymes, 2001). The WRAM model was designed to be applicable to different regions and different terrain characters including inland, ocean and lake coastal areas. The inputs for WRAM model included a 1-km^2 Digital Elevation Map (DEM), and three types' meteorological inputs: wind power roses, vertical profiles of wind power, and where appropriate, open ocean wind power. The final wind power density was produced based on adjusting the base wind power density value for a particular grid cell to the factors like terrain blocking, relative and absolute elevation, aspects, distance from ocean or lake coastlines, and small-scale wind flow patterns such as local sea breezes (Heimiller and Haymes, 2001). The adjustment formula used for each grid is:

Wind Power Density = (base wind power density) times (terrain blocking factors) * (aspect factors) *(distance from coastline factors) * (relative elevation factors) * (small-scale wind-flow pattern factors). (Heimiller and Haymes, 2001; *Equ. 2.9)*

The WRAM model for calculating wind power density values is especially useful to areas with low roughness, such as grasslands (Heimiller and Haymes, 2001).

In the study of matching local end user demand with local renewable resources, Felder (2004) found climate and topographic variables are the most important factors influencing wind power. Her findings are consistent with one DOE report (US Department of Energy/NREL, 2011), which pointed out that the highest average wind speeds are generally shown along seacoasts, ridgelines, hilltops, and on the Great Plains. Felder (2004) also linked wind speed with the factors like orientation, shape, and slope of a ridge.

2.3.2 Insolation and Geography

According to Felder (2004), in the case of solar radiation, the latitude, topography, atmospheric conditions, orientation of sites, and shading conditions are micro-geographic factors that influence the amount of radiation one site receives. Areas with high cloud cover, pollution, smog, dust or shadow will obstruct solar access, while areas with more reflective surfaces such as lakes could have more solar intensity. Sun-facing slopes receive more solar radiation than other places (Felder, 2004).

Dubayah and Rich (1996) derived a specific solar radiation formula based on their study of applying GIS-based modeling. It was recognized by the authors that topographic factors, such as elevation, slope, aspect, and shadowing have great effects on solar radiation (Dubayah and Rich, 1996). They used geographic factors in a quantitative and systematic way by incorporating them into their modeling environment. Topographic factors like slope and canopy effects were also included in their model to obtain the final radiation data.

In another study of a GIS-based assessment of solar radiation conducted by the European Commission Joint Research Center (ECJRC, 2006), a set of models, publications, databases, and reports was published. The project explored how solar radiation interacts with the earth. According to the report, there are three groups of factors influencing the insolation on a location of the earth surface. The first group is the earth's geometry, revolution and rotation (which decide

declination), latitude, and solar hour angle. The second group is terrain factors such as elevation, surface inclination, orientation, and shadows. The third group is atmospheric attenuation, such as scattering, absorption by gases (air molecules, ozone, CO_2 and O_2), solid and liquid particles (aerosols, including non-condensed water), and clouds (condensed water) (ECJRC, 2006). Because the three group factors vary with time and location, solar radiation varies spatially and temporally.

In summary, most studies recognized the influences of geographic factors like topographic variables, climatic condition, and relative location on insolation. But how and to what extent each factor could affect the density of insolation at a site may be researched further.

2.4 Complementarity Related Studies Conducted in Other Fields

The concept of complementarity in general could have many implications and has been defined by a variety of disciplines from different angles. Since the world is comprised of complementary components and phenomena, the concept of complementarity has been used to define the structures and substructures of the world. The common point behind various kinds of complementarities is: there exist different components and each can be integrated into one system based on both their generality and otherness (AHDEL, 2007). Within the integrated systems, they functionally coordinate with each other and contribute to the performance of the whole system from each part (AHDEL, 2007).

To some extent, it is the complementarities in the world that provide the "necessary poles for dialectic process" (AHDEL, 2007). As a concept, complementarity either defines a relation between two opposite states or principles that together exhaust the possibilities, or defines the interrelation of reciprocity whereby one thing supplements or depends on the other (AHDEL, 2007). However, different fields have expanded the coherence of complementarity in differently. For the complementary nature of wind and solar radiation, the latter definition seems a better fit.

2.4.1. Definitions of Complementarity

The notion of complementarity was first used in economics by Edgeworth (1925). According to Edgeworth (1925), "two activities or properties are defined as complements if doing more of one thing increases the returns to doing (more of) the other". Mathematically, complementarity is also expressed in supermodularity f(x,y), which implies that the same direction of change in f(x,y) can be caused either when any component of $\boldsymbol{x}$ is increased or is non-decreasing in the other components of **y** (Kim, 2003). Therefore, the supermodularity of a function corresponds with complementarity among its arguments (Kim, 2003).

In different disciplines, depending on the specific research topic, complementarity is usually given a specialized definition. In physics, it usually refers to the particle-wave duality in the basic principle of quantum theory (Englert, Scully, and Walther, 1994; Bohr, 1999). In molecular biology, it could refer to the property of double-stranded nucleic acid such as DNA:RNA duplex (IHGSC, 2004). In social psychology, it implies the idea that people seek others with characteristics that are different from and complement their own attractiveness (Bluhm, Widiger, and Miele, 1990). In economics, complementarity means higher values in any variables increase the marginal returns to higher values in the remaining variables; a complement or complementary good is defined as good that should be consumed with another good and its cross elasticity of demand is negative (Kim, 2003). In management, according to Milgrom and Roberts, any two productive activities or practices in a firm are said to be complementary if the development of one increases the productivity of the other (Milgrom and Roberts, 1990). In network design, complementarity refers to the coordination effects of network service components (Kim, 2003). In the field of innovation of general purpose technology, a technology complementarity arises in any situation in which the past or present decisions of the initiating agents with respect to their own technologies affect the value of the receiving agent's existing technologies and their opportunities for making further technological changes (Carlaw and Lipsey, 2002).

The complementarity concept used in the present study on ***CWS*** combines the notion of Edgeworth (1925), which is similar to both the extension applied in management, and the coordination effect in network service. It is expected the ***CWS*** over time not only assures the increase of the total output of the two when either one of the two sources increases, but also improves the stability and reliability of the power provision system deploying both types of resources.

2.4.2 Quantification of Complementarity

Depending on the definition applied in different disciplines, quantification methods used in measuring the complementarity are different. In economics, complementarity emphasizes more of the supplemental feature of products. The cross elasticity of demand, which indicates the percentage change in quantity demanded for the first good that occurs in response to a percentage change in price of the second good, is used to measure the degree of complementarities (Bordley, 1985). The formula used is:

Ec= (x % change of demand in product X)/(y% change in price of product Y)

(Bordley,1985; *Equ. 2.10*)

In network design, according to Kim (2003), two ways are used to test and measure the complementarity between network components. One is the direct method, which focuses on how the network components affect the whole network performance; second is the indirect method, which is to recognize the relationship between network components.

In management, complementarity means the marginal improvement to overall performance is increasing when increasing the performance of one component; the same effect is expected when increasing the performance of the other components (Schaefer, 1999). In this case, the choices made by a firm in two complementary domains are coordinated. If the complementary variables of the production function increase simultaneously, the value of that function increases by more than the sum of the value of the changes induced by the increase in each of the variables when

taken separately (Schaefer, 1999). Two types of approaches for measuring the complementarities in management are suggested. One approach "relies on a regression of a measure of productivity on a set of regressors, including the interaction effect between different practices, as estimates of complementarity parameters" (Laursen and Mahnke, 2001). The other approach "tests if the correlation among practices is positive, conditional on observables" (Laursen and Mahnke, 2001).

When the complementarity between wind and insolation is measured for a location over an annual cycle, the methods used must differ from other fields because unlike other disciplines, the converse tendency occurs over the temporal axis. This is a special feature of ***CWS***. A method to quantify the complementing tendency between the two resources is introduced in Chapter Four of the present study.

2.5 Spatial Analysis Methodology

The present study attempts to investigate the relations of various geographic factors and the complementary nature of wind and insolation. Geographic analysis methodologies are used in revealing the relations of multiple geographic factors and their impacts on ***CWS***. To study the spatial variation and autocorrelation indicated in the ***CWS*** and impacting factors, GIS visualization tools and statistical analysis approach including factor analysis and principal components analysis (Giordani and Kiers 2006) were used before further modeling was conducted.

Mitasova et al. (1996) discussed four approaches using open GIS methods and tools in their study of spatial and temporal distributed phenomena, including: interpolations from multi-dimensionally scattered points of data, analysis of surface and hypersurface, modeling of spatial processes, and three-dimensional dynamic visualization. The general interpolation and approximation methods and examples were also investigated by the authors.

In their book regarding statistical techniques in geographic analysis, Shaw and Wheeler (1994) systematically introduced different statistical methods and their applications in geography studies, including factor analysis and principal components analysis. The authors discussed two major techniques of factor analysis. The first is R-mode factoring, in which the correlation matrix of selected variables is built. The second is Q-mode factoring, which is a better fit for geographic aerial analysis, comparing pairs of areas and their attributes. Principal components approach reduces a number of correlated variables into a smaller number of uncorrelated variables called principal components. For reducing data dimensionalities, either factor analysis or principal components analysis can be used. But in case where little data is known, principal components analysis is suggested.

For the present study, to discover constituents leading to variations and exceptions in the complementary nature of wind and insolation, spatial analysis methods like principal components analysis (PCA) and the geographic weighted regression (GWR) modeling were used. PCA analysis is the eigenvector-based multivariate analysis and good for exploratory spatial data analysis (Giordani and Kiers 2006). Because of the specialty of geographic phenomena, all factors of one location are inherently connected because they possess the same coordinate and geography background. This leads to embedded multicollinearity in geographic factors. PCA analysis helps to effectively reduce multicollinearity in data dimensions by decomposing eigenvalues into principal components (Giordani and Kiers 2006).

Fotheringham, Brunsdon and Charlton (2002) developed the geographic regression model (GWR) to reduce spatial autocorrelation and limit independent variables within smaller local areal units. Global statistics are non-mappable, aspatial and GIS-unfriendly because they emphasize similarities across space (Fotheringham, Brunsdon and Charlton, 2002). For geographic phenomena, the desegregation of global statistics is more meaningful than using single values. GWR modeling is also called local geographic modeling. It can be done through calibration

within different regions, or moving windows, or even through the geographic weighted models with fixed or adaptive spatial kernels (Fotheringham, Brunsdon and Charlton, 2002). In the GWR model, the weighting function could be in several different forms and the decision of bandwidth, which refers to the number of neighbors needed for local estimation, is part of the process of calibration depending on the data density. The general extension of the GWR model considers spatial heteroskedasticity a situation when the variance of the error terms as well as regression coefficients exhibits spatial non-stationarity (Fotheringham, Brunsdon and Charlton, 2002). The GWR method solves the modifiable area unit problem (MAUP) to some extent.

Geographic phenomena inherently contain both high spatial heterogeneity and homogeneity. The GWR approach successfully models the spatial variation and autoregression by desegregating global statistics into local statistics. It is a good choice for modeling complicated spatial phenomena. It was chosen to explore the influences of various geographic factors on the complementary nature of wind and insolation in this study.

2.6 Summary of Literature Review

Literatures cited in this chapter are direct or indirect references for the study of complementarity of wind and insolation, from both the concepts and methods perspective. A few studies targeted at the initial efforts of exploring the ***CWS*** nature, and exposed what needs to be studied further. Studies of complementarity in other fields are also useful guides to study the ***CWS*** considering there is some generality in complementary features. The Edgeworth notion (1925) about complementarity, the definitions of complementarity in management and network service, generalized supermodularity of complementarity, and quantification approaches of complementarity developed in other fields, all highlight how to define and measure the ***CWS***.

Scattered discussions in different studies regarding what and how geographic factors affect wind or solar radiation help to identify what geographic factors might be considered as influencing

factors on the complementarity between wind and insolation, and what should be included in modeling the relations of geography and the ***CWS***. For instance, the investigation should consider terrain type and features in different geographic regions, atmospheric conditions over inland, ocean or lake coastal areas, and different spatial processes ongoing in different terrain categories including complex, flat, or mixed types. Therefore, factors like absolute location, elevation, relative elevation, terrain type, terrain exposure, aspects, slope orientation, surface roughness, climatic zones, major climatic characteristics, and distance from major water bodies may all be combined into the investigation of the ***CWS***.

Various spatial analysis methodologies provide some potential approaches applicable for exploring the spatial patterns of the ***CWS*** and the potential correlations of geographic factors and the ***CWS*** nature. In this study, in addition to the explorative spatial data analysis methods like simple Pearson correlation analysis, backward stepwise regression analysis, principal components analysis and GWR modeling methods were used.

CHAPTER III

PROBLEM DEFINITION AND METHODOLOGY OUTLINE

3.1 Concepts Definition and Research Statement

Both wind and solar radiation vary from place to place and from moment to moment. With the variations in landscape from place to place, such as hills, valleys, river bluffs and lakes, or trees and buildings, a complex and highly variable wind regime is also created on the earth's surface (IEC, 2007). Climatic factors also affect the wind regime, as well as the case for solar radiation. Geography and climate in micro, regional, and macro scales affect both the wind and solar energy potential. Because the geographic factors, such as location, local topography, and local climate impact both wind and insolation in the same spot, they are believed to be affecting the complementarity between the wind and solar power potential at the place.

In addition, the complementarity between wind and insolation is a derived nature from the temporal variation of both wind and insolation. Because of the inherent temporal fluctuation of the two energy forms, complementarity between them becomes possible. For the purpose of this study, the concept of complementarity is defined as: during a specific period of time at one location, the extent the occurrence of the two tends to be converse with each other. Because of the converse tendency, the wind might be relatively strong when insolation is relatively low and the wind might be relatively weak when the insolation is relatively high. The more their occurrence tendency is converse to each other, the more they complement each other (see Figures 3.1 through 3.3).

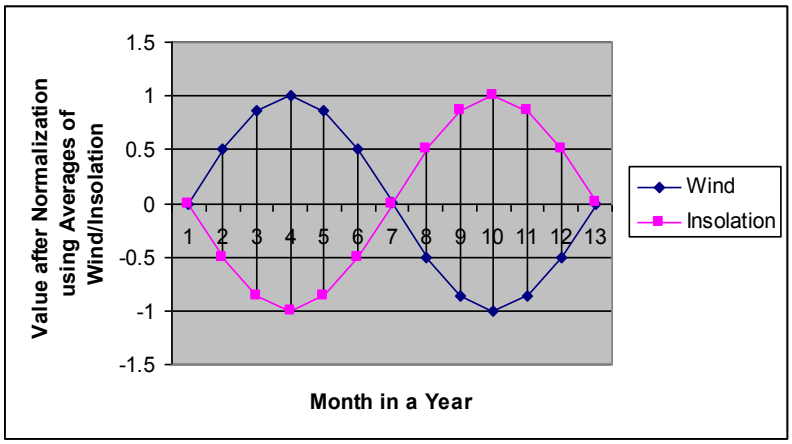

Figure 3.1 Perfectly Converse Occurrences of Wind and Insolation

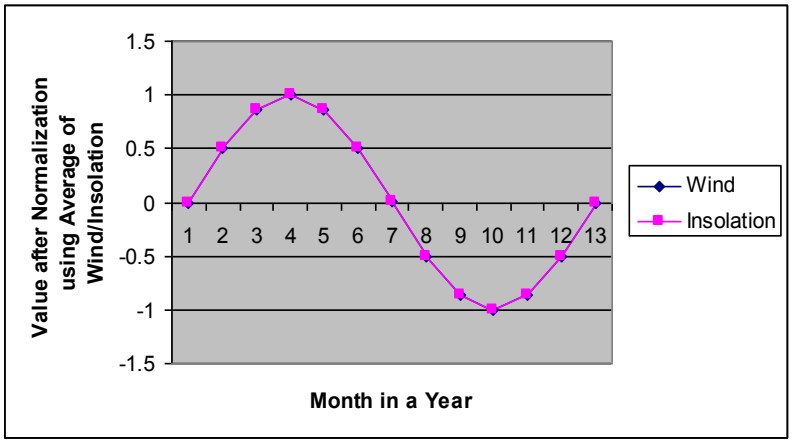

Figure 3.2 Perfectly Concordant Occurrences of Wind and Insolation

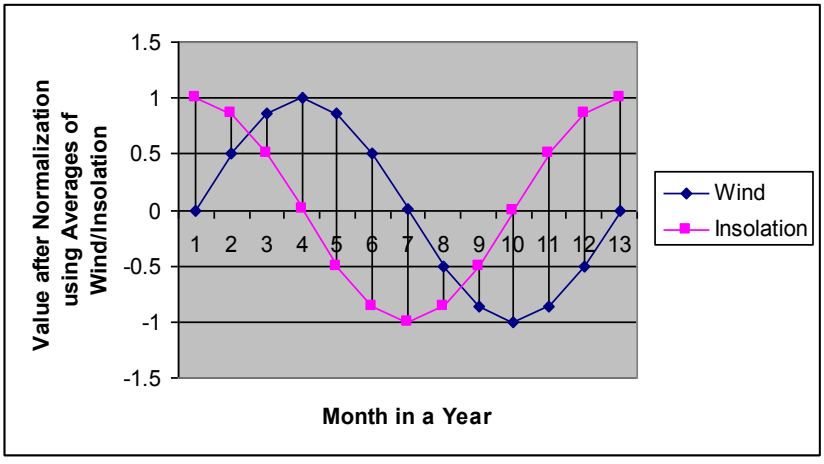

Figure 3.3 Partially Converse Occurrences of Wind and Insolation

When an electrical conversion system uses the wind and solar resources from a location, the total output of power of the integrated system depends on the complementarity of the temporal profiles of wind and solar sources. Adding the two resources over time tends to keep the total power productivity at a higher level with less temporal variation than using each source alone.

Accordingly, the research statement for this study is specified as following: at each location, on an annual and daily basis, the availability of wind energy and incident solar radiation energy tends to be complementary. This feature could keep the daily total amount of energy from the two sources at a more stable level than the use of only one resource. Furthermore, this complementary nature of wind and solar energy varies spatially. Geographic factors such as location, local terrain types, and local climate conditions can account for variations in the complementarity of these two energy resources.

There are several notions that need to be clarified in the above statement. First, this study focuses on the complementary tendency shown between the two energy forms over annual cycles, but the nature over daily cycles will be briefly examined as well. Features of the complementary nature of wind and solar radiation within monthly or seasonal cycles are not investigated. Second, the basic sub-period unit used depends on the time cycle studied. For instance, in this study, for annual cycles, a month is the sub-period unit used; for diurnal cycles, a 5-minute sub-period unit is used. Third, the complementarity between wind and insolation in this study involves two basic variables: long term average wind power density and long term average solar radiation density over corresponding sub-period unit. Fourth, it is assumed that this ***CWS*** exists in every place and there are differences in their complementary levels. This feature is referred to as the spatial heterogeneity of complementarities in this study. Fifth, geographic factors ranging from macro, meso to micro scales are considered as influencing factors of the spatial heterogeneity of complementarities. The scope of this research is limited to meso- and micro scale factors, which were investigated and linked with the ***CWS***.

3.2. Research Objectives

There are several specific objectives of this study:

(1) To examine the universal existence of the complementarities between the wind and solar resources beyond current sporadic observations;

(2) To quantify the complementarity for different places over specific periods of time, mainly during annual period, but the daily period will be observed;

(3) To identify the existence of the spatial variations of the complementarities between wind and solar radiation;

(4) To examine geographic factors affecting the complementarities;

(5) To investigate and model the relations of geographic factors and the spatial variations of the ***CWS***, and

(6) To explore and explain the dynamic mechanism behind the ***CWS*** preliminarily.

As indicated in Chapter 2, the nature of the ***CWS*** has been asserted by past research. However, most were based on observations in one or two locations. It is not known how general the phenomenon is and how it varies spatially. Through generating a numeric index to quantify the ***CWS*** over each place, this study provides an approach to identify the existence and level of the ***CWS*** nature at every place.

In the past, most studies used intuitive temporal profiles of both wind and solar energy to indicate the complementary nature observed. Some studies like the one by Takle and Shaw (1979), and the one by Sahin (2000) used statistical methods to assess the complementarity. To help further explore the ***CWS*** from a quantitative and spatial perspective, a numeric index to represent the ***CWS*** level at each location is more helpful. This study provides a standardized approach to quantify the ***CWS*** for different locations based on historical wind and insolation data. The index generated can be used in GIS or other explorative spatial analysis tools to illuminate spatial characteristics of the ***CWS***. It also can be used in quantitative models to relate the ***CWS*** to a set of

geographic factors. Although in this study the quantification method was applied in Oklahoma, it is applicable to any other place.

In this study, geographic factors that might influence the ***CWS*** are defined and the variable representing each factor were collected through primary or secondary data sources. The relations of various geographic factors with different levels of complementarity of wind and solar energy were then studied using the principal components analysis and the geographic weighted regression (GWR) model.

This study is mainly exploratory in nature. Because of data availability, the state of Oklahoma was used as an example in this study. Thirteen years of historical data for 127 Mesonet stations were used to study the ***CWS*** across Oklahoma. Mesonet is a statewide network to monitor the mesoscale environment and weather event in Oklahoma. It records observations of each site every 5 minutes, 24 hours per day (MESONET, 2008).

Several useful output results were generated in addition to the findings about spatial characteristics of ***CWS***, and modeled relations of geographic factors and the ***CWS***:

(1) Computer scripts and programs to automate the quantification and profile generation;

(2) A quantified complementarity index value representing the ***CWS*** of each location;

(3) A distribution profile showing daily average wind power and insolation density, and the variation over the annual cycle for each MESONET station;

(4) A normalized profile showing the variation over the annual cycle for each MESONET station;

(5) Long term observed geographic parameters defined as factors influencing the ***CWS*** of each MESONET location;

(6) GWR models to explain the possible spatial non-stationarity of complementarities using geographic factors, and

(7) Maps to display the spatial variations of complementarities, geographic factors, modeling coefficients, parameters, and error and residual terms. To ease reading, some of these results are included in the Appendix of this dissertation.

In the long run, world energy strategies should include as many renewable energy resources as possible. Research on the spatial features of the bilateral complementarity between wind power and insolation could initiate a better understanding of the relationship between renewable resources and possible geographic roles and processes behind them. Through studying the complementarities between wind and insolation, one potential application is to assess the interrelations between these two forms of renewable energy so that it can be used in future deployment designs of renewable systems. Another application is to help to explain how and what geographic factors are involved in shaping this nature so that some extrapolations and predications could be made based on the potential correlations. This study regarding the ***CWS*** will directly help to develop the temporal profile of wind and solar power at a specific location where specific geographic variables and conditions are known.

3.3. Approach Outline

The direct goal of this study is to provide a standardized approach to quantify and measure the complementary level of wind and insolation over different places, and to conduct an explorative study of the relations of the ***CWS*** and geographic factors. To serve this goal, the case of Oklahoma and its publicly available long-term Mesonet data were chosen as an example for the whole investigation. An outline of the data and methodology are presented below.

3.3.1 Data Used

Data needed in this study can be classified into three types: 1) sampled sites and their related information such as location and elevation information, 2) the attribute data recorded in a fixed interval for each chosen site, including the temperature, pressure, humidity, wind speed, solar

insolation, and 3) other data required by the study such as relative elevation information, terrain features, regional or local vegetation information, and microclimate and regional climatologic data.

In the case of Oklahoma, the basic data are 1994-2006 Oklahoma 5-minute Mesonet data including both wind speed and insolation. Other data recorded by Mesonet, including temperature, rainfall, pressure, and humidity of every five minutes, are also used in the study.

In addition to attribute variables, base data such as local topography, digital elevation models (DEM), landscape maps, and other vegetation maps are needed. Where no first-hand data source like the Mesonet was available, local historical climate data, summary products, and secondary data sources such as reanalysis data or gridded historical weather data produced by Nation Centers for Environmental Prediction (NCEP) or the National Center for Atmospheric Research (NCAR) could be employed. For example, NASA provides a measure of site-specific radiation data set based on a 10-year satellite study and an 11 x 11 grid cell data for specific latitudes and longitudes (CECCR, 2002). The Vegetation/Ecosystem Modeling and Analysis Project (VEMAP) generated grid-averaged surface wind speeds normalized at a 10m height for three-month seasonal and annual averages, which cover the entire conterminous U.S. in 0.5^{o} x 0.5^{o} grid cells (VEMAP, 2008). Other geophysical data such as elevation from USGS (USGS, 2008), land cover based on the images of the Advanced Very High Resolution Radiometer –AVHRR (NOAA, 2008), and vegetation maps from USGS may also be used as input data. In cases where there were multiple sources of data existing for one parameter, different sources of data were used as supplementary or corrective sources for each other.

The Oklahoma Mesonet provides base data and shapefiles of all Mesonet sites. Other data like Oklahoma administrative maps from Oklahoma Center for Geospatial Information (OCGI, 2008), 30m DEMs of Oklahoma from USGS (2008), OKGAP 90m from OCGI (2008), and Oklahoma

Land Cover/Land Use map from NLCD (2012) were obtained from corresponding sources. Topographic parameters for Mesonet sites, like aspects, slope, curvature, relative elevation, and hill shadow were derived for each site from DEM 30m maps. Land cover and land use within a 10km buffer area for each Mesonet site were calculated using the 2001 NLCD map of Oklahoma; direct distance to Gulf of Mexico of each site was also measured based on the shapefile Mesonet (2008) provided.

Considering the large amount of data used in the study, downloading, data cleaning, extracting, and complementarity calculation were semi-automated through the aid of both self-designed and commercially available computer programs.

For the Oklahoma Mesonet, batch data files were downloaded directly from Mesonet public data website and stored in a file-based database. Each month of each year had a folder to store the daily files from Mesonet. The database for original data files had the structure years-months-days, with one text file for each day of each month and year. There were 28 to 31 files contained in each monthly folder in total, depending on the length of that month. There were twelve month folders for each year and 13 year folders for the years 1994-2006. Metadata and map data were also fetched from secondary sources and stored in corresponding folders. All text based data were then inserted into the SQL server database through a specifically designed program.

3.3.2 Approach Outline

Micro-geography, regional geography, and quantitative geographic analysis methods were employed to investigate the spatial characteristics of wind and solar resources, and the ***CWS***. Once all data required for the study were organized in the database, the next step was data processing and analysis. There were several steps involved in spatial analysis of complementarities between wind and insolation and their relations with associated geographic factors.

The first was to preprocess the collected raw data and prepare the data for calculating the complementarities between wind and insolation for each selected location. In this step, daily average wind power density and daily average insolation density were calculated.

The second step was to quantify the complementarities of each sampled station. A method to calculate the complementarity for each location was developed so that the derived complementarities among different locations were comparable, and quantitative analysis became possible. The resulting indexes were used as major and dependent variables in spatial analysis. Details of the quantification approach are introduced in Chapter Four.

Third, an explorative data analysis was performed on the resulting complementarity index values to discover any obvious spatial patterns. General statistical methods and GIS tool was used to conduct the explorative study. In this step, the spatial pattern of heterogeneity and autocorrelation indicated in complementarity values can be visualized in an intuitive way through GIS mapping and interpolation.

Fourth was to choose geographic factors to be included in the correlation study as independent variables. Terrain types from complex, flat to mix, absolute and relative elevations, and absolute latitude and longitude were usually taken as first terrain factors affecting the complementarities. Aspect, slope, distance to major water bodies, climate and atmospheric characteristics were the secondary terrain attributes which are derivations of first terrain factors. Other factors from local, regional, and global scales were also examined. A stepwise regression model and principal components analysis were used in this stage to prune the number of factors.

Fifth, a comprehensive correlation model was built to connect the complementarity index with major geographic factors. In this step, the geographically weighted regression (GWR) method was used to explore and explain the relations between the dependent complementary index and various independent geographic variables. The model created could also be used for estimating

and predicting the complementarity level of wind and insolation in a specific site with specified values of various geographic parameters known. All results were mapped using GIS.

Lastly, an exploratory explanation of the modeling results was attempted. Internal mechanisms and processes leading to spatial relationships between geographic factors and the ***CWS*** are discussed.

The methodology employed by the present study is preemptive and tentative. The approaches need to be verified by applying it in more places other than Oklahoma. Future improvements in both the quantification approach and the modeling approach are still necessary in hoping to develop a widely feasible prediction and modeling method for assessing the ***CWS*** over different places.

CHAPTER IV

QUANTIFICATION OF THE COMPLEMENTARY NATURE OF WIND POWER AND INSOLATION

Quantification of the complementary nature of wind and insolation is helpful when exploring the spatial features of the complementary nature between the wind and solar energy (***CWS***). In this study, a standardized numeric index representing the complementary nature is developed. For simplicity, the complementarity *index* between wind power and incoming solar radiation (insolation) is abbreviated as ***CIWS***. This chapter outlines a quantification approach used in this study to derive such an index. Steps for this quantification method will be introduced below accompanied by a scenario using long-term high-resolution Oklahoma Mesonet data. The presented approach could be used in ***CIWS*** calculations for various time spans, including the annual and diurnal cycle. Because of time limitations, the annual ***CIWS*** is taken as the focus of this study, but a glimpse of applying the quantification approach to calculate the diurnal ***CIWS*** for Oklahoma is also provided in the last part of this chapter.

4.1. Data Preparation

The complementarity between wind power and solar radiation can be described as a feature located on the earth's surface within a specific period of time. This part of the study focuses on the complementarity between the two energy forms of wind and insolation observed in the period of annual cycles. The distinct sub-period unit of the annual cycle used in this study is the month.

Since each month contains 28 to 31 days, the daily average wind power density (*DAWD*) and daily average insolation power density (*DAID*) in each month was used to represent the wind power and insolation power density for that month respectively. In this study, the area between the annual variation curve of wind power density and that of insolation power density at the same height above the earth's surface is identified as the ***CIWS*** value (see the shaded area of Figure 4.1). The primary data needed to derive the area representing the complementarity index, ***CIWS***, for a site are the *DAWD* and *DAID* at the same height of a site for each month.

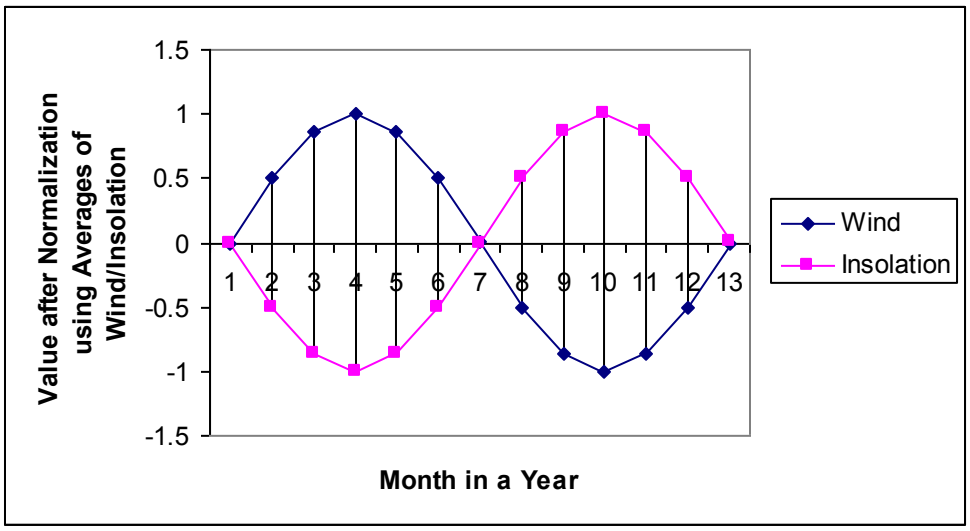

Figure 4.1 Shaded Areas between Annual Variation Curves of Wind and Insolation Power as ***CIWS***

Considering that the wind power density varies significantly across vertical distances above the earth's surface, and insolation power density shows little vertical variation within a range close to the earth's surface, the height used to derive the wind power density needs to be specified. The height could be determined based on either the basic height set for historic data observation, or the height a specific study is interested in. In this study, the height of 50m above land surface, a standard height for estimating wind power generation for wind farms, is chosen as the specified height for estimating ***CIWS***.

4.1.1. Data Extraction

DAWD and *DAID* are the major data needed to calculate ***CIWS*** in this study. If these data are available already, the annual profile chart displaying monthly wind density and solar power density, referred to as the basic profile, can be built. A normalization procedure is then carried out on the basic profile. The final ***CIWS*** value is calculated based on the normalized profile. However, most often, the *DAWD* and *DAID* data are not available and must be calculated first.

The necessary data for calculating *DAWD* of a site for each month is historically recorded wind speed data within each month. Other data needed include: monthly long-term temperature data, monthly long-term pressure data, and the elevation. The data needed for calculating the *DAID* of a site for each month is long-term solar radiation data. With the exception of the elevation data, it is better if all historic data observations were collected within a small interval of time during a day. The higher of the temporal resolution of historical data, the more statistically robust are the aggregated immediate results and the final *DAWD* and *DAID*. In this study, high temporal resolution refers to data recorded in the intervals of hours or minutes. It is also better if those historic data were recorded at a fixed height and a fixed interval of time. This makes the calculation of the *DAWD* easier to be accomplished in one formula (see Approach 1 below). However, if the temporal resolutions of the original data are low and height unfixed, a different approach can be taken to calculate the *DAWD* for each month (see Approach 2 below). If the heights of available recorded data are significantly different, some extrapolation of the original data might be needed before applying corresponding formulas. In addition, the longer term the historical observations spanned, the more representative are the *DAWD* and the final ***CIWS*** for the studied site.

In summary, the prerequisite data discussed above to be used in building annual profiles of wind and solar power density at one site are listed below:

(1) Wind speed measured in some fixed interval and fixed height;

(2) Temperature recordings measured in some fixed interval at the same or close height as wind speed;

(3) Pressure data measured in fixed intervals at the same or close height with as wind speed measurement;

(4) Site elevation;

(5) Solar radiation data measured in fixed intervals at the same or close height as wind speed.

The Oklahoma Mesonet is a densely spaced weather observation network set up for environmental monitoring since 1994. The term Mesonet is a combination of the words "mesoscale" and "network" (MESONET, 2008). In meteorology, "mesoscale" refers to weather events that last from several minutes to several hours, and range in size from about one mile to 150 miles (MESONET, 2008). The Mesonet consists of over 110 automated stations across Oklahoma, with at least one Mesonet station in each of Oklahoma's 77 counties (MESONET, 2008). Figure 4.2 and Figure 4.3 are the Mesonet maps created based on 2005 Mesonet data (which are used by this study), with the former one labeling sites using full location names, and the latter one using corresponding short names.

At each Mesonet site, the environment parameters are measured by a set of instruments located on or near a 10m tower. The measurements are packaged into “observations” and transmitted to a central facility every 5 minutes, 24 hours per day year-round (MESONET, 2008). The Oklahoma Climatological Survey at the University of Oklahoma receives the observations and verifies the quality of the data (MESONET, 2008). In this study, these Mesonet data were used as base study to study the complementary nature between wind and solar radiation in Oklahoma. The height at which the complementarity was investigated was around 50 meters above the surface, extrapolated from original 10m wind data and 2m solar data.

Figure 4.2 Map of Mesonet Sites with Full Name (based on 2005 Mesonet Data)

Figure 4.3 Map of Mesonet Sites with Short Name (based on 2005Mesonet Data)

The detailed list of data extracted from the Mesonet database (MESONET, 2008) outlined in section 3.3.1and used in calculating *DAWD* and *DAID* included:

(1) *TAIR*-site temperature at the height of 1.5m averaged every 5 minute (Celsius)

(2) *WSPD*-site wind speed at 10m averaged every 5 minutes (m/s)

(3) *PRES*-site pressure averaged every 5 minutes (millibars)

(4) *TA9M*-site temperature at height of 9m averaged every 5 minutes (Celsius)

(5) *SRAD*-site solar radiation above ground averaged every 5 minutes (watt/m^2)

The elevation data for each site provided by the Mesonet is:

(6) *ELEV*-elevation for each Mesonet site, a fixed value for each location (m)

The raw Mesonet data for 127 stations between 1994 and 2006 were extracted with about 158 million records. Each record includes 26 different column types, including those listed above.

4.1.2. Data Processing

Once the data sources and data types were determined, all needed data were migrated into one integrated database for further processing. The original data amounts were usually huge; and it was expedient to use SQL server or Oracle database servers to store the raw data because they are especially suitable for huge and growing databases, and can provide quick data transactions. For the case of Oklahoma, all Mesonet data were imported into one table CLIMATOLOGYDATA in a SQL server database through programs designed for this purpose (see Appendix A).

After the basic database and data table were built, depending on the available parameter data, one of the two different approaches was employed to calculate the *DAWD* on original data for each month of a year. The method for calculating *DAID* is the same under both approaches.

Approach 1: Calculation of *DAWD* based on Interval Wind Power Density

In the example of Mesonet data, the formulas for the first approach are:

$$WPD5min10m = 0.5*(PRES*100/(287*(TA9M+273)))*\text{power}(WSPD, 3) \qquad \textit{(Equ. 4.1)}$$

WPD5min50m=*WPD5min10m**power (5, 3/7) *(Equ. 4.2)*

WPD50mMthAvg=sum (*WPD5min50m* within same month same year)/count (*WPD5min50m* within same month same year) *(Equ. 4.3)*

DAWD=*WPD50mbyMth*=Sum (*WPD50mMthAvg*)/Count (*WPD50mMthAvg* for same month of a year) *(Equ. 4.4)*

Where the *PRES*, *TA9M* and *WSPD* were all from the original data records of Mesonet; *WPD5min10m* and *WPD5min50m* are the estimated wind power density every 5-minute at 10m and 50m respectively; *WPD50mMthAvg* is the average daily wind power density (Stadler and Hughes 2005) at the height of 50m for each site within the same month during 1994-2006; *WPD50mbyMth* is the average daily wind power density for corresponding months at each site based on all years from 1994-2006; the unit used for *WPD5min10m, WPD5min50m, WPD50mMthAvg,* and *WPD50mbyMth* is watts/m^2.

Approach 2: Calculation of *DAWD* based on Average Wind Speed

In the example of Mesonet data, the major formulas are:

PRESMAvg =SUM (*PRES* within same month same year)/count (*PRES* within same month same year) *(Equ. 4.5)*

TA9MMAvg= SUM (*TA9M* within same month same year)/count (*TA9M* within same month same year) *(Equ. 4.6)*

WSPDMAvg= SUM (*WSPD* within same month same year)/count (*WSPD* within same month same year) *(Equ. 4.7)*

WPDMthly10m=0.5*1.91*(*PRESMAvg**100/(287*(*TA9MMAvg*+273)))*power(*WSPDMAvg*,3) *(Equ. 4.8)*

WPDMthly50m=WPDMthly10m * power(5, 3/7) *(Equ. 4.9)*

DAWD=WPD50mbyMth=Sum(*WPDMthly50m*)/Count(*WPDMthly50m* for same month of a year) *(Equ. 4.10)*

As in Approach 1, where the *PRES*, *TA9M* and *WSPD* are all from the original data records from the Mesonet, *PRESMAvg, TA9MMAvg,* and *WSPDMAvg* are the estimated monthly average pressure, temperature and wind speed at a height of 10m respectively; *WPDMthly10m* and *WPDMthly50m* are the estimated daily wind power density at 10m and 50m respectively for each month during 1994-2006 at the site based on the second approach; *WPD50mbyMth* is the average daily wind power density for corresponding months of each site based on all years from 1994-2006; the unit used for *WPDMthly10m, WPDMthly50m, WPDMthly50m,* and *WPD50mbyMth* is watts/m^2. If this approach is used in other studies, the *PRESMAvg, TA9MMAvg,* and *WSPDMAvg* data could be already available from some historical data collection.

A note here is that in both approaches for the Oklahoma Mesonet, the basic data used were *PRES*, *TA9M* and *WSPD* from the original Mesonet data. However, there are some observations in which the *PRES* and *TA9M* data were missing or not valid for use. In this case, alternative formulas using variables of TAIR and ELEV from the Mesonet, combined with variable WSPD, are used to estimate the wind power density.

Under both approaches, the formulas applied to calculate the average daily insolation power density of each month for Mesonet were:

SRADmthlyAvg=Sum (*SRAD* within same month same year)/Count (*SRAD* within same month same year) *(Equ. 4.11)*

DAID=MthlyAvgSRAD=Sum(*SRADmthlyAvg*)/ Count (*SRADmthlyAvg* for same month of a year) *(Equ. 4.12)*

Where *SRAD* is the original 5-minute solar radiation data recorded around 2m height in the Mesonet data. In this study, the vertical variation of solar radiation is ignored and solar radiation is assumed to be received at a height of 50m, matching the wind power density data. Therefore, the resulting *SRADmthlyAvg* also represents the daily average solar radiation at a height of 50m for each month of each year at each location during 1994-2006; *MthlyAvgSRAD*

represents the average daily solar insolation of each month at a height of 50m for all years from 1994-2006 at each site; the unit for both S*RADmthlyAvg* and *MthlyAvgSRAD* is watts/m^2.

4.1.3 Building Monthly Wind and Solar Power Density Profile

All the above operations on original data were conducted using the SQL query functions provided by SQL server or Oracle. Intermediate and final results were also stored in respective tables in the same database for future use. Table 4.1 and Figure 4.4, and Table 4.2 and Figure 4.5, show the results for Mesonet's ACME station by using the Approach 1 and 2 respectively. As seen in the tables and charts, the calculated *DAWD,* based on the above two approaches, were close though not completely identical. This confirms both approaches were valid to quantify the ***CWS***. A separate study may be conducted in the future on how significant the difference is in the results from the two approaches and what may be a most appropriate method for calculating *DAWD*. In this study, in later part, only the results from Approach 1 for Mesonet sites will be demonstrated and employed.

After the *DAWD* and *DAID* were obtained through calculations explained above, a profile to combine both wind and solar power density in an annual cycle was built to indicate the complementary trend between wind and insolation power density. For example, Figure 4.4 and Figure 4.5 describe the basic profiles for ACME station; Figure 4.6 is the basic profile drawn for another station BOIS (results based on Approach 1). All charts indicate the complementary nature between wind and insolation (See Appendix F). The basic profiles generated in this stage were used in further normalization procedures to calculate a final ***CIWS*** value for each site. A two-step normalization procedure is introduced below to perform on the basic profiles of each site.

4.2. Normalization of the Annual Wind and Insolation Power Density Profile

As suggested in the basic profiles, the complementary nature between wind power and solar radiation is not just a feature manifested through the increased total energy output by combining

the two energy forms, but also through the canceling effect of the opposite trend varying in time of the two energy forms, which might work together to increase the stability of hybrid systems. In this study, the complementarity level is defined by the area between the *DAWD* and *DAID* curves, which represents the annual variation of wind and insolation power density in the basic profile for each site. To obtain a complementarity index representing the complementary nature for each location, normalization is needed to make it comparable across locations. A two-step normalization procedure was developed to standardize the basic profiles for calculating the ***CIWS*** index. Details of the normalization procedures are presented below, with the example applied to the basic profiles obtained for Oklahoma Mesonet sites.

STID	STNM	Month	DAWD	DAID
ACME	110	1	276.88	114.20
ACME	110	2	297.93	143.03
ACME	110	3	364.63	186.32
ACME	110	4	378.04	233.91
ACME	110	5	279.82	253.52
ACME	110	6	196.65	279.81
ACME	110	7	131.37	290.97
ACME	110	8	106.40	258.67
ACME	110	9	135.20	214.58
ACME	110	10	215.05	161.16
ACME	110	11	258.77	117.71
ACME	110	12	241.72	104.01

Table 4.1 ACME 13-Year Averaged *DAWD* and *DAID* using Approach 1

STID	STNM	Month	DAWD	DAID
ACME	110	1	263.10	114.20
ACME	110	2	268.49	143.03
ACME	110	3	364.49	186.32
ACME	110	4	401.33	233.91
ACME	110	5	307.09	253.52
ACME	110	6	212.48	279.81
ACME	110	7	157.38	290.97
ACME	110	8	116.26	258.67
ACME	110	9	125.14	214.58
ACME	110	10	207.17	161.16
ACME	110	11	245.94	117.71
ACME	110	12	221.76	104.01

Table 4.2 ACME 13-Year Averaged *DAWD* and *DAID* using Approach 2

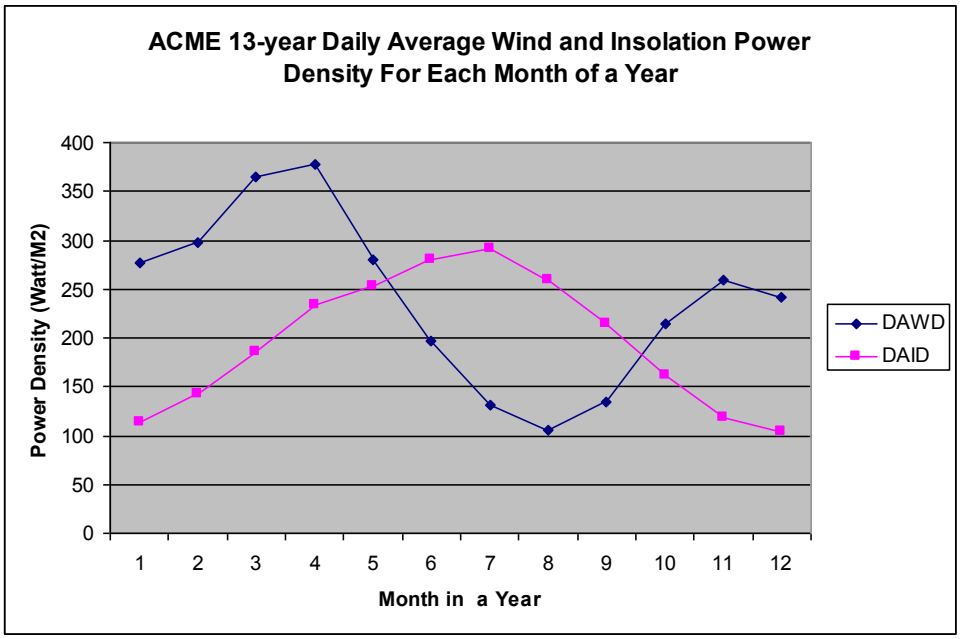

Figure 4.4 ACME Basic Profiles of *DAWD* and *DAID* based on Approach 1

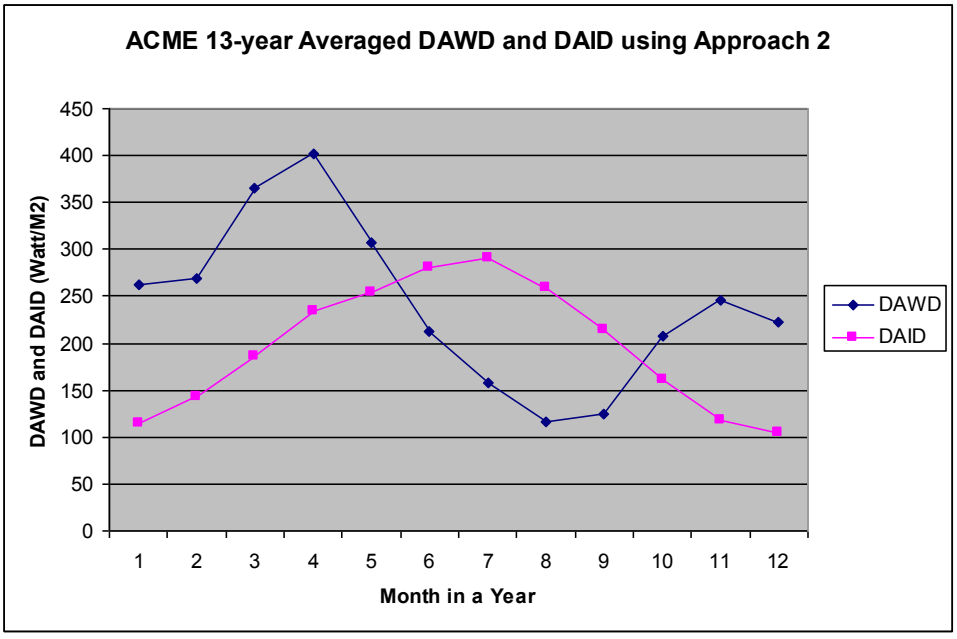

Figure 4.5 ACME Basic Profiles of *DAWD* and *DAID* based on Approach 2

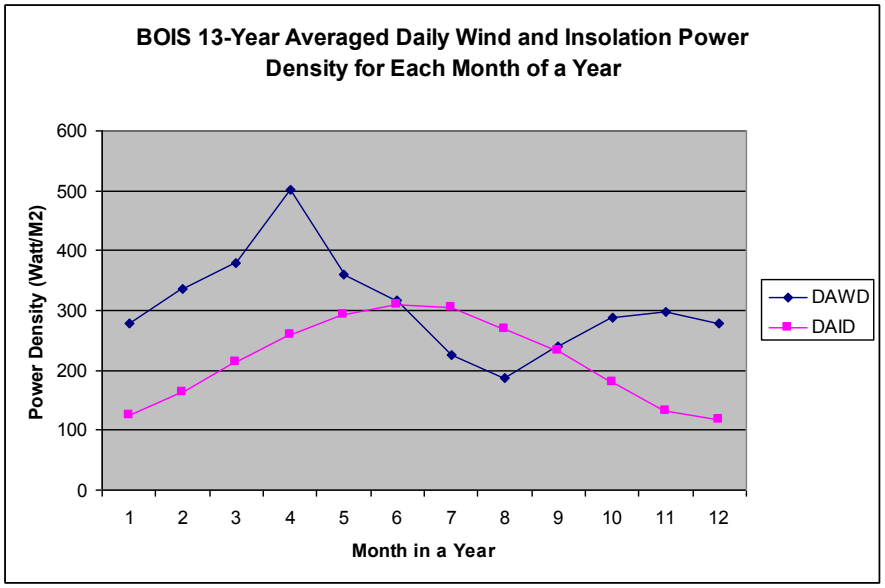

Figure 4.6 BOIS Basic Profiles of *DAWD* and *DAID* (based on Approach 1)

4.2.1 First-step Normalization by Yearly Average

At each site, in the annual cycle, the daily averaged wind and solar power density fluctuate around their yearly average level. Therefore, in the first step of normalization, the *DAWD* and *DAID* of each month were normalized using the yearly average of *DAWD* and *DAID* correspondingly. This was done through following steps:

1. Yearly average *DAWD* (abbreviated as *YDAWD*) and yearly average *DAID* (abbreviated as *YDAID*) were calculated based on the obtained *DAWD* and *DAID* for 12 months in annual cycle.
2. Calculate the percentage of *DAWD* and *DAID* of their yearly average. The formulas applied were of the form: *PCNT_DAWD=DAWD/YDAWD* and *PCNT_DAID=DAID/YDAID*. The results from this step for each month could be either greater than 1 or less than 1 depending on whether the monthly *DAWD* or *DAID* is greater than or less than their yearly average level.
3. Subtract 1 from the percentage of *PCNT_DAWD* and *PCNT_DAID* to obtain how much of each month's *DAWD* and *DAID* differ from their yearly average levels.

The results from this step are named *NA_DAWD* and *NA_DAID* respectively. The formulas applied were: *NA_DAWD=PCNT_DAWD*-1 and *NA_DAID=PCNT_DAID*-1.

The results after conducting the first-step normalization for the Mesonet station ACME (using the results of Approach 1) was presented in the following Tables 4.2, 4.3 and 4.5.

STID	STNM	Month	DAWD	DAID	YDAWD	YDAID
ACME	110	1	276.88	114.2	240.21	196.49
ACME	110	2	297.93	143.03	240.21	196.49
ACME	110	3	364.63	186.32	240.21	196.49
ACME	110	4	378.04	233.91	240.21	196.49
ACME	110	5	279.82	253.52	240.21	196.49
ACME	110	6	196.65	279.81	240.21	196.49
ACME	110	7	131.37	290.97	240.21	196.49
ACME	110	8	106.40	258.67	240.21	196.49
ACME	110	9	135.20	214.58	240.21	196.49
ACME	110	10	215.05	161.16	240.21	196.49
ACME	110	11	258.77	117.71	240.21	196.49
ACME	110	12	241.72	104.01	240.21	196.49

Table 4.3 Results of Yearly Average DAWD and DAID at Station ACME

STID	STNM	Month	DAWD	DAID	PCNT_DAWD	PCNT_DAID
ACME	110	1	276.88	114.20	1.15	0.58
ACME	110	2	297.93	143.03	1.24	0.73
ACME	110	3	364.63	186.32	1.52	0.95
ACME	110	4	378.04	233.91	1.57	1.19
ACME	110	5	279.82	253.52	1.16	1.29
ACME	110	6	196.65	279.81	0.82	1.42
ACME	110	7	131.37	290.97	0.55	1.48
ACME	110	8	106.40	258.67	0.44	1.32
ACME	110	9	135.20	214.58	0.56	1.09
ACME	110	10	215.05	161.16	0.90	0.82
ACME	110	11	258.77	117.71	1.08	0.60
ACME	110	12	241.72	104.01	1.01	0.53

Table 4.4 Percentage of Monthly DAWD and DAID over the Yearly Average for ACME

STID	Month	DAWD	DAID	NA_DAWD	NA_DAID
ACME	1	276.88	114.20	0.15	-0.42
ACME	2	297.93	143.03	0.24	-0.27
ACME	3	364.63	186.32	0.52	-0.05
ACME	4	378.04	233.91	0.57	0.19
ACME	5	279.82	253.52	0.16	0.29
ACME	6	196.65	279.81	-0.18	0.42
ACME	7	131.37	290.97	-0.45	0.48
ACME	8	106.40	258.67	-0.56	0.32
ACME	9	135.2	214.58	-0.44	0.09
ACME	10	215.05	161.16	-0.10	-0.18
ACME	11	258.77	117.71	0.08	-0.40
ACME	12	241.72	104.01	0.01	-0.47

Table 4.5 Results after First-step Normalization for Station ACME

4.2.2 Second-step Normalization around Peak Value

After the first-step of normalization, the daily average wind and insolation power densities for each month have been normalized over the yearly average level of each. Figure 4.7 below shows the results after the first normalization for station ACME. Different from Figure 4.4, the Y-axis now refers to how much each month's *DAWD* and *DAID* differ from their yearly average level respectively, not the actual *DAWD* and *DAID* as in Figure 4.4. However, the peak values of resulting *NA_DAWD* and *NA_DAID* after the first normalization are inconsistent with each other and vary from site to site. For instance, *NA_DAWD* at ACME has a range of -0.6 to 0.6, while *NA_DAID* for this site falls between -0.5 to 0.5. In addition, the ranges of both *NA_DAWD* and *NA_DAID* are different from station to station. For instance, different from station ACME, in Figure 4.8, *NA_DAWD* for station BOIS has a range of 0.39 to 0.63, while *NA_DAID* has the ranges of -0.46 to 0.43.

The inconsistency of the range of peak values indicates the results from the first normalization fluctuate among different ranges. This means the final ***CIWS*** values calculated based on the area between the two curves representing annual wind and insolation power density would also fluctuate. This would make it difficult to compare the final calculated complementarity index

among different sites because the areas between the two curves representing wind and solar power density would also fluctuate. A second step of normalization around the peak values was conducted on the results of the first-step normalization, so that the curve areas for the final ***CIWS*** values fell into a constant range.

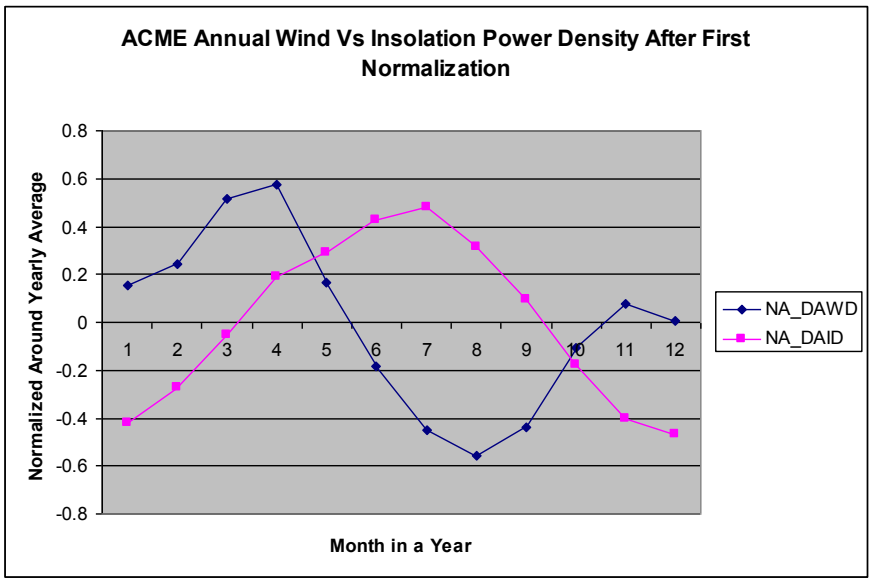

Figure 4.7 Results of ACME after First Normalization

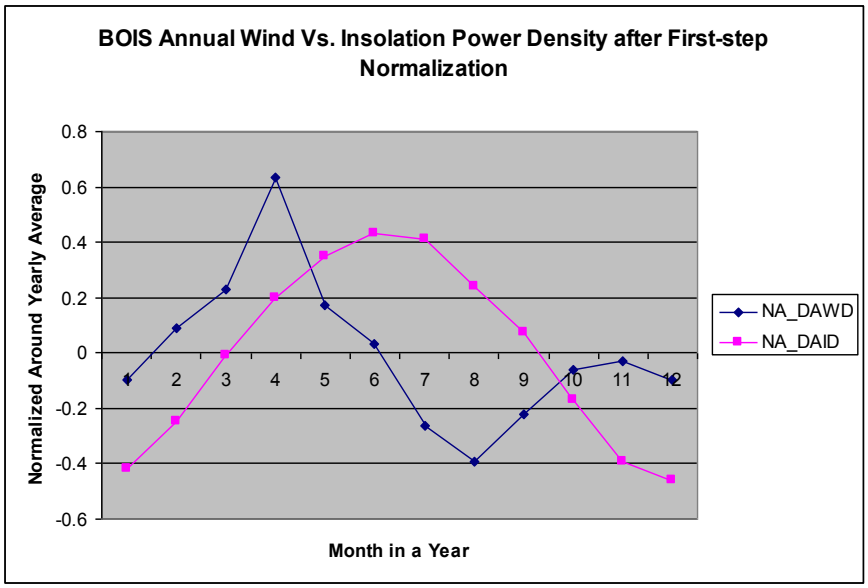

Figure 4.8 Results of BOIS after First Normalization

In this second stage of normalization, the results from the first-step normalization of *NA_DAWD* and *NA_DAID* for each month were normalized again using the absolute maximum value of each in the annual cycle. The detailed steps are:

1. Determine which *NA_DAWD* and *NA_DAID* has the highest absolute value in annual cycle and name them as *PK_NADAWD* and *PK_NADAID* correspondingly.
2. Divide the *NA_DAWD* and *NA_DAID* for each month of the site by the maximum absolute values *PK_NADAWD* and *PK_NADAID* respectively to calculate how much each month's *NA_DAWD* and *NA_DAID* are away from the absolute peak value of each. The results are named *NPK_NADAWD* and *NPK_NADAID*. The formulas applied are *NPK_NADAWD=NA_DAWD/PK_NADAWD* and *NPK_NADAID = NA_DAID/PK_NADAID*.

Table 4.6 and Table 4.7 show the results after the second normalization for Mesonet station ACME. Figure 4.9 displays the normalized profile for station ACME after second normalization.

STID	STNM	Month	NA_DAWD	NA_DAID	PK_NADAWD	PK_NADAID
ACME	110	1	0.15	-0.42	0.57	0.48
ACME	110	2	0.24	-0.27	0.57	0.48
ACME	110	3	0.52	-0.05	0.57	0.48
ACME	110	4	0.57	0.19	0.57	0.48
ACME	110	5	0.16	0.29	0.57	0.48
ACME	110	6	-0.18	0.42	0.57	0.48
ACME	110	7	-0.45	0.48	0.57	0.48
ACME	110	8	-0.56	0.32	0.57	0.48
ACME	110	9	-0.44	0.09	0.57	0.48
ACME	110	10	-0.10	-0.18	0.57	0.48
ACME	110	11	0.08	-0.40	0.57	0.48
ACME	110	12	0.01	-0.47	0.57	0.48

Table 4.6 Results from Step 1 of Second Normalization for Station ACME

When both normalization procedures discussed above was performed using the basic profiles of each site, the normalized profiles for all sites were built. Charts based on these normalized profiles for all sites with valid data demonstrate the complementary nature between wind power and solar radiation in a more standardized way compared with basic profiles. The range of the

normalized values on the Y-axis is between -1 and 1, the range of months on the X axis is from 0 to 12, and the maximum area difference between the two curves as shown in Figure 4.9 can be as large as the rectangular area: (12-0)*(1-(-1)) = 24, which is a unitless constant for all sites. Theoretically, the areas between the curves therefore range between 0 and 24.

STID	Month	NPK_NADAWD	NPK_NADAID
ACME	1	0.27	-0.87
ACME	2	0.42	-0.57
ACME	3	0.90	-0.11
ACME	4	1.00	0.40
ACME	5	0.29	0.60
ACME	6	-0.32	0.88
ACME	7	-0.79	1.00
ACME	8	-0.97	0.66
ACME	9	-0.76	0.19
ACME	10	-0.18	-0.37
ACME	11	0.13	-0.83
ACME	12	0.01	-0.98

Table 4.7 Results of Second Normalization around Absolute Peak Values of ACME

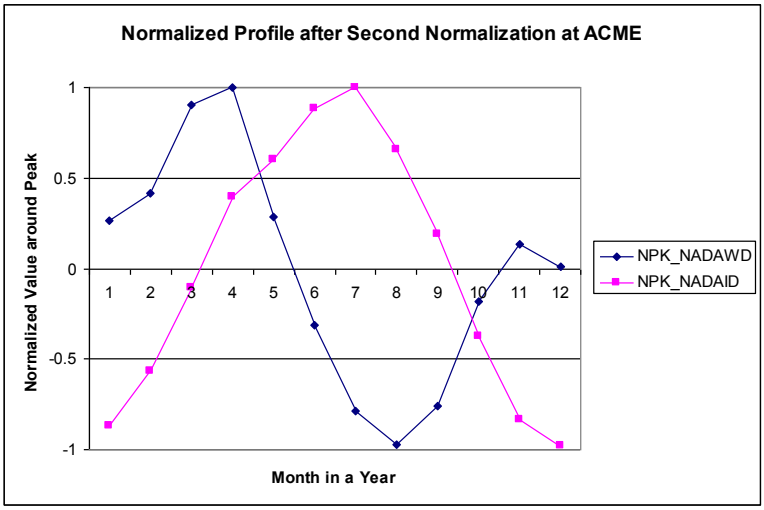

Figure 4.9 Normalized Profile after Second-step Normalization at Station ACME

4.3. Calculating the Annual Complementarity Index

The last step of the quantification approach is to calculate the final ***CIWS*** index which is also the area between the two normalized curves (see Figure 4.10). Since the curves are not smoothed, equations are not available for describing the curves. To obtain the approximate integrated area

between two curves, the area between the two normalized curves of wind power and insolation power density was estimated through adding each small triangle and trapezoid in the area between the two curves. Here are the steps performed:

1. In the charts drawn based on normalized profiles, lines were dropped between the two points representing the normalized results of *NPK_NADAWD* and *NPK_NADAID* for each month (see Figure 4.10).
2. To calculate the area of each triangle and trapezoid formed by the two curves and newly dropped lines:
    1) First calculate the difference between the connected pair of points of each month by using the equation (*NPK_NADAWD-NPK_NADAID*). Results were stored under the variable name *LENGTH_BETWEEN*. The absolute value of each *LENGTH_BETWEEN* variable represents the length of the line dropped in step 1. If the variable of *LENGTH_BETWEEN* is negative, the *NPK_NADAID* of the month is higher than that month's *NPK_NADAWD* value, and vice versa.
    2) Calculate the area of each single triangle or trapezoid by applying corresponding formulas to each. If the values of the variable *LENGTH_BETWEEN* for two adjacent months with same sign, a trapezoid shape is formed within the two normalized curves and the lines dropped for adjacent months; the formula to calculate the trapezoid area will be used, and the two bases are the lengths of the dropped lines for the two adjacent months respectively. If the sign of the *LENGTH_BETWEEN* variable for two adjacent months are different, two small triangles are formed within the two normalized curves; and each of the two lines dropped for the adjacent months is the base of each triangle respectively; in this case, the triangle formula is applied twice and the areas of the two

small triangles are summed to get the total areas between the two lines for two adjacent months.

3. Summarize all estimated areas between the two curves from step 2 and the final summed value is the ***CIWS*** for the site.

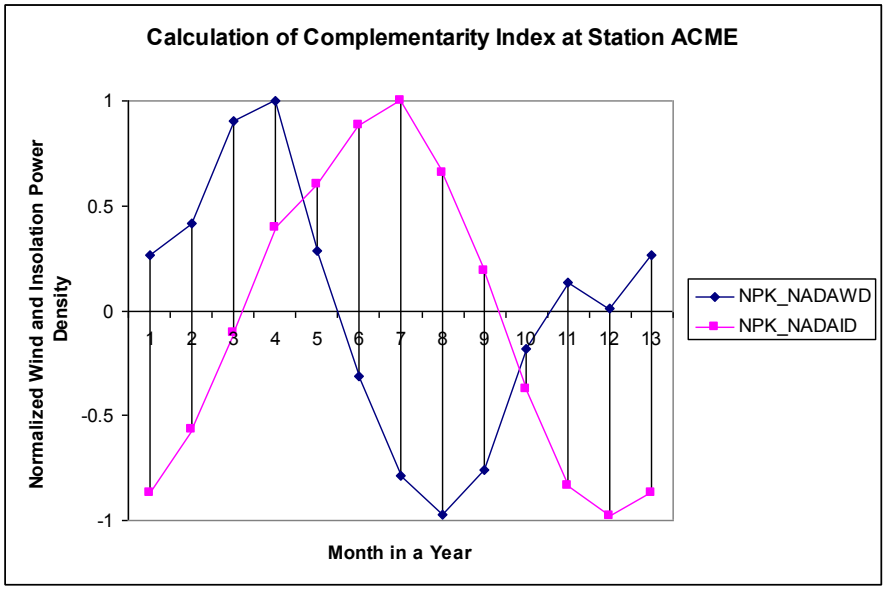

Figure 4.10 Display Complementarity Areas between two Curves for Station ACME

The steps described above are illustrated using the example of Mesonet station ACME. Figure 4.10 is the chart drawn based on the normalized profile after the second normalization for ACME. Lines were dropped between points representing normalized results of wind and insolation respectively for each month. The size of the shaded area between the two normalized curves defines the value of ***CIWS*** for station ACME. Intermediate and final results in this stage are given in Table 4.8.

To calculate the total area of the shaded part, steps described above were followed. Additionally, after the line was dropped between the two paired points on wind and isolation curve for Month 12, an additional line was created between the two paired points representing wind and isolation on curves for Month 1 so that the ***CIWS*** value includes a cycle of one complete year. Figure 4.10

shows this extension. As the last step, areas for all small triangles and trapezoids in this chart were summed up as the final ***CIWS*** value for site ACME, which is 11.4 (see Table 4.9) out of 24.

STID	STNM	Month	NPK_NADAWD	NPK_NADAID	LENGTH_BETWEEN
ACME	110	1	0.27	-0.87	1.14
ACME	110	2	0.42	-0.57	0.98
ACME	110	3	0.90	-0.11	1.01
ACME	110	4	1.00	0.40	0.60
ACME	110	5	0.29	0.60	-0.32
ACME	110	6	-0.32	0.88	-1.20
ACME	110	7	-0.79	1.00	-1.79
ACME	110	8	-0.97	0.66	-1.63
ACME	110	9	-0.76	0.19	-0.95
ACME	110	10	-0.18	-0.37	0.19
ACME	110	11	0.13	-0.83	0.97
ACME	110	12	0.01	-0.98	0.99

Table 4.8 Calculation of Difference of Pair Points on Two Curves for ACME

The normalization steps described above were carried out through automatic calculation scripts (see Appendix A) in SQL queries with final and intermediate results stored in corresponding tables automatically. A program for generating the basic and normalized profiles to display in batch format was also developed so that results could be presented visually (see Appendix B).

STID	Month	NPK_NADAWD	NPK_NADAID	LENGTH_BETWEEN	AREA_BETWEEN
ACME	1	0.27	-0.87	1.14	1.06
ACME	2	0.42	-0.57	0.98	1.00
ACME	3	0.90	-0.11	1.01	0.81
ACME	4	1.00	0.40	0.60	0.25
ACME	5	0.29	0.60	-0.32	0.76
ACME	6	-0.32	0.88	-1.20	1.49
ACME	7	-0.79	1.00	-1.79	1.71
ACME	8	-0.97	0.66	-1.63	1.29
ACME	9	-0.76	0.19	-0.95	0.41
ACME	10	-0.18	-0.37	0.19	0.58
ACME	11	0.13	-0.83	0.97	0.98
ACME	12	0.01	-0.98	0.99	1.06
Area Total					11.40

Table 4.9 Calculation of Area Differences between Two Curves for ACME

4.4 Mapping the Annual *CIWS*

Once the complementarity index, ***CIWS***, was calculated for all targeted locations, a map to display the complementarity index for Mesonet sites was created. Because the calculated ***CIWS*** values are point-based data, interpolation techniques were used to generate a map to display the ***CWS*** level across sampled regions based on the sampled sites.

Figure 4.11 shows the ***CIWS*** values across Oklahoma after kriging (Oliver and Webster 1990) all obtained ***CIWS*** values of the Mesonet sites using Approach 1 described in section 4.2. The map indicates that the locations having a higher level of annual ***CIWS*** values are mostly located in eastern Oklahoma, while the sites on the west side of Oklahoma have a relatively lower annual ***CIWS***. This is interesting because the resources of wind and solar energy are each greater in the western part of the state than the eastern part with the greatest complementarity occurring in eastern Oklahoma. In next chapter, spatial analysis was conducted to further explore this mapped pattern.

4.5 Cross Verification from Different Quantification Approach

Section of 2.1.3 of this dissertation introduced an approach developed by Sahin (2000) based on Pearson correlation. Although the present study does not favor Sahin's approach because of its limitation of requiring the normalized distribution of wind and solar profile data, Sahin's approach was still applied to Oklahoma data to check if the computed complementarity values show similar spatial tendencies while used on these non-normal data. The formulas used for computation was listed in section 2.1.3.

The computed results of ***CIWS*** for Mesonet sites were also kriged. Figure 4.12 is the resulting map of ***CIWS*** values across Oklahoma based on Sahin's approach. This map shows a general correspondence with Figure 4.11. Higher levels of complementarity between wind and solar energy arise in eastern Oklahoma, and less in the west.

The results from the experimental application of Sahin's approach helps to confirm that the quantification approach for deriving ***CIWS*** values developed by this study is reasonable, and it strengthens confidence that the approach could be extended to more areas when needed.

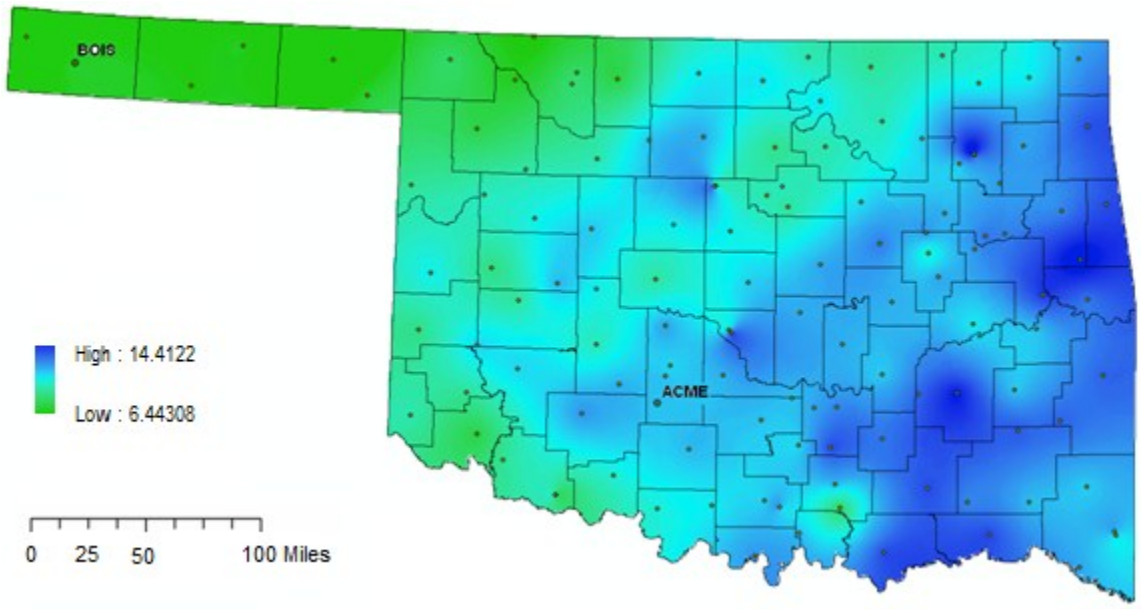

Figure 4.11 Kriged Map of Annual ***CIWS*** Values for Oklahoma

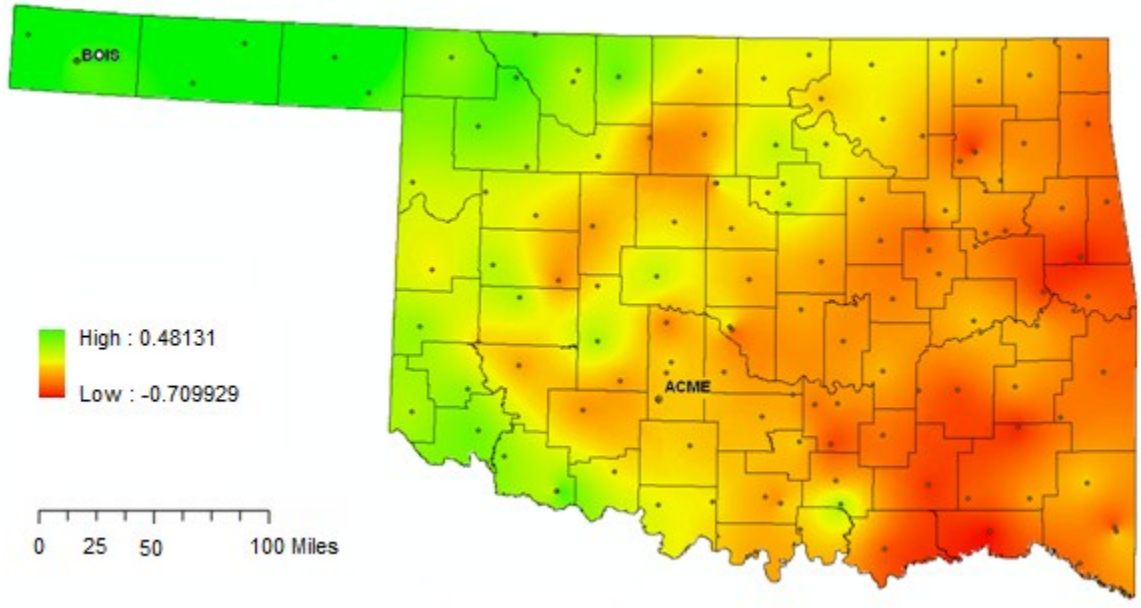

Figure 4.12 Kriged Map of Annual ***CIWS*** based on Sahin's Approach

4.6 A Glimpse of the Calculation of Daily *CIWS*

The approach described above can be altered to calculate the ***CIWS*** value for each site within a daily cycle. In contrast to deriving the ***CIWS*** values within the annual cycle, the area between two curves representing the average variations of wind and insolation power density within 24-hour period is defined as the diurnal ***CIWS*** value for the site. The distinct sub-period unit chosen for the diurnal calculation could be in hour or minute.

In the case of the Oklahoma Mesonet, a 5-minute interval was used as the sub-diurnal unit considering the availability of 5-minute interval data. In total, there are 288 5-minute periods in the daily cycle. Each 5-minute averaged wind power density (abbreviated as *M5AWD*) and 5-minute averaged insolation power density (abbreviated as *M5AID*) in the daily cycle needed to be calculated first to derive the daily ***CIWS***, just as the *DAWD* and *DAID* were calculated before deriving annual ***CIWS***. The original raw data needed for calculating Oklahoma *M5AWD* and *M5AID* was same as the imported raw data used in 4.1.1 for calculating *DAWD* and *DAID*. Other steps involved in calculating the annual ***CIWS*** were also correspondingly modified to obtain the daily ***CIWS***. In the following part, calculations of ***CIWS*** for the day April 15 of year 2000 for all Mesonet stations were chosen to demonstrate the general steps involved. Appendix C contains the SQL scripts used to calculate the daily ***CIWS*** for Oklahoma Mesonet stations based on Mesonet data. Considering the great similarity to deriving annual ***CIWS***, a relatively concise introduction of the procedures is presented below.

4.6.1. Calculation of *M5AWD* and *M5AID*

In this part of study, to build the daily variation profile of wind and insolation, for each of the daily 288 5-minute intervals, the averaged wind power density for the 5-minute *M5AWD* and averaged insolation power density for the 5-minute interval *M5AID* were calculated first. The height used to observe the *M5AWD* and *M5AID* was still set to 50m. Therefore, an extrapolation of power density from 10m to 50m was also needed. Different from the annual ***CIWS***

calculation, the sub-period unit used for the daily ***CIWS*** in this study was also the basic data recording interval of Mesonet data. Therefore, there is only one simple approach applicable to calculate the averaged 5-minute wind power density *M5AWD*, which is to apply formulas on each measurement record directly.

To study a sample day, all original data records for April 15 of 2000 for different sites were withdrawn from the raw data table in SQL database to a new table. Then, the following formulas were applied on the raw data of each site including variables like *TAIR*, *WSPD, PRES, TA9M, SRAD*, and *ELEV*:

$$WPD5min10m = 0.5*(PRES*100/(287*(TA9M+273)))*\text{power}(WSPD, 3) \quad \textit{(Equ. 4.13)}$$

$$WPD5min50m = WPD5min10m*\text{power}(5, 3/7) \quad \textit{(Equ. 4.14)}$$

$$M5AWD = WPD5min50m \quad \textit{(Equ. 4.15)}$$

$$M5AID = SRAD \text{ of same 5-minute time interval at April 15 of 2000 as wind} \quad \textit{(Equ.4.16)}$$

Where the *PRES*, *TA9M* and *WSPD* were all from the original Mesonet data, *WPD5min10m* and *WPD5min50m* are the estimated wind power density every 5-minute at 10m and 50m respectively for the day of April 15, 2000; the unit used for *WPD5min10m, WPD5min50m,* and *M5AWD* is watts/m^2. *SRAD* is the original 5-minute solar radiation data recorded at 2m by the Mesonet. This study ignores the vertical variation of solar radiation and assumes solar radiation is the same at the height of 2m and 50m for each site. Therefore, the *SRAD* also represents the average solar radiation at the height of 50m for each 5-minute time interval for April 15 of 2000 at each location. The unit used for both *SRAD* and M5*AID* was watts/m^2.

4.6.2. Building Daily Basic Profiles of M5AWD and M5AID

After the *M5AWD* and *M5AID* were calculated for April 15 of 2000 for all sites, basic profiles describing the diurnal variations of wind and insolation could be built. The complementarity of wind and insolation during daily cycles can be visually indicated using the basic profiles. Figures 4.13 and 4.14 are the basic profiles drawn for ACME and BOIS stations on April 15 of 2000,

which show the diurnal variation of wind and insolation power density and the complementary features in the two stations. The diurnal basic profile for each site was then normalized through a two-step normalization procedure similar to that applied to derive annual ***CIWS***.

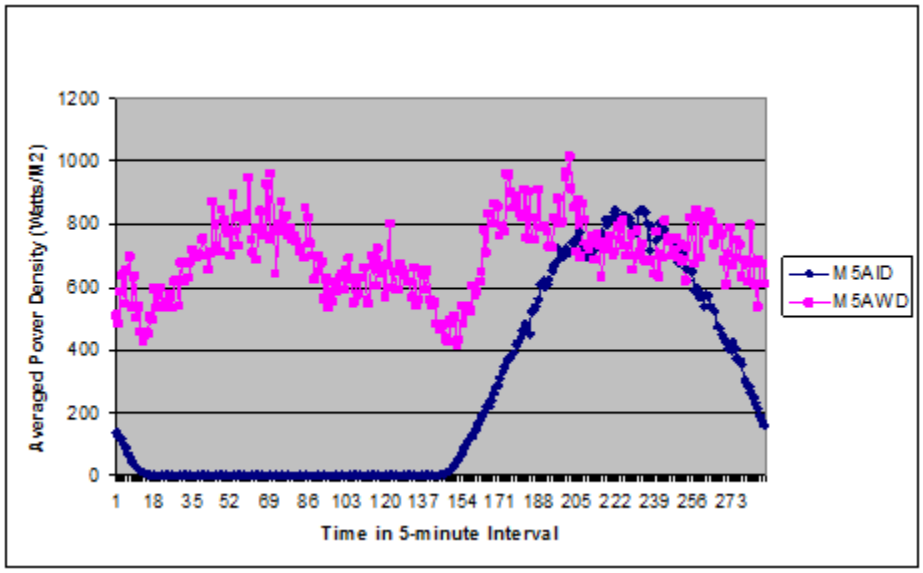

Figure 4.13 Daily Wind and Insolation Power Density for ACME at April 15 of 2000

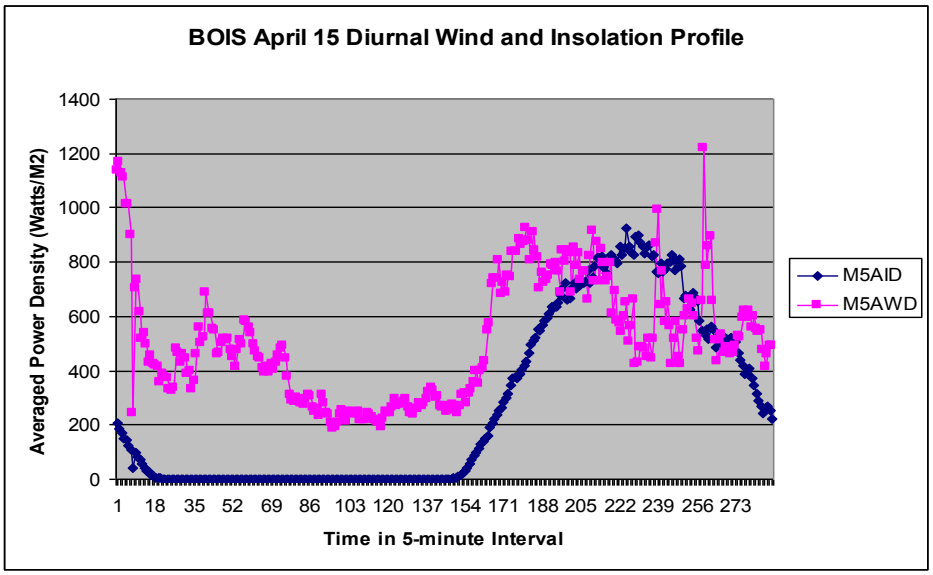

Figure 4.14 Daily Wind and Insolation Power Density for BOIS at April 15 of 2000

4.6.3. Normalization of Diurnal Basic Profiles

To standardize the diurnal basic profiles, similar to that of the annual ***CIWS***, the two-step normalization procedures by daily averaged power density and by peak values were conducted.

4.6.3.1 First-Step Normalization by Daily Averaged Wind and Insolation Density

The first step of normalization by daily average wind and insolation power density was performed on each *M5AWD* and *M5AID* in a diurnal period. The detailed procedures are as following:

1. Calculate the daily averaged *M5AWD* (abbreviated as *DAMWD*) and daily averaged *M5AID* (abbreviated as *DAMID*) based on the obtained *M5AWD* and *M5AID* for 288 intervals in a daily cycle.
2. Apply the formula below to calculate the percent of each *M5AWD* and *M5AID* of their daily averaged value of *DAMWD* and *DAMID*: PCNT_M5AWD=M5AWD/DAMWD and PCNT_M5AID=M5AID/DAMID.
3. Subtract 1 from the percentage of *PCNT_M5AWD* and *PCNT_M5AID* to determine how much each *M5AWD* and *M5AID* values differ from their respective daily average levels. The results from this step are named *NA_M5AWD* and *NA_M5AID*. The formulas applied are: *NA_ M5AWD =PCNT_ M5AWD* -1 and *NA_M5AID =PCNT_M5AID* -1.

For the example of Mesonet station ACME, Figure 4.15 shows the resulting profile after this step of normalization for April 15 of 2000.

4.6.3.2 Second-Step Normalization by Daily Peak Wind and Insolation Density

In the second stage of normalization, the results from the first-step normalization of *NA_ M5AWD* and *NA_ M5AID* for each 5-minute interval were normalized again using the absolute maximum value of *NA_ M5AWD* and *NA_ M5AID* in the cycle respectively. The detailed steps are:

1. Determine the *NA_M5AWD* and *NA_ M5AID* value which has the highest absolute value in daily cycle and name them as *PK_NAM5AWD* and *PK_NAM5AID* correspondingly.
2. Calculate how much each *NA_M5AWD* and *NA_M5AID* differ from their absolute peak value by dividing the *NA_M5AWD* and *NA_M5AID* for each 5-minute interval of April 15 of 2000 of the site by the maximum absolute values *PK_NAM5AWD* and *PK_NAM5AID* respectively. The results are named as *NPK_NAM5AWD* and *NPK_NAM5AID*. The formulas applied are *NPK_NAM5AWD=NA_M5AWD/PK_NAM5AWD* and *NPK_NAM5AID =NA_ M5AID /PK_NAM5AID*.

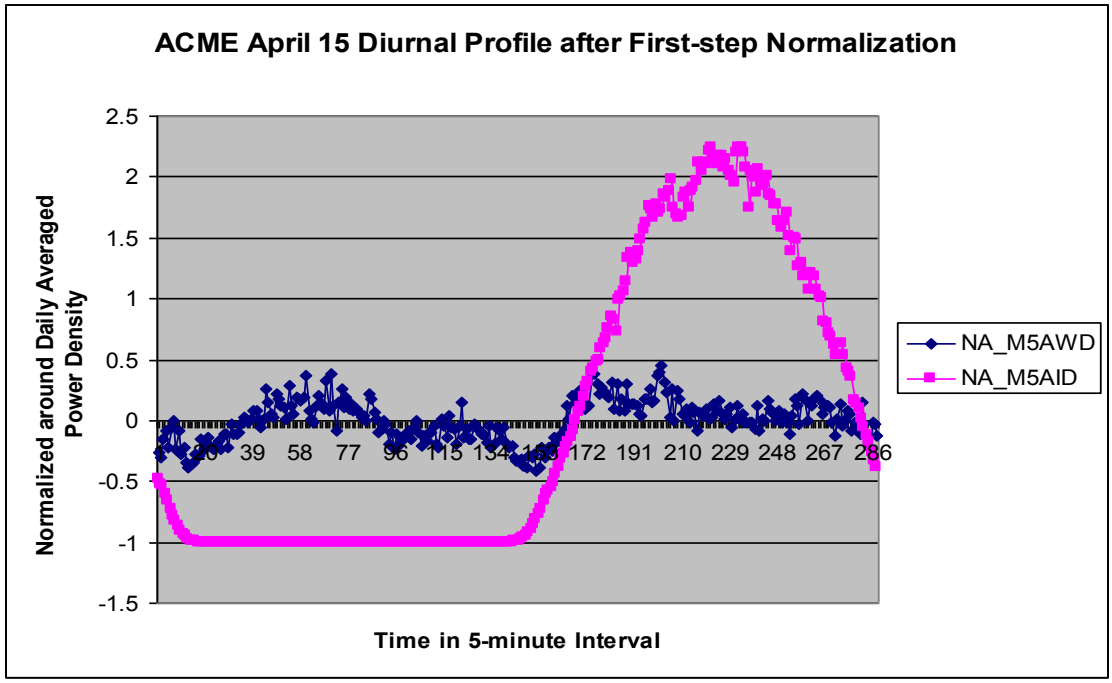

Figure 4.15 ACME Diurnal Profile at April 15 of 2000 after First-step Normalization

The result after this second step of normalization for ACME on April 15 of 2000 is shown in Figure 4.16, in which both normalized power density for wind and insolation falls within the range of -1 and 1. Different from the basic and normalized profiles for the annual ***CIWS***

calculation, the duration of time in diurnal profiles become 288 instead of 12 because the sub-period unit was 5-minute for the daily case. Therefore, the maximum possible area between the two normalized curves of wind and insolation for the diurnal cycle is 288*2= 576, different from the one for the annual cycle which is 12*2=24. To make the ***CIWS*** index comparable between annual and diurnal cycles, a normalization of calculated areas on their maximum ranges for annual and diurnal cycle respectively was conducted. Part 4.6.5 gives more discussion of this.

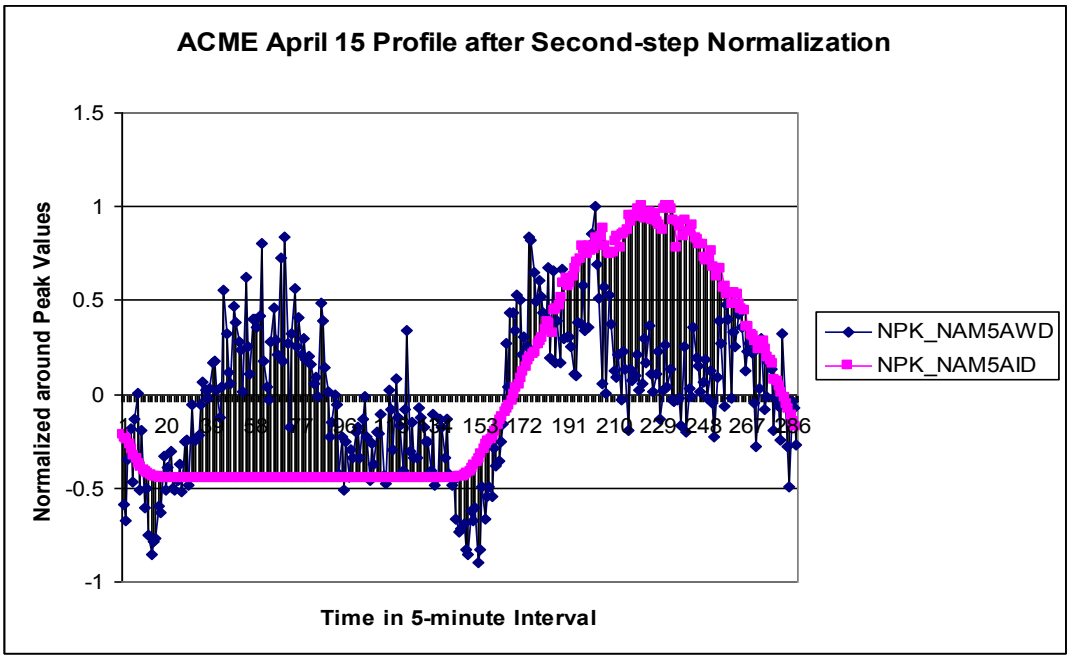

Figure 4.16 ACME Diurnal Profile of April 15 of 2000 after Second Normalization

4.6.4. Calculating Daily *CIWS* and Mapping the Results

As in the case of calculating the annual ***CIWS***, the area between two normalized curves represents the variation of complementary wind and insolation power density in daily cycles, and is estimated through adding each small triangle and trapezoid between the two curves. The following steps describe the detailed procedures:

1. In the charts drawn based on second normalized profiles, drop lines between the two points representing the normalized results of *NPK_NAM5AWD* and

NPK_NAM5AID for each site.

2. Calculate the area of each triangle and trapezoid formed by the two curves and newly dropped lines.
3. Summarize all estimated areas between the two curves from step 2 and the final summed value is the daily ***CIWS*** for the site.

For the example of Mesonet ACME station, the obtained daily ***CIWS*** of April 15, 2000 is 116.92. The map created for daily ***CIWS*** for all Mesonet Sites on April 15 of 2000 is shown in Figure 4.17. Compared with Figure 4.11 for Oklahoma annual ***CIWS***, this kriged map indicated a different spatial tendency of daily ***CIWS*** from annual ***CIWS***, where the north western and north eastern parts of Oklahoma show relatively higher daily complementarity of wind and insolation than south eastern part on April 15 of 2000. Two other maps of daily ***CIWS*** were also generated by applying the procedures presented in this section to Mesonet data of July 15 and December 15 of 2000 respectively (Figure 4.18 and Figure 4.19).

4.6.5 Comparison of Daily and Annual *CIWS*

As mentioned earlier, since the ranges of the annual and daily ***CIWS*** values in the quantification approach described above are different, a simple normalization is needed upon resulted ***CIWS*** values to make the calculated ***CIWS*** values standardized and comparable for different temporal spans. In this study, the result of annual ***CIWS*** is between 0 and 24, and the result for daily ***CIWS*** is between 0 and 576. A normalization based on the corresponding maximum range values can be conducted on each ***CIWS*** value. For example, in the case of Oklahoma, annual ***CIWS*** will be normalized by 24 and daily ***CIWS*** will be normalized by 576 for each site in this study. With this normalization, ***CIWS*** values for any span of time falls into the same range of 0 and 1. The higher of this normalized value, the better complementarity between wind and insolation is implied.

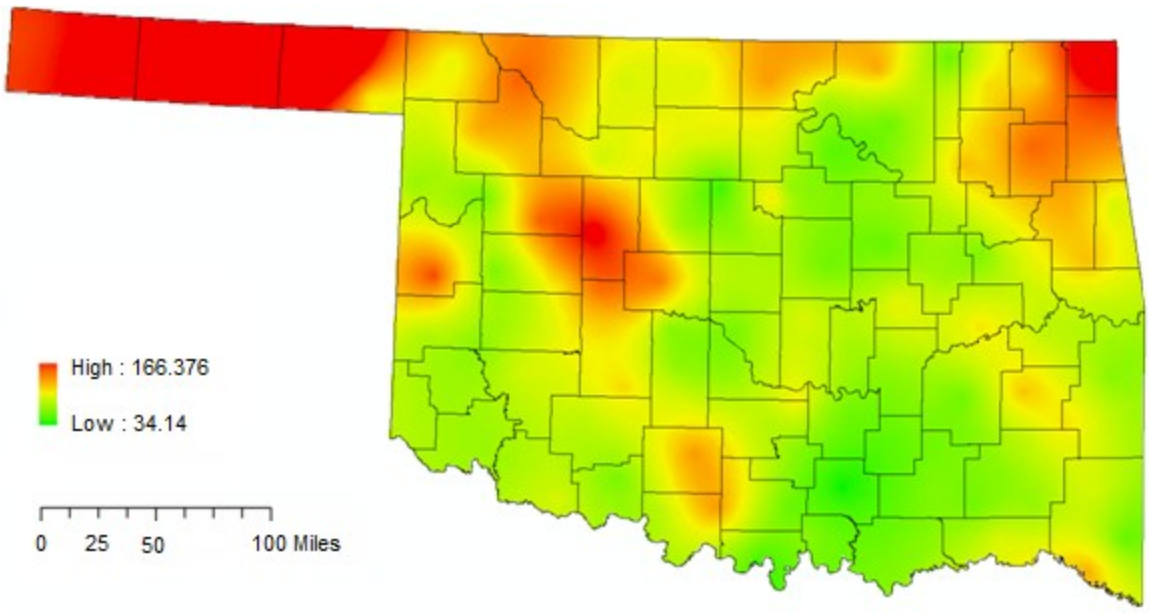

Figure 4.17 Kriged Daily ***CIWS*** of April 15 of 2000 for Oklahoma

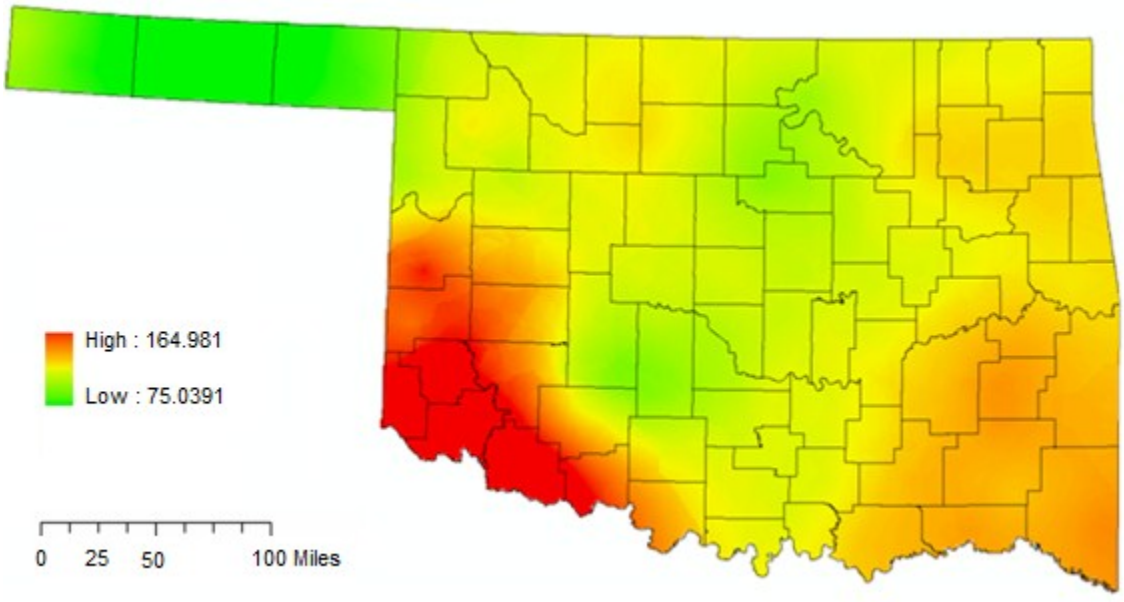

Figure 4.18 Kriged Daily ***CIWS*** for July 15 of 2000 for Oklahoma

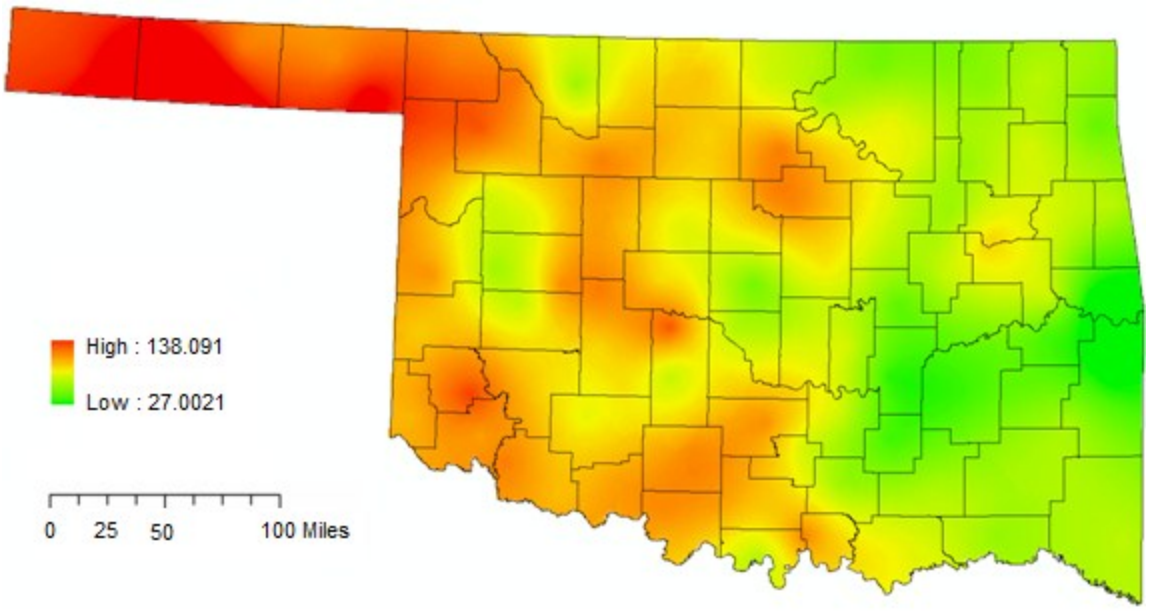

Figure 4.19 Kriged Daily ***CIWS*** for Dec. 15 of 2000 for Oklahoma

For the Oklahoma Mesonet station ACME, the daily ***CIWS*** value after above normalization, for the day of April 15 of 2000 is 69.79/576 = 0.1212, for the day of July 15, 2000 is 89.33/576=0.155, and for the day of December 15, 2000 is 71.77/576=0.125, while the annual ***CIWS*** for ACME is 11.405/24 = 0.475. Obviously, there is a temporal variation of the daily ***CIWS***. Besides, at station ACME, long term annual ***CIWS*** is better than the daily ***CIWS*** indicated in the three sampled days in year 2000. This conforms to what was found by Takle and Shaw (1979) in their study. Whether this is a universal feature needs more verification .

The spatial variation of daily ***CIWS*** on April 15, July 15, December 15 of 2000 and the annual ***CIWS*** across Oklahoma can be visualized through the kriged map in Figures 4.17, 4.18, 4.19, and 4.11. Differing spatial distributions are apparent in the two sets of maps. For instance, in Figure 4.17, daily ***CIWS*** values increase from east to west for daily ***CIWS*** on April 15 of 2000, but the opposite pattern occurs for annual ***CIWS*** on Figure 4.11. This implies that in Oklahoma, the spatial distribution of ***CIWS*** values for different days is inconsistent from day to day; there must be more days showing distribution patterns close or similar to annual ***CIWS*** maps that

distributions of annual ***CIWS*** can be completely different from some of the days. Figures 4.18 and 4.19 are kriged maps for daily ***CIWS*** of July 15 and December 15 of 2000 respectively. Figure 4.18 for July 15 of 2000 indicates the highest values of daily ***CIWS*** are mostly located in the southwestern part of Oklahoma, with eastern Oklahoma showing the second. Figure 4.19 indicates the highest ***CIWS*** values expand from the northwestern part of the state towards the eastern part of Oklahoma on December 15 of 2000. Considering the annual ***CIWS*** is some kind of combined results of daily ***CIWS*** for the year, it can be assumed that if maps of daily ***CIWS*** are created for each day of the year, there should be a dominance of maps indicating a high to low level of ***CIWS*** from east to west than those showing a different distribution. Because of time limitations, this is not fully confirmed in this study, which could be examined through generating actual diurnal ***CIWS*** maps for each day or more sample days in a year in Oklahoma.

The different spatial patterns of daily and annual ***CIWS*** values for the same region are actually useful for analyzing the impacts of geographic factors on the nature of ***CWS***, assuming that geographic factors affect the daily and annual ***CWS*** in the same way, or via the same mechanism. This will be discussed further in the next chapter.

4.7 Explorative Spatial Analysis on Complementarity Index

Exploratory spatial data analysis (ESDA) is explorative data analysis for the purpose of discovering spatial patterns in an intuitive and visualized way (De Smith, Goodchild and Longley, 2007). There are multiple ways to conduct ESDA. But simple statistical analysis and using GIS interpolation techniques are sufficient for this study. A simple statistical analysis of resulting ***CIWS*** values indicates the average annual ***CIWS*** for Oklahoma is 10.99, about 46 percent of the theoretical maximum value of 24.0; the standard deviation is 1.5. Approximately 57 percent of the sites have above-average ***CIWS*** values. Also, the annual complementarity is spatially skewed with highest ***CIWS*** values falling in the east where both wind and solar energy are less abundant.

The interpolated maps of the ***CIWS*** values tell the spatial features of ***CWS***. In Oklahoma, the maps for both the annual and diurnal time periods indicate the complementary nature of wind power and insolation varies from place to place; spots with extreme values are outlined clearly; spatial patterns for daily and annual ***CIWS*** are different as shown by the map for the diurnal ***CIWS*** values of April 15 of 2000 (see Figure 4.17), indicating relatively higher ***CIWS*** in the middle to western part of Oklahoma while the annual ***CWS*** is relatively higher in eastern Oklahoma (see Figure 4.11).

However, to better explore the causes of the spatial heterogeneity of the ***CWS***, and to help predict the ***CIWS*** in various space and time dimensions, further studies other than the ESDA are usually needed. The next parts of the study link various geographic factors related to ***CWS*** and investigate their influences on the spatial variations of the ***CWS***.

CHAPTER V

GEOGRAPHIC FACTORS AFFECTING THE COMPLEMENTARITY

As shown in the case of Oklahoma, the nature of complementarity of wind and insolation (***CWS***) varies over space. Considering both wind and solar radiation are geographic phenomena affected by various geographic factors, it is logical to believe that the ***CWS*** is inherently linked to various geographic factors. However, geographic factors are a huge and complicated collection. They are embedded in each geographic location and vary over space. In addition, they are usually interdependent and could both be the causes and the results of different kind of phenomena on the earth's surface at the same time.

An investigation of the spatially varying effects of geographical factors on ***CWS*** is useful for both theoretical and practical reasons. From a theoretical perspective, geographic processes and variables as well as their impacts on ***CWS*** are likely to be different at different places. Examining the variations of geographic factors and their potential associations with the nature of ***CWS*** might help to develop a better understanding of underlying geographic processes. From a practical standpoint, finding geographic factors that are important to local areas might help to better predict the ***CWS*** level locally and temporally and make it possible to build a numeric model for prediction. Additionally, through analyzing the spatial variation of relationships helps uncover those relevant geographic factors for improving model performance.

To identify key factors impacting the ***CWS***, this study went through three steps. First, based on

literature and past studies regarding the effects of different geographic factors on wind and insolation, enlist those possible factors linked to wind and insolation as potential independent variables affecting the ***CWS***. Second, statistical methods like simple Pearson correlation analysis and stepwise regression analysis are used to find key factors impacting on the ***CIWS***. Third, if there were no consistent marked out factors related to ***CIWS*** found, principal components analysis is used to compress multiple geographic variables and to reduce the multicollinearity among variables. Results from Pearson correlation analysis and stepwise regressions are used to assist with identifying the principal components and naming each principal dimension from the principal components analysis (PCA).

5.1 Determination of Geographic Factors Influencing the *CWS*

Wind and solar radiation are two major climatological phenomena on earth. Three categories of factors are identified as having a major impact on them: 1) climate - atmosphere, 2) timing - decided by the relative locations between the Sun and the earth, and 3) the terrain conditions. In this study, all three groups of factors are referred to as geographic factors or spatial factors, because they are geographic phenomena, affected by location and affecting other spatial conditions.

It is speculated that if there is perfect complementarity between the wind and solar power with time in various places, then the combination of the above three categories of driving forces in each place should play inverse impact on wind or insolation received at a location. If the complementarity only exists to some extent, then the combination of these driving forces may only make converse impact to some extent. By examining the three groups of factors in different locations, their relationship with wind and solar power, and their relationship with the variation of complementarity nature, it might be better known how geographic factors influence the ***CWS***.

In the three categories of geographic factors identified above, time is unique. It is also a type of

space since it is determined by the relative location between the Sun and the earth. Because of its highly dynamic nature, time is relatively difficult to model. A panoramic model including full time spans with varying relative relations between the earth and the Sun requires more dynamic data collection and complex computation modeling, and thus is excluded by this study. Instead, this study picked two temporal cycles - annual and diurnal - to examine the ***CWS***. The absolute location of sampled sites, plus the averaged climatic parameters and relatively static terrain conditions, might be considered to indirectly reflect the impacts of relative relations between the earth and the Sun. Therefore, in this study the geographic factors linked to the complementary relationship of wind and insolation are categorized into three types: locational factors, climatic factors, and terrain factors.

Each of the above three categories includes some representative variables. The list of variables is not exhaustive, but attempts to include as much as is practical for the preliminary stage of the study. In the case study of Oklahoma, 57 variables were identified; the numeric measurement of each variable for each sampling site is recorded in one table.

5.1.1 Spatial Scoping of Impacting Geographic Factors

The hallmark of all geographic phenomena are continuity and contingency in space, which makes scale of study an issue that could impact analytical results and conclusions. Scales in this study could range among micro, meso and macro scales with no definite boundaries between adjunct scales. Because of the complexity of natural phenomena, impacting factors and processes can cross multiple levels of scales and vary within each. The larger the scale used, the more complicated the interrelationships between scale levels might be. Although the scale of investigated spatial factors affecting the ***CWS*** involves any of the above ranges, considering time limitations and the convenience of data collection, this study focuses on the micro to meso scale perspective to study the influences of geographic factors on ***CWS***, leaving the full-scale exploration of this relationship for the future.

To mitigate the uncertainty from the scale factor in this study, original data collection of various geographic variables covers both micro and meso scale, leaving the variable dimension reduction to statistic tools like principal components analysis. For instance, for geographic variables with varying spatial scope, measurements are collected within different spatial ranges, such as aspect within 1 kilometer, 5 kilometer and 10 kilometer of a Mesonet site respectively. For variables varying within temporal scope - such as temperature, rain, and pressure - measurements are averaged to different seasons to increase temporal coverage. All measurements are point-based. Details of data contained in each category are described in the following section using the example of Oklahoma.

5.1.2 Variables Contained in Corresponding Categories of Geographic Factors

In the case of Oklahoma, there were 57 variables identified in three major categories of geographic factors. Table 5.1 shows the abbreviation and full name of variables for each of the three categories.

As shown in Table 5.1, three variables are included in the location related geographic factors of each Mesonet site: latitude, longitude and elevation. They define the absolute location of each site on the earth's surface. Since these location variables are relatively fixed in macro background, to some extent they reflect the influence of macro impacts on the ***CWS***. They are also the most basic and important geographic factors in any sense.

Variable numbers 4 to 22 and number 52 to 57 in Table 5.1 are some terrain factors associated with each Mesonet site, including linear distance to Gulf of Mexico, aspect within 1km, 5km and 10km range, slope within 1km, 5km and 10km, curvature within 1km, 5km and 10km, hillshade within 10km, relative elevation within 5km and 10km toward east, south, west, and north respectively, and land use and land cover. The latter one includes percentage of water surface, residential use, pasture, barren soil, shrub, and forest within 10km of each site.

No	Abbreviation	Full Name	No	Abbreviation	Full Name
1	LAT	Latitude	30	PRESWINT	Average pressure in winter
2	LON	Longitude	31	RELHSPRI	Relative humidity in spring
3	ELEV	Elevation	32	RELHSUMM	Relative humidity in summer
4	DISTANCE	Distance to Gulf Mexico	33	RELHWINT	Relative humidity in winter
5	ASPCT1K	Aspect within 1km range	34	RELHFALL	Relative humidity in fall
6	ASPCT5K	Aspect within 5km range	35	TAIRSPRI	Average temperature in spring
7	ASPCT10K	Aspect within 10km range	36	TAIRSUMM	Average temperature in summer
8	SLOPE1K	Slope within 1km range	37	TAIRFALL	Average temperature in fall
9	SLOPE5K	Slope within 5km range	38	TAIRWINT	Average temperature in winter
10	SLOPE10K	Slope within 10km range	39	SPRIMAX	Maximum daily temperature in Spring
11	CURVAT1K	Curvature within 1km range	40	SPRIMIN	Minimum daily temperature in Spring
12	CURVAT5K	Curvature within 5Km range	41	SPRIDIFF	Average daily temperature difference in Spring
13	CURVA10K	Curvature within 10Km range	42	SUMMMAX	Maximum daily temperature in Spring
14	HILSH10K	Hill shade within 10K range	43	SUMMMIN	Minimum daily temperature in Summer
15	DFEV5KE	Relative elevation 5km east	44	SUMMDIFF	Average daily temperature Difference in Summer
16	DFEV5KS	Relative elevation 5km south	45	FALLMIN	Fall minimum daily temperature
17	DFEV5KW	Relative elevation 5km west	46	FALLMAX	Fall max daily temperature
18	DFEV5KN	Relative elevation 5km north	47	FALLDIFF	Average daily temperature difference in fall
19	DFEV10KE	Relative elevation 10km east	48	WINTMAX	Winter maximum daily temperature
20	DFEV10KS	Relative elevation 10km south	49	WINTMIN	Winter minimum daily temperature
21	DFEV10KW	Relative elevation 10km west	50	WINTDIFF	Average daily temperature Difference in winter
22	DFEV10KN	Relative elevation 10km north	51	CINDX	Average Annual Cloud Index
23	RAINSPRI	Average rain in Spring	52	W_PRCT	Water surface percentage in 10km
24	RAINSUMM	Average rain in Summer	53	R_PRCT	Residential percentage in 10km
25	RAINFALL	Average rain in Fall	54	P_PRCT	Pasture percentage in 10km range
26	RAINWINT	Average rain in Winter	55	B_PRCT	Barren surface percentage in 10km
27	PRESSPRI	Average pressure in Spring	56	S_PRCT	Shrug percentage in 10km range
28	PRESSUMM	Average pressure in Summer	57	F_PRCT	Forest percentage in 10km range
29	PRESFALL	Average pressure in Fall			

Table 5.1 Geographic Factors Investigated for Mesonet Sites

Climate-atmosphere related variables investigated include the averaged rainfall, averaged air pressure, averaged relative humidity, and averaged air temperature for each site in each of the four seasons, as shown in Table 5.1 variable numbers 23 to 38. Maximum and minimum air temperatures and temperature differences in each season for each site are also identified as possible factors. These factors are temporally varied, and therefore are seasonally averaged to mitigate the impacts of average numbers by longer periods and elucidate mesoscale climatic characteristics. Another factor, variable number 39, the average yearly cloud index (abbreviated as CINDX), defined by formula *Equ. 5.3* in this study, was speculated to be an important climate-atmosphere factor in shaping the temporal and spatial variation of the ***CWS***, considering cloudiness is a special climatic phenomenon and usually related with transformation of atmosphere condition. The presence and features of clouds directly affect both wind and insolation.

5.1.3 Data Collection and Derivation

In this study, most data, especially location and climate-atmosphere related data regarding Mesonet sites, are directly collected from or calculated based on information published on the official Mesonet website (MESONET, 2008), They have been quality assured (Fiebrich, et al., 2006; McPherson, et al., 2007). Latitude, longitude and elevation data are provided by the Mesonet site through downloadable Excel files and GIS compatible shape-files. Data like average rainfall, air pressure, air temperature in different seasons, and yearly cloud index for each site are calculated based on 5-minute interval Mesonet data using SQL queries in the SQL server (see Appendix A, C and D).

Because of the availability of the high-resolution temporal data of the Mesonet, it becomes much easier to calculate the yearly cloud index of each site in Oklahoma. This might be impossible in many other places because of the lack of quality data like what the Mesonet provides for Oklahoma. SQL scripts developed for deriving the *CINDX* in SQL server database are included in

Appendix D. The major formulas for calculating the yearly cloud index of each site is as follows:

Average Yearly SRAD of Each Site = (Sum of Yearly SRAD)/ (Number of Years Averaged) *(Equ.5.1)*

Average Yearly Maximum SRAD of Each Site = (Sum of Yearly Maximum SRAD)/ (Number of Years Averaged) *(Equ.5.2)*

CINDX = (Average Yearly SRAD of each site)/ (Average Yearly Maximum SRAD) *(Equ.5.3)*

Terrain-related data were withdrawn from several digital maps, including the Mesonet shape-files, a projected Oklahoma map, the most recent 30 meters digital elevation model (DEM), and national landcover and landuse data published in 2001 (NLCD, 2012). The Oklahoma map used in this study was downloaded from the OCGI site (OCGI, 2008). The DEM map was obtained from the USGS site (USGS, 2008). Tools provided in Raster Surface Analysis of ArcToolBox in ArcGIS version 9.0, such as curvature, hillshade, slope and aspect calculation are used for obtaining terrain data for each site, and the zoning area calculation tool were used to calculate the percentage of each type of land use type for each Mesonet site.

5.2 Pruning of Geographic Factors through Exploratory Analysis

Complementarity between wind and insolation as a geographic phenomenon could be caused by a wide range of geographic factors and complicated spatial processes. Linking the variations of the ***CWS*** with potential spatial factors through spatial statistics provides a way to identify those hidden key factors and processes.

Before further modeling efforts are carried out in this study, preliminary analysis such as simple correlation analysis, stepwise regression, and principal components analysis, from relatively simple to relative complicated, were attempted in succession on data representing the dependent and independent variables, expecting that some specific factors were marked out from the long list of potential factors as significant ones for modeling. However, no consistent results were obtained from different statistical methods, and high multicollinearity was found in variables that

it is difficult to explicitly identify individual factors as explanatory variables. This leads to the use of principal components analysis to determine independent predictors. Various exploratory statistical analysis used in this step helped to prune the explanatory variables, isolate and identify those key factors affecting the ***CWS***, and helped to prepare principal components used in further modeling of the relationship between ***CWS*** and various geographic factors. It also aided in examining and naming major dimension factors after a model was built. SPSS (UCLA-ATS, 2011) is used as the major statistic tool in this study to conduct the simple correlation analysis, stepwise regression analysis, and principal components analysis.

5.2.1 Simple Bivariate Correlation Analysis

The simple correlation analysis relates ***CIWS*** values with data obtained for each geographic variable by calculating the bivariate Pearson correlation coefficient using SPSS software. As shown in Table 5.2, 16 variables positively correlated with ***CIWS*** with a correlation value greater than 0.5. They are listed last in Table 5.2, including the location's longitude (LON), minimum air temperature averaged for winter, fall and spring season (WINTMIN, FALLMIN, and SPRIMIN), air pressure averaged for each of the four seasons (PRESSUMM, PRESSPRI, PRESFALL and PRESWINT), averaged relative humidity level for spring, summer and fall season (RELHSPRI, RELHSUMM and RELHFALL), averaged temperature for fall season and winter season (TAIRFALL and TAIRWINT), averaged rainfall in fall and winter season (RAINFALL and RAINWINT), and percentage of forest within 10 kilometers (F_PRCT). The results imply that longitude, seasonal temperature difference, seasonal average air pressure, seasonal average air temperature, seasonal rainfall or humidity level, and cloud index are some relatively important factors that may positively affect the ***CWS***. Except the variable LON - longitude and F_PRCT - percentage of forest coverage, most of the factors positively and significantly correlated with ***CWS*** come from the category of climate-atmosphere related.

In Table 5.2, 6 variables that are negatively correlated with ***CIWS*** with correlation values smaller than -0.5 are also listed, including average air temperature difference for spring, winter, fall and summer (SPRIDIFF, WINTDIFF, FALLDIFF and SUMMDIFF), distance to Gulf of Mexico (DISTANCE), and elevation of each site (ELEV). This means variables like seasonal average air temperature difference, distance to Gulf of Mexico, and the elevation of each site are some key factors that are inversely related to the ***CWS*** of each site. Again, most of them are climate-atmosphere related.

Variable	Corr_CIWS		Variable	Corr_CIWS
SPRIDIFF	-0.713		PRESFALL	0.581
WINTDIFF	-0.696		PRESSPRI	0.582
DISTANCE	-0.672		TAIRWINT	0.586
ELEV	-0.662		RAINFALL	0.587
FALLDIFF	-0.584		TAIRFALL	0.596
SUMMDIFF	-0.559		RELHSUMM	0.598
CINDX	0.486		SPRIMIN	0.646
RELHFALL	0.526		RELHSPRI	0.651
F_PRCT	0.543		FALLMIN	0.659
RAINWINT	0.565		WINTMIN	0.693
PRESSUMM	0.580		LON	0.727
PRESWINT	0.580			

Table 5.2 Simple Pearson Correlation between Various Factors and ***CIWS***

By further examining the paired correlation of some specific variables with ***CIWS***, more detailed information could be obtained. For instance, the relationship between the annual cloud index (CINDX) and ***CWS*** was exposed through the tendency chart of CINDX and ***CIWS***. Figure 5.1 charts 13 years' average cloud index values and the ***CIWS*** values for each site. Obviously the two lines show great correspondence in general trend although the correlation coefficient between the two is around 0.49. Considering the impact from replacing some missing data using the designated formula in calculating cloud index, the actual bivariate correlation value might be a bit higher.

Figure 5.1 Correlation shown by Tendency Lines of Annual Cloud Index and ***CIWS***

Another example is the co-varying tendency of the variable SPRIDIFF and ***CIWS***. The high negative correlation value between SPRIDIFF and ***CIWS*** implies that if a location has a relatively high daily temperature difference in the spring, it could mean a low annual ***CWS*** level for this location.

In general, based on the information in Table 5.2, it seems that both locational and climatic factors play important roles in shaping the complementarity of wind and insolation. Influences from terrain factors except the percentage of forest, distance to Gulf of Mexico, and elevation, which are also moisture-related factors, are relatively minor. Combined with the results in this simple correlation analysis, future studies of the relationship between geographic factors and ***CWS*** could be fruitful.

5.2.2 Backward Stepwise Regression Analysis

Backward stepwise regression is another method of exploratory analyses. It begins with a full model using all variables and then variables are eliminated from the model in an iterative process. According to Donoho and Johnstone (1994), the fit of the model is tested using residual sum of square (RSS) to ensure that the model still adequately fits the data when eliminating each variable. When no more variables can be eliminated from the model to improve the RSS, the analysis has been completed. The drawback of this procedure is fitting new data in this model is usually not as good as fitting current data.

The backward stepwise regression analysis in SPSS was conducted for all Oklahoma data obtained in this study, including 57 independent variables and the dependent variable ***CIWS***. After excluding variables step by step, 16 variables remained for a best-fitting model. These variables include: LON, DISTANCE, ASPCT10K, SLOPE10K, CURVAT1K, HILSH10K, DFEV10KS, DFEV10KW, RAINSPR, RELHFALL, TAIRSUMM, SUMMMAX, WINTDIFF, W_PCT, R_PCT, and S_PCT. Figure 5.2 shows the final optimal residual line obtained. The good fit between the observed data and the expected data implies an optimal model was built matching current collected data although how well this model can be fit with future data is uncertain. Table 5.3 is the model summary after the last variable removed. The adjusted R square in this table told an overall good model fit with about 76% variance explained by the model. The Durbin-Watson value, very close to 2, implied that no significant autocorrelation found in the final model. The ANOVA test results shown in Table 5.4 verified that there is a significant relationship between dependent variable ***CIWS*** and the remaining 16 predictors in the model at the 95% confidence level.

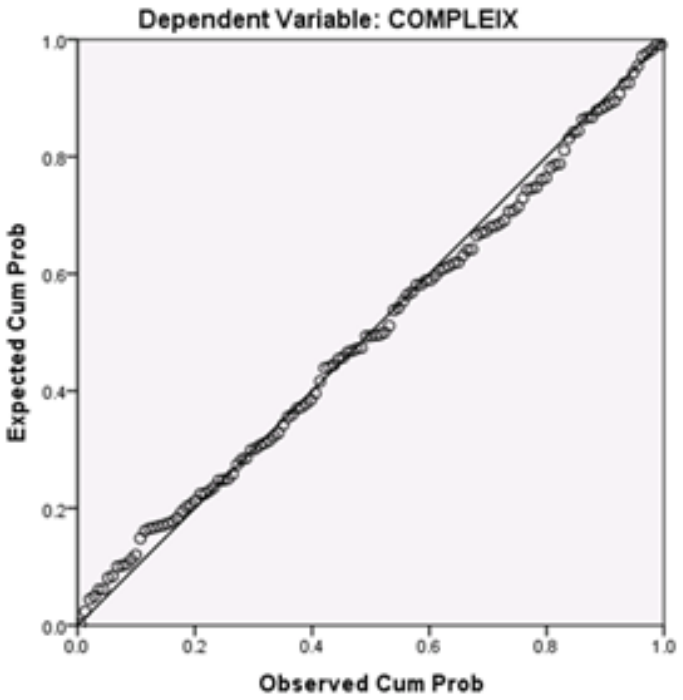

Figure 5.2 Normal Plot of Regression Standardized Residual for Mesonet Data

R	R Square	Adjusted R Square	Std. Error of the Estimate	Change Statistics			Durbin-Watson
				R Square Change	F Change	df1	
.888	.789	.758	.737930144	-.003	1.799	1	1.979

Table 5.3 Model Summary after Last Variable Removed

Model	Sum of Squares	df	Mean Square	F	Sig.
Regression	223.982	16	13.999	25.708	.000
Residual	59.899	110	.545		
Total	283.881	126			

Table 5.4 ANOVA Test after Last Variable Removed

Table 5.5 provides more information about the results from the last step of the backward regression. While the B value in the table gave the actual predictor unit for each variable, the standardized coefficients in the table indicated the relatively influential level of each variable in the model. Variable LON, SUMMDIFF, FALLDIFF, DISTANCE, and RELHFALL, were shown as the most significantly influencing ones in the model. It is noteworthy, that these marked-out variables are also identified by the simple correlation analysis in section 5.2.1 to be significant factors, and belong to the two major categories of location and climate, although more variables were marked out by simple correlation analysis.

However, the results in Table 5.5 also suggest that there is significant multicollinearity found in the five significant variables. The value of VIF in this table indicates the level of multicollinearity for each variable, with a VIF of a variable greater than 5 usually linked with high multicollinearity. Therefore, simply using results from this model, it is still difficult to explain the influences of each individual factor on the ***CWS***.

Model		Unstandardized Coefficients		Standardized Coefficients	*t*	Sig. VIF	Collinearity Statistics
		B	Std. Error	Beta			VIF
Step 35	(Constant)	125.171	12.215			.000	
	LON	.827	.113	.955	8.87	.000	8.875
	DISTANCE	-.009	.002	-.768	21.2	.000	21.284
	ASPCT10K	.004	.001	.169	1.53	.002	1.538
	SLOPE10K	-5.051	1.438	-.214	1.94	.001	1.941
	CURVAT1	-179.864	62.488	-.162	1.65	.005	1.653
	HILSH10K	.000	.000	.148	1.10	.002	1.109
	DFEV10KS	-.009	.005	-.132	2.28	.049	2.287
	DFEV10K	.021	.006	.274	3.45	.001	3.458
	RAINSPRI	-.005	.002	-.181	3.64	.033	3.648
	RELHFAL	-.259	.041	-.673	5.95	.000	5.958
	SUMMDIF	.895	.205	.602	9.87	.000	9.878
	FALLMIN	-.503	.238	-.479	26.7	.037	26.708
	FALLDIFF	-1.322	.231	-1.014	16.4	.000	16.402
	W_PRCT	-.067	.022	-.149	1.25	.003	1.257
	R_PRCT	.039	.016	.121	1.36	.020	1.364
	S_PRCT	.016	.009	.095	1.55	.086	1.554

Table 5.5 Coefficients after Last Variable Removed

5.2.3 Automatic Linear Modeling using Forward Stepwise Regression

Automatic linear modeling is a feature provided by SPSS to build powerful linear models in an easier manner than before. It is also good for data mining. It uses the Akaike Information Criterion (AIC) as the criteria to decide variables to be included in the model (Fotheringham, Brunsdon and Charlton, 2002). Models with smaller AIC value are better fitted to the data. Data for the original predictor variables usually are transformed first by trimming outliers to increase the effectiveness and accuracy of modeling.

Tables 5.6 and 5.7 are the summary report from the automatic linear modeling using forward stepwise regression on Oklahoma data. Based on each variable's contribution to the model

accuracy, seven transformed variables are identified as important factors by the modeling for an optimal AIC value of -31.9, including LON, WINTMIN, CURVT1k, HILLSH10k, RELHSUMM, TAIRFALL, and DFELV10KS. Compared with findings from backward stepwise regression, there are only one common variable - LON - which appear important in both models. Compared with results from simple correlation analysis, LON, WINTMIN, RELHSUMM, and TAIRFALL are the four variables that appear in both as significant factors.

Target	**COMPLEIX**
Automatic Data Preparation	On
Model Selection Method	Forward Stepwise
Information Criterion	-31.902

Table 5.6 Model Summary

Importance Ranking	**Variable**
1	LON_transformed
2	WINTMIN_transformed
3	CURVAT1K_transformed
4	HILSH10K_transformed
5	RELHSUMM_transformed
6	TAIRFALL_transformed
7	DFEV10KS_transformed

Table 5.7 Variable Importance Ranking

5.2.4 Principal Components Analysis

Since no consistent marked-out variables were obtained from approaches above, and there is un-ignorable multicollinearity observed in the variables, principal components analysis is chosen as the final exploratory analysis to help to prepare major components for further modeling. The point of principal components analysis is to redistribute the variance in the correlation matrix using the method of eigenvalue decomposition to redistribute the variance to first components

extracted (UCLA-ATS, 2011). It reduces data dimensions and multicollinearity between independent variables, while taking account of each potential factor's influences.

Principal components analysis is related and similar to factor analysis, but they are not identical. PCA performs a variance-maximizing rotation of the variable space while taking into account all variability in the variables (UCLA-ATS, 2011). In contrast, factor analysis estimates how much of the variability is due to common factors - communality. The two methods would become essentially equivalent if the error terms in the factor analysis model, the variability not explained by common factors, was found to have the same variance (UCLA-ATS, 2011).

Running PCA on the Oklahoma data, obtained outputs including commonalities, correlation matrixes, total variance explained by each variable, a scree plot, a component matrix, and rotated component matrix tables. However, after the first run of PCA, the correlation matrix shows it was a non-positive definite matrix, which implies linear dependency existing among the 57 independent variables. To exclude the linear dependency, variables were removed step by step through re-running PCA analysis on the raw data. Examining the result indicated that the linear dependency was caused by three sets of temperature variables: average daily temperature difference for each season, average daily maximum temperature for each season, and average daily minimum temperature for each season. This seemingly obvious linear dependency was missed in data collection stage since these data were respectively calculated from raw Mesonet data. By comparing the result of Kaiser-Meyer-Olkin Measure (KMO) and Barlette's tests (UCLA-ATS, 2011), four variables representing the average daily maximum temperature for each season (SPRIMAX, SUMMMAX, FALLMAX, and WINTMAX) were then removed from the variable sets. There were a total of 53 variables left to join further PCA analysis.

The KMO test is often used to measure the sampling adequacy. The value of KMO varies between 0 and 1, and values closer to 1 are better (UCLA-ATS, 2011). The Bartlett's test inspects

the null hypothesis that the correlation matrix is an identity matrix, in which all of the diagonal elements are 1 and all off diagonal elements are 0 (UCLA-ATS, 2011). The null hypothesis therefore needs to be rejected. These tests taken together provide a minimum standard which should be passed before a PCA analysis should be conducted further (UCLA-ATS, 2011). The results in Table 5.8 indicate that PCA applied in this study on Oklahoma data passed these minimum tests.

Kaiser-Meyer-Olkin Measure of Sampling Adequacy		.817
Bartlett's Test of Sphericity	Approx. Chi-Square	15792.821
	Df.	1378
	Sig.	.000

Table 5.8 KMO and Bartlett's Test Results

Figure 5.3 is the scree plot, which indicates eigenvalue of each principal component (PC). The eigenvalue also reperents the fraction of total variance in the data as explained by each PC (UCLA-ATS, 2011). Table 5.9 gives the contribution of total variance explained by the first ten PCs. As it is shown in Figure 5.3, from about the eleventh component on, the scree plot line is almost flat, meaning that each successive component is accounting smaller and smaller amounts of the total variance. Table 5.9 lists ten initial eigenvectors with eigenvalues greater than 1, which explained 82.8 percent of the variance in the original data. In general, only those principal components whose eigenvalues greater than 1 are important because the components with an eigenvalue less than 1 account for less variance than did the original variable, which had a variance of 1, and so are of little use (UCLA-ATS, 2011). The first ten principal factors with eigenvalue greater than 1 from this procedure were actually saved and used as principal components for further modeling the relationship of geographic factor and the nature of ***CWS*** later (see Appendix E).

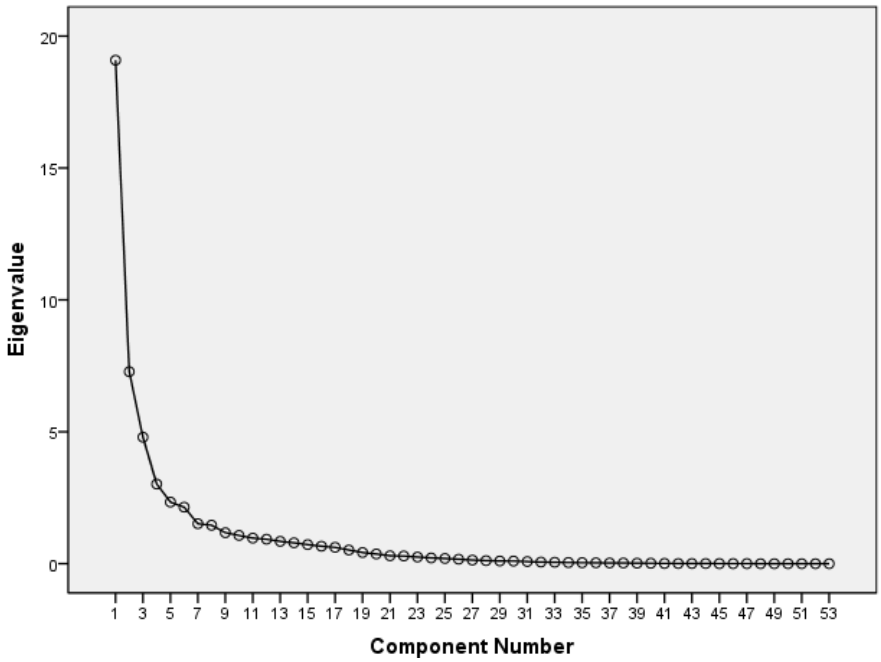

Figure 5.3 Scree Plot of PCA on Oklahoma Mesonet Data

Component	Initial Eigenvalues			Extraction Sums of Squared Loadings		
	Total	% of Variance	Cumulative %	Total	% of Variance	Cumulative %
1	19.087	36.013	36.013	19.087	36.013	36.013
2	7.278	13.732	49.745	7.278	13.732	49.745
3	4.794	9.045	58.791	4.794	9.045	58.791
4	3.019	5.696	64.487	3.019	5.696	64.487
5	2.334	4.403	68.890	2.334	4.403	68.890
6	2.141	4.040	72.930	2.141	4.040	72.930
7	1.515	2.858	75.788	1.515	2.858	75.788
8	1.456	2.746	78.534	1.456	2.746	78.534
9	1.175	2.217	80.751	1.175	2.217	80.751
10	1.069	2.017	82.768	1.069	2.017	82.768

Table 5.9 Total Variance Explained by First Ten Components

Table 5.10 is the output component matrix for the first ten principal components extracted. The table contains component loadings, which are the correlations between the variable and the PC. An examination of the components reveals that the first three components, comprising of 58.8 percent of the variance, are explainable, and they were termed as the "Moisture," "Landscape", and "Temperature" dimensions respectively. The major variables included in each of the dimensions are given in Table 5.11. All correlations in this table are statistically significant at the .01 level. Of note is the logical nature of signs of most of the simple correlations between each variable and ***CIWS***.

The effectiveness of PCA analysis is reflected through the reproduced correlation matrix and the residual table. The reproduced correlation matrix is based on the extracted components. If the reproduced correlation matrix is similar to the original correlation matrix before extraction, it suggests the components that were extracted accounted for a great deal of the variance in the original correlation matrix, and that PCs sufficiently represent the original data (UCLA-ATS, 2011). For the same reason, if the values in the residual table, which are calculated as the difference between the observed and reproduced correlation, are close to zero, it indicates a good representation of components. The results in the residual table of this study provided such a proof.

5.3 Speculation on Results of Exploratory Analysis

Based on the above exploratory studies on the relationship between collected variables and calculated ***CIWS***, some variables from the three categories, location, terrain or atmosphere, may play more important roles than others in shaping a higher ***CWS*** level at a location. However, results obtained from different methods indicated different focus in general. In addition, severe multicollinearity among variables was confirmed by the method of backward stepwise regression analysis. Jointly examining the results from different approaches helps to make some inferences.

Variable	Component									
	1	2	3	4	5	6	7	8	9	10
LAT	-.538	-.008	-.666	-.336	-.242	.141	-.155	.070	.001	-.009
LON	.887	.086	-.355	.060	-.089	-.039	-.021	-.056	-.060	-.037
ELEV	-.935	-.064	.027	.158	.088	.047	.000	-.056	.023	-.016
DISTANCE	-.880	-.027	-.315	-.250	-.101	.103	-.101	.076	.044	.013
ASPCT1K	.211	.075	-.220	-.176	.513	-.053	-.290	.102	-.271	.250
ASPCT5K	.368	.171	-.353	.064	.607	-.007	-.283	.138	.261	.049
ASPCT10K	.346	.079	-.326	.104	.449	.010	.027	.210	.273	-.245
SLOPE1K	-.021	-.205	-.123	.566	-.150	.197	-.323	.137	.088	.096
SLOPE5K	-.273	.099	-.030	.741	-.210	-.001	-.226	.241	.114	.041
SLOPE10K	-.429	.168	-.001	.638	-.138	.168	.008	.274	-.031	-.040
CURVAT1K	.054	-.653	.004	-.104	-.122	-.593	-.068	-.079	.071	-.050
CURVAT5K	.067	-.642	-.237	.165	.269	.446	.281	.075	-.006	.002
CURVA10K	-.057	-.478	-.061	.096	.297	.537	.385	.093	-.117	-.002
HILSH10K	.118	.013	.029	-.100	.246	-.107	.199	-.375	.260	-.220
DFEV5KE	.181	.724	-.029	.007	.467	.305	-.074	-.084	.050	.045
DFEV5KS	-.058	.665	.162	.042	.001	.531	.090	-.308	.161	-.073
DFEV5KW	-.282	.663	.219	.184	-.290	.351	.133	.043	-.108	-.023
DFEV5KN	.023	.737	-.014	.105	.270	-.123	-.055	.277	-.214	.163
DFEV10KE	.264	.788	.024	-.168	.336	.014	-.179	-.132	.150	-.036
DFEV10KS	-.139	.737	.212	-.051	-.186	.260	-.139	-.319	.130	.003
DFEV10KW	-.370	.663	.315	.074	-.429	.044	-.111	.016	-.129	.015
DFEV10KN	.084	.784	.043	.048	.092	-.405	-.144	.145	-.119	.084
RAINSPRI	.739	.190	-.428	.022	-.172	-.012	.075	.010	.063	.113
RAINSUMM	.474	.009	-.507	.008	-.102	.044	.088	-.117	-.189	.242
RAINFALL	.794	.027	-.191	.279	-.108	-.145	.179	-.184	.032	.184
RAINWINT	.791	.168	-.178	.293	-.075	-.133	.157	-.126	.013	.200
PRESSPRI	.813	.339	.089	-.249	-.108	.111	.045	.205	-.050	-.075
PRESSUMM	.807	.342	.090	-.251	-.107	.115	.045	.208	-.052	-.077
PRESFALL	.813	.338	.092	-.253	-.108	.111	.045	.207	-.049	-.074
PRESWINT	.815	.336	.090	-.255	-.109	.109	.045	.206	-.047	-.073
RELHSPRI	.889	.217	-.205	-.014	-.105	-.053	.156	.105	.016	-.062
RELHSUMM	.777	.150	-.467	.113	-.066	-.127	.061	-.131	-.113	-.107
RELHWINT	.685	.304	-.257	-.211	-.130	-.133	.236	.169	.174	-.009
RELHFALL	.820	.256	-.244	-.112	-.062	-.136	.222	.034	.073	-.046
SPRIDIFF	-.875	.277	.155	-.003	.078	-.138	.213	.008	.024	.012
SUMMDIFF	-.709	.482	.210	.026	.030	-.216	.279	.050	.003	-.029
FALLDIFF	-.711	.514	.165	.068	.113	-.252	.185	-.095	-.099	-.006
CINDX	.671	.217	-.389	.171	-.101	-.020	-.023	.007	.107	.059
WINTDIFF	-.813	.351	.211	.042	.167	-.219	.164	-.063	-.040	.010
W_PRCT	.259	.075	.024	-.021	-.178	.011	-.507	-.224	.204	-.300
R_PRCT	.211	-.129	-.086	-.289	.074	.212	-.212	-.427	-.411	.192
P_PRCT	-.505	-.039	.029	-.373	.029	.116	-.144	.181	-.061	.132
B_PRCT	-.018	.083	.012	-.101	-.164	.055	.103	-.140	.465	.665
S_PRCT	-.440	.054	.231	.213	.240	-.130	.041	.061	.133	.152
F_PRCT	.603	.121	-.233	.515	.064	-.005	-.061	-.214	-.106	-.106
TAIRSPRI	.685	-.037	.679	.012	.110	-.039	-.007	.009	-.073	.044
TAIRSUMM	.322	-.172	.757	-.261	-.043	.042	-.003	.200	.207	.115
TAIRFALL	.824	-.102	.511	.157	.074	-.040	.000	-.028	-.008	.012
TAIRWINT	.720	-.073	.532	.302	.152	-.086	.028	-.151	-.133	.004
SPRIMIN	.864	-.201	.405	.010	.036	.046	-.111	.017	-.056	.025
SUMMMIN	.655	-.398	.440	-.190	-.072	.138	-.135	.128	.167	.098
FALLMIN	.876	-.280	.348	.100	.022	.055	-.054	.020	.026	.005
WINTMIN	.840	-.205	.391	.226	.071	.001	-.028	-.089	-.091	.003

Table 5.10 Component Matrix

COMPONENT	DIMENSION NAME	SIMPLE CORRELATIONS WITH SIGN
FAC1	Moisture	Season Rain/Relative humidity +
		Longitude +
		Cloud Index +
		Forest Coverage +
		Season Minimum Temperature +
		Season Pressure +
		Elevation –
		Distance from Gulf of Mexico –
		Season Temperature Difference–
		Pasture land coverage –
FAC2	Landscape	Relative elevation 10 km/5km +
		Curvature –
FAC3	Temperature	Season Temperature +
		Latitude –
		Rain/Relative humidity –
FAC4	Landscape	Slope 5km/10km/1km +
		Forest Coverage +
FAC5	Landscape	Aspect 5km/1km +
		Relative elevation 10km–
FAC6	Landscape	Curvature 10km +
		Curvature 1km–
FAC7	Landscape	Curvature 10km +
		Water surface percentage –
FAC8	Landscape	Residential land Percentage –
FAC9	Landscape	Barren land percentage +
		Residential land percentage –
FAC10	Landscape	Barren land percentage +

Table 5.11 Explanation of First Ten Principal Components

Results from simple correlation analysis indicates that factors like longitude, averaged daily lowest temperature for the fall and winter season, averaged daily temperature difference for spring and winter, distance to Gulf of Mexico, elevation, averaged air pressure in four seasons, relative humidity in all four seasons, averaged rain amount in all four seasons, averaged daily

temperature in fall, annual cloud index, and averaged forest coverage, are all significantly related to the variations of the ***CWS*** level of a location. Terrain factors like relative elevation, slope, curvature, and hill shade are not identified as relatively significant factors by the bivariate analysis. Looking further into these variables identified, most of them fall into two categories; one is the location-related category, and the other is the atmospheric condition including the air moisture level. Topographic factors of a location indicate relatively minor importance by this approach.

Results from backward regression analysis based on historic data included 16 key factors, crossing the three categories of geographic dimensions. But the most important five factors are from location and atmosphere category, suggesting similar focus as the method of simple correlation analysis, that is, location and atmospheric factors may play more important roles than terrain variables when linking with the higher level of ***CWS***. However, multicollinearity was discovered in the five key factors by this method. Although multicollinearity might not impact on the predictability of the whole regression model, but it made it difficult to examine the actual influences of each factor on the ***CIWS***.

The results of both automatic linear regression and PCA approaches show a mixed emphasis about the key factors affecting the ***CWS*** level of a location. That is, factors from all three categories are playing important roles in shaping the ***CWS*** and affecting the ***CWS*** level. This can be seen from Tables 5.7 and 5.11, which display results of the two methods respectively. However, like the other two methods - simple correlation analysis and backward stepwise regression - the most important categories of factors still belongs to the location and atmosphere dimensions. In Table 5.7, the first two factors ranked as the most important are LON and WINTMIN; In Table 5.11, the first principal component contains location and atmospheric variables, and is named as the moisture dimension.

Obviously, differing statistical approaches have generated different list of predictors in relating with ***CWS*** because different pruning criteria were used. But one speculation, based on the study of the case of Oklahoma thus far, might be that, moisture and moisture-related geographic factors at a location play the most important roles in affecting the ***CWS*** level of a site. Longitude, elevation, distance to a big water body like the Gulf of Mexico, rain amount, forest coverage, relative humidity, temperature, and pressure all could be interpreted as directly related with the air humidity level of a location, and furthermore, they are the first category of factors directly affecting the ***CWS*** of a location.

Another speculation is that most of these geographic factors are also related to the amount of surface friction, which is an important factor affecting wind. It seems that, from the case of Oklahoma, the more varied the terrain conditions around a location, the higher ***CIWS*** potential for the location. Considering wind is a transformative type of energy from solar energy, derived from an unbalanced distribution of solar energy received in air and on the earth's surface, it might be speculated that terrain variation is another key factor impacting on the ***CWS*** by either directly affecting the distribution of both insolation and wind energy, or indirectly affecting the ***CWS*** through affecting the moisture level of air.

Therefore, other landscape factors, or location related factors other than moisture or terrain conditions, may be categorized as factors indirectly affecting ***CWS***, through affecting the air moisture level or terrain variation. This may explain why southeastern Oklahoma, with more forest coverage, complicated landscapes types, and higher water body coverage, is showing higher annual ***CIWS*** values than western Oklahoma, where both wind and solar resources are higher but moisture level is lower and the landscape is relatively single-toned. It seems that focusing on the view of micro and meso scales, higher air moisture levels and terrain variation increases the possibility of a higher complementarity between wind and insolation in the location.

Because of the complexity of geographic phenomena and the relatively brief data used in numeric modeling, it is difficult to definitely isolate affecting factors and their influences toward a spatial phenomenon. Not only is there multicollinearity among spatial variables of one location, but there is also autocorrelation of one variable over space. The spatial delay impacts of geographic factors, including of variables in the three categories of this study (location, atmosphere, and terrain conditions), leads to the influences of a variable on ***CWS*** usually transformed with distance and mirrored in different time and locations. In addition, geographic variables themselves, especially atmosphere-related factors, are temporally varied, so is the nature of ***CWS*** at the site. Therefore, associations of geographic factors with ***CWS*** appear both spatially and temporally dynamic and somewhat indefinite.

Under current limitations, it is still not possible to build a dynamic or macro model to reflect the temporally varying relationship of various geographic factors on the ***CWS***. This study simply tried to model the spatial variation of this relationship, using data averaged from long term span and over the micro to meso scale of space. Principal components analysis, considered to be the optimal one to reduce the inherent multicollinearity among various geographic factors comparing with other methods, was used to determine independent explanatory variables for further regression modeling. In Chapter Six, the first ten PCs obtained in this chapter for Oklahoma (see Appendix E) were used as the independent variables in geographically weighted regression (GWR) to model the relationship between the geographic factors and the ***CIWS***, and to further examine the speculations from above.

CHAPTER VI

MODELING THE RELATIONSHIP OF GEOGRAPHIC FACTORS AND THE COMPLEMENTARY NATURE OF WIND POWER AND INSOLATION

After the examination of which geographic factors might be linked with the complementary nature between wind and insolation in the previous chapter, the present chapter will focus on modeling how these identified factors impact on the complementary nature of wind power and solar radiation (***CWS***) combined or individually. Statistical geographic modeling approach was employed to accomplish the task. As discussed earlier, at each location there is a list of possible geographic factors linked with a geographic phenomenon like the ***CWS***. These factors incessantly take part in varied geographic processes. It is difficult to build a quantitative model to include all possible factors in one geographic setting, just as it is difficult to build a panoramic model to replicate all real-time processes in which these factors are involved. Modeling the real-world scenario using geographic statistical modeling is one of the most realistic choices. It is useful to construct a numeric model to expose some key empirical relationships based on high quality unit observations at various scales. A single numeric model not only helps to acquire a better understanding of how all independent variables are integrated to impact on the ***CWS***, it also helps to find out how each individual variable affects the ***CWS*** by analyzing the tendency of each model coefficient.

As discussed in section 5.1, geographic phenomena are those affected by location and location-

related factors, or so called spatial/geographic variables. Each spatial variable is also associated with a set of spatial processes which usually involves variables active in wider spatial scales. For geographic variables, space functions like a special type of time. Variables use space as an evolving stage, changing conditions over their evolving course in space. This leads to the nature of spatial autocorrelation and spatial heterogeneity embedded in each spatial variable. Spatial processes involving various spatial variables in various kinds of interwoven relationships are therefore not spatially static, but intrinsically manifest spatial autocorrelation and spatial heterogeneity just as the associated variables. Spatial relationships behind these spatial processes over space thus vary by place.

There may be two aspects regarding the variation of the relationship between one geographic phenomenon and a set of impacting geographic variables. On the one hand, the list of geographic variables linked with the phenomenon could vary with location. On the other hand, the way each of the variables is involved with the studied phenomenon could be non-constant over space. Spatial modeling examines and analyzes the variation of spatial relationships in both respects by one model. Compared with traditional global statistical modeling, local spatial analytical approaches are more proper for studying spatially non-static relationships by calculating spatially varying parameter estimates for each model variable. In this study, geographically weighted regression (GWR) modeling, which is one local statistical modeling approach to model spatially varying relationships, is used to investigate the relationship between the complementary nature of wind and insolation and its linked geographic factors.

6.1 GWR as a Local Analysis Approach

Statistical spatial modeling delineates a spatial relationship through linking the studied geographic phenomenon and those impacting phenomena in a relationship as between dependent variable and independent variables. Traditional global statistical modeling emphasizes a relatively uniform representation of characteristics of whole study area, reflecting little or no variation of

the relationships in the local level (Yu and Wei, 2006). By using one single value, the global statistic approach tries to expose general regularities or laws and focuses on similarities across space (Yu and Wei, 2006). However, global statistical analysis is aspatial since it cannot give correct attribute information about different locations. Thus, it is GIS-unfriendly because the results lack detail on maps. In contrast, local analytical approaches build global models with spatially varying attributes, depicting both similarities and differentiation over space, and are good for mapping in GIS.

Different from how traditional models adopt a single statistic value, local geographic modeling usually uses calibration within different regions, or moving windows. There have been various kinds of local analytical approaches developed. For instance, the local univariate spatial data analysis approaches include local point pattern analysis such as GAM (Lloyd, 2007), local graphic analysis such as XLispstat (Tierney, 1990), and MANET (Fotheringham, Brunsdon and Charlton, 2002), local filters approach for remote-sensing images, and local measures of spatial dependency such as Moran's I. Approaches of multivariate spatial data analysis include, the spatial expansion method in the form of $y_i=\alpha_i+\beta x_{i1}+\ldots+\tau x_{im}+\varepsilon_i$, and $\alpha_{i=}\ \alpha_{0+}\ \alpha_{1Ui+}\alpha_{2Vi,}\ \beta_{i=}\ \beta_{0+}\ \beta_{1Ui+}\beta_{2Vi,}\ \tau_{i=}\ \tau_{0+}\ \tau_{1Ui+}\tau_{2Vi}$, the spatially adaptive filtering method, multilevel modeling approaches, random coefficient models, spatial regression models and local methods for spatial flow modeling, etc. (Yu and Wei, 2006).

The geographic weighted modeling uses fixed or adaptive spatial kernels to catch disseminated global statistics over local scale. According to Fotheringham, Brunsdon and Charlton (2002), the mathematic mechanics of GWR are derived from matrix calculation. In classic regression, the matrix used is like:

$Y= X\beta + \varepsilon$, where $\beta= (X^TX)^{-1}X^TY$ (Fotheringham, Brunsdon and Charlton, 2002*; Equ. 6.1*)

But in the GWR modeling, the equivalent is:

$Y=(\beta xX)*1 + \varepsilon$, where $\beta=(X^T\ W(i)X)^{-1}X^TW(i)Y$ (Fotheringham, Brunsdon and Charlton, 2002; *Equ. 6.2*)

In GWR modeling, the weighting function of W(i) could be any of the following cases:

if W_{ij}=1 for all i, j, GWR will become Ordinary Least Square (OLS);

if W_{ij} = 1 if $d_{ij} \leq d$, and W_{ij} = 0 otherwise, the discrete wight function is used;

if $W_{ij} = exp(- d_{ij}^2 / h^2)$, where h is referred to as the bandwidth, continuous weighting function is used.

if $W_{ij} = [1 - (d_{ij} / hi)^2]^2$ if $d_{ij} < hi$, and W_{ij}= 0 otherwise, the spatially adaptive weighting functions is used.

(Source: Fotheringham, Brunsdon and Charlton, 2002)

Whichever weighting function is selected, the estimated parameter surfaces will be, in part, functions of the defined weighting function. When the bandwidth of h is close to indefinite, the weights tend to be 1.0 for all pairs of points, so that the estimated parameters become uniform and GWR becomes equivalent to OLS (Fotheringham, Brunsdon and Charlton, 2002). Conversely, when the bandwidth h becomes smaller, the parameter estimates will increasingly depend on observations in close proximity of point *i* and hence will have increased variance (Fotheringham, Brunsdon and Charlton, 2002). The key issue of GWR, therefore, becomes how to select the optimal bandwidth.

The optimal bandwidth usually changes with calibration strategy, depending on using fixed or adaptive weighting schema (Yu and Wei, 2006). Several different criteria could be used to decide the optimal bandwidth of GWR modeling, including the approach to calculate the cross-validation score, the approach to calculate the generalized cross-validation score, the minimized Akaike Information Criterion (AIC), and the Bayesian Information Criterion (Claeskens and Hjort, 2008). Considering the bias-variance trade off features, the corrected AIC approach was believed to be more justified for determining optimal bandwidth in GWR (Fotheringham, Brunsdon and Charlton, 2002).

According to Fotheringham, Brunsdon and Charlton (2002), there are at least two exclusive

benefits from applying GWR modeling. The first is GWR modeling reduces the spatial auto-correlated error terms by allowing geographically varying relationships to be modeled through spatially varying parameter estimates rather than through the error terms in a model (Fotheringham, Brunsdon and Charlton, 2002). By comparing the GWR models with and without autoregressive parts, it was found that the distributions of the local parameter estimates from the two kinds of models are identical. This suggests that whatever causes the local variation in parameter estimates in the model is not accounted for by the addition of an autoregressive term to the local modeling framework (Fotheringham, Brunsdon and Charlton, 2002). GWR is therefore good at depicting both spatial non-stationarity and spatial dependency.

Another benefit of applying GWR is that it solves the modifiable area unit (MAUP) problem to some extent (Fotheringham, Brunsdon and Charlton, 2002). There are two types of MAUP problem identified in geography. One is the scale effect, which refers to how different results can be obtained from the same statistical analysis at different levels of spatial resolution. The other is the zoning effect, which refers to how different results can be obtained due to the regrouping of zones at a given scale. GWR modeling aims to solve the MAUP problem through determining the appropriate partitioning of space to study the relationships between dependent variable and independent variables and insure the relationships examined are relatively homogenous within the partition (Fotheringham, Brunsdon and Charlton, 2002). GWR does not imply a scale, and the zones for a process is determined inherently (Yu and Wei, 2006). Bandwidth is a measure of spatial scale of analysis in GWR. The micro details could be highlighted with the change of scale, and decrease of degrees of freedom, and also an increased homogeneity. The selection of bandwidth in GWR is part of the calibration process which helps to solve the MAUP problem.

Both the complementary nature of wind and insolation and its linked geographic factors are spatially varying phenomena, exhibiting spatial autocorrelation and spatial heterogeneity like many other geographic phenomena. The complexity of spatial conditions and processes behind

them leads to the assumption that the relationship between the ***CWS*** and its impacting factors may not be static over space. GWR as one of the optimizing techniques available for local geographic analysis is a more suitable choice for modeling the relationship between the ***CWS*** and a wide range of geographic factors than traditional global regression models. This assumption is tested and examined further by applying GWR to the case study of Oklahoma.

6. 2. Using GWR to Model the Relationship of the Geographic Factors and the *CWS*

Fotheringham and his colleagues developed the GWR software for implementing GWR modeling for various tasks (Fotheringham, Brunsdon and Charlton, 2002). Detailed instructions about how to use the software are provided (UBC, 2011). This study used GWR3.0 to model the influences of various geographic factors on the nature of ***CWS*** for the example of Oklahoma. One exceptional advantage of using the GWR software is its output also includes statistics for corresponding global regression model besides the output of local statistics and parameter estimates using the same set of variables. This feature helps to determine improvements of the GWR model over global models and identify a statistically sound GWR model.

6.2.1 Data for GWR Modeling

In the case study, the major goal was to explore how the levels of ***CWS*** in various locations affected by various geographic factors linked with different spatial scales, extended from the specific Mesonet sites. The response variable used in GWR modeling for Oklahoma is the calculated complementarity index of wind power and solar radiation (***CIWS)*** for each Mesonet site as described in Chapter Four. The predictor variables used are the ten principal components as described in section 5.2.4.

To apply the GWR software, the original data file stored in Excel was first converted to a comma separated CSV file format. In the final transformed data file, there were a total of 127 regression points, and 13 variables, including the dependent variable ***CIWS***. Independent variables included

longitude and latitude plus the ten PCA components for each site. Appendix E is the complete converted data file used in GWR modeling for this study. In this file and all following analysis, the ten variables FAC1, FAC2, FAC3…FAC10, refer to the corresponding principal components used as the explanatory variables in GWR modeling. In the present study, the major variables dominating the ten dimensions were identified and presented in Table 5.8, which fall into three major categories: moisture, landscape, and temperature.

6.2.2 Performing GWR Modeling

A control file based on the converted data file was generated for further GWR modeling. The GWR software provides a Model Editor interface to accomplish this job (see Figure 6.1). The dependent and independent variables of GWR modeling, location variables in the data file, weighting schemes and calibration method, and the type of output for parameter estimates files were specified through this step in the control file. Since the measurement of all independent and dependent variables in this study are continuous, Gaussian modeling was selected. In this study, the kernel type chosen was adaptive, and the bandwidth selection method was based on the corrected AIC. The type of parameter estimates file was set to spreadsheet format, so that the output could be imported and displayed in ArcGIS later. The viewable listing file as output was also chosen so that more statistical information could be acquired about the modeling procedure. Once the control file was created and saved, running the software generated outputs. There were two major parts of output for this study based on control file settings. The first part was the parameter estimate file saved into the format of spreadsheet. The other part was the optional output listing file in text format.

To study the relationship between geographic factors and ***CIWS*** in Oklahoma, GWR modeling was performed using different lists of the predictor variables as shown in Table 6.2. Whether or not a variable was picked for GWR modeling was based on its *t* value in global OLS regression, which is the statistic for the hypothesis $\alpha=0$ (Yu and Wei, 2006). By looking into the global

regression statistics included in output listing of GWR on all ten PCs (see Table 6.1), it was found that not all the ten PCs are significantly related with the ***CIWS***. Table 6.1 lists the coefficient, standard error, *t* value, and corresponding *p* value for each PC in global OLS regression modeling. Based on the *p* value in the table, principal components FAC1, FAC4, FAC6, FAC9 defined in Table 5.8 are significantly related to ***CWS*** at a 95% above confidence level and FAC5 was related to ***CWS*** at a 85% level. Studies indicate that only using globally verified predictor variables in GWR can effectively minimize multicollinearity that would otherwise appear in local model (Qiu & Wu, 2011). Therefore, the other five PCs, FAC2, FAC3, FAC7, FAC8, FAC10 were excluded from various runs of GWR modeling (see Table 6.2).

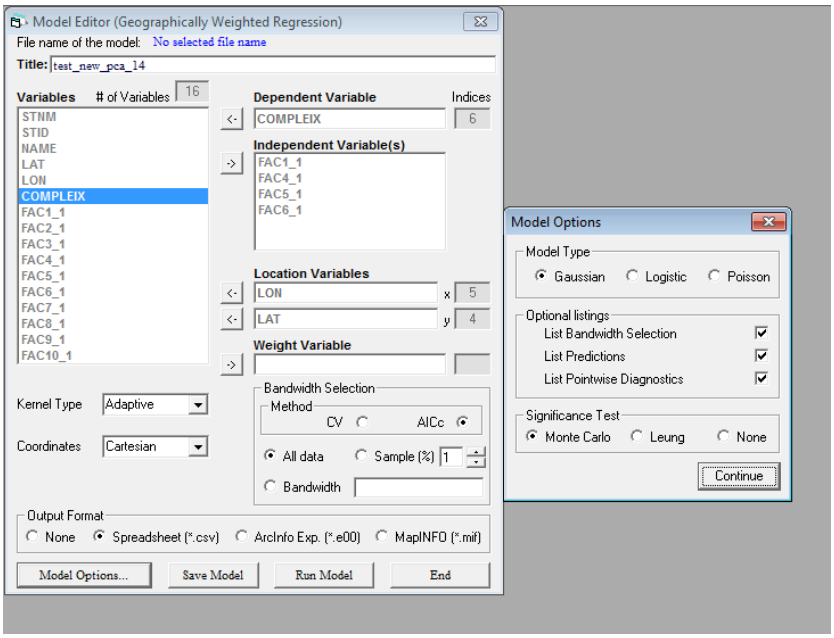

Figure 6.1 Setup of GWR Model Editor

Through comparing results from GWR modeling within cases using different lists of predictor variables, it was further found that the GWR local model did not always outperform the corresponding global ordinary least square (OLS) regression. According to Fotheringham, Brunsdon and Charlton (2002), GWR modeling can be regarded as successful if the AIC score for the local GWR model is decreased more than 3 from OLS. Table 6.2 provides a summary of the

statistics of GWR on different cases. Only three cases indicate an AIC improvement of greater than 3. Of the three cases, two of them included FAC3, which was one of the five PCs (see Table 5.8 for PC details) identified as not significantly related with ***CWS***. To minimize multicollinearity, cases 5 and 7 were excluded. Case number 10 which used FAC1, FAC4, FAC5 and FAC6 as explanatory variables met the criteria of a successful GWR modeling and was left for further analysis.

Parameter	Estimate	Std. Err	*t* Value	*p* Value
Intercept	10.99	0.09	128.97	0
FAC1	1.11	0.09	12.94	0
FAC2	-0.06	0.09	-0.76	0.45
FAC3	-0.09	0.09	-1.00	0.32
FAC4	0.18	0.09	2.15	0.03
FAC5	0.12	0.09	1.46	0.15
FAC6	0.2	0.09	2.31	0.02
FAC7	0.03	0.09	0.36	0.72
FAC8	0.07	0.09	0.76	0.45
FAC9	-0.27	0.09	-3.11	0
FAC10	0.01	0.09	0.09	0.93

Table 6.1 Global Regression Statistics for First Ten PCs

From Table 6.2, in the case of number 10, the global OLS model using FAC1, FAC4, FAC5 and FAC6 as independent variables explained about 57% of total variance in ***CWS***. But the respective GWR model explained about 70% of variance in ***CWS*** of Oklahoma, a good improvement from the global OLS model.

Table 6.3 lists the original variables composed of each selected PC by this model. The variance explained by each PC in the principal components analysis is also included. In this table, most variables were assigned to no more than one principal component dimension. If one variable is the most significant within more than one dimension, it was assigned to the principal component with which it had the highest correlation value. Variables' effects on the ***CWS*** are examined in the following section using information in Table 6.3 and the surface maps for the parameter estimates.

Case Number	Number of PCs	Components List	Regression Type	Coefficient of Determination	Adjusted R-Square	AIC	AIC Improvements by GWR
1	10	FAC1,FAC2,FAC3, FAC4,…,FAC10	OLS	0.623	0.587	365.45	-2.56
			GWR	0.660	0.607	368.01	
2	9	FAC1,FAC2,FAC3, FAC4,…,FAC9	OLS	0.623	0.590	363.02	-1.49
			GWR	0.658	0.610	364.51	
3	8	FAC1,FAC2,FAC3, FAC4,…,FAC8	OLS	0.591	0.560	370.81	-0.35
			GWR	0.715	0.642	371.16	
4	7	FAC1,FAC2,FAC3, FAC4,…FAC7	OLS	0.589	0.562	369.04	1.64
			GWR	0.704	0.638	367.40	
5	6	FAC1,FAC2,FAC3, FAC4,FAC5,FAC6	OLS	0.589	0.565	366.85	5.54
			GWR	0.700	0.642	361.31	
6	6	FAC1,FAC3,FAC4, FAC5,FAC6,FAC9	OLS	0.619	0.596	357.35	0.98
			GWR	0.709	0.654	356.37	
7	5	FAC1,FAC3,FAC4, FAC5,FAC6	OLS	0.587	0.567	365.15	9.07
			GWR	0.705	0.652	356.08	
8	5	FAC1,FAC4,FAC5, FAC6,FAC9	OLS	0.615	0.596	356.15	0.74
			GWR	0.657	0.622	355.44	
9	4	FAC1,FAC4,FAC6, FAC9	OLS	0.609	0.592	356.17	0.21
			GWR	0.643	0.613	355.96	
10	4	FAC1,FAC4,FAC5, FAC6	OLS	0.584	0.567	363.91	4.09
			GWR	0.704	0.647	359.82	

Table 6.2 Results of Performing GWR on Different Lists of PCs

Predictor Factor	Dimension Name	Significant Components	Variance Explained (%)
FAC1	Moisture	Season Rain/Relative humidity + Longitude + Cloud Index + Elevation – Distance from Gulf of Mexico – Season Temperature Difference–	36.01
FAC4	Landscape	Slope 5km/10km/1km + Forest Coverage +	5.70
FAC5	Landscape	Aspect 5km/1km + Relative elevation 10km–	4.40
FAC6	Landscape	Curvature 10km + Curvature 1km -	4.04

Table 6.3 Variables and Predictor Principal Components in GWR

6.2.3. Analysis of Modeling Results

Monte Carlo test included in the output listing of the GWR model tests the spatial variability in the local parameter estimates. The results in Table 6.4 indicate that there is significant spatial variation in the local parameter estimates for intercept and the predictor variable FAC1. There is weakly significant variation in FAC5 at a 90% confidence level. The spatial variation in the remaining variables, FAC4 and FAC6, is not significant at all and there is a reasonably high probability that their variations occurred by chance. Based on this information, in terms of mapping the local estimates, concentration was put on FAC1 and FAC5 plus the intercept, for which the local estimates exhibit significant spatial non-stationarity. Maps of local estimates were not made for the other two variables: FAC4 and FAC6.

Parameter	P-value	Significant
Intercept	0	Yes
FAC1	0	Yes
FAC4	0.26	n/s
FAC5	0.1	weak/s
FAC6	0.77	n/s

Table 6.4 Monte Carlo Test of Spatial Variability of Parameter Estimates

Based on information in Table 6.1, the *t* value for FAC1, FAC4, FAC5 and FAC6 in the global model indicates that each of them is positively related with ***CIWS***. However, FAC1 indicates the strongest relationship with ***CIWS***, while FAC6 and FAC4 hold weaker positive relationships, and FAC5 has the weakest relationship with ***CIWS***. Combined with the information in Table 6.3, it can be inferred that, in Oklahoma, the higher average seasonal rain amount, relative humidity, longitude, and higher annual cloud index of a location, generates a higher annual ***CIWS***. In contrast, factors like higher elevation, greater distance to Gulf of Mexico, and higher average seasonal temperature differences, could likely create a relatively low annual ***CIWS*** for a location.

The landscape dimensions of high slope and forest coverage, high aspect value in 5km and 1km ranges, high curvature value in the 10km range, low relative elevation within 10km, and low curvature value within 1km, all are linked with higher annual ***CIWS***. Whether these tendencies based on the global model are applicable to everywhere in Oklahoma were examined through the local parameter estimates in the GWR model. Results from GWR modeling were mapped into graduated point data first using five classes of natural break, and then was interpolated into area based using ordinary spherical kriging in ArcGIS. Graduated colours represent various values.

Figure 6.2 maps the coefficients for the first principal component FAC1, which is named as the moisture dimension. Different from what the global model depicts, the local model reveals that the coefficients for FAC1 are not constant over places in Oklahoma. The lowest regression coefficients are in the southeastern mountains and central part of Oklahoma, which are the parts of the state most often in the path of plentiful moisture from the Gulf of Mexico. The highest regression coefficients are in northeastern Oklahoma, and the second highest are in the western Oklahoma, which is also considered to be the driest part of the state. Therefore, it seems that same amount of change in the moisture level will bring a higher amount of change in ***CIWS*** in the northeastern area and the relatively drier western area than in the moister southeastern part.

Figure 6.3 is the map of *t* values for FAC1. A *t* value here indicates the statistical significance level of corresponding parameter estimates at each location. The map affirms that the relationship between ***CWS*** and FAC1 is not significant everywhere in Oklahoma. A strong positive relationship between ***CWS*** and FAC1 appears in western and northeastern Oklahoma, while a weak negative relationship between the two appears in southeastern and central Oklahoma. This is different from what the global model suggests that the same strength of positive relationship between the ***CWS*** and the moisture dimension occurs everywhere in Oklahoma. Table 6.3 indicates variables like seasonal rain, relative humidity, and longitude and cloud index of a location positively affect the moisture dimension, and variables like elevation, distance from Gulf

of Mexico and seasonal temperature difference of the location are negatively related to the moisture dimension. However, the *t* value distribution map indicates that, the combined influences from these factors in the moisture dimension on the nature of ***CWS*** seem higher in drier areas than in moister areas. This feature can be visualized by contrasting the *t* value map with the surface map drawn based on FAC1 values in Figure 6.4.

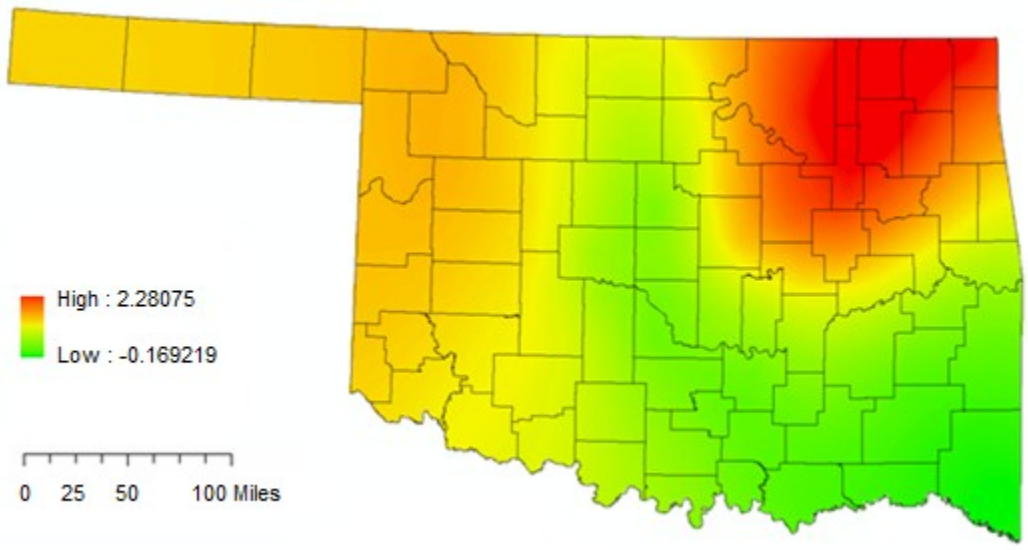

Figure 6.2 Parameter Estimates of Moisture Dimension (FAC1)

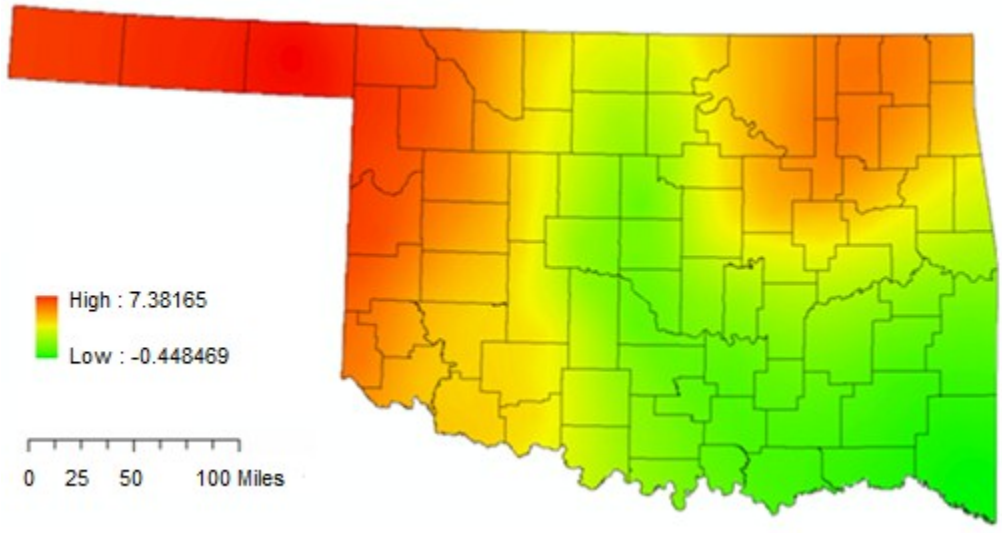

Figure 6.3 *t* Value for Moisture Dimension (FAC1)

Maps were created for most variables in FAC1 to check how the *t* value map varies with the geographic factors contained in FAC1, the moisture dimension. Maps for two variables, distance to Gulf of Mexico and the pasture coverage, indicate the most co-varying patterns with FAC1. The farther the distance is from the Gulf of Mexico and the higher the pasture coverage is, the place is more likely to have a more significant correlation of ***CWS*** and moisture.

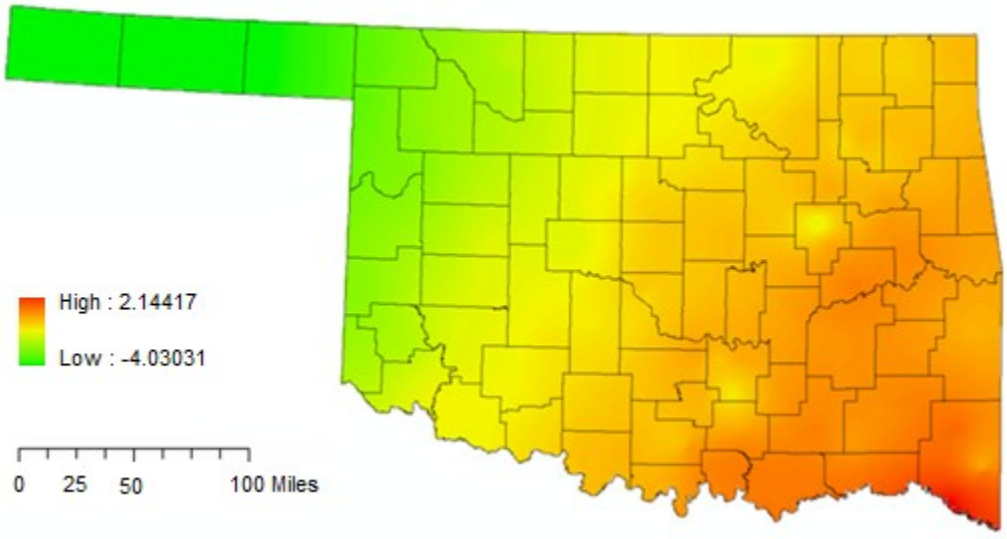

Figure 6.4 Surface Map for FAC1 Values (Moisture Dimension)

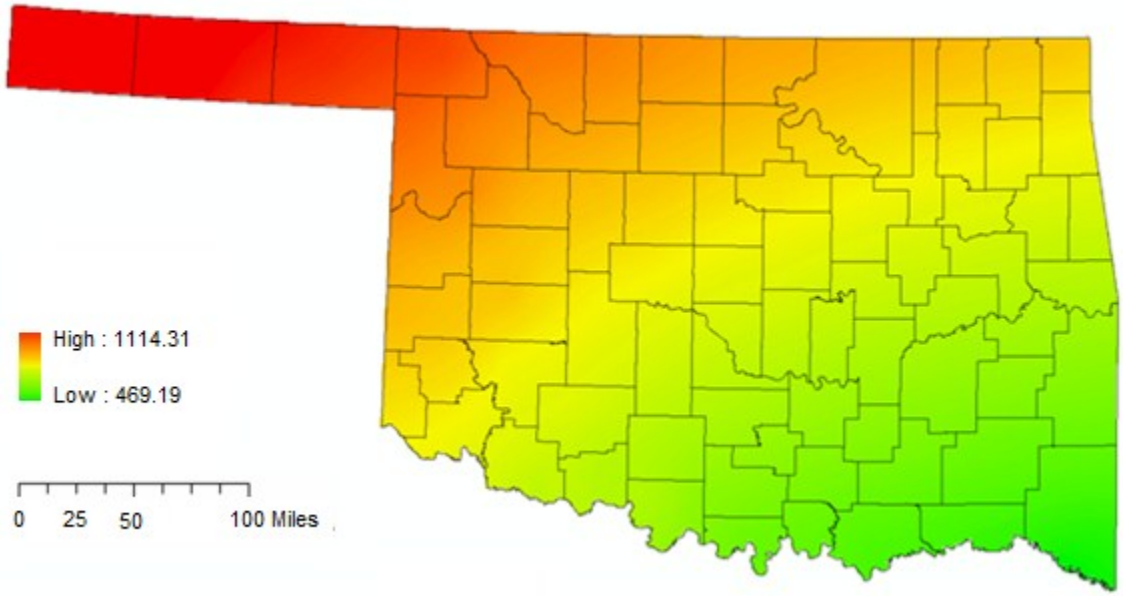

Figure 6.5 Surface Map for Distance to Gulf of Mexico

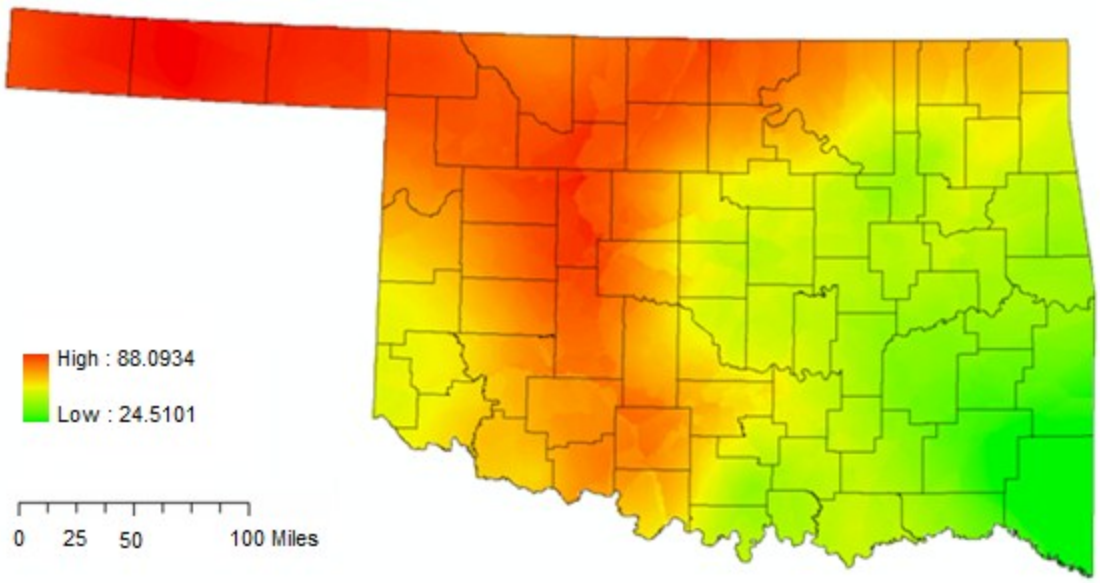

Figure 6.6 Surface Map for Pasture Coverage Percentage

Figure 6.7 is the map of parameter estimates for FAC5, which is largely composed of the variable of aspect within 5km and 1km and the relative elevation within 10km. This map indicates that the higher regression coefficients for FAC5 are in the northern part of Oklahoma, and the lower regression coefficients are in southern Oklahoma. The same amount of change in FAC5 will bring more changes to ***CIWS*** in the northern part of Oklahoma than in the southern. The map of *t* value for FAC5 (Figure 6.8), indicates the same pattern as the coefficient map in Figure 6.7, showing that in northern Oklahoma the positive relationship still holds, but in southern Oklahoma this relationship reverses. Considering the variables of aspect within 5km and 1km are positively related to FAC5 and the relative elevation within 10km are negatively related to FAC5, the distribution of FAC5 should indicate the synthesized result from the two categories of variables, plus other affecting variables. Figure 6.9 indicates that aspect within 5km is high in eastern and southern Oklahoma, but low in north western Oklahoma. Figure 6.10 shows a different pattern of relative elevation westward within 10km. Simply by combining the results from these two maps, it can be inferred that FAC5 is probably low in north-western Oklahoma, and high in eastern Oklahoma. The *t* value map in Figure 6.8 indicates that the influence of FAC5 on ***CWS*** is

relatively high in north-western and north-eastern portion of the state, where the FAC5 is relatively low.

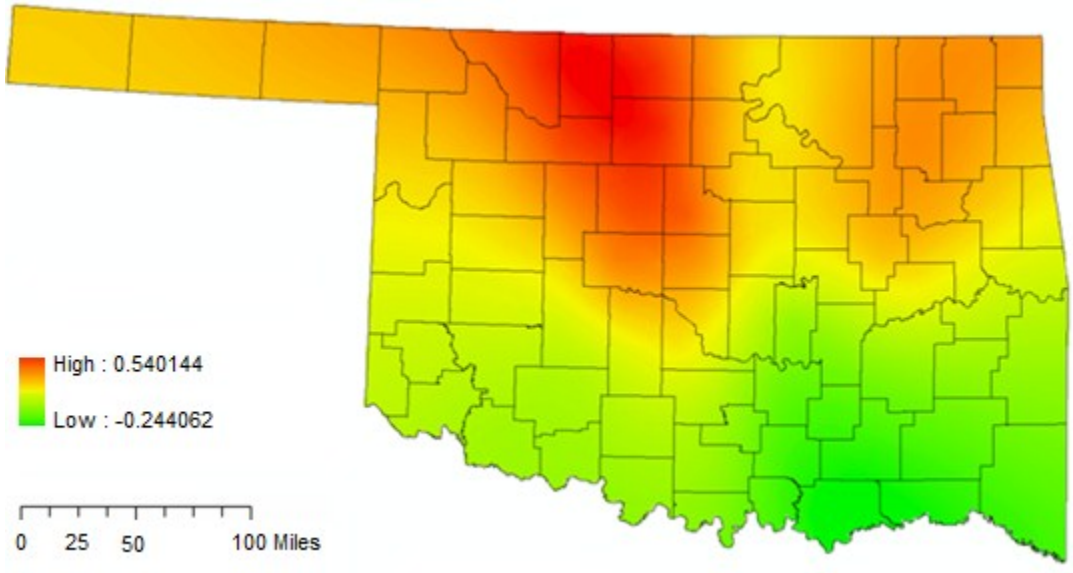

Figure 6.7 Parameter Estimates for Aspect and Relative Elevation Dimension (FAC5)

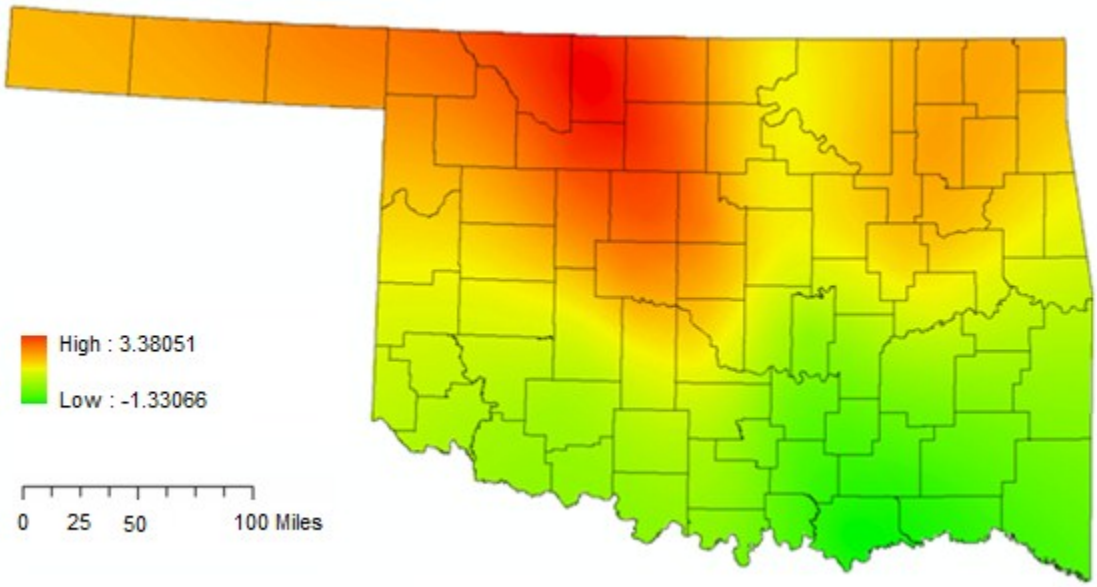

Figure 6.8 *t* Value for Aspect and Relative Elevation Dimension (FAC5)

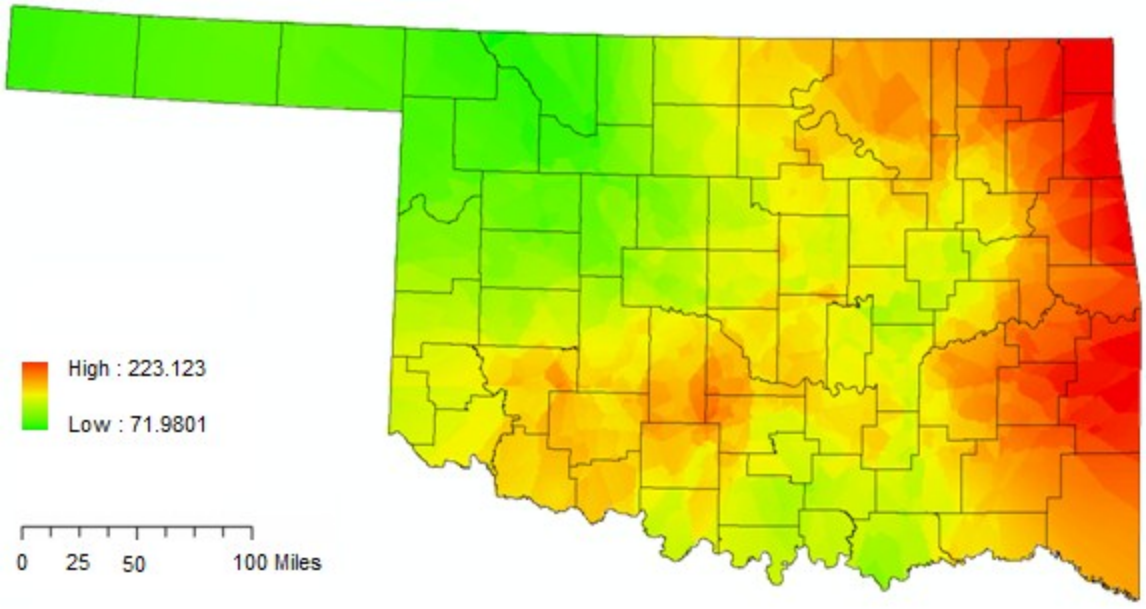

Figure 6.9 Surface Map of Variable Aspect within 5km (ASPECT5K)

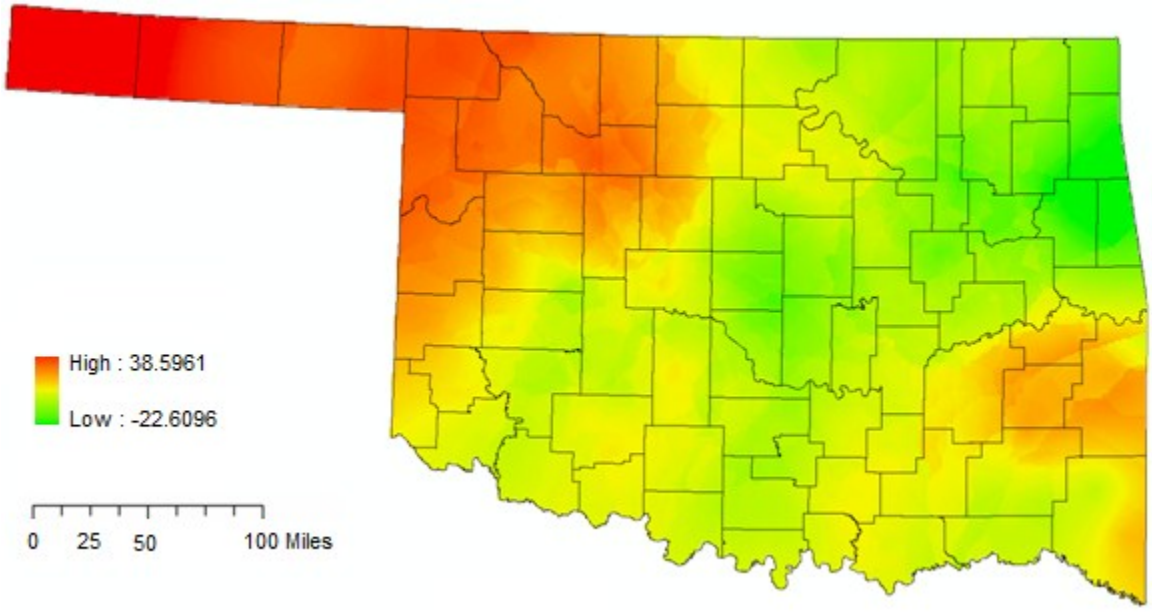

Figure 6.10 Surface Map of Variable Relative Elevation in 10km (DEFV10K)

Figure 6.11 maps the intercepts of the model. Intercepts represent the average effect on the

dependent variable with all the independent variables excluded from the model. The intercept values decreased with distance northwest in Oklahoma and can be interpreted as the model performing modestly differently over the state. The distribution pattern of Figure 6.11 is similar to the distribution of the annual ***CIWS*** in Oklahoma, with the highest values dominating the southeastern Oklahoma. This seems to imply that there are still some other factors that have not been captured explicitly in the GWR, especially factors affecting the nature of ***CWS*** in southeastern Oklahoma.

Maps for the estimates of FAC4 and FAC6 were skipped considering their spatial variations probably occur by chance based on the Monte Carlo significance test (Table 6.4). Combined with information in Table 6.5, FAC4 and FAC6 are identified as significantly related with local landscape dimensions of slope, forest coverage, and curvature condition. They are influential factors on ***CWS***, but the influences from these factors seem only to be determined by the absolute value of these factors, and do not vary so much with the location of these factors. Therefore, the coefficients from global modeling for these two components may also be used as the coefficients for the two factors in the local model.

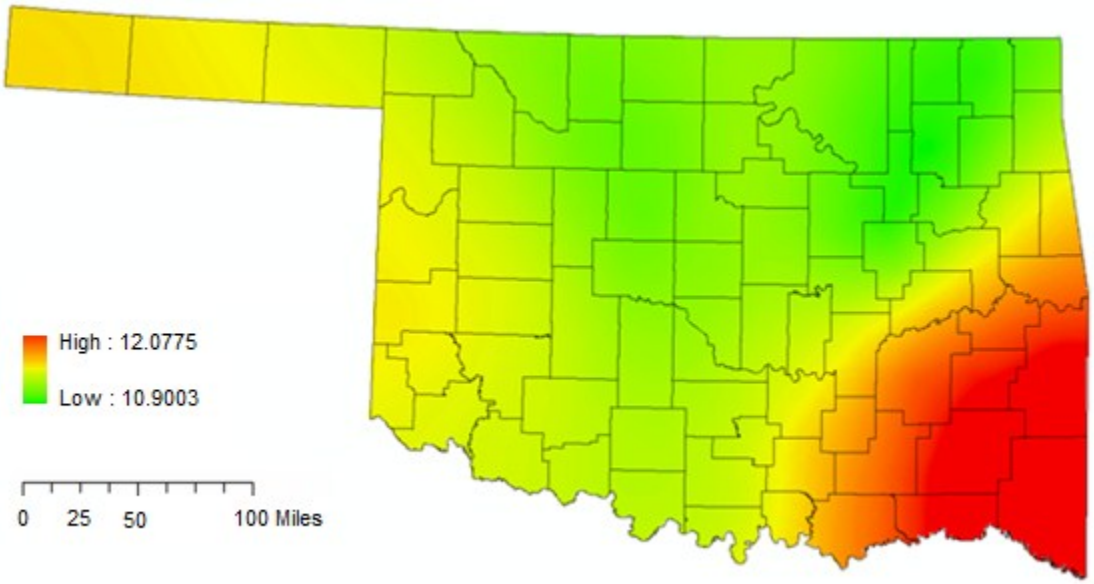

Figure 6.11 Parameter Estimates for Intercept

6.2.4 Statistics of GWR Model

GWR modeling provides some diagnostic statistics regarding how well the GWR model replicates the relationship between ***CWS*** and predictor variables. Table 6.5 provides the ANOVA test result for comparing the results of global model with the GWR model. The F test in this table indicates that the GWR model is a significant improvement from the global model for Oklahoma ***CWS*** data.

Source	SS	DF	MS	F
OLS Residuals	118.1	5.00		
GWR Improvement	34.0	15.31	2.2199	
GWR Residuals	84.1	106.69	0.7886	2.8148

Table 6.5 ANOVA Test Result from GWR Output Listing

Figure 6.12 is the local R-square map. The map indicates that not everywhere in Oklahoma is well explained by this GWR model. The model performed best in panhandle and western parts of Oklahoma, explaining at most about 82% percent of data variance, but in part of south central Oklahoma, this number dropped to about 21% at worst. The R-square is best in the western and northeastern parts of Oklahoma, matching most parts of the *t* value map for FAC1 (Figure 6.3), and, partially matching the *t* value map of FAC5 (Figure 6.8). This means that FAC1 and FAC5 are proper explanatory variables for this GWR model. Figure 6.13 is the residual map. Generally, this map shows a random distribution of residuals, and suggests that the model does fine for the state as a whole.

6.3 Some Discussion

This study built a statistical model for studying geographic variations of meso to micro scale of factors of ***CWS*** values in the case of Oklahoma. Considering the non-stationarity of geographic

phenomena, the local modeling approach of GWR was chosen. The thirteen years of 5-minute Mesonet data for 127 sites were the sample data. Principal components from PCA analysis on 53 geographic factors at Mesonet sites were used as the explanatory variables and the annual ***CIWS*** of Mesonet sites was used as response variable. GWR modeling was performed on different lists of independent variables using the first ten PCs.

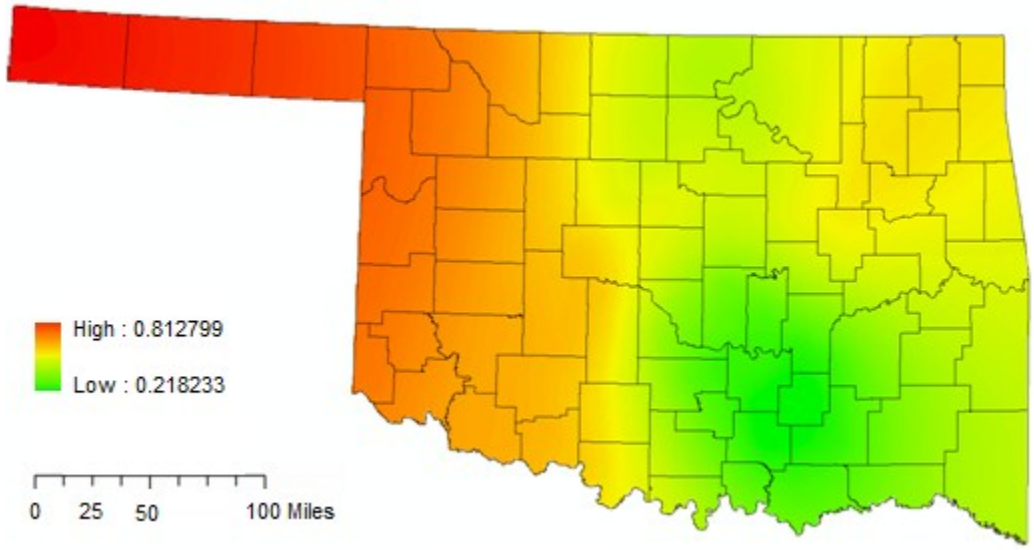

Figure 6.12 Surface of Local R-Square

The statistics from global modeling (Table 6.1) indicate that only FAC1, FAC4, FAC5, FAC6, and FAC9 are significantly related with ***CIWS***. The five PC factors correspond to moisture, landscape focusing on slope/forest coverage, landscape focusing on aspect/relative elevation, landscape focusing on curvature, and landscape focusing on barren and residential land percentage (Table 6.3). FAC9 is negatively related to ***CIWS***, and the four other PCs are positively related to the ***CIWS***. The higher the level of seasonal rain and humidity, longitude, cloud index, slope and forest coverage is, and the lower the elevation, the closer distance to Gulf of Mexico, and the smaller the average seasonal temperature difference is, could mean a higher level of ***CIWS*** at the location. In contrast, the factor FAC9, focusing on barren and residential land

percentage, is negatively related to ***CIWS*** and suggests higher percentage of barren land and lower percentage of residential land could mean lower ***CIWS***.

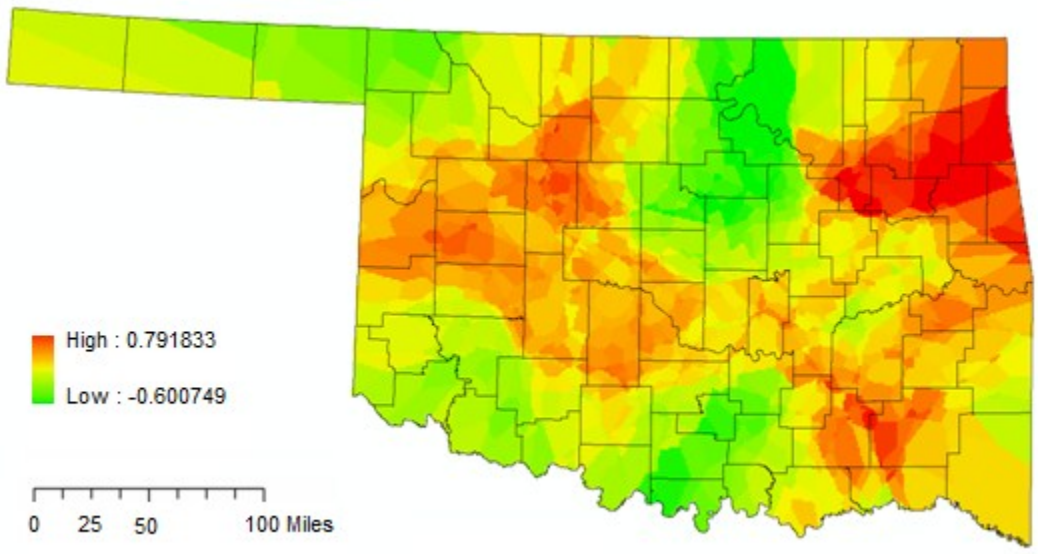

Figure 6.13 Surface of Residual

The results from running GWR using different lists of independent variables indicate that, in most cases, GWR models do not outperform global models in replicating the relationship between the ***CIWS*** and independent variables (see Table 6.2). There is only one case of the GWR model that outperforms the global OLS model, which used FAC1, FAC4, FAC5 and FAC6 as valid predictor variables. This model explains about 65% of data variance statewide. In this model, the principal components FAC1 and FAC5 are the two indicating spatial variation, while the other two (FAC4 and FAC6) do not vary much with locations.

The model of GWR using FAC1, FAC4, FAC5 and FAC6 as predictor variables has local R-squares between 0.20 and 0.88. In all of the GWR models using different lists of principal factors as explanatory variables, FAC1 is found to be the only factor indicating strong spatial variation in each case of models besides the intercept of each model. This suggests that among all identified factors, the moisture dimension in climate category is the most important spatial factor

influencing the level of ***CWS***. Considering that factors in climate category are also the ones most temporarily volatile, this feature may be used to predict the temporal changes in ***CIWS*** due to the varied climatic variables. The weak spatial variation in FAC5 indicates that the influences from the dimensions of aspect and relative elevation on ***CIWS*** only vary weakly with places. Combined with the inference that little spatial variation found in the estimates for FAC4 and FAC6, the influences from the landscape dimension variables on ***CIWS*** generally vary little with geography as compared with the influences of the moisture dimension on ***CIWS***. However, the three landscape dimensions are still important predictor variables of ***CIWS*** in the global model.

Based on the results of the only valid GWR model, the spatial patterns in the coefficients of FAC1 and FAC5 indicate that the positive relationship between ***CIWS*** and FAC1 and FAC5 in the global model does not hold everywhere in the local model and, in some places, a negative relationship between the ***CIWS*** and the two predictor variables occurs. Besides, it seems that in the locations with lower levels of moisture, the relationship between ***CIWS*** and the moisture factors are more statistically significant than in places with higher level of moisture (Figure 6.3). In addition, by comparing the map of the *t* values for FAC1 (Figure 6.3) with the distribution maps of variables within FAC1 (Figure 6.4), the variable distance to Gulf of Mexico and the variable pasture land coverage are most similar. This suggests that these two variables may affect the parameter estimates for FAC1 most.

The map of the intercepts of the GWR model (Figure 6.11) displays a pattern similar to the dependent variable ***CIWS***. It suggests that there are some unexplained variations in the GWR model, which may be due to some factors not included in the current modeling. Since most geographic variables in the meso to micro scale with the possibility of affecting the ***CWS*** have been considered in this study, the pattern of intercepts implies that the unexplained variations may be due to more to the macro nature of ***CWS***, which refers to the fact that the ***CWS*** and all associated geographic factors and processes behind are actually phenomena ongoing in much

wider spatial scale, crossing local points and regions. However, in this study, the nature of ***CWS*** was isolated to individual points and the level of ***CWS*** is assumed to be only directly related to a local or regional level of location, climate, and landscape factors. Obviously, the factors in the model were simplified and there is possible deficiency from surrogating of individual points from the macro background for explaining the ***CWS*** variations. According to Qiu and Wu (2011), the imperfection of a local modeling may be due to uncertainty of data aggregation on independent factors. Because of autocorrelation between geographic phenomena, for both the dependent variable ***CIWS*** and the list of independent variables, the variations within wider scale could contribute to unexplained variations of a local statistic model. For the purposes of investigating geographic variations of influential factors and examining spatial commonalities and dissimilarities in statistical analysis across Oklahoma, this study treated local ***CWS*** nature as single entities and necessarily disregarded the complex processes behind such a macro phenomenon. This seems to be an inherent deficiency to statistical geographic modeling, but it might be dealt with if GWR modeling is performed using a series of spatial units of local regression (Qiu and Wu, 2011), instead of using explanatory variables of a mix of scales like in this study.

CHAPTER VII

CONCLUDING REMARKS AND FUTURE WORK

This study investigated how the average level of complementarity between wind and insolation at a location is affected by geographic features of various scales. A case study was conducted over the state of Oklahoma using Oklahoma Mesonet data from 1994 through 2006. Quantification approaches, statistics and geographic weighted regression were employed in this study. Although much more could be done regarding this topic in the future, some basic conclusions could be drawn based on the current study. Potential applications and some future work in this field are discussed later in this chapter.

7.1 Concluding Remarks

First, the complementary nature of wind and insolation at a location can be quantified through long-term observed wind and insolation data. The quantification approach developed in this study calculates the dimensionless annual complementarity index, ***CIWS***, through normalizing original data of wind power and solar radiation over a yearly cycle. A similar approach was developed to calculate the daily ***CIWS***. Detailed procedures of the quantification approach are provided in Chapter Four. This approach is also cross validated by another method used by Sahin (2000), which is primarily based on Pearson correlation.

Second, the quantification approach was applied to Oklahoma and generated annual ***CIWS*** values for all Mesonet sites. The values fall between 0.28 and 0.62 if 1 is the highest. The interpolated

surface (Figure 4.11) using kriging created a map of annual ***CIWS*** for the entire state. In the case of Oklahoma, the nature of ***CWS*** does vary from place to place and there is notable spatial heterogeneity of the ***CIWS*** from eastern to western Oklahoma. In neighboring areas, the distribution pattern of ***CIWS*** manifests spatial auto-correlation, which refers to the tendency for nearby things to be more similar than distant things (De Smith, Goodchild and Longley, 2007).

Third, it was observed from the ***CIWS*** distribution map of Oklahoma shown in Figure 4.11 that, greater complementarity existed in eastern Oklahoma as opposed to western Oklahoma where both solar and wind energy are more plentiful. Therefore, a higher potential of wind or solar resources in a location as compared to other places does not necessarily mean a higher level of ***CIWS*** at that location. In western Oklahoma, areas with less climatic or terrain variation seem to have lower level of annual ***CIWS*** than eastern locations with more complex or mixed climatic and terrain conditions.

Fourth, based on the distribution pattern of the annual ***CIWS*** in Oklahoma shown in Figure 4.11, the ***CIWS*** seems to co-vary with elevation, the distance to Gulf of Mexico, latitude and longitude. Relating the ***CIWS*** with three categories of factors -- climate, location, and terrain -- 57 spatial variables from all three categories at local and micro scales were identified. Through correlation analysis, elevation, distance to Gulf of Mexico, longitude, plus spring humidity level and daily temperature difference in different seasons, were found to be significantly co-related with ***CIWS***. Through principal components analysis, the significantly co-related indicators were compressed into the three key dimensions: moisture, landscape and temperature.

Fifth, in the case of Oklahoma, by running a geographically weighted regression to model the relationship between the first ten principal components of PCA analysis and ***CIWS***, it was found that only four out of the first ten principal components were significantly related to ***CIWS*** at a 95% confidence level. These components represented the dimensions of moisture, landscape

focusing on slope/forest coverage, landscape focusing on curvature, and landscape focusing on barren and residential land coverage respectively. Another principal component factor of landscape focusing on aspect/relative elevation was significantly related to ***CIWS*** at an 85% confidence level. With many spatial variables potentially impacting on the ***CIWS*** within the three major categories of climate, location and terrain, only the four significant principal factors identified are valid for further local or global regression modeling (Qiu and Wu, 2011).

Sixth, through running the geographically weighted regression to model the relationship between the valid principal components and ***CIWS***, it was found that local models do not necessarily outperform global models, which means there may be a global relationship between those indicators and the ***CIWS***. The global model could provide another potential way to estimate ***CIWS*** for different locations other than the quantification approach. However, the local model works better for analyzing the relationship between geographic factors and ***CIWS*** than global models, because a local model provides localized parameter estimates, *t* values (significance test of parameter estimates) and error terms.

Seventh, in global models, among the significant principal component factors, the factor of landscape focusing on barren and residential land percentage was found negatively related to ***CIWS***, while the other three were all positively related to ***CIWS***. But based on the results of local model, the positive or negative relationship between ***CIWS*** and those valid indicators do not always hold and may reverse in different places. The signs of their relationships with ***CIWS*** also help to explain why, in Figure 4.11, eastern Oklahoma with generally higher levels of moisture, local slopes, forest coverage, local curvature or relative elevation has higher annual ***CIWS***.

Eighth, regression modeling found that ***CIWS*** generally has the closest relation with the moisture dimension principal component. This component includes the average relative humidity in the spring, average minimum temperature in all seasons, average temperature in the fall, average air

pressure in all seasons, average rainfall in all seasons, the annual cloud index, and average forest coverage in the region. The second category of principal components impacting most on ***CIWS*** is terrain variation, such as relative elevation of the location. Average curvature and aspect of a location may be listed as the third and fourth factors affecting the nature of ***CWS***.

Ninth, in the case of Oklahoma, there is only one case where the GWR model outperforms its corresponding global model. In this local model, the moisture dimension is the only one indicating significant spatial variation. This suggests that locations with higher levels of moisture may expect higher ***CIWS***, but the influences of moisture on ***CWS*** in wet regions lower than that in drier regions. Considering moisture is also a climatic variable varying with time, and the nature of ***CWS*** also varies temporally, it can be surmised that moisture could be a key factor behind both the temporal and spatial variation of ***CWS***.

Finally, for either the global model or local model of the relationship between spatial factors and ***CIWS***, there is still about 40% of data variation not explained by either. It is believed there are measurements of factors beyond local and regional scales affecting the nature of ***CWS***. Most likely some factors crossing local scales and with macro backgrounds also play important roles on the ***CWS***. This is based on the fact that both the response variables of wind/insolation and those explanatory spatial variables are macro phenomena over global scales, and actually are spatially undivided, while in modeling efforts, they are usually deliberately split into pieces in different scales for convenience of the study.

7.2 Some Potential Applications

There are several potential applications of the intermediate and final modeling results obtained from this study. First, based on this study, in Oklahoma, about one-half of Oklahoma has the normalized annual ***CIWS*** values above 50%, with the other half having less than 50%. This means that, when taking advantage of the complementary nature of wind and insolation in an

actual system design, a hybrid system deploying both wind and solar power as energy sources can be assured of adequate combined input at least 50% of the time in the eastern half of Oklahoma. But, in the western part of Oklahoma, the duration of acceptable combined input in a year is most likely to be less than half the time. Therefore, the backup systems designed for such hybrid systems should assure a stable energy provision for at least half of the time.

Second, the annul ***CIWS*** values and their annual complementarity profiles of wind and insolation generated for Oklahoma Mesonet sites in this study are of direct use to guide the planning and design of hybrid systems that hold much promise for the combined exploitation of wind and solar energy. It is rational to consider building wind/solar hybrid systems in places with relatively rich wind and solar resources and with good complementarity because this would require less energy storage and facilitate economical operation. Detailed annual or daily profiles of wind and solar power potential is necessary in design of both hybrid and standalone systems using wind and solar resources. Annual profiles generated by batch for all Mesonet sites are included in Appendix F.

Third, the findings of the relationship between geographic factors and ***CIWS*** in Oklahoma imply that areas with simple pattern of climatic or terrain conditions and with lower moisture levels may have lower level of annual ***CIWS***. If this relationship stands universally, hybrid deployment of wind and insolation in this type of area needs to consider more on-site storage for backup. The findings in this dissertation could help to decide the relative feasibility of installing hybrid wind/solar systems in a specific location. The more detailed arrangement of solar/wind systems, and the more exact demand of storage, can be determined further by observing the different levels of complementarity and energy use patterns.

Fourth, prediction and estimation of the complementarity index seems possible for areas with no long-term actual measurements of wind/solar data but with long-term climatology data available,

through applying the GWR model built in this study.

Finally, this study provides some standardized approaches to quantify ***CIWS*** for different locations with known interval wind/insolation data. Programs to help automate the quantification process have been developed (see Appendices A, B and C). Programs to create profile charts of wind power and solar radiation in annual or daily cycles are also available for similar usage.

7.3 Suggestions for Future Work

This study explored and quantification of the nature of ***CWS***, and investigated the relationship between geographical features and ***CWS***. There is scope of considerably more research on this topic. The following part suggests several avenues for future work.

First, the method employed to calculate annual ***CIWS*** is not finalized for the quantification of complementarity considering the normalization procedure could be further simplified and improved. The case study is positioned in a data-rich state like Oklahoma. Other approaches might be developed given the varying quantity and quality of wind, solar, and geographic data in other regions of the world. In addition, in this study, the aggregate unit for calculating annual ***CIWS*** is by month, and for deriving daily ***CIWS*** is a specific day; when investigating the nature of ***CWS*** in regions with rich resources of either insolation (such as Arizona), or wind (such as western of Oklahoma), the aggregate unit could be replaced by specific day/night time intervals, and may be by seasons. This could also be tested using Oklahoma data first.

Second, this study investigates how ***CIWS*** is impacted by local and regional geographic variables using geographically weighted regression. The distribution of local R-square and the intercept indicates there is still some variance unexplained by the local variables chosen for this study. Macro factors may be more significant for understanding the complementarity. Because of the complexity of geographic phenomena, the exploration is still based on point-based or region-based observations, and inductive models such as extrapolation. But no matter how small the

observation unit is, the background setting of geography is always continuous and the spatial processes taking place are continuous. How the larger scale variations of those geographic factors are related to the ***CWS*** index needs additional study.

Third, temporal patterns of complementarity in diurnal, seasonal, and annual cycles are not the focus of this study, but are important and deserve more study. How the ***CWS*** in the three temporal levels differ from each other needs additional study. To make a better match with local electrical load level using energy generated from both wind and solar resources, it will be necessary to create the temporal profile of wind and solar for each location. The more detailed the temporal coverage, the more useful it will be in actual engineering and market design. The temporal pattern of ***CWS*** is not only useful in actual system design for hybrid systems of both wind and solar resources in each location but also in forming a complete picture about the dynamic nature of ***CWS***.

Fourth, study of the spatial factors behind temporal variations of ***CWS*** in different locations and comparing with results of this study would be helpful to deepen the understanding of how the nature of ***CWS*** is related to various geographic factors.

Fifth, this study used only Oklahoma and only the Mesonet data from 1994-2006 in the case study. The methods applied in this study should be extended to include more recent Mesonet data and applied to other regions so that the GWR results can be tested and verified. The geographic factors identified as related with the ***CWS,*** and the global and GWR models can be also tested using other data-rich locations in United States.

Sixth, in the present study, conversion efficiency (Kaltschmitt, Streicher, and Weise, 2009), land use conflicts, and other economic and social factors (Abbasi and Abbasi, 2000; Simon, 2009), which might be keys to installation of hybrid systems, have been excluded. Likewise, determination of optimal scales of generation and equipment specifications were beyond the

scope of this study. As such, the current analysis was dictated by the natural resources and geographic background rather than extant wind and solar technologies. Additional studies could bring these non-geographic factors into focus.

Seventh, the present analysis is for a part of the United States where distribution and transmission lines are well-developed. Hybrid projects using wind and solar energy might be coupled or not coupled to an existing or future electrical grid depending upon economics and the wishes of the developer. However, large expanses of the Third World lacking electrical transmission will adopt off-grid generation. These are important differences in terms of how hybrid projects will be implemented, but have not been included in this study.

Eighth, this study implicitly focuses on rural areas because rural landscapes with wind/solar hybrid systems are more readily sited and because of the relative lack of land use conflicts and electrical grid connections. The Oklahoma Mesonet stations serving as the data source were originally sited to be representative of rural surroundings within a few kilometers. This avoided complicated urban temperature and wind variations so well-established over the micro- and meso-scales (Geiger, Aron, and Todhunter, 2005). It is surmised that statewide complementarity maps such as presented in this study would not change with the inclusion of urban data, but that nuances in urban areas would need to be explored for individual siting decisions within cities.

Ninth, there are many unknown factors about the causes and spatial processes behind the nature of ***CWS***, and they need more exploration and modeling analysis. The negative feedback mechanism behind solar and wind energy may be of theoretical value to further study this dynamic nature of ***CWS***. Negative feedback could be the cause of complementarity of wind and insolation. Based on the general definition of feedback by Ramaprasad (1983), any change in the environment leading to additional and enhanced changes in that system is the result of a positive feedback mechanism. Alternatively, if a change in the environment leads to a compensating

process that mitigates the change, it is a negative feedback mechanism (Ramaprasad, 1983). Based on the definition of the ***CWS***, it describes a tendency taking place on earth's surface that when insolation onto one location tends to decrease, at the same time, wind power, the redistributed solar energy accumulated from different places and time may increase at the same point. This fits the concept of negative feedback. In addition, identification of atmospheric variables as first-level of impacting factors on ***CWS*** emphasizes the fact that wind energy is a redistributed type of energy from solar energy in the moving atmosphere. The study of the relationships between wind and insolation is essentially a study of the redistribution mechanics of solar to wind energy. There is some kind of negative feedback behind the process of solar energy redistributing to wind energy. Variables representing atmospheric movement and conditions are the most direct factors driving negative feedback formed in the redistribution processes. Other geographic factors such as absolute location and landscape conditions affect the feedback formation through impacting on the atmospheric variables first. So, they are secondary factors on the nature of ***CWS***. To learn more about how geographic factors influence the ***CWS*** also means to learn more about mechanics behind the forming of the negative feedbacks between solar and wind energy.

Finally, in situations where just wind and insolation in one location cannot meet the local energy demand, the knowledge of complementarity of these energy sources in a wider geographic area could be vital. Wind energy measured at one location is a demonstration of delayed redistribution of solar energy, which reaches the earth surface at a different time and location usually. Because of the complexity and uncertainty of geographic processes behind this redistribution, the temporal variation of the complementarity of wind and insolation at a location is inherent in nature. However, it is possible this temporal variation may be mitigated through deployment of wind and solar energy from a wider geographic area (Jacobson, 2009). Therefore, investigation of

complementarity of renewable energy sources within a region rather than at a point seems worthy of future work.

By studying the complementarities between wind and insolation, one major goal is to verify the interrelations between these two forms of renewable energy so that its features can be used as a guide in future deployment of renewable resources. An overarching goal is to try to explain how and what geographic factors help to shape the complementary nature between them so that some extrapolations and predications can be made based on an appropriate correlation model. Understandings of some spatial characteristics and processes taking place behind the two renewable resources might also be deepened.

Undoubtedly, future global energy strategies will include more renewable energy resources. Research on the spatial feature of bilateral complementarity between wind power and insolation should initiate further attempts to study the relationship between renewable resources and the possible geographic roles and processes behind them.

REFERENCES

Abbasi, S. A. and N. Abbasi. 2000. The likely adverse environmental impacts of renewable energy sources. *Applied Energy* 65:121-44.

Ai, B., H. Yang, H. Shen., and X. Liao. 2003. Computer-aided design of PV/wind hybrid systems. *Renewable Energy* 28:1491-12.

Aitken, D., Billman, L., and Bull, S. 2004. The Climate Stalization Challenge: Can Renewable Energy Sources Meet the Target? *Renewable Energy World* 7(6): 56-69.

American Heritage Dictionary of the English Language (AHDEL), 4th Edition. 2007. Boston, USA: Houghton Mifflin Company.

Archer, C. and M. Jacobson. 2005. Evaluation of global wind power. *Journal of Geophysical Research – Atmospheres* 110:D12110.

Barley, C., L. Dennis, D. J. Lew, and L. T. Flowers. 1997. *Sizing wind/photovoltaic hybrids for households in Inner Mongolia.* National Renewable Energy Laboratory website: http://www.nrel.gov/docs/legosti/fy97/23116.pdf (last accessed on 11 August, 2011).

Bluhm, C., Widiger, T. A., and Miele, G. M. 1990. Interpersonal complementarity and individual differences. *Journal of Personality and Social Psychology* 58: 464-471.

Bohr, N. 1999. *Neils Bohr collected works*, Volume 10, *Complementarity beyond physics (1928-1962),* ed. D. Flavholdt. Amsterdam, Elsevier.

Bordley, R. 1985. Relating elasticities to changes in demand. *Journal of Business and Economic Statistics* 3(2): 156-58.

BP Review. 2011. Global Natural Gas Reserve. Retrieved from BP company website: http://www.bp.com/sectiongenericarticle800.do?categoryId=9037178&contentId=7068624 (last accessed on June 30, 2012).

California Energy Commission Consultant Report (CECCR). 2002. New Wind Energy Resource Maps of California. Retrieved from California Energy Commission website: http://www.energy.ca.gov/reports/2004-07-14_500-02-055F.PDF (last accessed on August 20, 2011).

Carlaw, K. and Lipsey, R. 2002. Externalities versus technological complementarities: a model of GPT-driven, sustained growth. *Research Policy* 31(8–9):1305-1315.

Claeskens, G. and Hjort, N. L. 2008. Cambridge Series in Statistical and Probabilistic Mathematics - Model Selection and Model Averaging: The Bayesian information criterion, p.70-98. Cambridge, United Kingdom: Cambridge University Press,

Cleveland, J. Cutler. 2007. Energy Transitions Past and Future. *Encyclopedia of Earth*. April, 2007. Retrieved from http://www.eoEarth.org/article/Energy_transitions_past_and_future (last accessed on Apr. 2012).

De Smith, M., Goodchild, M., and Longley, P. 2007. *Geospatial Analysis - a comprehensive guide*. 2nd edition, p.181. Leicester, UK: Troubador Publishing Ltd.

Dogniaux, R. 1994. Prediction of solar radiation in areas with a specific microclimate. Commission of the European communities. Dordrecht: Kluwer Academic Publishers.

Donoho, David L. and Iain M. Johnstone. 1994. Ideal spatial adaptation by wavelet shrinkage, *Biometrika* 81(3):425-455.

Dubayah, Ralph and Rich, M. Paul. 1996. GIS-based Solar Radiation Modeling. In: *GIS and Environmental Modeling: Progress and Research Issues*. Editors: Goodchild, M. F., Steyaert, L. T., Parks, B. O., Johnston, C., Maidment, D., Crane, M., and Glendinning, S. GIS World Books: Colorado, 1996: 129.

Edgeworth, F.Y., 1925. The pure theory of monopoly. In: *Papers Relating to Political Economy,* Vol.1, London, MacMillan: 111–142.

Energy Information Administration (EIA). 2010. *Table of Primary Energy Review 1949-2009*. EIA website: http://www.eia.doe.gov/emeu/aer/txt/ptb0101.html (last accessed August 15, 2010).

Englert, Berthold-Georg, Scully, M. O., and Walther, H. 1994. The Duality in Matter and Light. *Scientific American* 27(6): 56-61.

European Commission Joint Research Center (ECJRC). 2006. GIS Assessment of Solar Energy Resources in Europe. Nov. 12, 2006. Institute of Energy and Transport of European Commission website: http://www.ec-gis.org/project.cfm?id=621&db=project (last accessed May 2, 2012).

Felder, Deborah. 2004. A regionally based energy end-use strategy: Case studies from Centre Country, Pennsylvania. *The Professional Geographer* 56:185-200.

Fiebrich, Christopher A., David L. Grimsley, Renee A. McPherson, Kris A. Kesler, Gavin R. Essenberg, 2006: The Value of Routine Site Visits in Managing and Maintaining Quality Data from the Oklahoma Mesonet. *J. Atmos. Oceanic Technol.*, **23**, 406–416.

Fotheringham, A., C. Brunsdon, and M. Charlton. 2002. *Geographically weighted regression: the analysis of spatially varying relationships*. Chichester, UK: John Wiley & Sons, LTD.

Geiger, R., R. Aron, and P. Todhunter. 2005. *The climate near the ground.* Lanham, UK: Rowman and Littlefield Publishers, Inc.

Giordani, P. and H. Kiers. 2006. A comparison of three methods for principal component analysis of fuzzy interval data. *Computational Statistics & Data Analysis* 51(1): 379-97.

Gül, Timur. 2004. "Integrated Analysis of Hybrid Systems for Rural Electrification in Developing Countries". http://www2.lwr.kth.se/Publikationer/PDF_Files/LWR_EX_04_26.PDF (last accessed July 22, 2012).

Heimiller, D.M. and Haymes, S.R. 2001. *Geographic Information Systems in Support of Wind Energy Activities at NREL's WARM model*. US Department of Energy Wind Powering America website: http://www.windpoweringamerica.gov/pdfs/gis_nrel.pdf (last accessed Sept. 19, 2011).

Internation Energy Agency (IEA). 2012. IEA wind annual report 2012. IEA website: http://www.iea.org/aboutus/faqs/renewableenergy/ (last accessed from on May 2, 2012).

International Human Genome Sequencing Consortium (IHGSC). 2004. Finishing the euchromatic sequence of the human genome. *Nature* 431 (7011): 931-45.

Iowa Energy Center (IEC). 2007. Wind Energy Manual. IEC website: http://www.energy.iastate.edu/renewable/wind/wem/wem-08_power.html (last accessed Jan. 2, 2011).

Intergovernmental Panel on Climate Change. 2007. Summary for Policy makers. *IPCC AR4: p.13.* Website: http://www.ipcc.ch/pdf/assessment-report/ar4/wg1/ar4-wg1-spm.pdf (last accessed July 22, 2012).

Jacobson, M. Z. 2009: Review of solutions to global warming, air pollution, and energy security. *Energy and Environmental Science* 2:148-73.

Kaltschmitt, M., W. Streicher, and A. Weise, eds. 2009. *Renewable energy, technology, economics, and environment*. Berlin, Springer.

Kim, H. 2003. Measuring complementarity in network design using structural equation modeling (SEM) technique with LISREL software. *The IEEE Xplore* 2:1513-19.

Kimura, Y., Y. Onai, and I. Ushiyama. 1996. A demonstrative study for the wind and solar hybrid power system. *Renewable Energy* 9:895-98.

Laursen, K. and Mahnke, V. 2001. Knowledge strategies, firm types, and complementarity in human-resource practices. *Journal of Management and Governance* 5: 1–27.

Lincoln, S. 2005. Fossil fuels in the 21st century. *Ambio* 34: 621-27.

Lloyd, C. D. 2007. Local Models Spatial Analysis. 1st Edition. CRC Press: USA.

Macken, K.J.P., Bollen, M.H.J. and Belmans, R.J.M. 2004. Mitigation of voltage dips through distributed generation systems. *IEEE Transactions on Industry Applications* 40: 1686-92.

McPherson, R. A., C. Fiebrich, K. C. Crawford, R. L. Elliott, J. R. Kilby, D. L. Grimsley, J. E. Martinez, J. B. Basara, B. G. Illston, D. A. Morris, K. A. Kloesel, S. J. Stadler, A. D. Melvin, A.J. Sutherland, and H. Shrivastava. 2007: Statewide monitoring of the mesoscale environment: A technical update on the Oklahoma Mesonet. *Journal of Atmospheric and Oceanic Technology* 24: 301-321.

Meyer, R. 2008. The potential of solar energy for replacing fossil fuels. *Barcelona, Spain: The VII ASPO Conference Presentations*. http://www.aspo-spain.org/aspo7/presentations/Meyer-CSP-ASPO7.pdf (last accessed on August 15, 2010).

MESONET, 2008. Mesonet basic site information and map. From website: http://www.mesonet.org/index.php/site/sites/station_names_map (last accessed on August 21, 2011).

Milgrom, P. and Roberts, J. 1990. The Economics of Modern Manufacturing: Technology, Strategy and Organization. *American Economic Review* 80: 511-28.

Mitasova, H., Mitas, L., Brown, W.M., Gerdes, D.P., Kosinovsky I., and Baker, T. Modeling Spatial and Temporal Distributed Phenomena: New Methods and Tools for Open GIS. *GIS and Environmental Modeling: Progress and Research Issues*. GIS World Books: Colorado, 1996:345.

National Energy Education Project (NEED). 2011. *Wonders of wind-teacher's guide*. NEED websitehttp://www.need.org/needpdf/Wonders%20of%20Wind%20Teacher%20Guide.pdf (last accessed on April 2, 2012).

National Land Cover Databse (NLCD). 2012. NLCD 2001 map from Multi-resolution Land Characteristics Consortium website: http://www.mrlc.gov/nlcd01_data.php (last accessed on July 2, 2012).

National Oceanic and Atmospheric Administration (NOAA). 2008. Retrieved from website: http://noaasis.noaa.gov/NOAASIS/ml/avhrr.html (last accessed on July 29, 2012).

Oklahoma Center for Geospatial Information (OCGI). 2008. OCGI website: http://www.ocgi.okstate.edu/ (last accessed on June 1, 2012).

Oklahoma Wind Power Initiative (OWPI). 2007. OWPI site: http://www.ocgi.okstate.edu/owpi/ (last accessed on May 2, 2012).

Office of Engineering Research, Oklahoma State University (OSU Report). 1962. *Report on Energy Storage-Key to Our Economic Future*. Sept., 1962: 171.

Oliver, M. A. and R. Webster. 1990. Kriging: a method of interpolation for geographical information systems. International Journal of Geographical Information Science 4 (3): 313-32.

Qiu, Xiaomin and Wu, Shuo-sheng. 2011. Global and local regression analysis of factors of American College Test (ACT) score for public high schools in the state of Missouri. *Annals of the Association of American Geographers,* Routledge, 101(1): 63-83.

Ramakumar, Rama. 2001. Electricity From Renewable Energy: A Timely Option. *Keynote Address on National Seminar on Renewable Energy Sources.* Pune, Maharashtra, India, 2001.

Ramaprasad, Arkalgud. 1983. On the definition of feedback. *Behavioral Science*: Vol. 28(1): 4–13.

Reichling, J. and F. Kulacki. 2008. Utility scale hybrid wind–solar thermal electrical generation: a case study for Minnesota. *Energy* 33 (4): 626-38.

Rockwell, R.C. 1998. From a Carbon Economy to a Mixed Economy: A Global Opportunity. *Consequences* Vol. 4(1). Website: http://www.gcrio.org/consequences/ (last accessed July 12, 2012).

Sahin, A.Z. 2000. Applicability of wind-solar thermal hybrid power systems in the northeastern part of the Arabian Peninsula. *Energy Sources, Part A: Recovery, Utilization, and Environmental Effects* 22: 845-50.

Sawin, J. 2004. *Mainstreaming Renewable Energy in the 21st Century.* Washington, D.C.: Worldwatch Institute, 18.

Schaefer, Scott. 1999. Product design partitions with complementary components. *Journal of Economic Behavior & Organization* Vol. 38 (1999): 311-330.

Shaw, G., and Wheeler, D. 1994. Statistical techniques in geographical analysis, 2nd Edition. London: David Fulton Publishers,

Simon, C. A. 2009. Cultural constraints on wind and solar energy in the U.S. Context. *Comparative technology transfer and society* 7 (3):252-69.

Sims, R. 2004. Renewable energy: a response to climate change. Solar Energy, Volume 76 (1-3): page 9-17. From website: http://www.sciencedirect.com/science/article/pii/S0038092X03001014 (last accessed Nov. 12, 2012).

Solar Radiation Monitoring Lab (SRML), University of Oregon. 2007. SRML website: http://solardat.uoregon.edu/SolarRadiationBasics.html (last accessed on January 2, 2011).

Stadler, S. and T. Hughes. 2005. Wind power climatology. In *Encyclopedia of World Climatology*, ed. J. Oliver, 807-13. Dordrecht, Neth.: Springer.

Takle, E. S. and Shaw, R. H. 1979. Complimentary nature of wind and solar energy at a continental mid-latitude station. *International Journal of Energy Research* 3: 103-12.

Tierney, Luke. 1990. LISP-STAT: An Object-Oriented Environment for Statistical Computing and Dynamic Graphics, NewYork, NY: Wiley.

University of California Los Angeles: Academic Technology Services, Statistical Consulting Group (UCLA-ATS). 2011. *Introduction to SPSS*. Retrieved from website: http://www.ats.ucla.edu/stat/SPSS/output/principal_components.htm (last accessed August 05, 2011).

University of British Columbia, Department of Geography (UBC), 2011. *GWR 3 Mannual*. Website: http://www.geog.ubc.ca/courses/geob479/labs/GWR3manual.htm (last accessed on May 20, 2011).

US Department of Energy. 2010. *Glossary of energy-related terms*. US DOE website: http://www1.eere.energy.gov/site_administration/glossary.html (last accessed Jan. 2, 2012)

US Department of Energy/NREL, 2011. Small wind electric systems- a Maryland consumer's guide. NREL website: http://www.nrel.gov/docs/fy09osti/45911.pdf (last accessed on May 21, 2012).

U.S. Geological Survey (USGS). 2008. USGS website: http://tahoe.usgs.gov (last accessed on July 2, 2012).

Vegetation/Ecosystem Modeling and Analysis Project (VEMAP). 2008. Retrieved from website: http://daac.ornl.gov/VEMAP/vemap.shtml (last accessed July 20, 2012).

Wang, Caisheng and Nehrir, M. Hashem. 2005. Analytical Approaches for Optimal Placement of Distributed Generation Sources in Power Systems. *IEEE Transactions on power systems* 19 (4): 2068-76.

Yu, Danlin and Wei, Yehua Dennis. 2006. Introduction to Geographically weighted regression. http://pages.csam.montclair.edu/~yu/GISDay_GWR.ppt (last accessed on Jan. 8, 2012).

Zhou, W., C. Lou, Z. Li, C. Lu, and Yang, H. 2010. Current status of research on optimum sizing of stand-alone hybrid solar–wind power generation systems. *Applied Energy* 87: 380-89.

APPENDIX A

SQL SCRIPTS FOR CALCULATING ANNUAL *CIWS* ON MESONET DATA

```
If exists (select * from dbo.sysobjects where id = object_id(N'[dbo].[ClimatologyData]') and
OBJECTPROPERTY(id, N'IsUserTable') = 1)
drop table [dbo].[ClimatologyData]
GO

---create table ClimatologyData to store all text data downloaded from Mesonet
CREATE TABLE [dbo].[ClimatologyData] (
        [DateTimeStamp] [varchar] (50) COLLATE SQL_Latin1_General_CP1_CI_AS NULL ,
        [STID] [varchar] (10) COLLATE SQL_Latin1_General_CP1_CI_AS NULL ,
        [STNM] [int] NULL ,
        [TIME] [int] NULL ,
        [RELH] [int] NULL ,
        [TAIR] [decimal](18, 2) NULL ,
        [WSPD] [decimal](18, 2) NULL ,
        [WVEC] [decimal](18, 2) NULL ,
        [WDIR] [decimal](18, 2) NULL ,
        [WDSD] [decimal](18, 2) NULL ,
        [WSSD] [decimal](18, 2) NULL ,
        [WMAX] [decimal](18, 2) NULL ,
        [RAIN] [decimal](18, 2) NULL ,
        [PRES] [decimal](18, 2) NULL ,
        [SRAD] [decimal](18, 2) NULL ,
        [TA9M] [decimal](18, 2) NULL ,
        [WS2M] [decimal](18, 2) NULL ,
        [TS10] [decimal](18, 2) NULL ,
        [TB10] [decimal](18, 2) NULL ,
        [TS05] [decimal](18, 2) NULL ,
        [TB05] [decimal](18, 2) NULL ,
        [TS30] [decimal](18, 2) NULL ,
        [TR05] [decimal](18, 2) NULL ,
        [TR25] [decimal](18, 2) NULL ,
        [TR60] [decimal](18, 2) NULL ,
        [TR75] [decimal](18, 2) NULL

) ON [PRIMARY]
GO

--create table to summarize WSPD data
CREATE TABLE WindSpdDaySummery (
IndicatorNo int null,
YearNo int null,
MonthNo int null,
DayNo int null,
STID varchar(5),
STNM int null,
WSPDDaySum decimal(10,2) null,
WSPDDayCount int null,
WSPDDayAvg decimal(10,6) null
)

-- Insert Data into  new table
```

```
INSERT INTO WindSpdDaySummery
(
IndicatorNo ,
YearNo,
MonthNo,
DayNo,
STID,
STNM,
WSPDDaySum,
WSPDDayCount,
WSPDDayAvg
)
SELECT IndicatorNo,
YearNo,
MonthNo,
DayNo,
STID,
STNM,
SUM(WSPD) as WSPDDaySum,
count(WSPD) WSPDDayCount,
SUM(WSPD)/count(WSPD) as WSPDDayAvg
FROM  ClimatologyData
WHERE WSPD>=0
GROUP BY IndicatorNo, YearNo, MonthNo, DayNo, STID,
STNM

--create new table to summarize TAIR data
CREATE TABLE TAIRDaySummery
(
IndicatorNo int null,
YearNo int null,
MonthNo int null,
DayNo int null,
STID varchar(5),
STNM int null,
TAIRDaySum decimal(10,2) null,
TAIRDayCount int null,
TAIRDayAvg decimal(10,6) null
)

-- Insert Data into  new table
INSERT INTO TAIRDaySummery
(
IndicatorNo ,
YearNo,
MonthNo,
DayNo,
STID,
STNM,
TAIRDaySum,
TAIRDayCount,
```

```
TAIRDayAvg
)
SELECT IndicatorNo,
YearNo,
MonthNo,
DayNo,
STID,
STNM,
SUM(TAIR) as TAIRDaySum,
count(TAIR) TAIRDayCount,
SUM(TAIR)/count(TAIR) as TAIRDayAvg
FROM  ClimatologyData
WHERE TAIR>-500
GROUP BY IndicatorNo, YearNo, MonthNo, DayNo, STID,
STNM

--create new table to summarize PRES data
CREATE TABLE PRESDaySummery
(
IndicatorNo int null,
YearNo int null,
MonthNo int null,
DayNo int null,
STID varchar(5),
STNM int null,
PRESDaySum decimal(10,2) null,
PRESDayCount int null,
PRESDayAvg decimal(10,6) null
)

-- Insert Data into  new table
INSERT INTO PRESDaySummery
(
IndicatorNo ,
YearNo,
MonthNo,
DayNo,
STID,
STNM,
PRESDaySum,
PRESDayCount,
PRESDayAvg
)
SELECT IndicatorNo,
YearNo,
MonthNo,
DayNo,
STID,
STNM,
SUM(PRES) as PRESDaySum,
count(PRES) PRESDayCount,
```

```
SUM(PRES)/count(PRES) as PRESDayAvg
FROM  ClimatologyData
WHERE PRES>0
GROUP BY IndicatorNo, YearNo, MonthNo, DayNo, STID,
STNM

--Create new table to join WSPD and TAIR data
SELECT WindSpdDaySummery.IndicatorNo,
WindSpdDaySummery.YearNo,
WindSpdDaySummery.MonthNo,
WindSpdDaySummery.DayNo,
WindSpdDaySummery.STID,
WindSpdDaySummery.STNM,
WindSpdDaySummery.WSPDDaySum,
WindSpdDaySummery.WSPDDayCount,
WindSpdDaySummery.WSPDDayAvg,
TAIRDaySummery.TAIRDaySum,
TAIRDaySummery.TAIRDayCount,
TAIRDaySummery.TAIRDayAvg
INTO JOINWindTair
FROM WindSpdDaySummery
LEFT JOIN TAIRDaySummery
ON WindSpdDaySummery.IndicatorNo=TAIRDaySummery.IndicatorNo and
WindSpdDaySummery.YearNo=TAIRDaySummery.YearNo and
WindSpdDaySummery.MonthNo=TAIRDaySummery.MonthNo and
WindSpdDaySummery.DayNo=TAIRDaySummery.DayNo and
WindSpdDaySummery.STID=TAIRDaySummery.STID and
WindSpdDaySummery.STNM=TAIRDaySummery.STNM

--Create new table by join tables for WSPD, TAIR, and TA9M
SELECT WindSpdDaySummery.IndicatorNo,
WindSpdDaySummery.YearNo,
WindSpdDaySummery.MonthNo,
WindSpdDaySummery.DayNo,
WindSpdDaySummery.STID,
WindSpdDaySummery.STNM,
WindSpdDaySummery.WSPDDaySum,
WindSpdDaySummery.WSPDDayCount,
WindSpdDaySummery.WSPDDayAvg,
TAIRDaySummery.TAIRDaySum,
TAIRDaySummery.TAIRDayCount,
TAIRDaySummery.TAIRDayAvg,
TA9MDaySummery.TA9MDaySum,
TA9MDaySummery.TA9MDayCount,
TA9MDaySummery.TA9MDayAvg
INTO JoinWindTairTa9m
FRom WindSpdDaySummery
left join TAIRDaySummery
ON WindSpdDaySummery.IndicatorNo=TAIRDaySummery.IndicatorNo and
WindSpdDaySummery.YearNo=TAIRDaySummery.YearNo and
WindSpdDaySummery.MonthNo=TAIRDaySummery.MonthNo and
```

```
WindSpdDaySummery.DayNo=TAIRDaySummery.DayNo and
WindSpdDaySummery.STID=TAIRDaySummery.STID and
WindSpdDaySummery.STNM=TAIRDaySummery.STNM
left join TA9MDaySummery
ON WindSpdDaySummery.IndicatorNo=TA9MDaySummery.IndicatorNo and
WindSpdDaySummery.YearNo=TA9MDaySummery.YearNo and
WindSpdDaySummery.MonthNo=TA9MDaySummery.MonthNo and
WindSpdDaySummery.DayNo=TA9MDaySummery.DayNo and
WindSpdDaySummery.STID=TA9MDaySummery.STID and
WindSpdDaySummery.STNM=TA9MDaySummery.STNM

--Create new table to summarize SRAD data
CREATE TABLE SRADDaySummery
(
IndicatorNo int null,
YearNo int null,
MonthNo int null,
DayNo int null,
STID varchar(5),
STNM int null,
SRADDaySum decimal(10,2) null,
SRADDayCount int null,
SRADDayAvg decimal(10,6) null
)

--Insert data to new table
INSERT INTO SRADDaySummery
(
IndicatorNo ,
YearNo,
MonthNo,
DayNo,
STID,
STNM,
SRADDaySum,
SRADDayCount,
SRADDayAvg
)
SELECT IndicatorNo,
YearNo,
MonthNo,
DayNo,
STID,
STNM,
SUM(WSPD) as SRADDaySum,
count(WSPD) SRADDayCount,
SUM(WSPD)/count(WSPD) as SRADDayAvg
FROM  ClimatologyData
WHERE SRAD>=0
GROUP BY IndicatorNo, YearNo, MonthNo, DayNo, STID,
STNM
```

APPENDIX B

MAIN PROGRAM FOR CREATING BASIC PROFILES AUTOMATICALLY

(MODIFIED FROM OPENSOURCE-ZEDGRAPH)

```
using System;
using System.Data;
using System.Drawing;
using System.Drawing.Imaging;
using System.IO;
using System.Configuration;
using System.Web;
using System.Web.Security;
using System.Web.UI;
using System.Web.UI.WebControls;
using System.Web.UI.WebControls.WebParts;
using System.Web.UI.HtmlControls;
using ZedGraph.Web;
using ZedGraph;

public partial class _Default : System.Web.UI.Page
{

   private string saveImagePath =
System.Configuration.ConfigurationManager.AppSettings["SaveImagePath"];
   private string SaveImageName =
System.Configuration.ConfigurationManager.AppSettings["SaveImageName"];
   private string ApplicationName =
System.Configuration.ConfigurationManager.AppSettings["ApplicationName"];
   private string ImageSubDirectory =
System.Configuration.ConfigurationManager.AppSettings["ImageSubDirectory"];
   DataSet locDataset = new DataSet();
   //database connection function
   DataFunctions datafunction = new DataFunctions();

   protected void Page_Load(object sender, EventArgs e)
   {
      if (!Page.IsPostBack)
      {
         //get location name for dropdown list
         locDataset = datafunction.GetLocationData();
         this.ddlLocations.DataSource = locDataset;
         this.ddlLocations.DataValueField = "STID";
         this.ddlLocations.DataTextField = "STID";
         this.ddlLocations.DataBind();
         this.ddlLocations.SelectedIndex = 0;
      }
   }

   protected void btnOneLocation_Click(object sender, EventArgs e)
   {
       singlegraph(this.ddlLocations.SelectedValue);
   }
   protected void btnAllLocation_Click(object sender, EventArgs e)
   {
      //get location name
```

```
        locDataset = datafunction.GetLocationData();
        //create one graph for each location
        for (int i = 0; i < locDataset.Tables[0].Rows.Count; i++)
        {
singlegraph(locDataset.Tables[0].Rows[i]["STID"].ToString());
        }
    }
    protected void singlegraph(string STID)
    {
        // get one location data
        DataTable dt = datafunction.GetData(STID);

        //create image full name with path use STID for image save
        //Name looks like -- ACME.jpg
        string filename = STID + ".jpg";

        //full Name looks like -- C:/inetpub/wwwroot/ZedGraphWebApp/tempImages/ACME.jpg
        // ***   All Image goes to C:/inetpub/wwwroot/ZedGraphWebApp/tempImages/   ***
        string imageFullName = saveImagePath + filename;

        //create graph use VerticalBarsWithLabels class, this is the only implement class
        //change the code in this class if you want format the graph or any other changes
        //Some sample codes can be found in function createGraph() of AppChartBase.cs class
        VerticalBarsWithLabels vg = new VerticalBarsWithLabels(imageFullName, 800, 600, dt);

        // relative path looks like -- http://localhost/ZedGraphWebApp/
        string ApplicationRelativePath = "http://" + Request.ServerVariables["SERVER_NAME"] +
"/" + ApplicationName + "/";

        if (vg.IsImageCreated)
        {   //add the image to web page one the image created
            System.Web.UI.WebControls.Image img = new System.Web.UI.WebControls.Image();
            //image id on page
            img.ID = STID;
            //ImageUrl looks like --  http://localhost/ZedGraphWebApp/tempImages/ACME.jpg
            img.ImageUrl = ApplicationRelativePath + ImageSubDirectory.Replace("\\","/") +
filename;
            img.Visible = true;
            imgPanel.Controls.Add(img);
        }
        vg = null;
    }
}
```

APPENDIX C

SCRIPTS FOR CALCULATING DAILY *CIWS* OF APRIL 15 OF 2000 FOR MESONET SITES

```
Begin select IndicatorNo, STID, STNM, YearNo, MonthNo, DayNo, TIME, RELH, TAIR,
WSPD, RAIN, PRES, SRAD, TA9M into AllSites0415_2000 from ClimatologyData where
(MonthNo=4 and DayNo=15 and YearNo =2000)

alter table AllSites0415_2000 add  WPD5min10m decimal(18,2) null, WPD5min50m decimal
(18,2) null, calc_flag int null

alter table AllSites0415_2000 add ELEV int null

update AllSites0415_2000  SET Elev=397 Where STNM=110

    (**calc_flag can be
    0-when WSPD, TA9m, PRES data used for calculating WPD, or none of them are null.
        1-when WSPD, TAIR, PRES data used for calculating WPD, or TA9m is null, but
        WSPD, TAIR, PRES are not.
        2-when WSPD, TA9m, Elev used for calculating WPD, or PRES is null, but WSPD,
        TA9m are not,
        3-when WSPD, TAIR, Elev used for calculating WPD, or TA9m and PRES are null, but
        WSPD, TAIR are not null.
        4-when WSPD, Elev used for calculating WPD, or TA9m, TAIR and PRES are null, but
        WSPD is not.
        -1-when WSPD is null)

        Update AllSites0415_2000 SET
        WPD5min10m=0.5*(PRES*100/(287*(TA9M+273)))*power(WSPD,3),
        WPD5min50m=WPD5min10m*1.993235,  calc_flag=0
where (WSPD>=0) and (PRES >0) and (TA9M >-500)


update AllSites0415_2000
SET WPD5min10m=0.5*(PRES*100/(287*(TAIR+273)))*power(WSPD,3),
WPD5min50m=WPD5min10m*1.993235,
calc_flag=1
where (WSPD>=0) and (PRES >0) and (TA9M<-500) and (TAIR >-500)


update AllSites0415_2000
        SET WPD5min10m=0.5*(101325/(287*(TA9M+273)))*EXP(-
        9.8*1267/(287*(TA9M+273)))*POWER(WSPD,3),
WPD5min50m=WPD5min10m*1.993235,
calc_flag=2 where (WSPD>=0) and (PRES<-500) and (TA9M >-500)


update AllSites0415_2000
        SET WPD5min10m=0.5*(101325/(287*(TAIR+273)))*EXP(-
        9.8*1267/(287*(TAIR+273)))*POWER(WSPD,3),
WPD5min50m=WPD5min10m*1.993235,
     calc_flag=3
where (WSPD>=0) and (PRES <-500) and (TA9M <-500) and (TAIR >-500)

    update AllSites0415_2000
```

```
SET WPD5min10m=0.5*(1.225-(1.194/10000)*1267)*POWER(WSPD,3),
    WPD5min50m=WPD5min10m*1.993235,
    calc_flag=4
Where (WSPD>=0) and (TA9M <-500) and (TAIR <-500)

update AllSites0415_2000
SET calc_flag=-1
where (WSPD<0)


update AllSites0415_2000
SET WPD5min50m=WPD5min10m*1.993235
where WPD5min10m is not null
```

APPENDIX D

SCRIPTS FOR CALCULATING ANNUAL CLOUD INDEX FOR MESONET STATIONS

```
update ClimatologyData
set MonthNo=SUBSTRING(DateTimeStamp,7,2)

alter table ClimatologyData
add MaxSRAD decimal(12,2) null

alter table ClimatologyData
drop column MaxSRAD

update ClimatologyData
set MaxSRAD=max(SRAD)
group by MonthNo and DayNo and TIME

create table MaximumSRAD
(
STID varchar(5) null,
STNM int null,
MonthNo int null,
DayNo int null,
TIME int null,
MaxSRAD decimal(10,2) null
)

Insert into MaximumSRAD
(
STID,
STNM,
MonthNo,
DayNo,
TIME,
MaxSRAD
)
select
STID,
STNM,
MonthNo,
DayNo,
TIME,
Max(SRAD)
from ClimatologyData
GROUP BY STID, STNM,MonthNo,DayNo,TIME

create table MaximumSRAD2
(
```

```
STID varchar(5),
STNM int null,
MonthNo int null,
DayNo int null,
TIME int null,
MaxSRAD decimal(10,2) null
)

Insert into MaximumSRAD2
(
STID,
STNM,
MonthNo,
DayNo,
TIME,
MaxSRAD
)
select distinct * from MaximumSRAD

CREATE INDEX INDXSTID
ON MaximumSRAD (STID)

INSERT INTO SRADDaySummery
(
STID,
STNM,
YearNo,
MonthNo,
DayNo,
SRADDaySum,
SRADDayCount,
SRADDayAvg
)
SELECT
STID,
STNM,
YearNo,
MonthNo,
DayNo,
SUM(SRAD) as SRADDaySum,
count(SRAD) SRADDayCount,
SUM(SRAD)/count(SRAD) as SRADDayAvg
FROM  ClimatologyData
WHERE SRAD>=0
```

```
GROUP BY STID,STNM, YearNo, MonthNo, DayNo

SELECT
STID,
STNM,
MonthNo,
DayNo,
SUM(SRAD) as SRADDayMax
into SRADDayMaximum
FROM  MaximumSRAD2
GROUP BY STID,STNM, MonthNo, DayNo

create table SRADDaySum
(
STID varchar(5) null,
STNM int null,
YearNo int null,
MonthNo int null,
DayNo int null,
SRADDayTotal decimal(10,2) null
)

insert into SRADDaySum
(
STID,
STNM,
YearNo,
MonthNo,
DayNo,
SRADDayTotal
)
SELECT
STID,
STNM,
YearNo,
MonthNo,
DayNo,
SUM(SRAD) as SRADDayTotal
FROM  ClimatologyData
WHERE SRAD>=0
GROUP BY STID,STNM, YearNo, MonthNo, DayNo

SELECT SRADDaySum.STID,
SRADDaySum.STNM,
```

```
SRADDaySum.YearNo,
SRADDaySum.MonthNo,
SRADDaySum.DayNo,
SRADDaySum.SRADDayTotal,
SRADDayMaximum.SRADDayMax
INTO JoinSRADDaySUMMax
FRom SRADDaySum
left join SRADDayMaximum
ON
SRADDaySum.MonthNo=SRADDayMaximum.MonthNo and
SRADDaySum.DayNo=SRADDayMaximum.DayNo and
SRADDaySum.STID=SRADDayMaximum.STID and
SRADDaySum.STNM=SRADDayMaximum.STNM

select STID, STNM, Sum(SRADDayMax) as SRADMonthMax from SRADDayMaximum into
SRADMaxbyMonth group by STID, STNM, MonthNo

select STID, STNM, Sum(SRADMonthMax) as SRADYearMax into SRADMaxbyYear from
SRADMaxbyMonth group by STID, STNM

select STID, STNM, YearNo, MonthNo, Sum(SRADDayTotal) as SRADMonthSum into
SRADSumbyMonth from SRADDaySum group by STID, STNM, YearNo, MonthNo

ALTER TABLE SRADDaySummery
ADD SRADDayTotal decimal (10,2) null

UPDATE SRADDaySummery
SET SRADDayTotal = SRADDaySum
WHERE SRADDayCount = 288

update SRADDaySummery
set SRADDayTotal=288*
(select AvgedDaySRAD
from SRADDayAvg
where SRADDaySummery.STID=SRADDayAvg.STID and
SRADDaySummery.STNM=SRADDayAvg.STNM and
SRADDaySummery.MonthNo=SRADDayAvg.MonthNo and
SRADDaySummery.DayNo=SRADDayAvg.DayNo
)
where SRADDayCount<288

create table SRADComDay
(
STID varchar(5),
```

```
STNM int null,
YearNo,
MonthNo int null,
DayNo int null,
SRADDaySum decimal(10,2) null,
SRADDayAvg decimal(10,2) null,
)

insert into SRADComDay
(
STID,
STNM,
YearNo,
MonthNo,
DayNo,
SRADDaySum,
SRADDayAvg,
)
select
STID,
STNM,
YearNo,
MonthNo,
DayNo,
SRADDaySum,
SRADDayAvg
from SRADDaySummery
where SRADDayCount=288

select STID, STNM, MonthNo, DayNo, Count(YearNo) as AvgedYears, Sum(SRADDayAvg) as
SummedAvgSRAD, Sum(SRADDayAvg)/Count(YearNo) as AvgedDaySRAD
into SRADDayAvg
from SRADDaySummery
where SRADDayCount=288
group by STID, STNM, MonthNo, DayNo
(46089 row(s) affected)

create table SRADAvgforTime
(
STID varchar(5) null,
STNM int null,
MonthNo int null,
DayNo int null,
TIME int null,
```

```
SumTIMESRAD decimal(10,2) null,
CountofTIME int null,
SRADAvgbyTime decimal(10,2) null
)

Insert into SRADAvgforTIME
(
STID,
STNM,
MonthNo,
DayNo,
TIME,
SumTIMESRAD,
CountofTIME,
SRADAvgbyTime
)
select
STID,
STNM,
MonthNo,
DayNo,
TIME,
Sum(SRAD),
Count(TIME),
Sum(SRAD)/Count(TIME)
from ClimatologyData
where SRAD>=0
GROUP BY STID, STNM,MonthNo,DayNo,TIME

create table MaximumSRAD3
(
STID varchar(5) null,
STNM int null,
MonthNo int null,
DayNo int null,
TIME int null,
MaxSRAD decimal(10,2) null
)

Insert into MaximumSRAD3
(
STID,
STNM,
MonthNo,
```

```
DayNo,
TIME,
MaxSRAD
)
select
STID,
STNM,
MonthNo,
DayNo,
TIME,
Max(SRAD)
from ClimatologyData
where SRAD>=0
GROUP BY STID, STNM,MonthNo,DayNo,TIME
```

select * into MaximumSRAD4 from MaximumSRAD2 (make a copy of MaximumSRAD2 before update)

```
update MaximumSRAD2
set MaxSRAD= (select SRADAvgbyTime from SRADAvgforTime where
SRADAvgbyTime.STID=MaximumSRAD2.STID and
SRADAvgbyTime.STNM=MaximumSRAD2.STNM and
SRADAvgbyTime.MonthNo=MaximumSRAD2.MonthNo and
SRADAvgbyTime.DayNo=MaximumSRAD2.DayNo and
SRADAvgbyTime.TIME=MaximumSRAD2.TIME)
where MaxSRAD<0

update ClimatologyData
set SRAD= (select SRADAvgbyTime from SRADAvgforTime where
SRADAvgforTime.STID=ClimatologyData.STID and
SRADAvgforTime.STNM=ClimatologyData.STNM and
SRADAvgforTime.MonthNo=ClimatologyData.MonthNo and
SRADAvgforTime.DayNo=ClimatologyData.DayNo and
SRADAvgforTime.TIME=ClimatologyData.TIME)
where SRAD<0

create table SRADDaySum2
(
STID varchar(5) null,
STNM int null,
YearNo int null,
MonthNo int null,
DayNo int null,
DayCount int null,
```

```
SRADDayTotal decimal(10,2) null
)

insert into SRADDaySum2
(
STID,
STNM,
YearNo,
MonthNo,
DayNo,
DayCount,
SRADDayTotal
)
SELECT
STID,
STNM,
YearNo,
MonthNo,
DayNo,
Count(SRAD) as DayCount,
SUM(SRAD) as SRADDayTotal
FROM  ClimatologyData
WHERE SRAD>=0
GROUP BY STID,STNM, YearNo, MonthNo, DayNo

--remove doubled value of IDAB in SRADDaySum2
update SRADDaySum2 set DayCount=DayCount/2
where STID='IDAB'

update SRADDaySum2 set SRADDayTotal=SRADDayTotal/2
where STID='IDAB'

select STIM, STNM, MonthNo, DayNo, Sum(SRADAvgbyTime) as
SRADDaySum,Count(TIME) as DayCount
into SRADDayTotalfromAvg
from SRADAvgforTime
group by STIM, STNM, MonthNo, DayNo

update SRADDaySum2
set SRADDayTotal = (select SRADDaySum from SRADDayTotalfromAvg where
SRADDayTotalfromAvg.STID=SRADDaySum2.STID
and SRADDayTotalfromAvg.STNM=SRADDaySum2.STNM and
SRADDayTotalfromAvg.MonthNo=SRADDaySum2.MonthNo
and SRADDayTotalfromAvg.DayNo=SRADDaySum2.DayNo)
```

```
where DayCount<288

SELECT
STID,
STNM,
MonthNo,
DayNo,
Count(TIME) as DayCountofMax,
SUM(MaxSRAD) as SRADDayMax
into SRADDayMaximum2
FROM  MaximumSRAD2
GROUP BY STID,STNM, MonthNo, DayNo

SELECT SRADDaySum2.STID,
SRADDaySum2.STNM,
SRADDaySum2.YearNo,
SRADDaySum2.MonthNo,
SRADDaySum2.DayNo,
SRADDaySum2.DayCount,
SRADDayMaximum2.DayCountofMax
SRADDaySum2.SRADDayTotal,
SRADDayMaximum2.SRADDayMax
INTO JoinSRADDaySUMMax2
FRom SRADDaySum2
left join SRADDayMaximum2
ON
SRADDaySum2.MonthNo=SRADDayMaximum2.MonthNo and
SRADDaySum2.DayNo=SRADDayMaximum2.DayNo and
SRADDaySum2.STID=SRADDayMaximum2.STID and
SRADDaySum2.STNM=SRADDayMaximum2.STNM

select STID, STNM, YearNo, MonthNo, count(SRADDayTotal) as CountofSRADDay,
Count(SRADDayMax) as CountofDayMax, Sum(SRADDayTotal) as SRADMonthSum,
Sum(SRADDayMax) as SRADMonthMax into SRADSumMaxbyMonth from
JoinSRADDaySUMMax2 group by STID, STNM, YearNo, MonthNo

select STID, STNM, YearNo, Sum(SRADMonthSum) as SRADYearSum,
Sum(SRADMonthMax) as SRADYearMax into SRADSumMaxbyYear from
SRADSumMaxbyMonth group by STID, STNM, YearNo

select STID, STNM, Sum(SRADYearSum) as SRADSiteSum,count(SRADYearSum) as
AvgedSumYears,Sum(SRADYearSum)/count(SRADYearSum) as AvgedSiteSum,
Sum(SRADYearMax) as SRADYearMax, count(SRADYearMax) as AvgedMaxYears,
Sum(SRADYearMax)/count(SRADYearMax) as AvgedSiteMax
```

```
into SRADAvgSumMaxbySite from SRADSumMaxbyYear group by STID, STNM

select STID, STNM, YearNo, Count(MonthNo) from SRADSumMaxbyMonth
group by STID, STNM, YearNo having count(MonthNo)<12 order by STID, YearNo

select * from ClimatologyData where STID='ALVA' and YearNo=1999 order by MonthNo,
DayNo, TIME

create table SRADAvgforMonth
(
STID varchar(5) null,
STNM int null,
MonthNo int null,
MonthCount int null,
SumSRADMonth decimal(10,2) null,
SRADAvgbyMonth decimal(10,2) null
)

insert into SRADAvgforMonth
(
STID,
STNM,
MonthNo,
MonthCount,
SumSRADMonth,
SRADAvgbyMonth
)
SELECT
STID,
STNM,
MonthNo,
Count(SRADMonthSum) as MonthCount,
Sum(SRADMonthSum) as SumSRADMonth,
Sum(SRADMonthSum)/Count(SRADMonthSum) as SRADAvgbyMonth
FROM  SRADSumMaxbyMonth
WHERE (CountofSRADDay=31 and MonthNo=1) or (CountofSRADDay=31 and MonthNo=3)
or (CountofSRADDay=31 and MonthNo=5) or
(CountofSRADDay=31 and MonthNo=7) or (CountofSRADDay=31 and MonthNo=8) or
(CountofSRADDay=31 and MonthNo=10)
or (CountofSRADDay=31 and MonthNo=12) or (CountofSRADDay=30 and MonthNo=4) or
(CountofSRADDay=30 and MonthNo=6) or
(CountofSRADDay=30 and MonthNo=9) or (CountofSRADDay=30 and MonthNo=11) or
(CountofSRADDay=28 and MonthNo=2) or
(CountofSRADDay=29 and MonthNo=2)
```

```
GROUP BY STID,STNM, MonthNo

update SRADSumMaxbyMonth
set SRADMonthSum= (select SRADAvgbyMonth from SRADAvgforMonth where
SRADAvgforMonth.STID=SRADSumMaxbyMonth.STID and
SRADAvgforMonth.STNM=SRADSumMaxbyMonth.STNM and
SRADAvgforMonth.MonthNo=SRADSumMaxbyMonth.MonthNo)
where (CountofSRADDay<31 and MonthNo=1) or (CountofSRADDay<31 and MonthNo=3) or
(CountofSRADDay<31 and MonthNo=5) or
(CountofSRADDay<31 and MonthNo=7) or (CountofSRADDay<31 and MonthNo=8) or
(CountofSRADDay<31 and MonthNo=10)
or (CountofSRADDay<31 and MonthNo=12) or (CountofSRADDay<30 and MonthNo=4) or
(CountofSRADDay<30 and MonthNo=6) or
(CountofSRADDay<30 and MonthNo=9) or (CountofSRADDay<30 and MonthNo=11) or
(CountofSRADDay<28 and MonthNo=2)

update SRADSumMaxbyMonth
set SRADMonthSum= (select SRADAvgbyMonth from SRADAvgforMonth where
SRADAvgforMonth.STID=SRADSumMaxbyMonth.STID and
SRADAvgforMonth.STNM=SRADSumMaxbyMonth.STNM and
SRADAvgforMonth.MonthNo=SRADSumMaxbyMonth.MonthNo)
where (CountofSRADDay<29 and MonthNo=2 and YearNo=1996) or (CountofSRADDay<29
and MonthNo=2 and YearNo=2000)
or (CountofSRADDay<29 and MonthNo=2 and YearNo=2004)

select STID, STNM, YearNo, count(SRADMonthSum) as CountofSRADMonth,
count(SRADMonthMax) CountofMonthMax,
as Sum(SRADMonthSum) as SRADYearSum, Sum(SRADMonthMax) as SRADYearMax into
SRADSumMaxbyYear2 from SRADSumMaxbyMonth
group by STID, STNM, YearNo

select * from SRADSumMaxbyYear2 where CountofSRADMonth<12
order by STID, STNM, YearNo

select STID, STNM, Sum(SRADYearSum) as SRADSiteSum, count(SRADYearSum) as
AvgedSumYears,Sum(SRADYearSum)/count(SRADYearSum) as AvgedYearSRAD,
Sum(SRADYearMax) as SRADYearMax, count(SRADYearMax) as AvgedMaxYears,
Sum(SRADYearMax)/count(SRADYearMax) as AvgedYearMax
into SRADAvgSumMaxbyYearSite2 from SRADSumMaxbyYear2 where
CountofSRADMont=12 group by STID, STNM

--after above operations, the tables ClimatologyData,
JoinSRADDaySUMMax2,SRADSumMaxbyMonth, SRADSumMaxbyYear2,  and
```

SRADAvgSumMaxbyYearSite2 are representing SRAD and SRADMax by TIME, DAy, Month, Year, and site correpondingly.

```
alter table SRADAvgSumMaxbyYearSite2
add AvgedYearlyCloudIndex decimal (5,2)

update SRADAvgSumMaxbyYearSite2
set AvgedYearlyCloudIndex=1-(AvgedYearSRAD/AvgedYearMax)
```

APPENDIX E

PRINCIPAL COMPONENTS FROM PCA ANALYSIS USED IN GWR MODELING

STNM	LAT	LON	FAC1	FAC2	FAC3	FAC4	FAC5	FAC6	FAC7	FAC8	FAC9	FAC10
1	34.7989	-96.6692	0.68	-0.23	0.48	-0.13	-0.27	1.16	-0.03	-1.50	-1.00	0.23
2	34.5872	-99.3378	-0.39	-0.25	1.46	-0.81	2.21	-0.07	-0.28	-0.12	-0.33	0.65
3	36.7797	-98.6717	-0.83	-0.59	-0.53	-1.00	-1.31	-0.07	0.95	-0.76	1.05	-1.16
4	34.2242	-95.7006	0.83	0.32	0.08	0.58	-0.56	-0.82	0.44	-2.95	-0.40	-1.02
5	34.1922	-97.0850	0.85	-0.98	1.33	0.14	-0.69	0.23	0.33	-1.01	1.00	-0.92
6	36.0728	-99.9014	-1.73	-0.02	-0.18	1.39	0.92	-1.66	0.08	1.44	0.21	0.70
7	34.0144	-94.6131	1.30	1.53	0.00	1.68	-0.98	-1.79	1.61	-2.06	0.70	-0.90
8	36.8022	-100.5303	-2.37	0.46	0.03	-0.69	-0.28	-0.68	-1.29	-0.89	0.50	-0.54
9	35.4017	-99.0589	-0.71	-0.63	0.84	0.83	-0.35	-0.58	0.93	1.46	-0.10	0.94
10	35.9625	-95.8661	0.66	0.83	-0.28	-1.58	-0.22	-0.05	-1.26	0.14	-2.86	0.60
11	36.7544	-97.2539	-0.14	0.54	-1.12	-1.45	-0.27	-0.08	0.74	0.06	0.00	-0.05
12	36.6925	-102.4972	-3.76	0.28	-1.33	1.06	0.88	-0.54	-0.95	-1.86	-1.42	-0.99
13	35.1717	-96.6314	0.57	-0.08	-0.06	-0.16	-0.23	0.07	-0.66	-0.89	-0.80	-0.49
14	36.4119	-97.6942	-0.30	0.25	-0.29	-1.44	-0.34	0.57	1.20	0.05	-0.10	0.21
15	35.7808	-96.3539	0.33	0.94	-0.34	0.01	-0.87	1.06	0.01	-1.01	-0.58	-0.99
16	36.8314	-99.6408	-1.71	0.99	0.47	-0.30	-1.04	-0.31	0.30	0.62	0.00	-0.27
17	36.6342	-96.8111	-0.13	0.59	-1.42	0.40	0.23	-0.48	1.15	1.24	-0.76	0.94
18	33.8939	-97.2692	0.63	0.43	1.90	-0.19	-0.96	-0.73	-0.84	-0.78	1.26	0.60
19	35.5914	-99.2706	-1.05	0.67	0.99	-0.12	-1.09	-0.38	-1.03	0.19	0.88	-0.97
20	34.8497	-97.0033	0.77	-1.29	-0.09	0.16	1.18	1.03	-0.40	0.15	2.52	-1.00
21	34.9925	-96.3342	0.75	0.86	-0.05	-0.13	0.05	-0.81	-1.31	-0.06	0.72	1.02
22	36.0283	-99.3464	-1.46	1.32	-0.07	0.91	0.27	-1.17	-0.43	2.00	0.51	0.66
23	34.6086	-96.3331	0.83	0.71	0.13	0.21	1.08	0.45	0.38	-0.86	-0.09	-0.15
24	35.6528	-96.8042	0.48	-1.56	-0.55	-0.15	-0.33	-1.22	-0.72	0.72	-0.56	0.24
25	36.7481	-98.3628	-0.71	0.59	0.02	-1.81	-1.85	0.21	0.64	-0.92	3.47	6.25
26	35.5458	-99.7275	-1.33	-1.03	0.59	1.66	-1.83	3.16	-0.40	-0.08	1.94	1.42
27	35.0319	-97.9144	-0.05	1.10	1.00	-0.69	-0.38	-0.16	0.03	-0.78	0.48	-0.95
28	36.3172	-95.6417	0.54	-0.48	-1.24	-0.60	0.04	-1.49	0.66	-0.81	1.20	-1.31
29	34.6556	-95.3261	1.03	2.07	0.46	1.35	-0.46	0.11	-3.82	2.73	1.02	-0.38
30	34.2231	-95.2494	1.19	-0.07	-0.56	2.68	0.17	-0.62	1.93	-1.18	-0.41	-0.07
31	35.6794	-94.8486	0.81	0.95	-1.85	2.60	0.90	5.21	0.38	-0.77	1.28	-0.32
32	36.9097	-95.8853	0.26	0.02	-1.66	-1.17	1.06	0.29	-0.27	1.57	0.83	-1.02
33	33.9206	-96.3200	1.19	-0.44	1.28	0.62	0.32	0.09	1.09	0.12	-0.95	0.79
34	35.5481	-98.0358	-0.43	0.45	-0.13	-0.75	-1.06	0.34	0.48	-1.32	-0.34	-0.70
35	35.2047	-99.8033	-1.41	0.59	0.99	0.73	0.55	0.04	0.55	-1.12	0.27	0.67
36	35.3000	-95.6583	1.15	-0.41	0.43	-0.46	-1.94	0.61	-2.34	1.52	0.05	-2.80
37	36.2636	-98.4978	-0.81	0.50	0.97	0.04	-2.32	1.34	0.58	1.25	0.49	0.11
38	36.8403	-96.4278	-0.33	0.19	-1.40	0.22	-0.87	-0.28	2.10	0.88	-1.05	0.21
39	36.7256	-99.1422	-1.22	-0.96	-0.37	-0.80	-1.07	-0.84	0.19	-0.04	0.48	-0.32
40	35.1492	-98.4667	-0.24	-0.23	0.60	-0.18	-0.17	-0.13	-0.40	1.32	0.71	-0.96

STNM	LAT	LON	FAC1	FAC2	FAC3	FAC4	FAC5	FAC6	FAC7	FAC8	FAC9	FAC10
41	36.6017	-101.6014	-3.03	-0.03	-0.54	0.77	0.29	-0.46	0.17	-1.07	-0.86	-0.88
42	34.2392	-98.7397	-0.10	-0.39	1.93	-0.54	-0.22	-0.28	0.46	-2.02	1.38	-1.53
43	35.8489	-97.4800	0.25	-1.08	-0.14	-0.69	-0.24	-0.04	0.12	0.07	0.48	-0.99
44	35.7475	-95.6400	0.59	0.31	-0.35	-0.73	-1.32	-0.16	0.52	-0.80	-0.36	-0.31
45	35.4844	-98.4822	-0.40	-0.15	0.06	-0.68	-0.12	1.62	0.34	-0.54	-0.07	0.07
46	34.9897	-99.0525	-0.46	-0.60	0.85	-0.51	0.77	-0.38	0.23	-0.53	1.24	-0.06
47	34.6861	-99.8339	-1.08	0.28	1.58	0.70	2.23	-1.18	0.76	-0.28	0.16	0.58
48	36.8553	-101.2253	-2.80	0.56	-0.77	0.31	1.03	-0.75	0.43	-1.22	-0.60	-0.54
49	34.0308	-95.5400	1.28	-0.90	1.08	0.26	-0.66	0.56	0.49	-1.35	-0.12	-0.42
50	33.8303	-94.8806	2.15	1.06	-0.77	0.90	-0.70	-0.88	-0.36	-3.46	0.47	4.30
51	36.4817	-94.7831	0.47	0.05	-2.19	0.45	1.30	1.75	-0.42	0.57	1.17	-1.43
52	36.8297	-102.8781	-4.03	1.66	-0.38	1.41	0.08	1.12	-3.02	-1.36	-0.83	-0.23
53	34.5289	-97.7647	0.32	-0.14	0.94	0.39	0.47	-0.91	0.31	0.75	-0.09	-0.04
54	35.8806	-97.9111	-0.17	0.81	0.17	-1.56	-0.04	0.30	0.05	0.27	-0.19	0.81
55	36.3844	-98.1114	-0.50	-0.12	-0.51	-1.01	-0.64	-0.26	1.14	0.12	0.71	-0.51
56	34.3086	-95.9975	1.14	0.32	0.34	0.31	0.13	-0.41	0.06	-1.11	0.14	-0.63
57	34.0361	-96.9431	1.10	-0.50	1.15	0.57	0.69	-0.80	-0.87	1.21	0.73	-0.50
58	34.8361	-99.4239	-0.98	0.76	1.08	0.81	1.91	-1.35	0.87	-0.30	-0.15	0.69
59	36.0644	-97.2128	0.05	-0.63	-0.56	-0.22	-0.19	0.99	0.75	-0.44	-0.32	-0.65
60	36.1186	-97.6014	-0.03	0.25	-0.49	-0.88	0.64	-0.48	0.90	0.01	1.87	-1.18
61	36.9869	-99.0111	-1.24	-0.13	-0.26	0.47	-1.61	0.69	0.41	1.50	-0.10	0.30
62	34.8819	-95.7808	0.92	-0.09	0.22	-0.05	0.48	1.49	-0.03	-0.60	-1.54	0.97
63	36.7922	-97.7456	-0.31	0.22	-0.64	-1.58	0.26	-0.20	1.10	0.44	0.97	-0.35
64	34.7292	-98.5667	-0.21	-1.02	1.34	2.91	-0.77	1.90	1.72	3.04	-0.39	0.83
65	36.8886	-94.8447	0.49	0.41	-2.22	-1.24	0.37	-0.17	-0.24	0.26	0.31	1.01
66	35.2722	-97.9556	-0.04	-1.72	-0.19	0.28	-0.11	-1.35	1.45	0.86	0.46	-0.26
67	34.3108	-94.8228	1.40	-0.16	-1.39	2.73	1.37	0.35	-0.29	-0.69	0.72	-0.03
68	36.8981	-96.9106	-0.01	-0.88	-1.91	-0.83	0.37	-1.08	-0.15	1.08	1.00	-0.74
69	35.2556	-97.4836	0.37	-0.35	0.48	-0.60	0.40	0.01	0.03	-0.49	1.31	-0.63
70	36.7436	-95.6078	0.25	0.97	-1.64	-1.25	-0.10	-0.23	0.24	0.17	-0.65	-0.45
71	36.0314	-96.4972	0.28	1.43	-0.92	0.06	0.48	2.08	-0.58	-0.14	0.08	-0.30
72	35.4317	-96.2628	0.64	-0.01	-0.17	-0.55	-0.09	0.27	0.09	-0.76	-0.71	0.12
73	35.5811	-95.9150	0.68	0.60	-0.73	-0.45	0.64	-0.27	-0.50	-0.35	-1.01	0.40
74	34.7156	-97.2294	0.56	-0.63	0.90	-0.70	-0.10	-0.43	-0.72	0.29	-0.74	0.45
75	36.3611	-96.7697	0.08	-0.16	-0.55	-0.50	-0.65	-0.56	0.21	0.54	-0.64	0.45
76	35.9983	-97.0481	0.24	-0.46	-0.24	-0.73	0.17	-0.15	0.29	0.79	-0.19	0.35
77	36.3689	-95.2717	0.49	0.74	-1.55	-1.07	0.60	-0.27	0.46	0.09	-0.07	-0.02
78	35.8992	-98.9603	-0.91	-0.98	-0.20	-0.50	-0.16	0.33	0.18	-0.79	0.54	-0.72
79	36.3556	-97.1531	-0.12	0.68	-0.45	-1.09	-0.28	0.06	0.38	0.33	-0.71	0.59
80	35.1231	-99.3597	-0.78	-1.06	0.96	0.86	1.43	-0.92	0.90	0.76	0.71	0.48

STNM	LAT	LON	FAC1	FAC2	FAC3	FAC4	FAC5	FAC6	FAC7	FAC8	FAC9	FAC10
81	34.1939	-97.5883	0.55	-0.47	1.20	-0.25	1.81	-0.58	-0.10	1.12	0.83	0.07
82	35.4381	-94.7978	0.83	0.88	-0.37	-0.05	0.33	0.36	-0.32	0.49	0.09	-0.27
83	36.1903	-99.0406	-1.09	0.44	0.15	-0.70	-0.82	0.23	-0.17	-0.31	0.13	-0.22
84	35.3650	-96.9483	0.39	-0.83	0.30	-0.89	-0.17	0.58	-0.13	-0.11	-1.40	0.44
85	36.4147	-96.0372	0.44	-2.61	-1.23	1.32	-1.72	-0.40	1.59	1.41	-0.90	0.36
86	36.5969	-100.2619	-2.22	0.00	-0.15	0.70	-0.57	0.22	0.09	0.32	-0.15	0.45
87	35.5422	-97.3411	0.32	-1.09	-0.11	-0.72	0.66	1.42	-1.15	-0.02	-2.44	1.51
88	35.2653	-95.1814	0.89	0.61	-0.32	-0.37	-0.37	0.42	-0.53	-0.59	1.55	1.46
89	36.1211	-97.0950	0.06	0.99	-0.15	-0.99	-0.33	0.43	-0.66	0.43	-1.71	0.34
90	34.8764	-96.0700	0.88	-0.76	0.15	0.22	-0.63	-0.45	-0.64	-0.36	-0.48	-0.35
91	34.5661	-96.9506	0.60	0.95	0.17	0.65	1.66	1.17	-0.15	0.94	0.51	0.14
92	35.9728	-94.9869	0.60	-0.29	-1.82	0.52	1.19	1.36	0.53	-0.21	-0.47	0.19
93	34.7106	-95.0117	0.96	1.80	0.34	0.94	-1.45	-2.91	-2.74	1.17	0.11	0.84
94	34.4394	-99.1375	-0.16	0.41	1.69	-0.96	2.66	0.34	-0.32	0.39	1.53	0.36
95	34.3328	-96.6794	0.62	0.41	0.28	1.72	0.43	-0.98	1.47	0.56	-0.45	0.01
96	35.8397	-95.4133	0.82	-0.93	-0.38	-0.69	-1.64	-0.29	-0.05	-0.28	-0.07	-0.96
97	36.7753	-95.2211	0.22	0.96	-1.99	-0.86	-0.64	-0.95	0.59	0.25	-0.13	-0.26
98	34.3647	-98.3206	0.05	0.21	1.81	-0.56	0.50	0.18	0.50	-0.15	0.81	-0.30
99	34.9817	-97.5208	0.19	-0.04	0.24	0.75	0.50	0.04	1.33	0.76	-0.47	0.02
100	35.8422	-98.5261	-0.62	-0.98	0.24	0.96	-2.12	1.36	1.25	1.05	0.12	0.00
101	34.1678	-97.9878	0.43	-0.06	1.58	-0.63	1.63	-0.33	-0.32	0.42	0.37	0.24
102	35.5081	-98.7753	-0.37	-1.00	-0.52	-0.62	1.94	0.63	0.82	0.49	1.03	0.09
103	35.4728	-95.1322	1.02	1.12	-0.04	-0.38	-0.64	0.00	-0.58	-0.13	0.46	-1.36
104	36.0111	-94.6450	0.75	-1.04	-2.09	1.10	0.34	-1.21	-0.36	0.74	0.65	-0.07
105	34.9008	-95.3478	0.93	2.12	0.19	0.79	0.16	0.92	-1.39	-0.35	1.33	-1.02
106	34.9847	-94.6881	0.58	2.97	-0.21	1.97	-0.96	-1.66	0.09	1.49	-0.49	0.79
107	36.4233	-99.4169	-1.36	-0.51	0.48	0.08	-2.28	1.31	-1.26	0.55	-0.12	-0.12
108	36.5172	-96.3422	0.15	0.27	-1.05	0.05	0.51	-0.22	0.90	0.93	-0.70	0.36
109	34.9678	-97.9514	-0.01	-0.09	1.22	-0.28	-0.65	0.24	0.14	0.70	-0.66	0.69
110	34.8056	-98.0056	0.09	0.05	0.77	-0.38	1.87	1.36	-0.92	0.38	0.43	0.37
111	34.9139	-98.2917	0.02	-1.24	0.09	-0.53	1.52	-0.41	-0.27	0.50	0.80	0.31
112	36.2619	-95.7572	0.12	-2.61	-1.32	0.56	-0.99	-0.54	-1.91	-0.72	0.05	1.23
113	35.8436	-96.0056	0.57	-1.18	0.24	-0.46	-1.77	-0.25	-0.29	0.10	-0.32	-0.12
114	35.7247	-95.9886	-0.46	-4.68	-1.92	2.19	0.83	-1.77	-3.93	-1.76	0.60	0.76
115	34.7890	-96.8430	0.37	-0.34	0.96	0.12	-0.63	-0.11	-0.12	0.08	-0.88	0.24
116	36.7083	-98.7075	-1.10	0.54	0.12	-1.21	-0.11	0.02	0.64	0.26	-0.05	-0.11
117	34.2392	-98.7444	-0.21	-0.40	2.47	-0.98	0.30	0.01	0.53	-0.84	0.50	-0.55
118	35.8258	-95.5600	0.61	-0.63	-0.22	-0.83	-0.52	-0.34	-0.14	0.31	-0.26	-0.07
119	34.1905	-96.6435	1.11	0.72	0.93	-0.49	-0.13	-0.23	-1.36	0.93	-0.54	-1.31
120	36.1422	-95.4505	0.27	0.70	-1.17	-0.97	0.98	0.17	0.96	-0.02	-1.03	-0.15

STNM	LAT	LON	FAC1	FAC2	FAC3	FAC4	FAC5	FAC6	FAC7	FAC8	FAC9	FAC10
121	35.2361	-97.4649	0.16	-0.47	0.65	-1.35	1.41	1.01	-1.13	0.15	-2.67	1.60
122	36.3213	-95.6461	0.44	-0.54	-0.67	-0.91	0.82	-0.09	-0.46	0.60	-1.84	-0.05
123	34.2282	-97.2007	0.35	-1.09	1.63	0.62	-0.65	-0.49	0.48	-0.80	-0.64	-1.37
124	34.0433	-94.6244	0.67	2.40	0.22	2.56	-0.34	-1.21	0.99	-0.78	-1.13	-1.06
125	36.1168	-97.6068	-0.27	0.23	-0.08	-0.98	1.27	0.04	0.40	0.31	-0.95	0.09
126	34.1926	-97.0857	0.54	-1.17	1.94	0.06	0.17	0.75	-0.90	-0.86	-2.69	-0.01
127	34.5521	-96.7178	-0.07	-0.60	1.87	1.30	0.38	0.27	0.80	-0.10	-2.23	-0.17

APPENDIX F

ANNUAL PROFILES OF WIND AND SOLAR POWER FOR MESONET STATIONS

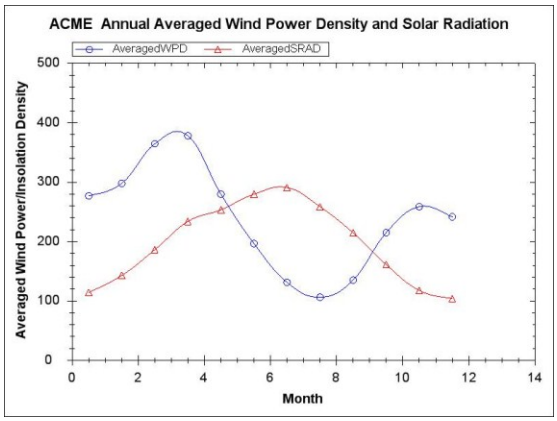
ACME Annual Averaged Wind Power Density and Solar Radiation
AveragedWPD
AveragedSRAD
Averaged Wind Power/Insolation Density
Month

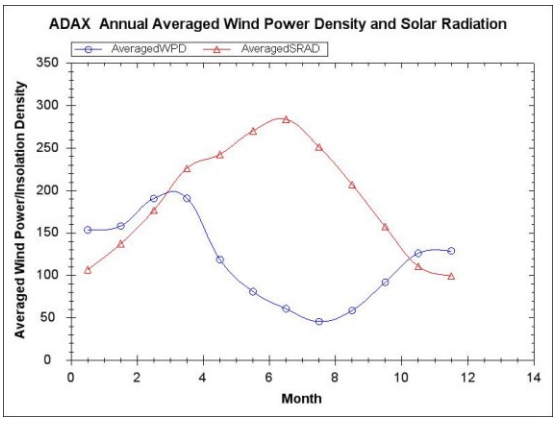
ADAX Annual Averaged Wind Power Density and Solar Radiation
AveragedWPD
AveragedSRAD
Averaged Wind Power/Insolation Density
Month

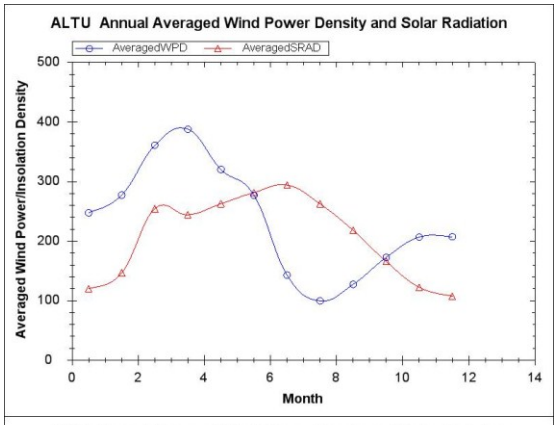
ALTU Annual Averaged Wind Power Density and Solar Radiation
AveragedWPD
AveragedSRAD
Averaged Wind Power/Insolation Density
Month

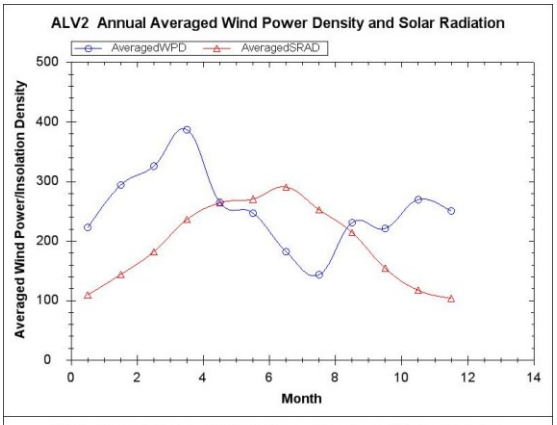
ALV2 Annual Averaged Wind Power Density and Solar Radiation
AveragedWPD
AveragedSRAD
Averaged Wind Power/Insolation Density
Month

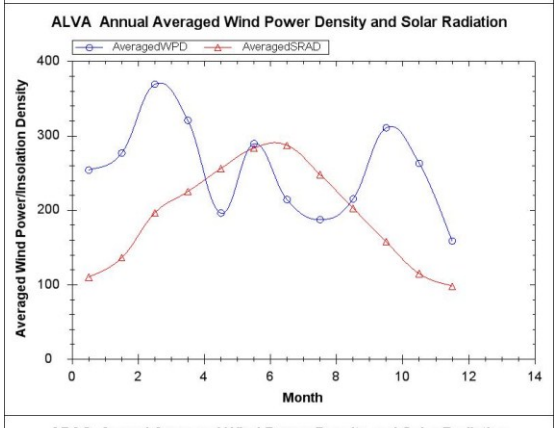
ALVA Annual Averaged Wind Power Density and Solar Radiation
AveragedWPD
AveragedSRAD
Averaged Wind Power/Insolation Density
Month

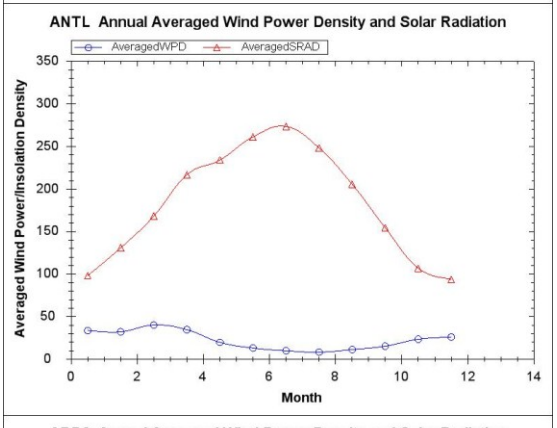
ANTL Annual Averaged Wind Power Density and Solar Radiation
AveragedWPD
AveragedSRAD
Averaged Wind Power/Insolation Density
Month

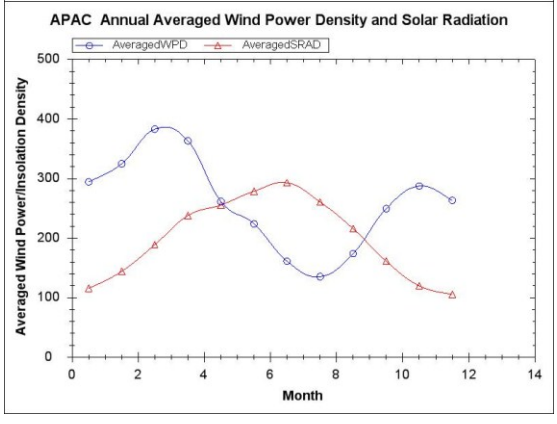
APAC Annual Averaged Wind Power Density and Solar Radiation
AveragedWPD
AveragedSRAD
Averaged Wind Power/Insolation Density
Month

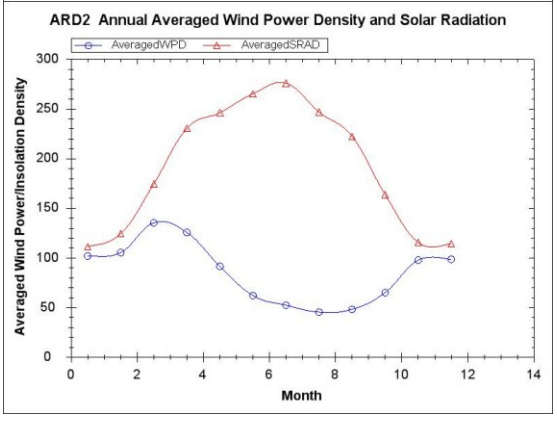
ARD2 Annual Averaged Wind Power Density and Solar Radiation
AveragedWPD
AveragedSRAD
Averaged Wind Power/Insolation Density
Month

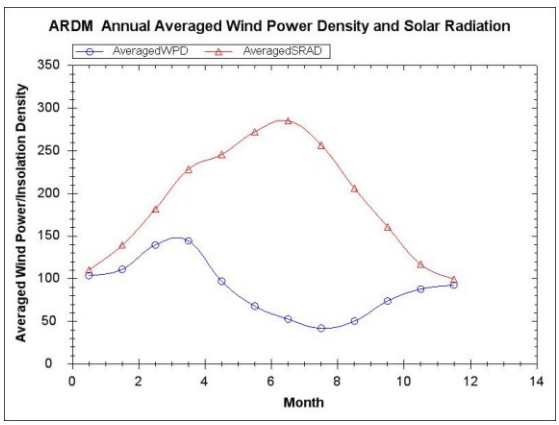
ARDM Annual Averaged Wind Power Density and Solar Radiation
AveragedWPD
AveragedSRAD
Averaged Wind Power/Insolation Density
Month

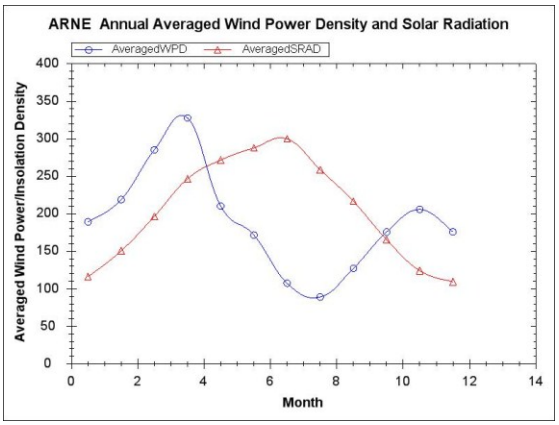
ARNE Annual Averaged Wind Power Density and Solar Radiation
AveragedWPD
AveragedSRAD
Averaged Wind Power/Insolation Density
Month

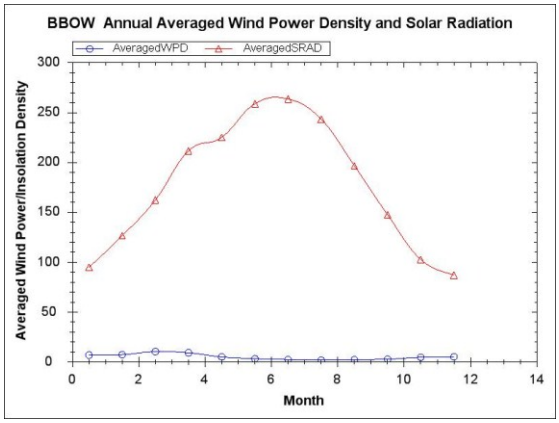
BBOW Annual Averaged Wind Power Density and Solar Radiation
AveragedWPD
AveragedSRAD
Averaged Wind Power/Insolation Density
Month

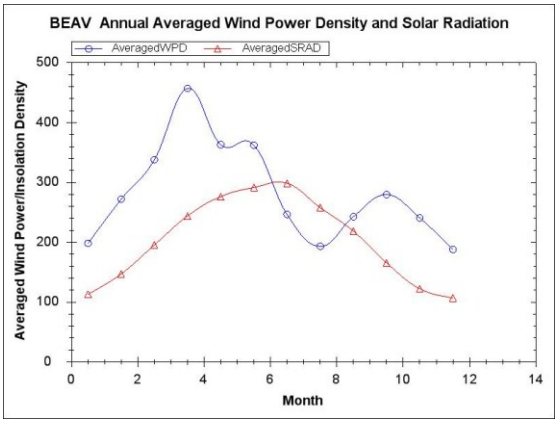
BEAV Annual Averaged Wind Power Density and Solar Radiation
AveragedWPD
AveragedSRAD
Averaged Wind Power/Insolation Density
Month

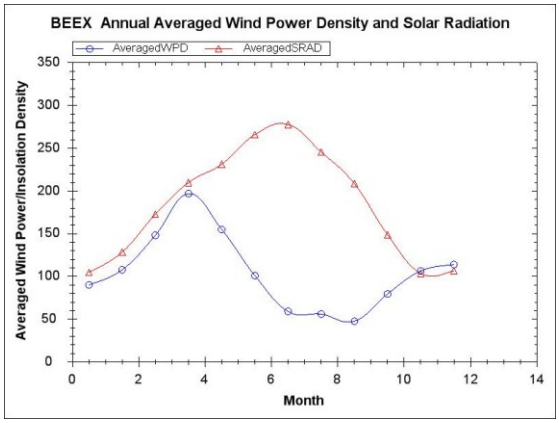
BEEX Annual Averaged Wind Power Density and Solar Radiation
AveragedWPD
AveragedSRAD
Averaged Wind Power/Insolation Density
Month

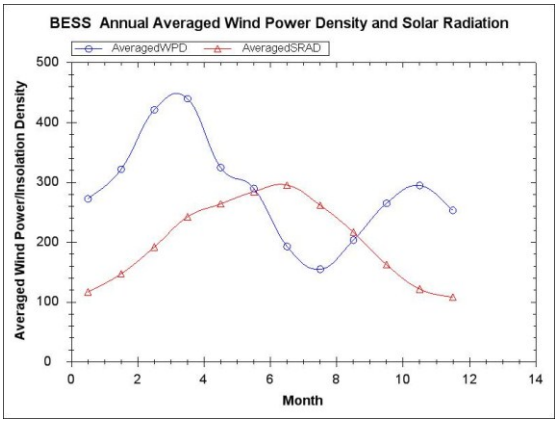
BESS Annual Averaged Wind Power Density and Solar Radiation
AveragedWPD
AveragedSRAD
Averaged Wind Power/Insolation Density
Month

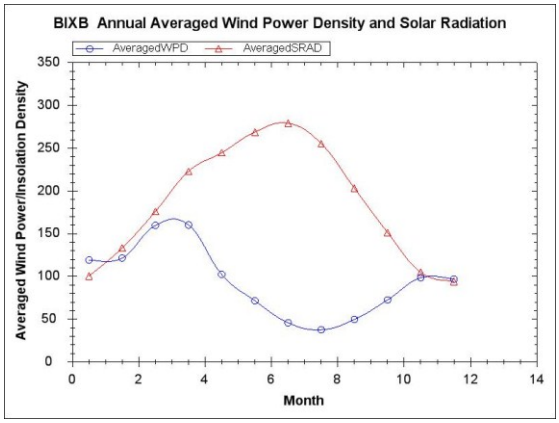
BIXB Annual Averaged Wind Power Density and Solar Radiation
AveragedWPD
AveragedSRAD
Averaged Wind Power/Insolation Density
Month

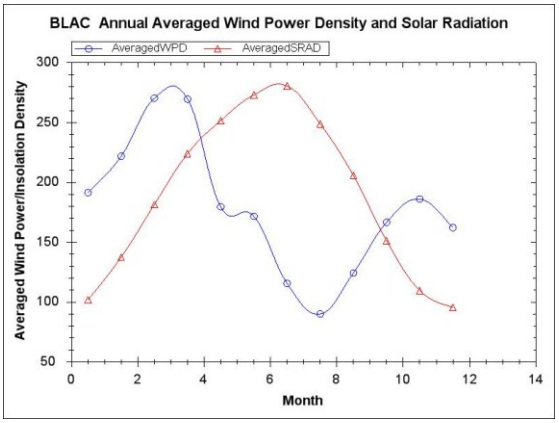
BLAC Annual Averaged Wind Power Density and Solar Radiation
AveragedWPD
AveragedSRAD
Averaged Wind Power/Insolation Density
Month

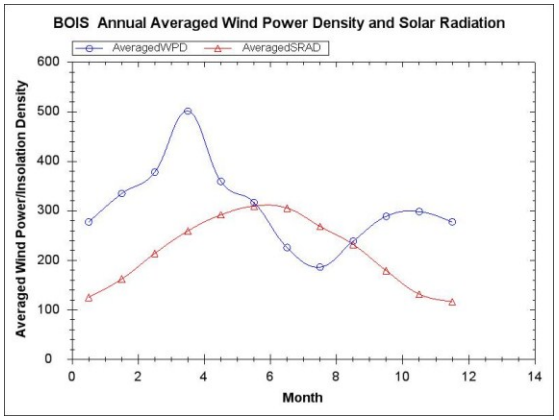
BOIS Annual Averaged Wind Power Density and Solar Radiation
AveragedWPD
AveragedSRAD
Averaged Wind Power/Insolation Density
Month

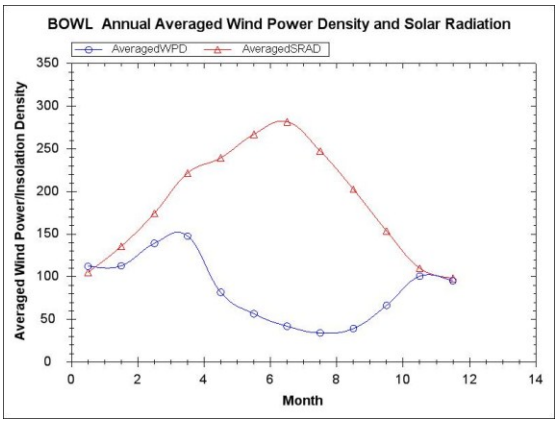
BOWL Annual Averaged Wind Power Density and Solar Radiation
AveragedWPD
AveragedSRAD
Averaged Wind Power/Insolation Density
Month

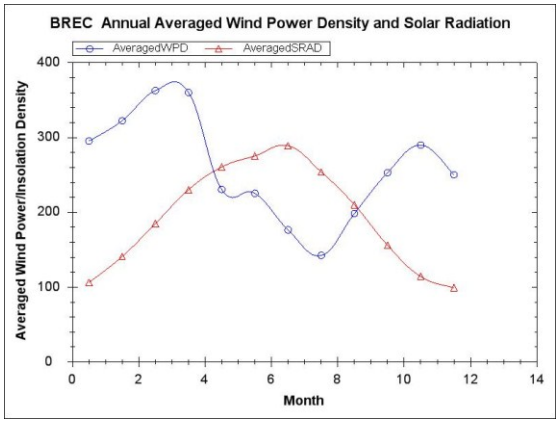
BREC Annual Averaged Wind Power Density and Solar Radiation
AveragedWPD
AveragedSRAD
Averaged Wind Power/Insolation Density
Month

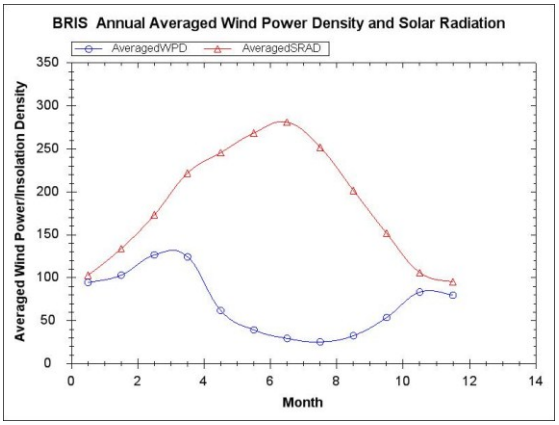
BRIS Annual Averaged Wind Power Density and Solar Radiation
AveragedWPD
AveragedSRAD
Averaged Wind Power/Insolation Density
Month

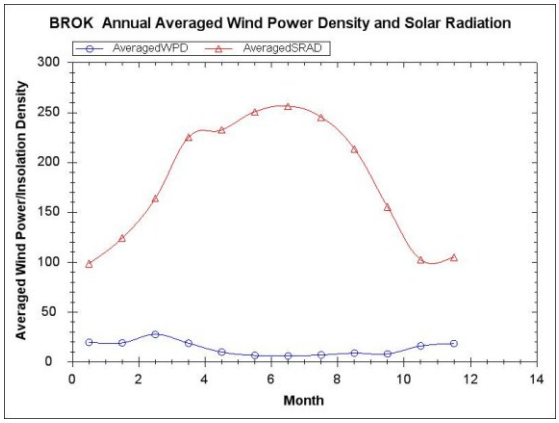
BROK Annual Averaged Wind Power Density and Solar Radiation
AveragedWPD
AveragedSRAD
Averaged Wind Power/Insolation Density
Month

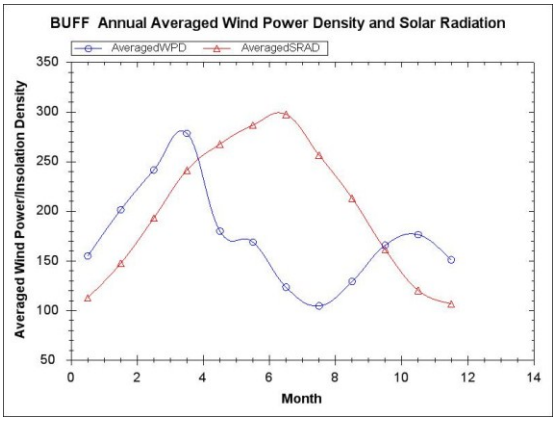
BUFF Annual Averaged Wind Power Density and Solar Radiation
AveragedWPD
AveragedSRAD
Averaged Wind Power/Insolation Density
Month

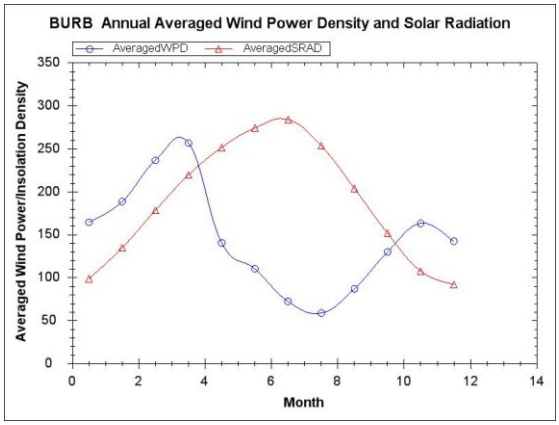
BURB Annual Averaged Wind Power Density and Solar Radiation
AveragedWPD
AveragedSRAD
Averaged Wind Power/Insolation Density
Month

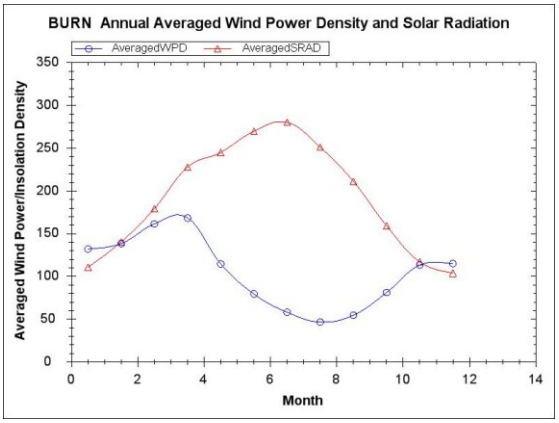
BURN Annual Averaged Wind Power Density and Solar Radiation
AveragedWPD
AveragedSRAD
Averaged Wind Power/Insolation Density
Month

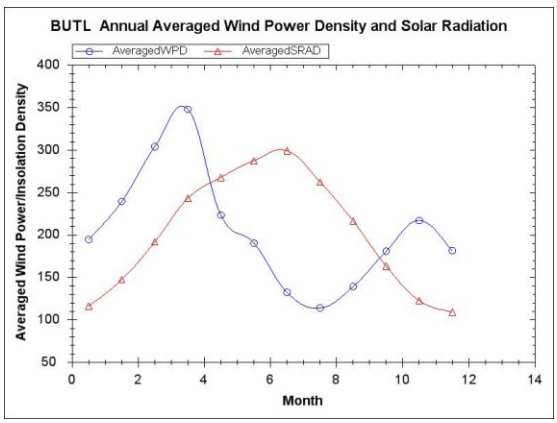
BUTL Annual Averaged Wind Power Density and Solar Radiation
AveragedWPD
AveragedSRAD
Averaged Wind Power/Insolation Density
Month

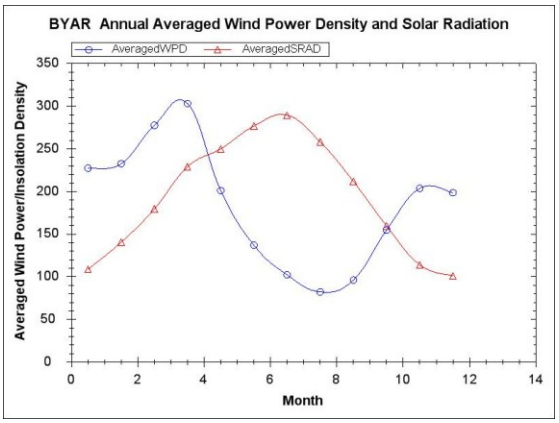
BYAR Annual Averaged Wind Power Density and Solar Radiation
AveragedWPD
AveragedSRAD
Averaged Wind Power/Insolation Density
Month

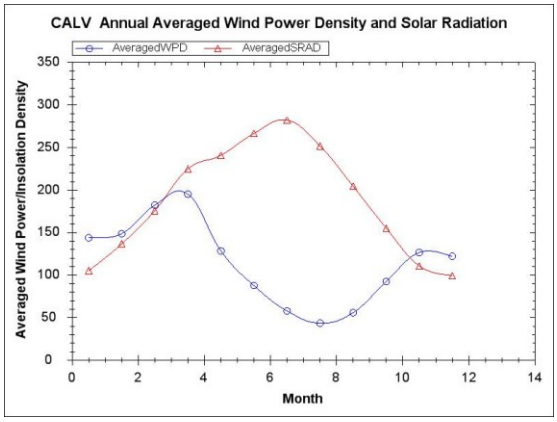
CALV Annual Averaged Wind Power Density and Solar Radiation
AveragedWPD
AveragedSRAD
Averaged Wind Power/Insolation Density
Month

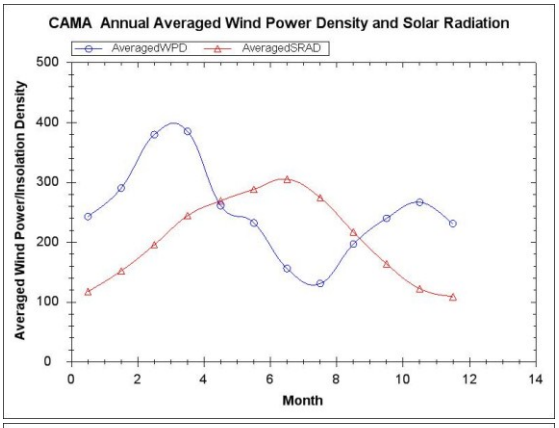
CAMA Annual Averaged Wind Power Density and Solar Radiation
AveragedWPD
AveragedSRAD
Averaged Wind Power/Insolation Density
Month

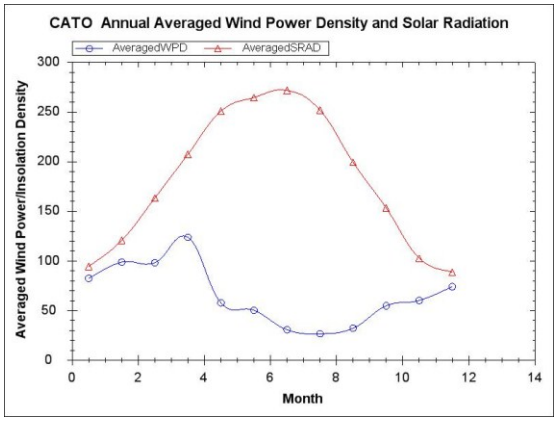
CATO Annual Averaged Wind Power Density and Solar Radiation
AveragedWPD
AveragedSRAD
Averaged Wind Power/Insolation Density
Month

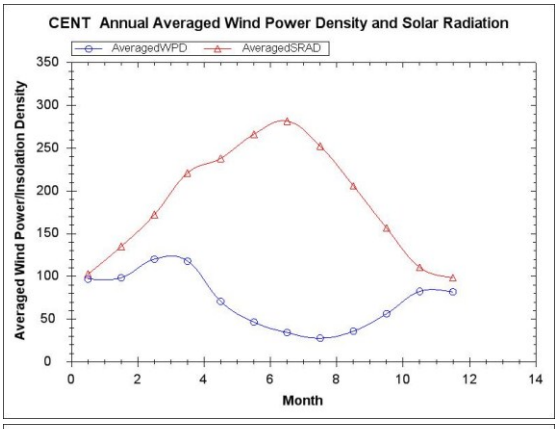
CENT Annual Averaged Wind Power Density and Solar Radiation
AveragedWPD
AveragedSRAD
Averaged Wind Power/Insolation Density
Month

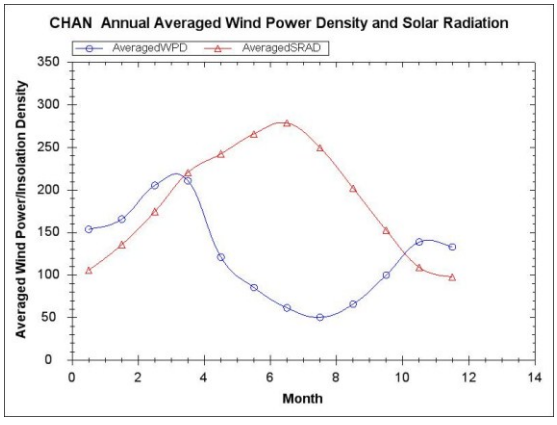
CHAN Annual Averaged Wind Power Density and Solar Radiation
AveragedWPD
AveragedSRAD
Averaged Wind Power/Insolation Density
Month

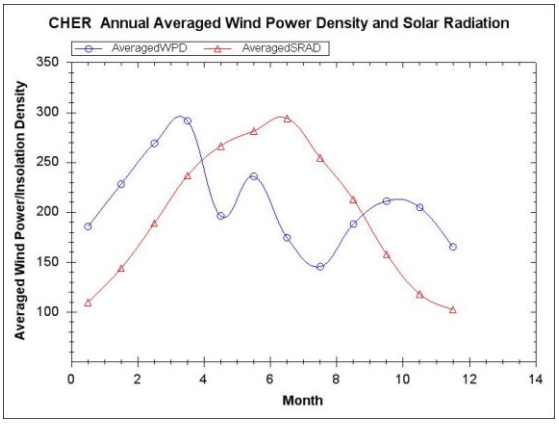
CHER Annual Averaged Wind Power Density and Solar Radiation
AveragedWPD
AveragedSRAD
Averaged Wind Power/Insolation Density
Month

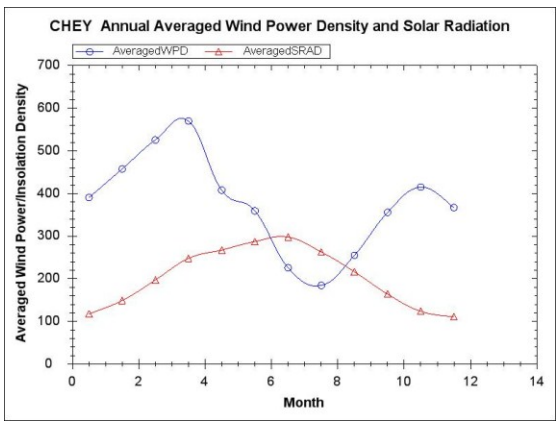
CHEY Annual Averaged Wind Power Density and Solar Radiation
AveragedWPD
AveragedSRAD
Averaged Wind Power/Insolation Density
Month

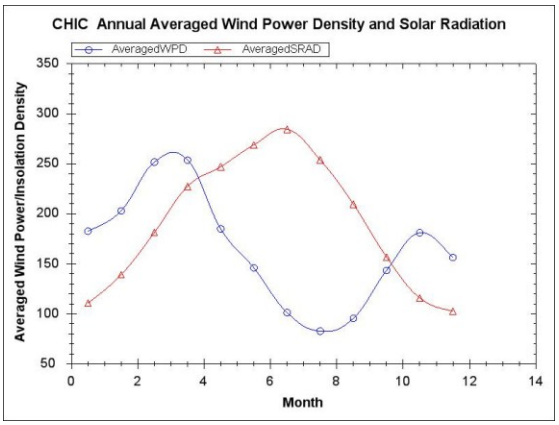
CHIC Annual Averaged Wind Power Density and Solar Radiation
AveragedWPD
AveragedSRAD
Averaged Wind Power/Insolation Density
Month

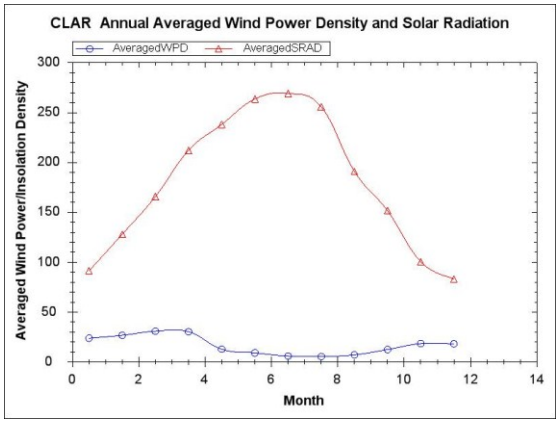
CLAR Annual Averaged Wind Power Density and Solar Radiation
AveragedWPD
AveragedSRAD
Averaged Wind Power/Insolation Density
Month

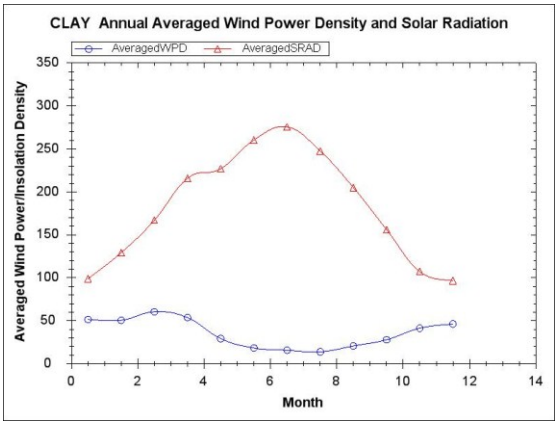
CLAY Annual Averaged Wind Power Density and Solar Radiation
AveragedWPD
AveragedSRAD
Averaged Wind Power/Insolation Density
Month

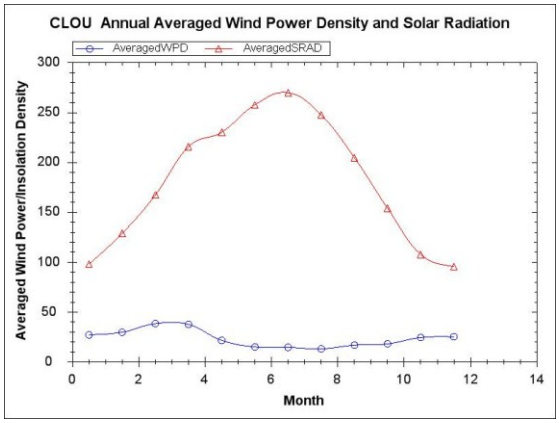
CLOU Annual Averaged Wind Power Density and Solar Radiation
AveragedWPD
AveragedSRAD
Averaged Wind Power/Insolation Density
Month

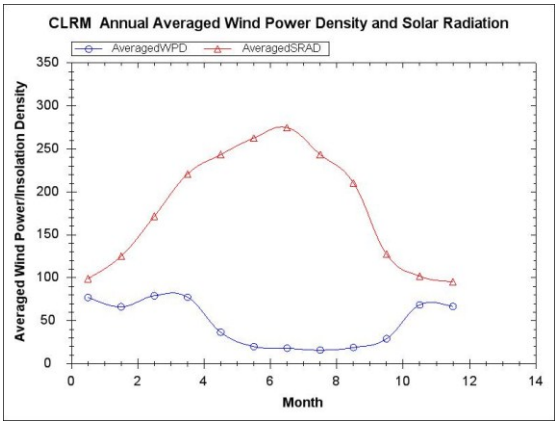
CLRM Annual Averaged Wind Power Density and Solar Radiation
AveragedWPD
AveragedSRAD
Averaged Wind Power/Insolation Density
Month

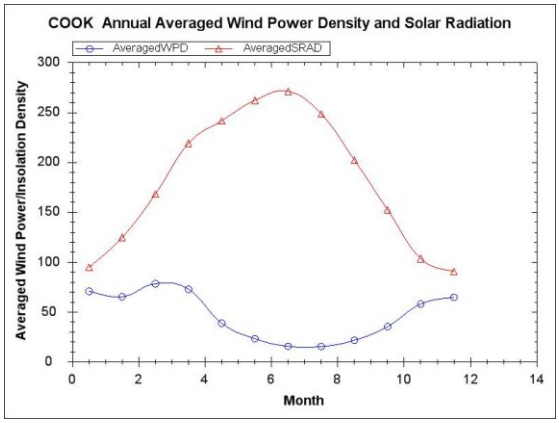
COOK Annual Averaged Wind Power Density and Solar Radiation
AveragedWPD
AveragedSRAD
Averaged Wind Power/Insolation Density
Month

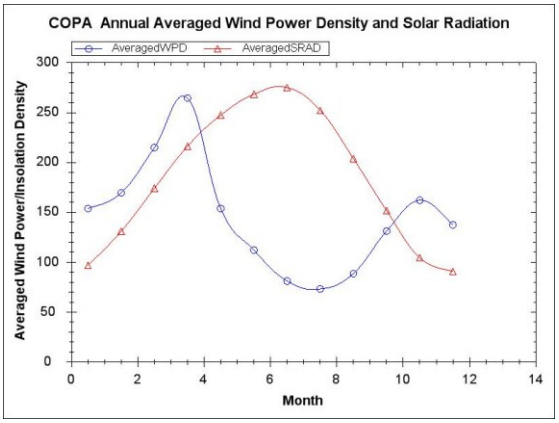
COPA Annual Averaged Wind Power Density and Solar Radiation
AveragedWPD
AveragedSRAD
Averaged Wind Power/Insolation Density
Month

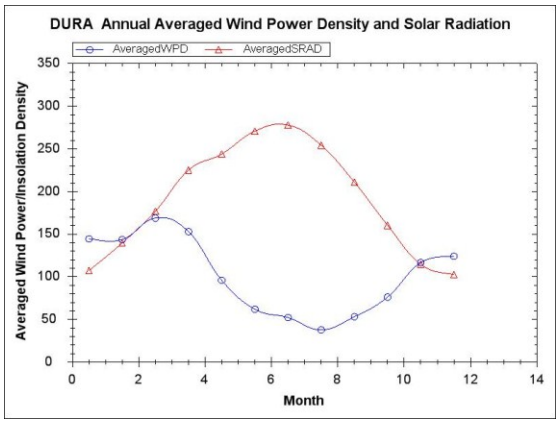
DURA Annual Averaged Wind Power Density and Solar Radiation
AveragedWPD
AveragedSRAD
Averaged Wind Power/Insolation Density
Month

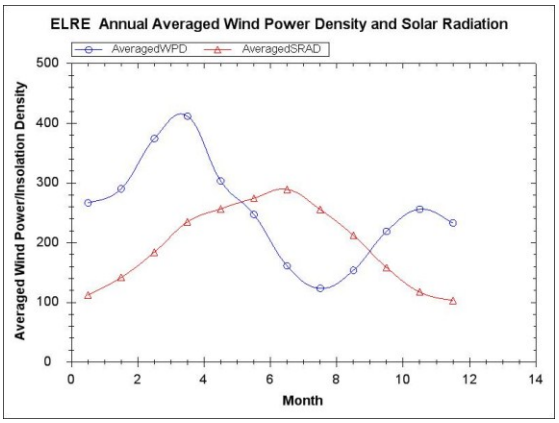
ELRE Annual Averaged Wind Power Density and Solar Radiation
AveragedWPD
AveragedSRAD
Averaged Wind Power/Insolation Density
Month

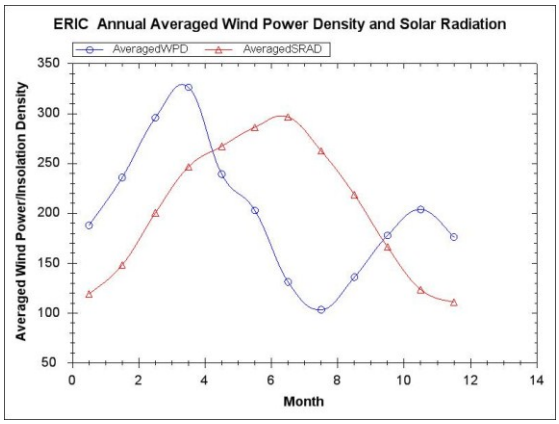
ERIC Annual Averaged Wind Power Density and Solar Radiation
AveragedWPD
AveragedSRAD
Averaged Wind Power/Insolation Density
Month

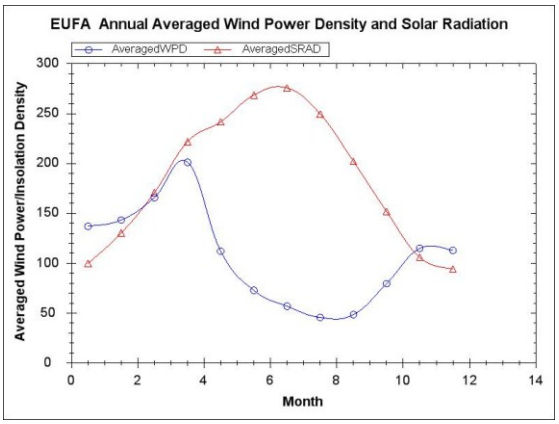
EUFA Annual Averaged Wind Power Density and Solar Radiation
AveragedWPD
AveragedSRAD
Averaged Wind Power/Insolation Density
Month

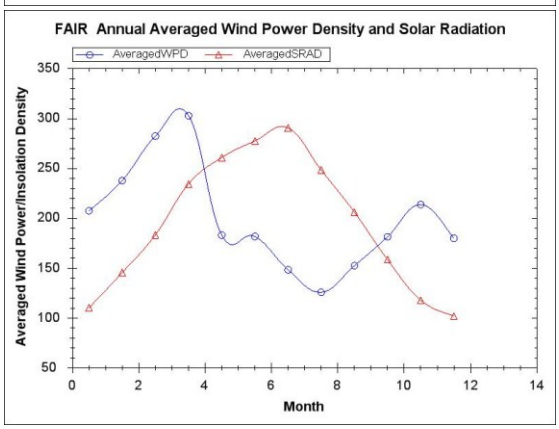
FAIR Annual Averaged Wind Power Density and Solar Radiation
AveragedWPD
AveragedSRAD
Averaged Wind Power/Insolation Density
Month

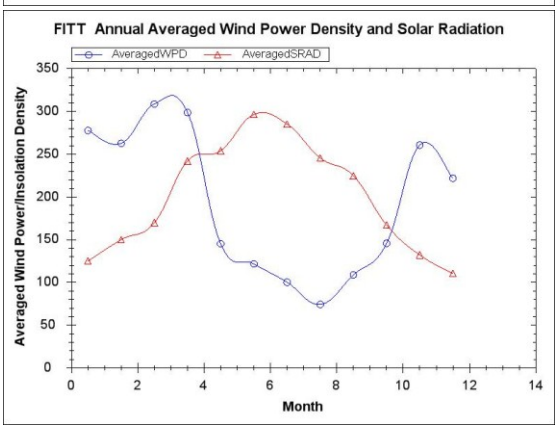
FITT Annual Averaged Wind Power Density and Solar Radiation
AveragedWPD
AveragedSRAD
Averaged Wind Power/Insolation Density
Month

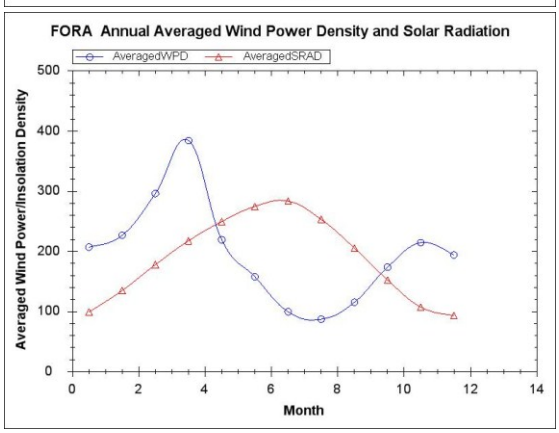
FORA Annual Averaged Wind Power Density and Solar Radiation
AveragedWPD
AveragedSRAD
Averaged Wind Power/Insolation Density
Month

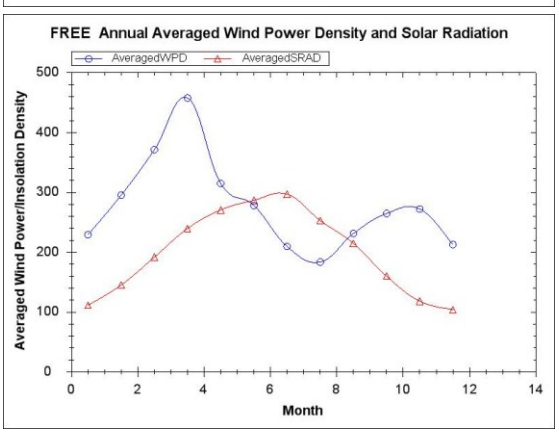
FREE Annual Averaged Wind Power Density and Solar Radiation
AveragedWPD
AveragedSRAD
Averaged Wind Power/Insolation Density
Month

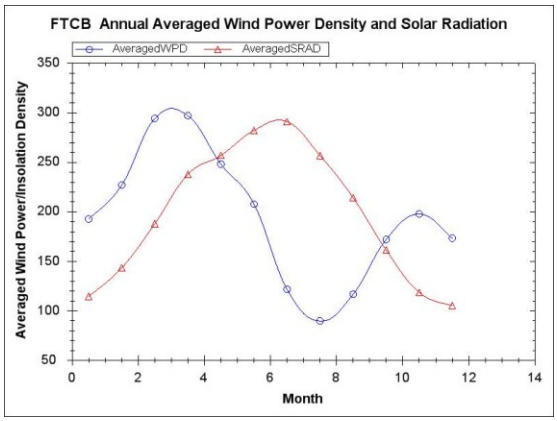
FTCB Annual Averaged Wind Power Density and Solar Radiation
AveragedWPD
AveragedSRAD
Averaged Wind Power/Insolation Density
Month

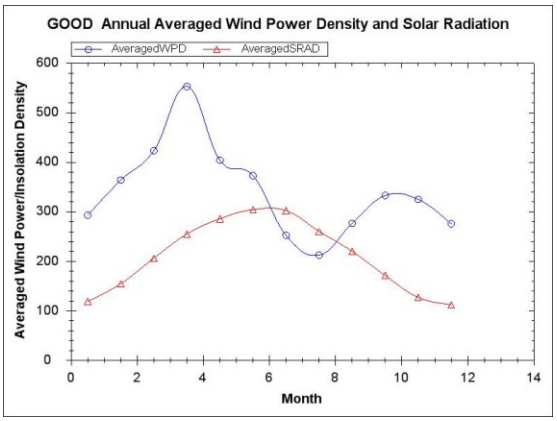
GOOD Annual Averaged Wind Power Density and Solar Radiation
AveragedWPD
AveragedSRAD
Averaged Wind Power/Insolation Density
Month

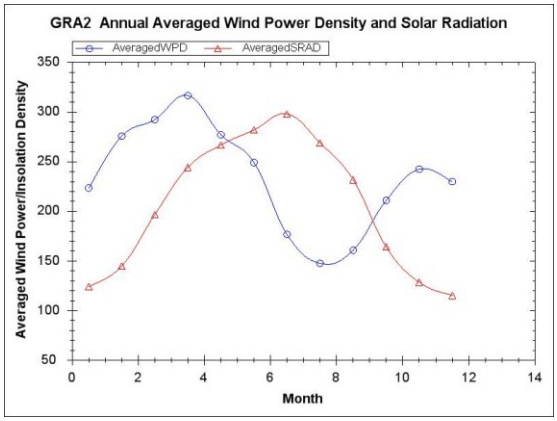
GRA2 Annual Averaged Wind Power Density and Solar Radiation
AveragedWPD
AveragedSRAD
Averaged Wind Power/Insolation Density
Month

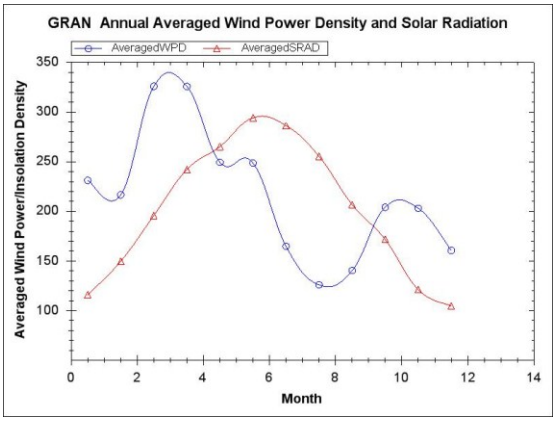
GRAN Annual Averaged Wind Power Density and Solar Radiation
AveragedWPD
AveragedSRAD
Averaged Wind Power/Insolation Density
Month

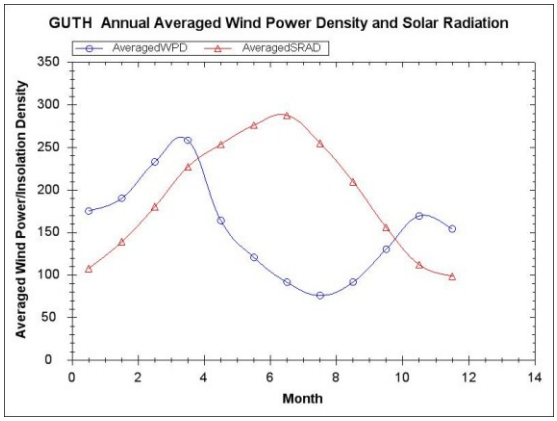
GUTH Annual Averaged Wind Power Density and Solar Radiation
AveragedWPD
AveragedSRAD
Averaged Wind Power/Insolation Density
Month

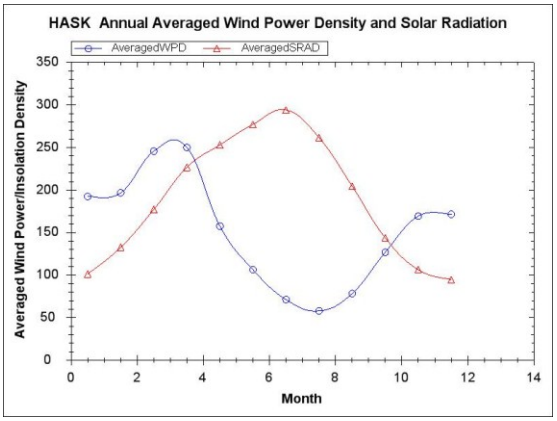
HASK Annual Averaged Wind Power Density and Solar Radiation
AveragedWPD
AveragedSRAD
Averaged Wind Power/Insolation Density
Month

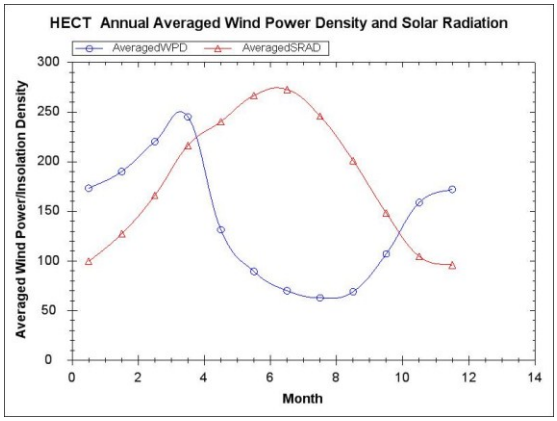
HECT Annual Averaged Wind Power Density and Solar Radiation
AveragedWPD
AveragedSRAD
Averaged Wind Power/Insolation Density
Month

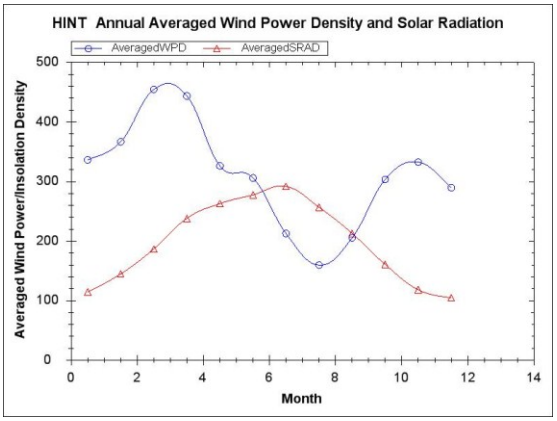
HINT Annual Averaged Wind Power Density and Solar Radiation
AveragedWPD
AveragedSRAD
Averaged Wind Power/Insolation Density
Month

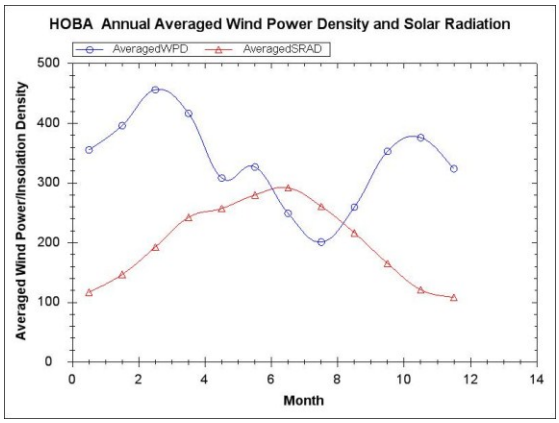
HOBA Annual Averaged Wind Power Density and Solar Radiation
AveragedWPD
AveragedSRAD
Averaged Wind Power/Insolation Density
Month

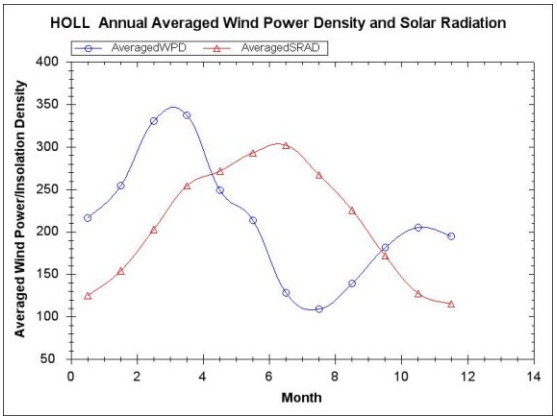
HOLL Annual Averaged Wind Power Density and Solar Radiation
AveragedWPD
AveragedSRAD
Averaged Wind Power/Insolation Density
Month

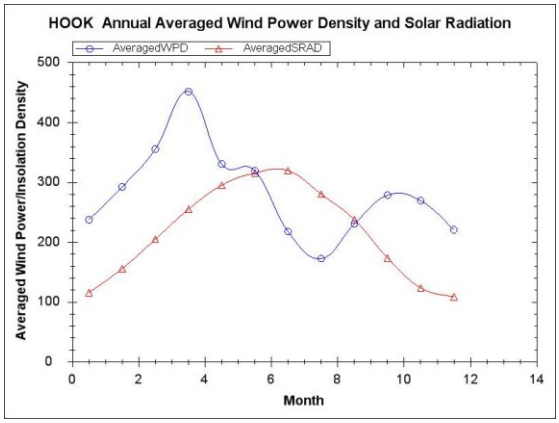
HOOK Annual Averaged Wind Power Density and Solar Radiation
AveragedWPD
AveragedSRAD
Averaged Wind Power/Insolation Density
Month

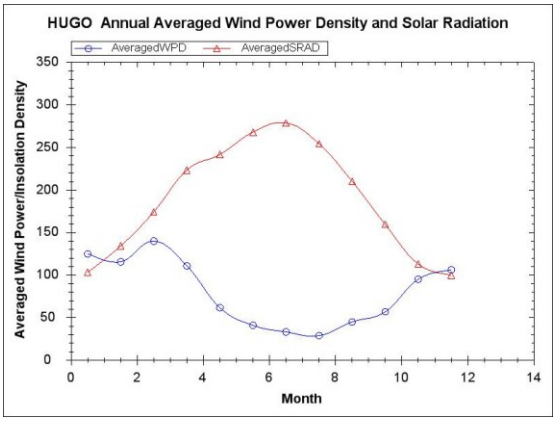
HUGO Annual Averaged Wind Power Density and Solar Radiation
AveragedWPD
AveragedSRAD
Averaged Wind Power/Insolation Density
Month

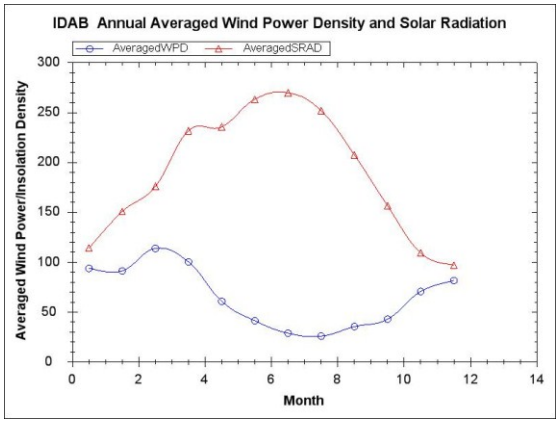
IDAB Annual Averaged Wind Power Density and Solar Radiation
AveragedWPD
AveragedSRAD
Averaged Wind Power/Insolation Density
Month

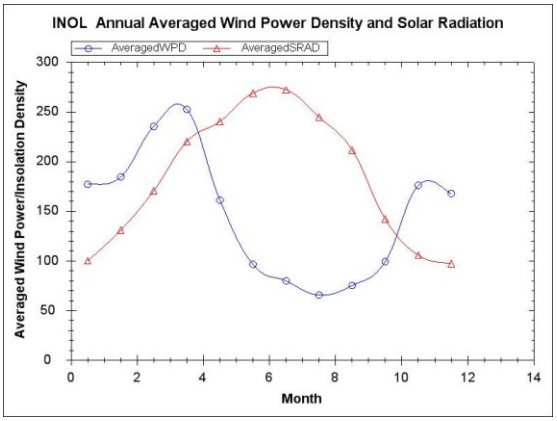
INOL Annual Averaged Wind Power Density and Solar Radiation
AveragedWPD
AveragedSRAD
Averaged Wind Power/Insolation Density
Month

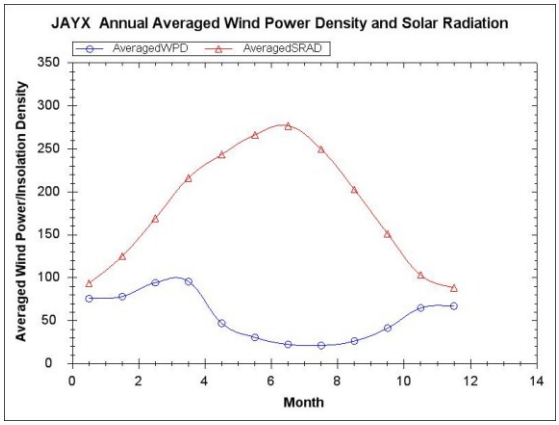
JAYX Annual Averaged Wind Power Density and Solar Radiation
AveragedWPD
AveragedSRAD
Averaged Wind Power/Insolation Density
Month

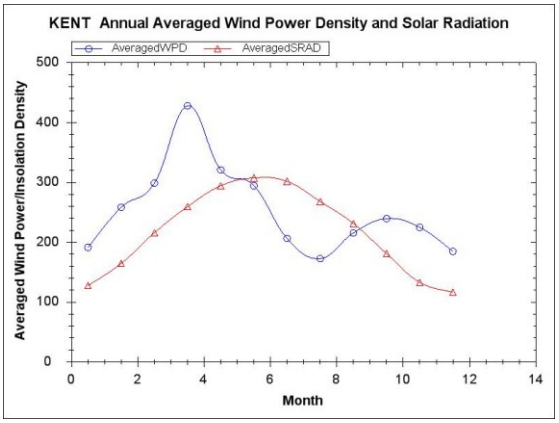
KENT Annual Averaged Wind Power Density and Solar Radiation
AveragedWPD
AveragedSRAD
Averaged Wind Power/Insolation Density
Month

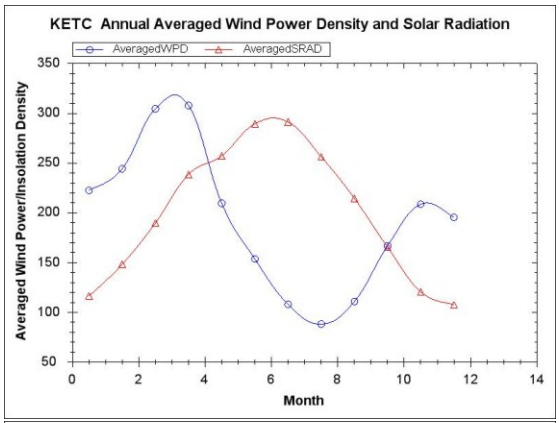
KETC Annual Averaged Wind Power Density and Solar Radiation
AveragedWPD
AveragedSRAD
Averaged Wind Power/Insolation Density
Month

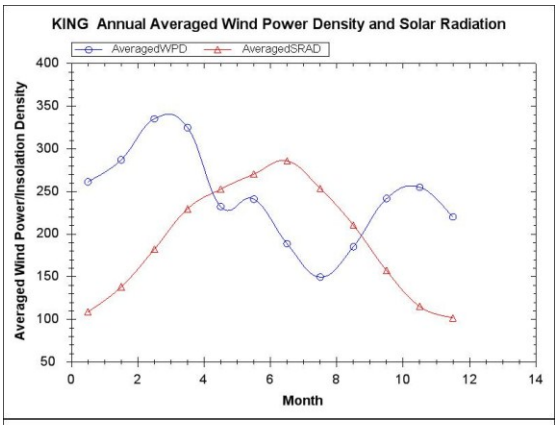
KING Annual Averaged Wind Power Density and Solar Radiation
AveragedWPD
AveragedSRAD
Averaged Wind Power/Insolation Density
Month

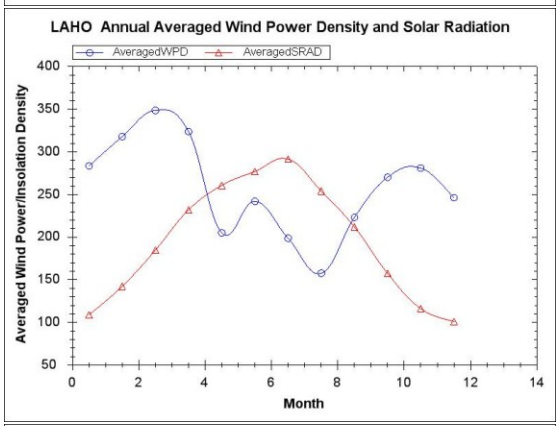
LAHO Annual Averaged Wind Power Density and Solar Radiation
AveragedWPD
AveragedSRAD
Averaged Wind Power/Insolation Density
Month

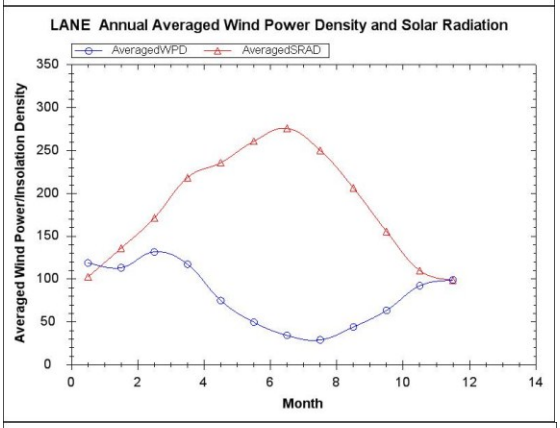
LANE Annual Averaged Wind Power Density and Solar Radiation
AveragedWPD
AveragedSRAD
Averaged Wind Power/Insolation Density
Month

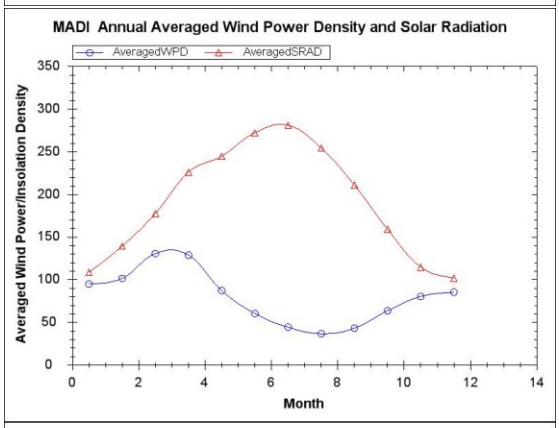
MADI Annual Averaged Wind Power Density and Solar Radiation
AveragedWPD
AveragedSRAD
Averaged Wind Power/Insolation Density
Month

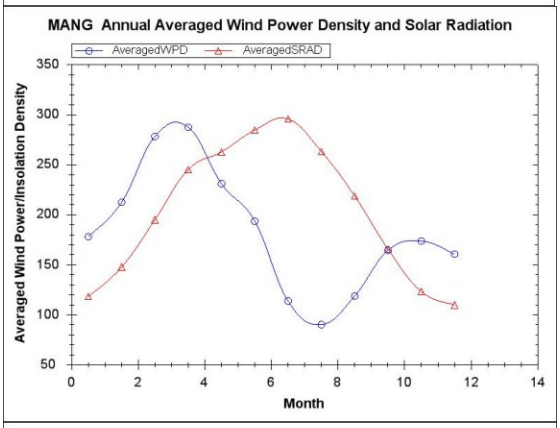
MANG Annual Averaged Wind Power Density and Solar Radiation
AveragedWPD
AveragedSRAD
Averaged Wind Power/Insolation Density
Month

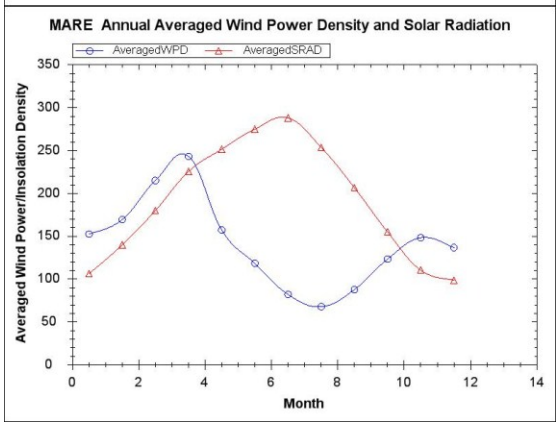
MARE Annual Averaged Wind Power Density and Solar Radiation
AveragedWPD
AveragedSRAD
Averaged Wind Power/Insolation Density
Month

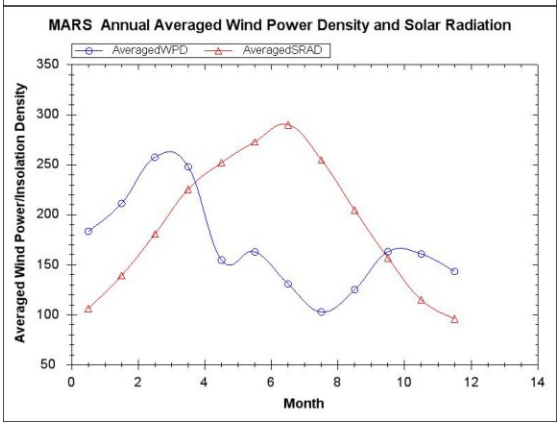
MARS Annual Averaged Wind Power Density and Solar Radiation
AveragedWPD
AveragedSRAD
Averaged Wind Power/Insolation Density
Month

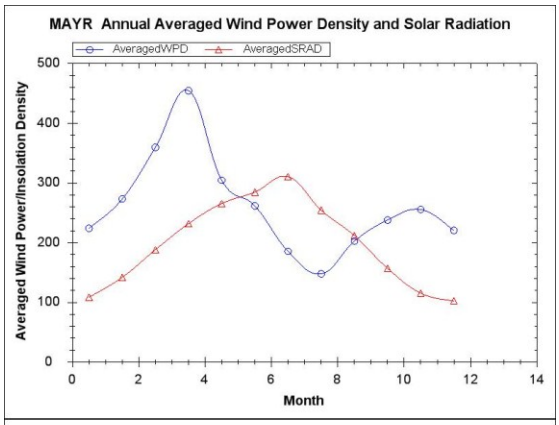
MAYR Annual Averaged Wind Power Density and Solar Radiation
AveragedWPD
AveragedSRAD
Averaged Wind Power/Insolation Density
Month

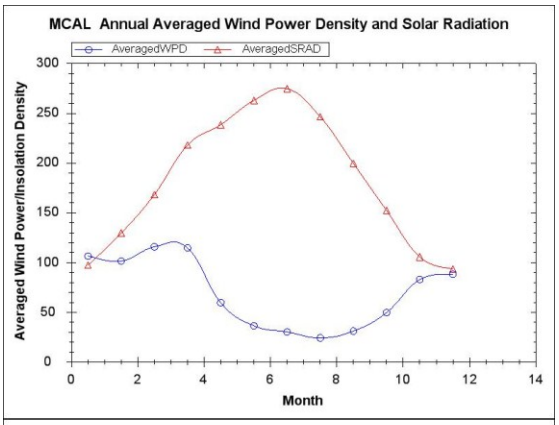
MCAL Annual Averaged Wind Power Density and Solar Radiation
AveragedWPD
AveragedSRAD
Averaged Wind Power/Insolation Density
Month

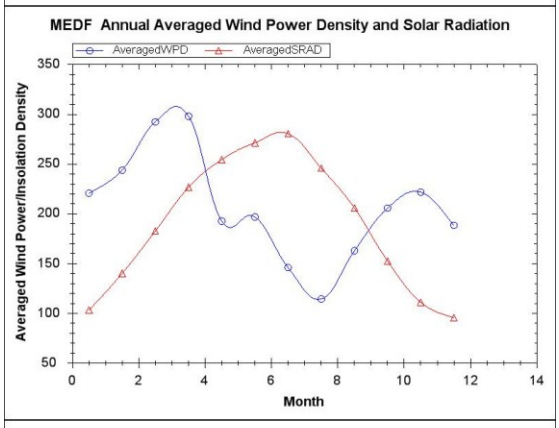
MEDF Annual Averaged Wind Power Density and Solar Radiation
AveragedWPD
AveragedSRAD
Averaged Wind Power/Insolation Density
Month

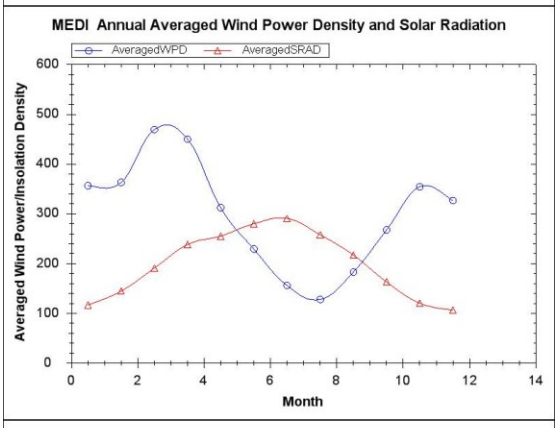
MEDI Annual Averaged Wind Power Density and Solar Radiation
AveragedWPD
AveragedSRAD
Averaged Wind Power/Insolation Density
Month

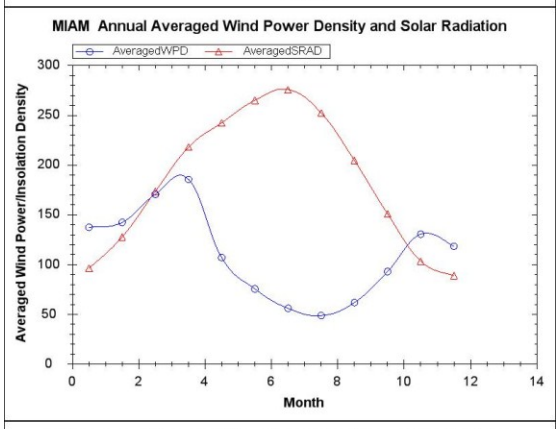
MIAM Annual Averaged Wind Power Density and Solar Radiation
AveragedWPD
AveragedSRAD
Averaged Wind Power/Insolation Density
Month

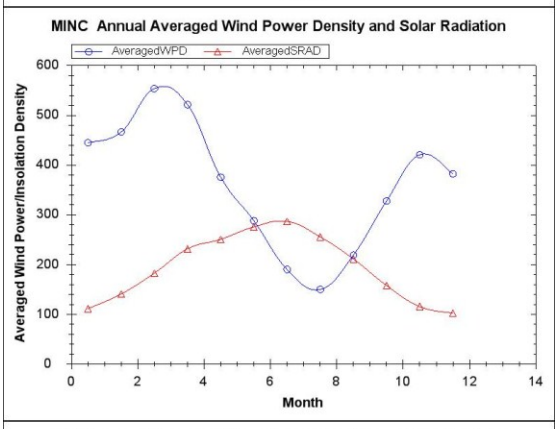
MINC Annual Averaged Wind Power Density and Solar Radiation
AveragedWPD
AveragedSRAD
Averaged Wind Power/Insolation Density
Month

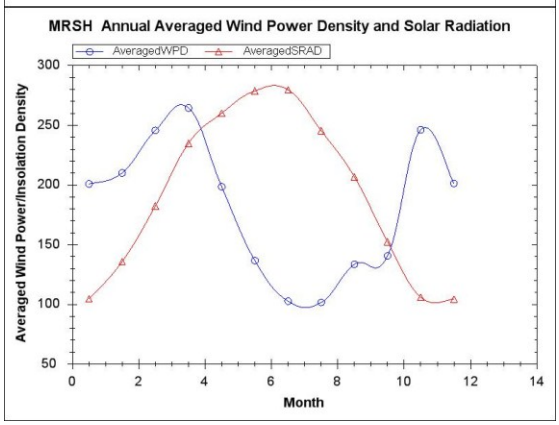
MRSH Annual Averaged Wind Power Density and Solar Radiation
AveragedWPD
AveragedSRAD
Averaged Wind Power/Insolation Density
Month

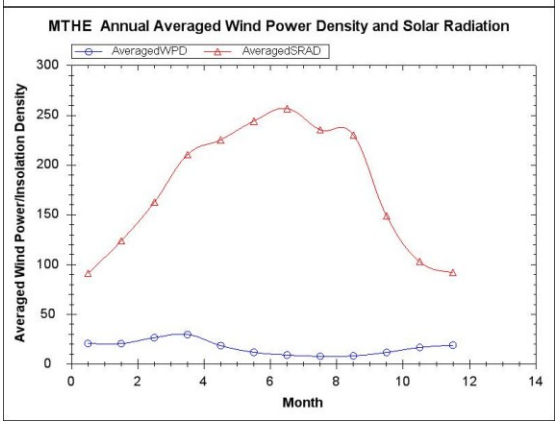
MTHE Annual Averaged Wind Power Density and Solar Radiation
AveragedWPD
AveragedSRAD
Averaged Wind Power/Insolation Density
Month

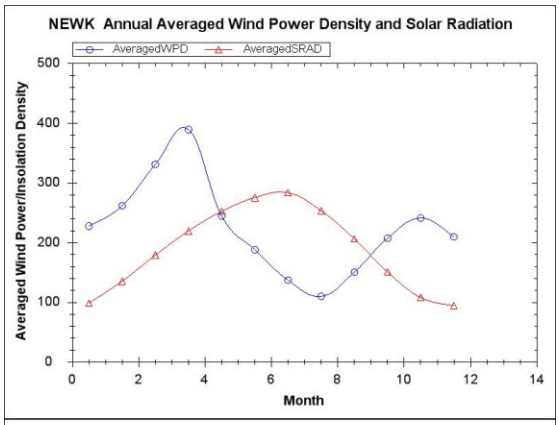
NEWK Annual Averaged Wind Power Density and Solar Radiation
AveragedWPD
AveragedSRAD
Averaged Wind Power/Insolation Density
Month

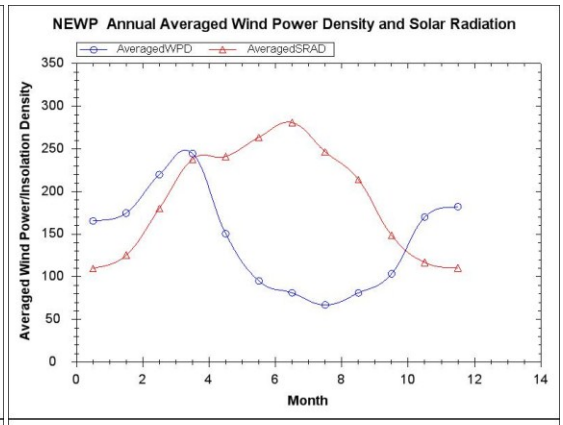
NEWP Annual Averaged Wind Power Density and Solar Radiation
AveragedWPD
AveragedSRAD
Averaged Wind Power/Insolation Density
Month

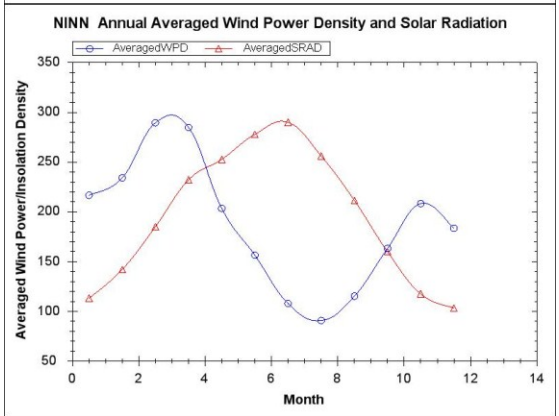
NINN Annual Averaged Wind Power Density and Solar Radiation
AveragedWPD
AveragedSRAD
Averaged Wind Power/Insolation Density
Month

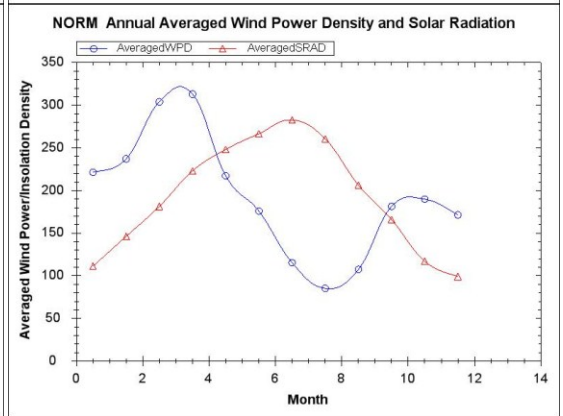
NORM Annual Averaged Wind Power Density and Solar Radiation
AveragedWPD
AveragedSRAD
Averaged Wind Power/Insolation Density
Month

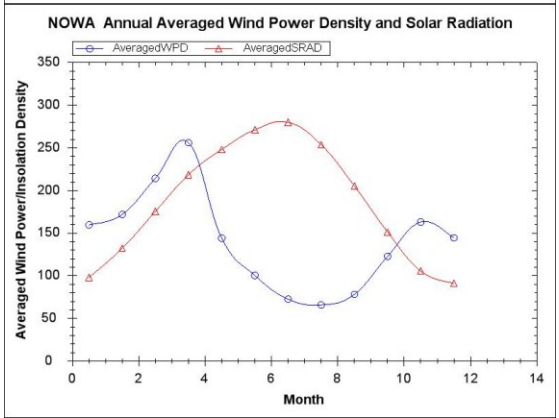
NOWA Annual Averaged Wind Power Density and Solar Radiation
AveragedWPD
AveragedSRAD
Averaged Wind Power/Insolation Density
Month

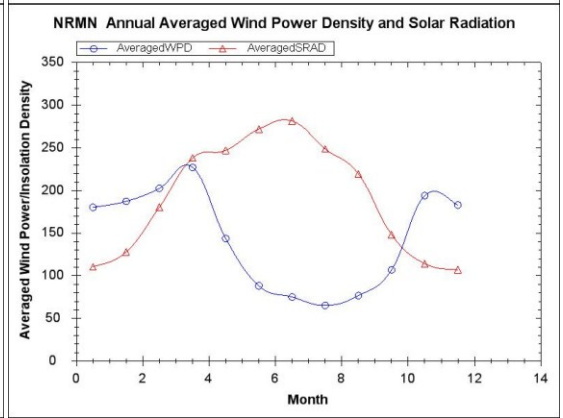
NRMN Annual Averaged Wind Power Density and Solar Radiation
AveragedWPD
AveragedSRAD
Averaged Wind Power/Insolation Density
Month

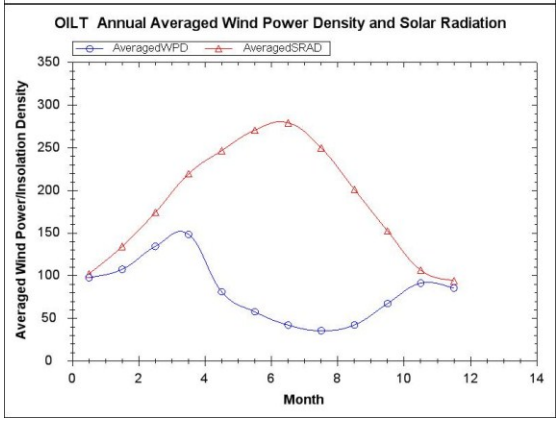
OILT Annual Averaged Wind Power Density and Solar Radiation
AveragedWPD
AveragedSRAD
Averaged Wind Power/Insolation Density
Month

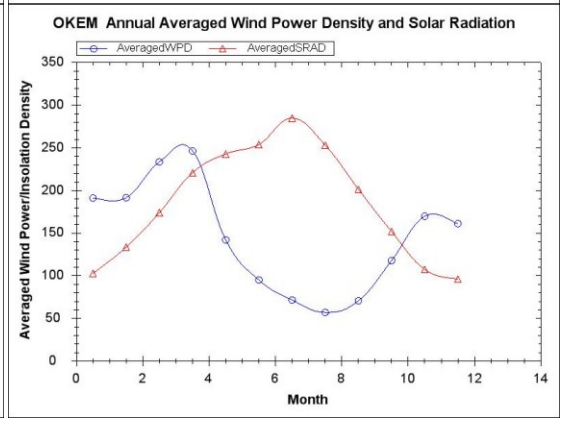
OKEM Annual Averaged Wind Power Density and Solar Radiation
AveragedWPD
AveragedSRAD
Averaged Wind Power/Insolation Density
Month

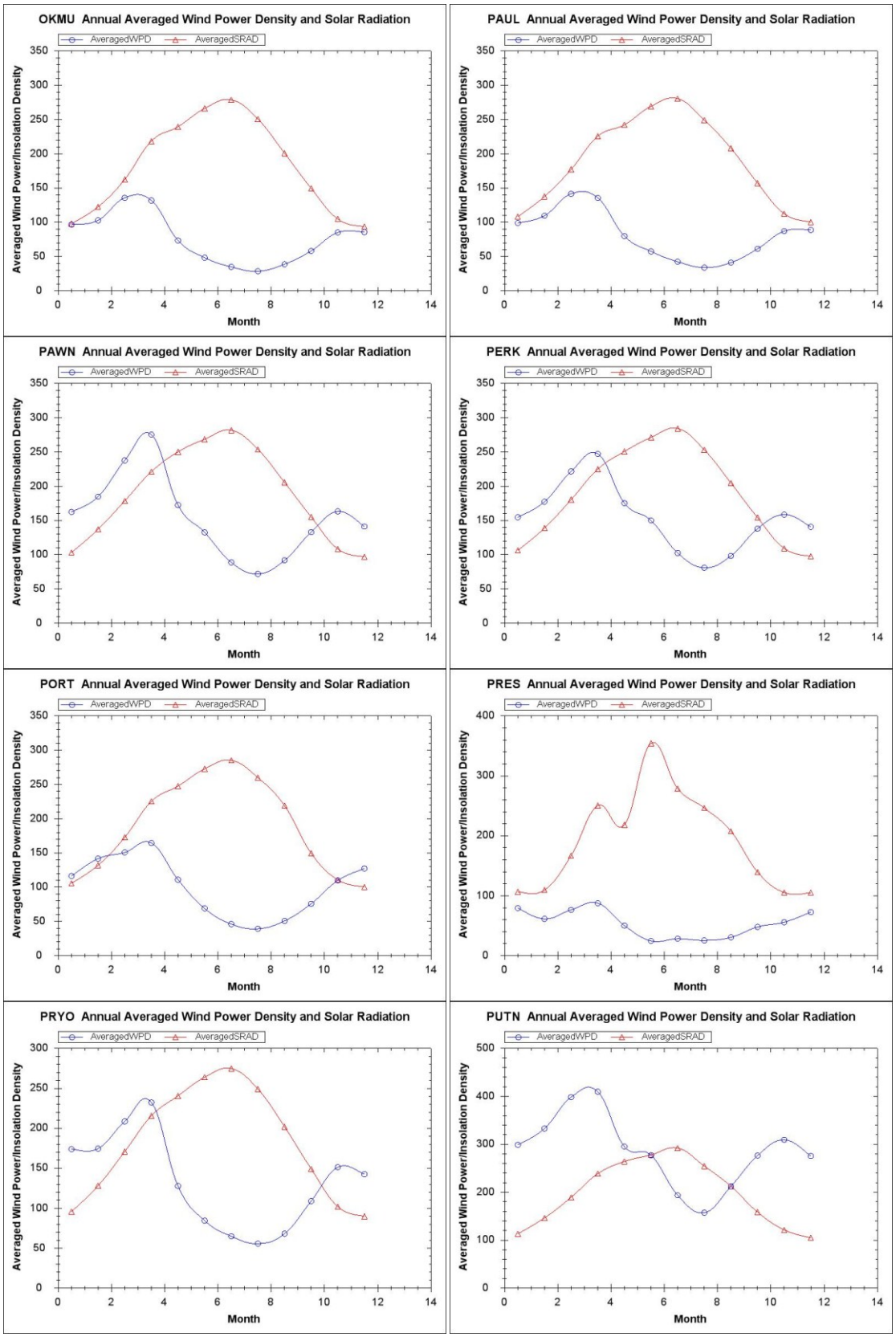
OKMU Annual Averaged Wind Power Density and Solar Radiation
PAUL Annual Averaged Wind Power Density and Solar Radiation
PAWN Annual Averaged Wind Power Density and Solar Radiation
PERK Annual Averaged Wind Power Density and Solar Radiation
PORT Annual Averaged Wind Power Density and Solar Radiation
PRES Annual Averaged Wind Power Density and Solar Radiation
PRYO Annual Averaged Wind Power Density and Solar Radiation
PUTN Annual Averaged Wind Power Density and Solar Radiation
AveragedWPD
AveragedSRAD
Averaged Wind Power/Insolation Density
Month

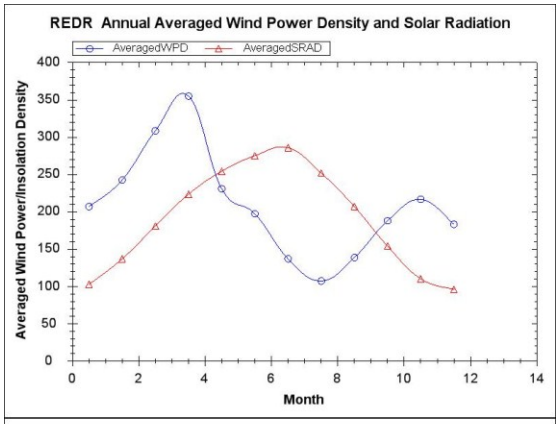
REDR Annual Averaged Wind Power Density and Solar Radiation
AveragedWPD
AveragedSRAD
Averaged Wind Power/Insolation Density
Month

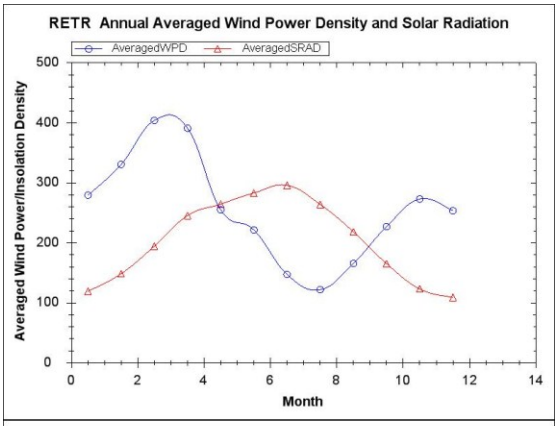
RETR Annual Averaged Wind Power Density and Solar Radiation
AveragedWPD
AveragedSRAD
Averaged Wind Power/Insolation Density
Month

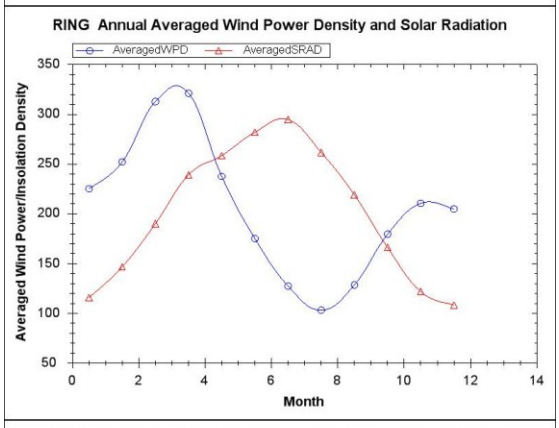
RING Annual Averaged Wind Power Density and Solar Radiation
AveragedWPD
AveragedSRAD
Averaged Wind Power/Insolation Density
Month

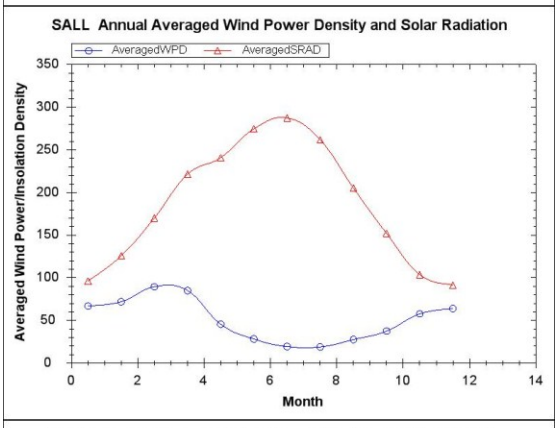
SALL Annual Averaged Wind Power Density and Solar Radiation
AveragedWPD
AveragedSRAD
Averaged Wind Power/Insolation Density
Month

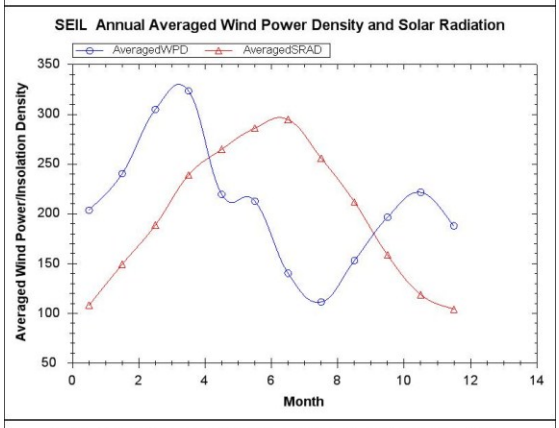
SEIL Annual Averaged Wind Power Density and Solar Radiation
AveragedWPD
AveragedSRAD
Averaged Wind Power/Insolation Density
Month

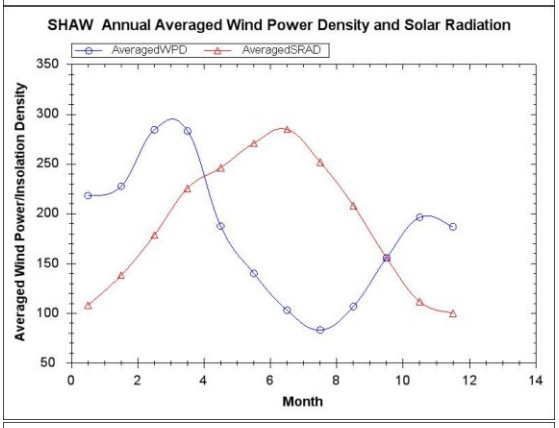
SHAW Annual Averaged Wind Power Density and Solar Radiation
AveragedWPD
AveragedSRAD
Averaged Wind Power/Insolation Density
Month

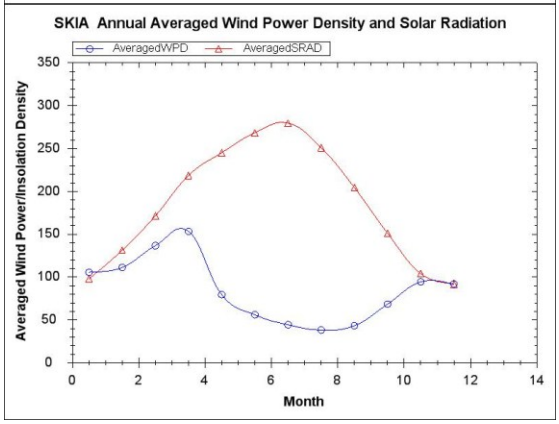
SKIA Annual Averaged Wind Power Density and Solar Radiation
AveragedWPD
AveragedSRAD
Averaged Wind Power/Insolation Density
Month

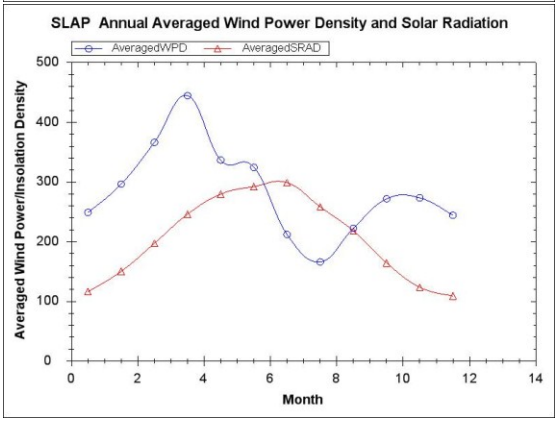
SLAP Annual Averaged Wind Power Density and Solar Radiation
AveragedWPD
AveragedSRAD
Averaged Wind Power/Insolation Density
Month

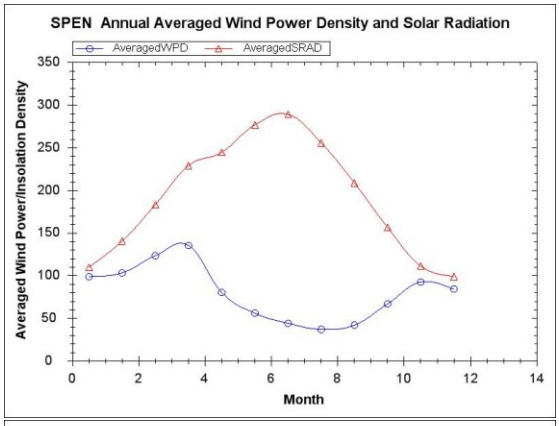
SPEN Annual Averaged Wind Power Density and Solar Radiation
AveragedWPD
AveragedSRAD
Averaged Wind Power/Insolation Density
Month

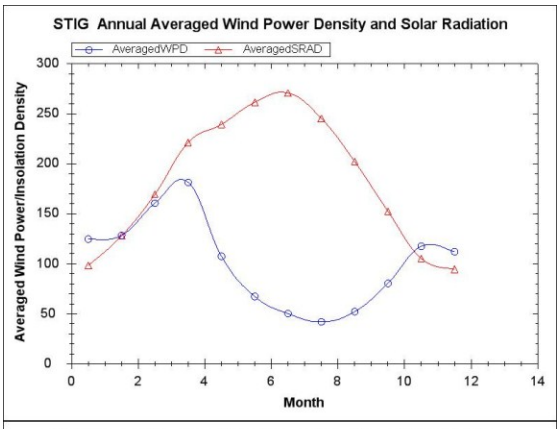
STIG Annual Averaged Wind Power Density and Solar Radiation
AveragedWPD
AveragedSRAD
Averaged Wind Power/Insolation Density
Month

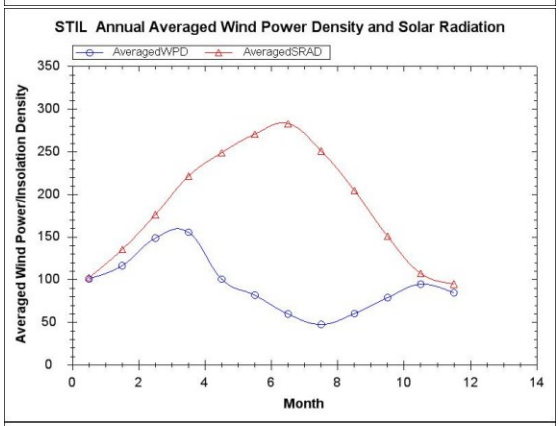
STIL Annual Averaged Wind Power Density and Solar Radiation
AveragedWPD
AveragedSRAD
Averaged Wind Power/Insolation Density
Month

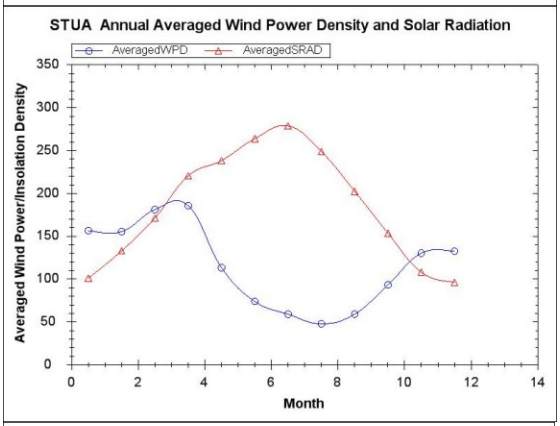
STUA Annual Averaged Wind Power Density and Solar Radiation
AveragedWPD
AveragedSRAD
Averaged Wind Power/Insolation Density
Month

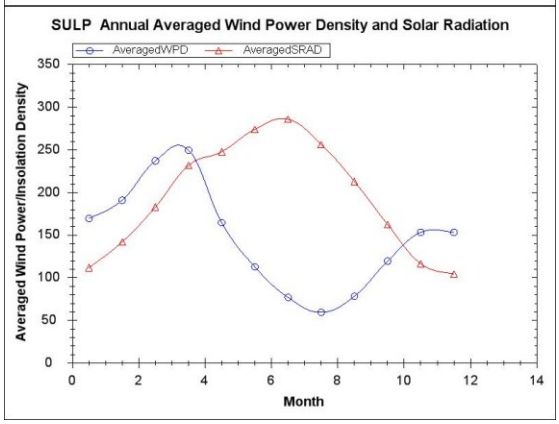
SULP Annual Averaged Wind Power Density and Solar Radiation
AveragedWPD
AveragedSRAD
Averaged Wind Power/Insolation Density
Month

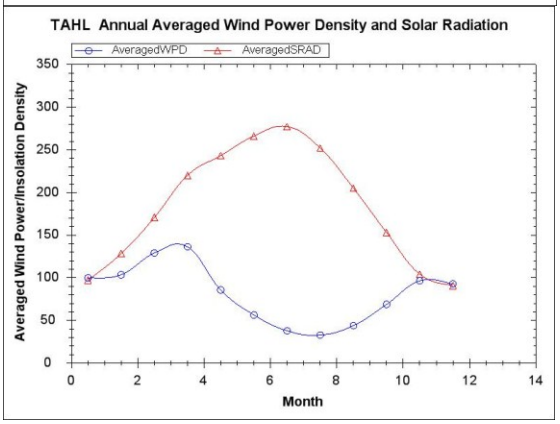
TAHL Annual Averaged Wind Power Density and Solar Radiation
AveragedWPD
AveragedSRAD
Averaged Wind Power/Insolation Density
Month

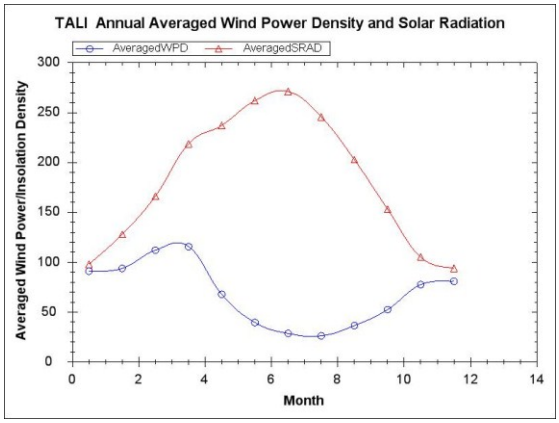
TALI Annual Averaged Wind Power Density and Solar Radiation
AveragedWPD
AveragedSRAD
Averaged Wind Power/Insolation Density
Month

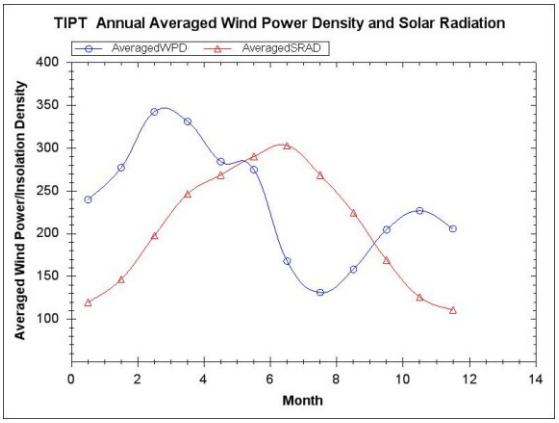
TIPT Annual Averaged Wind Power Density and Solar Radiation
AveragedWPD
AveragedSRAD
Averaged Wind Power/Insolation Density
Month

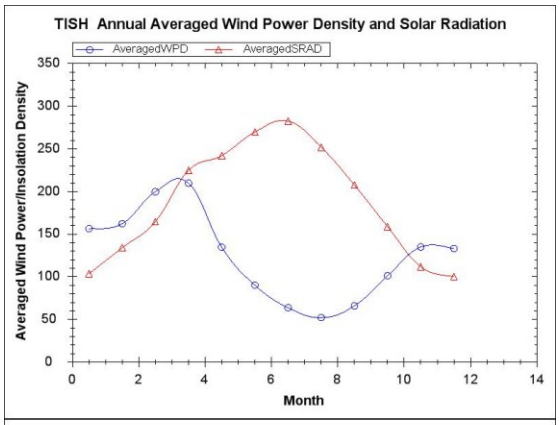
TISH Annual Averaged Wind Power Density and Solar Radiation
AveragedWPD
AveragedSRAD
Averaged Wind Power/Insolation Density
Month

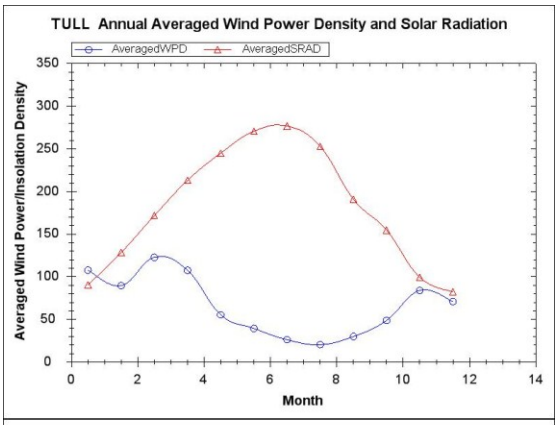
TULL Annual Averaged Wind Power Density and Solar Radiation
AveragedWPD
AveragedSRAD
Averaged Wind Power/Insolation Density
Month

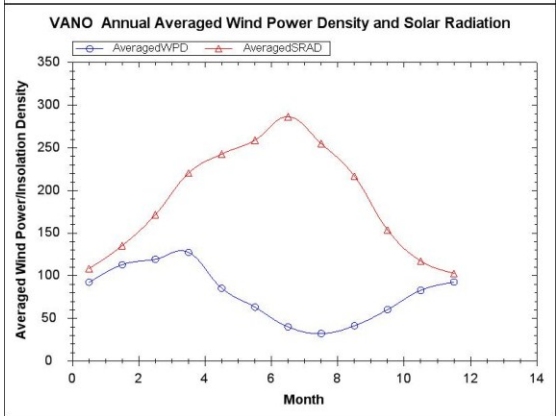
VANO Annual Averaged Wind Power Density and Solar Radiation
AveragedWPD
AveragedSRAD
Averaged Wind Power/Insolation Density
Month

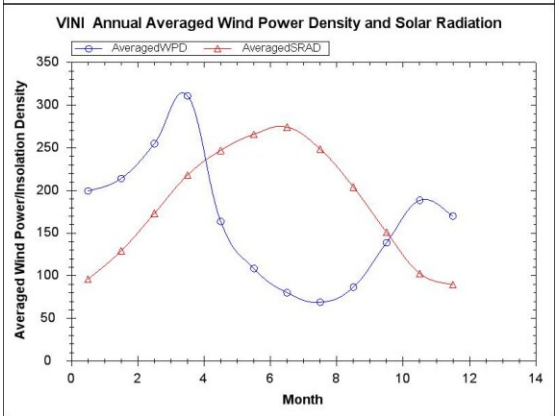
VINI Annual Averaged Wind Power Density and Solar Radiation
AveragedWPD
AveragedSRAD
Averaged Wind Power/Insolation Density
Month

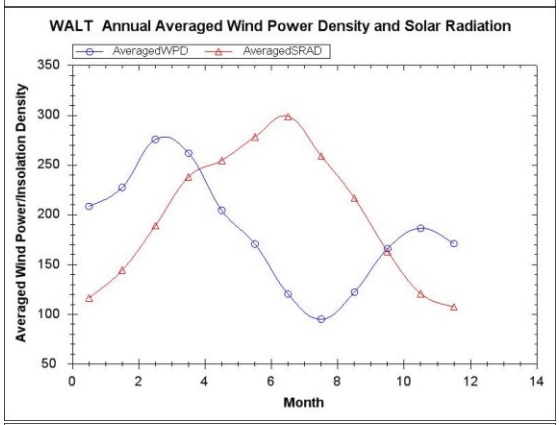
WALT Annual Averaged Wind Power Density and Solar Radiation
AveragedWPD
AveragedSRAD
Averaged Wind Power/Insolation Density
Month

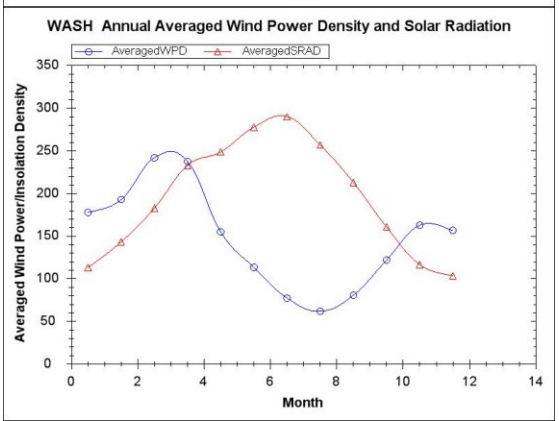
WASH Annual Averaged Wind Power Density and Solar Radiation
AveragedWPD
AveragedSRAD
Averaged Wind Power/Insolation Density
Month

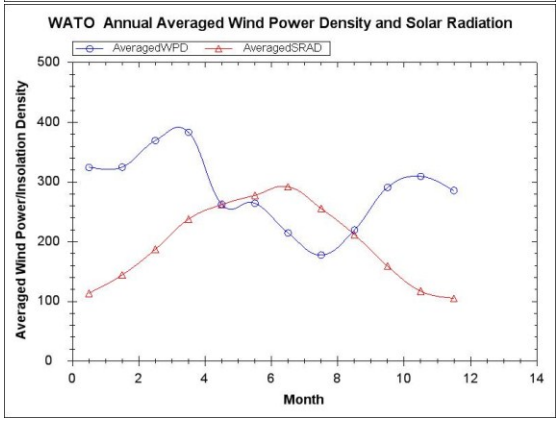
WATO Annual Averaged Wind Power Density and Solar Radiation
AveragedWPD
AveragedSRAD
Averaged Wind Power/Insolation Density
Month

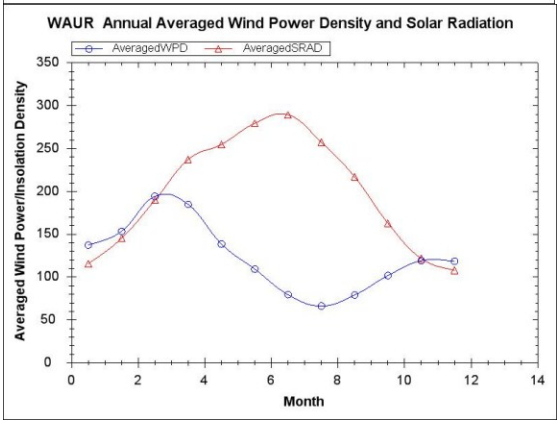
WAUR Annual Averaged Wind Power Density and Solar Radiation
AveragedWPD
AveragedSRAD
Averaged Wind Power/Insolation Density
Month

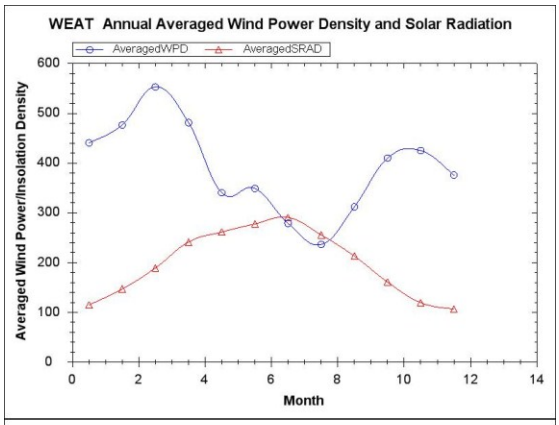
WEAT Annual Averaged Wind Power Density and Solar Radiation
AveragedWPD
AveragedSRAD
Averaged Wind Power/Insolation Density
Month

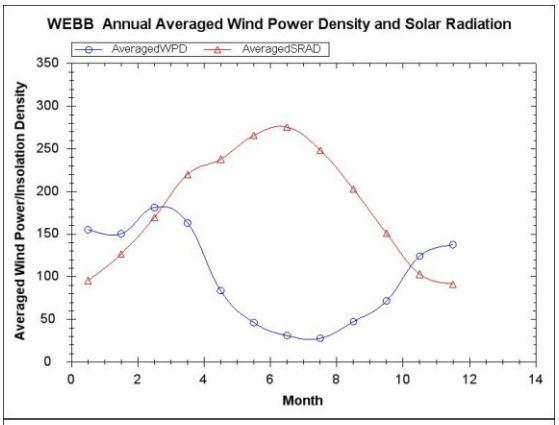
WEBB Annual Averaged Wind Power Density and Solar Radiation
AveragedWPD
AveragedSRAD
Averaged Wind Power/Insolation Density
Month

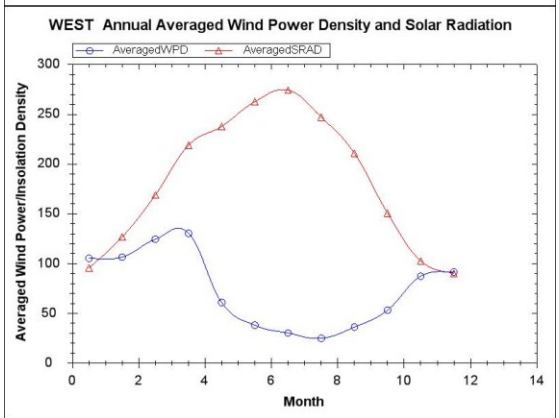
WEST Annual Averaged Wind Power Density and Solar Radiation
AveragedWPD
AveragedSRAD
Averaged Wind Power/Insolation Density
Month

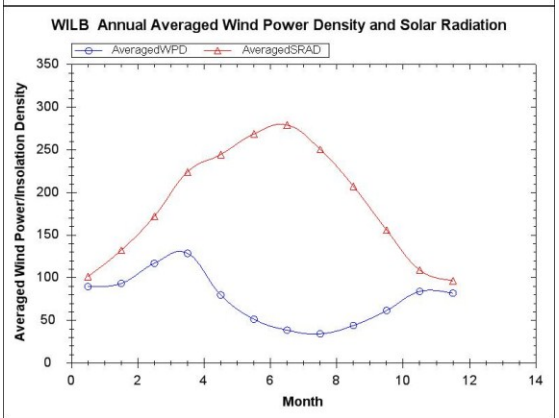
WILB Annual Averaged Wind Power Density and Solar Radiation
AveragedWPD
AveragedSRAD
Averaged Wind Power/Insolation Density
Month

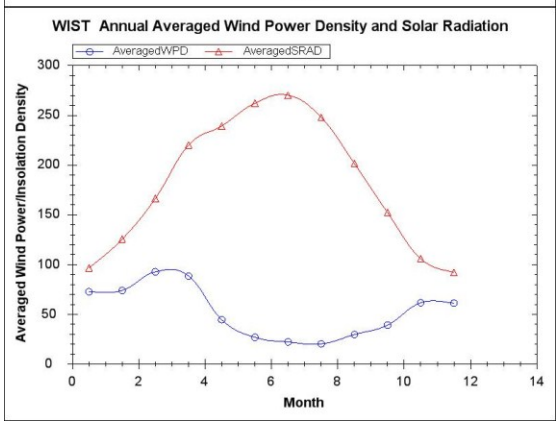
WIST Annual Averaged Wind Power Density and Solar Radiation
AveragedWPD
AveragedSRAD
Averaged Wind Power/Insolation Density
Month

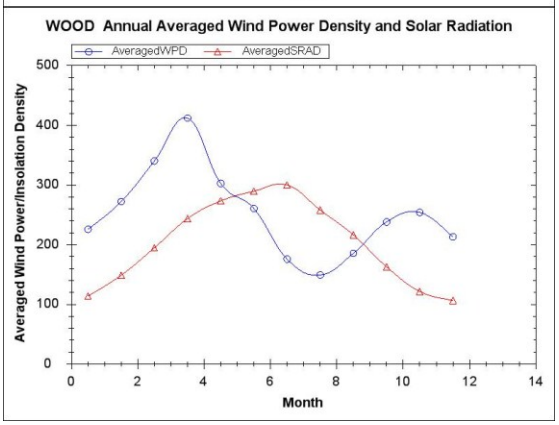
WOOD Annual Averaged Wind Power Density and Solar Radiation
AveragedWPD
AveragedSRAD
Averaged Wind Power/Insolation Density
Month

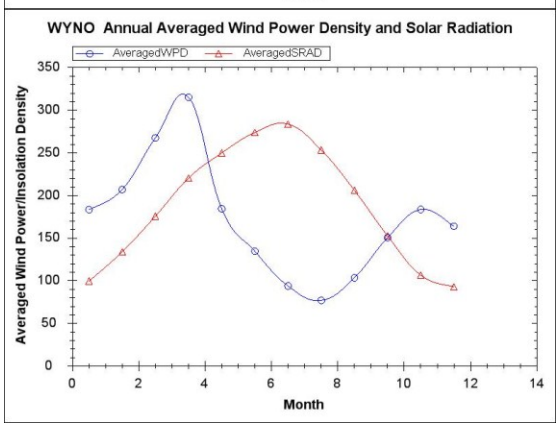
WYNO Annual Averaged Wind Power Density and Solar Radiation
AveragedWPD
AveragedSRAD
Averaged Wind Power/Insolation Density
Month

VITA

Weiping Li

Candidate for the Degree of

Doctor of Philosophy

Thesis: THE INFLUENCES OF GEOGRAPHIC FACTORS ON THE COMPLEMENTARY NATURE OF WIND POWER AND SOLAR ENERGY

Major Field: Geography

Biographical:

Education: Completed the requirements for the Doctor of Philosophy in Geography at Oklahoma State University, Stillwater, Oklahoma in December, 2012. Received Master of Science Degree in the major of Computer Science at Oklahoma State University, Stillwater, Oklahoma in May, 2000. Received Master of Arts in Economic Management from Nanjing University, Nanjing, China in June 1992. Received Bachelor of Science Degree in Economic Geography and Urban and Regional Planning from Nanjing University, Nanjing, China in June 1989.

Experience: Employed as application developer at Oklahoma State University from Feb, 2009 to present. Employed as research assistant and worked for Oklahoma Wind Power Initiative at Department of Geography, Oklahoma State University from August 2003 to December 2008. Employed as software engineer at Advanced Synergy Dynamics from November 2002 to August 2003 Norman, Oklahoma. Employed as software engineer at Factor of W.R. Hess, Oklahoma from October 2001 to October 2002 and from November 1999 to January 2001. Employed as software engineer at Virtual Class, Agoura Hills, California from January 2001 to October 2001.

Professional Memberships: Association of American Geographers (AAG), Gamma Theta Upsilon (GTU) - the international honor society in geography, Association for Computing Machinery (ACM).